ลักษณะสมบัติเชิงหน้าที่ของโปรตีนคล้ายคัลมอดุลิน CML3 จากข้าว *Oryza sativa* L.

นายอำนาจ ชินพงษ์พานิช

วิทยานิพนธ์นี้เป็นส่วนหนึ่งของการศึกษาตามหลักสูตรปริญญาวิทยาศาสตรดุษฎีบัณฑิต
สาขาวิชาชีวเคมีและชีววิทยาโมเลกุล ภาควิชาชีวเคมี
คณะวิทยาศาสตร์ จุฬาลงกรณ์มหาวิทยาลัย
ปีการศึกษา 2557

FUNCTIONAL CHARACTERIZATION OF CALMODULIN-LIKE PROTEIN CML3 FROM RICE *Oryza sativa* L.

Mr. Aumnart Chinpongpanich

A Dissertation Submitted in Partial Fulfillment of the Requirements
for the Degree of Doctor of Philosophy Program in Biochemistry and Molecular Biology
Department of Biochemistry
Faculty of Science
Chulalongkorn University
Academic Year 2014

Thesis Title	FUNCTIONAL CHARACTERIZATION OF CALMODULIN-LIKE PROTEIN CML3 FROM RICE *Oryza sativa* L.
By	Mr. Aumnart Chinpongpanich
Field of Study	Biochemistry and Molecular Biology
Thesis Advisor	Associate Professor Teerapong Buaboocha, Ph.D.
Thesis Co-Advisor	Professor Li-Jia Qu, Ph.D.

Accepted by the Faculty of Science, Chulalongkorn University in Partial Fulfillment of the Requirements for the Doctoral Degree

.....Dean of the Faculty of Science
(Professor Supot Hannongbua, Dr.rer.nat.)

THESIS COMMITTEE

.....Chairman
(Professor Anchalee Tassanakajon, Ph.D.)

.....Thesis Advisor
(Associate Professor Teerapong Buaboocha, Ph.D.)

.....Thesis Co-Advisor
(Professor Li-Jia Qu, Ph.D.)

.....Examiner
(Professor Aran Incharoensakdi, Ph.D.)

.....Examiner
(Assistant Professor Kuakarun Krusong, Ph.D.)

.....External Examiner
(Sittiruk Roytrakul, Ph.D.)

อำนาจ ชินพงษ์พานิช : ลักษณะสมบัติเชิงหน้าที่ของโปรตีนคล้ายคัลมอดุลิน CML3 จากข้าว *Oryza sativa* L. (FUNCTIONAL CHARACTERIZATION OF CALMODULIN-LIKE PROTEIN CML3 FROM RICE *Oryza sativa* L.) อ.ที่ปรึกษาวิทยานิพนธ์หลัก: รศ. ดร.ธีรพงษ์ บัวบูชา, อ.ที่ปรึกษาวิทยานิพนธ์ร่วม: ศ. ดร.ลี่เจีย ฉู่, หน้า.

จากการศึกษาที่ผ่านมาพบกลุ่มยีนคัลมอดุลิน (*Calmodulin, Cam*) และ *calmodulin-like protein* (*CML*) ขนาดใหญ่ในจีโนมข้าว (*Oryza sativa* L.) แต่ข้อมูลเชิงหน้าที่ของโปรตีนเหล่านี้ยังมีอยู่น้อยมาก ในงานวิจัยนี้ศึกษาสมบัติของโปรตีนรีคอมบิแนนต์บริสุทธิ์ OsCML3m ซึ่งเป็นโปรตีน OsCML3 ที่ขาดส่วนปลายคาร์บอกซิล (C-terminal extension) พบว่าโปรตีน OsCML3 และ OsCML3m สามารถจับกับแคลเซียมไอออนและเกิดการเปลี่ยนแปลงโครงรูป แต่ OsCML3m เท่านั้นที่สามารถจับกับเพปไทด์ของ CaMK II และจากการศึกษาโดยวิธี Circular dichroism (CD) พบว่าในภาวะที่มีแคลเซียม โปรตีน OsCML3m มี helical content สูงกว่า OsCML3 นอกจากนี้การศึกษา localization ภายในเซลล์พบว่า OsCML3 ส่วนใหญ่อยู่ที่ plasma membrane ในขณะที่ OsCML3m อยู่ในนิวเคลียส ก่อนหน้านี้โปรตีน OsPEBP และ OsHMGB1 ถูกระบุว่าเป็นโปรตีนเป้าหมายของ OsCML3m ในการศึกษาการเกิดอันตรกิริยาโดยวิธี yeast two hybrid พบว่าโปรตีน OsCML3 และ OsCML3s ที่ถูกทำให้เกิดการกลายพันธุ์ที่ตำแหน่งกรดอะมิโนซิสเทอีนไปเป็นเซรีนไม่สามารถเกิดอันตรกิริยากับโปรตีน OsPEBP และ OsHMGB1 ได้ขณะที่ OsCML3m ที่เชื่อมต่อกับ GAL4 DNA-binding domain เกิด self-activation และการวิเคราะห์ด้วยวิธี Bimolecular Fluorescence Complementation (BiFC) ไม่พบการเกิดอันตรกิริยาระหว่างโปรตีน OsPEBP กับโปรตีน OsCML3 OsCML3m และ OsCML3s ในขณะที่ OsHMGB1 สามารถจับกับโปรตีน OsCML3 OsCML3m และ OsCML3s ที่นิวเคลียส ซึ่งน่าจะผ่านทาง nuclear localization signal ของ OsHMGB1 ชี้ให้เห็นว่าโปรตีน OsHMGB1 เป็นโปรตีนเป้าหมาย *in planta* ของโปรตีน OsCML3 นอกจากนี้จากการทดสอบโดยวิธี Electrophoretic mobility shift assay (EMSA) พบว่าภายใต้สภาวะที่มีแคลเซียมโปรตีน OsCML3m สามารถลดการจับกันระหว่างโปรตีน OsHMGB1 กับ pUC19 double stranded DNA ในขณะที่โปรตีน OsCML3 ไม่มีผล ผลการทดลองทั้งหมดนี้ชี้ให้เห็นว่าส่วน C-terminus ของโปรตีน OsCML3 ส่งผลต่อการจับกับโปรตีนเป้าหมาย และการจับของ OsCML3 กับ OsHMGB1 ส่งผลขัดขวางการจับของ OsHMGB1 กับ DNA

การศึกษาการแสดงออกในระดับทรานสคริปของยีน *CML3* พบว่าภายใต้ความเค็มระดับการแสดงออกลดลงเพียงเล็กน้อยที่ชั่วโมงที่ 1 และพบระดับการแสดงออกที่เพิ่มขึ้นเมื่อทดสอบด้วยให้ 6-Benzylaminopurine (BA) และลดลงเพียงเล็กน้อยเมื่อให้ 3-Indoleacetic acid (IAA) ที่ชั่วโมงที่ 48 และมีระดับการแสดงออกเพิ่มสูงขึ้น 2-3 เท่า เมื่อได้รับภาวะเครียดจากความเย็น จากการตรวจสอบ บริเวณโปรโมเตอร์ของ *OsCML3* พบบริเวณที่อาจเป็น ABREs (ABA-responsive element) สองตำแหน่ง และ LTRE (low temperature responsive element) หนึ่งตำแหน่ง จากนั้นได้สร้างอราบิดอปซิสทรานเจนิกส์ที่มีระดับการแสดงออกเกินปกติของยีน *OsCML3* หรือ *OsCML3m* จากการทรานสฟอร์มโดยอาศัยอะโกรแบคทีเรียมได้พืชที่เป็น homozygous ที่เป็นอิสระต่อกันจำนวนอย่างละสี่สายพันธุ์ จากการตรวจสอบความสามารถในการทนเย็นของอราบิดอปซิสทรานเจนิกส์ในระยะงอกของเมล็ดพบว่า เมล็ดทรานเจนิกส์ในทุกสายพันธุ์ที่ถูกปลูกที่อุณหภูมิ 11 ºC มีอัตราการงอกที่สูงกว่าเมล็ด wild type และ อราบิดอปซิสทรานเจนิกส์ควบคุมที่ทรานสฟอร์มด้วยเวกเตอร์เปล่า ยกเว้นสายพันธุ์ 21014 เมื่อสังเกตที่วันที่ 14 นอกจากนี้ยังพบว่าน้ำหนักแห้งและน้ำหนักสดของพืชทรานเจนิกส์ที่ปลูกที่อุณหภูมิ 11 ºC ต่อที่อุณหภูมิปกติ (22 ºC) มีค่ามากกว่าของ wild type และอราบิดอปซิสทรานเจนิกส์ควบคุมที่ทรานสฟอร์มด้วยเวกเตอร์เปล่าโดยส่วนใหญ่ โดยสรุปแล้วโปรตีน OsCML3 มีความเป็นไปได้ที่จะทำหน้าที่ที่เกี่ยวข้องกับกลไกในการควบคุมการจับ DNA ของโปรตีน OsHMGB1 ในนิวเคลียสและส่วนปลายคาร์บอกซิล (C-terminal extension) ยังอาจทำหน้าที่ควบคุมนี้ นอกจากนี้การแสดงออกเกินปกติของยีน *OsCML3* หรือ *OsCML3m* สามารถเพิ่มความสามารถในการทนเย็นของพืชอราบิดอปซิสในระยะงอกและระยะต้นกล้าได้อีกด้วย

ภาควิชา ชีวเคมี	ลายมือชื่อนิสิต .....
สาขาวิชา ชีวเคมีและชีววิทยาโมเลกุล	ลายมือชื่อ อ.ที่ปรึกษาหลัก .....
ปีการศึกษา 2557	ลายมือชื่อ อ.ที่ปรึกษาร่วม .....

5373838323 : MAJOR BIOCHEMISTRY AND MOLECULAR BIOLOGY
KEYWORDS: CALMODULIN / CALCIUM RECEPTOR PROTEIN / CML3 / ORYZA SATIVA L.

AUMNART CHINPONGPANICH: FUNCTIONAL CHARACTERIZATION OF CALMODULIN-LIKE PROTEIN CML3 FROM RICE *Oryza sativa* L.. ADVISOR: ASSOC. PROF. TEERAPONG BUABOOCHA, Ph.D., CO-ADVISOR: PROF. LI-JIA QU, Ph.D., pp.

Previously, a large family of *Calmodulin* (*Cam*) and *calmodulin-like* (*CML*) genes has been identified in *Oryza sativa* L., but there is little detailed information on the functions of these proteins. Here, we examined properties of the purified recombinant protein encoded by *OsCML3m* (truncated *OsCML3* lacking the C-terminal extension (CTE) coding sequence). The rOsCML3 and rOsCML3m proteins were found to exhibit a Ca^{2+}-binding property and subsequent conformational change, but the ability to bind the CaM kinase II peptide was only observed for OsCML3m. Changes in their secondary structure upon Ca^{2+}-binding measured by circular dichroism revealed that OsCML3m had a higher helical content than OsCML3. Moreover, the subcellular localization of OsCML3 and OsCML3m revealed that OsCML3 was mainly localized at the plasma membrane, whereas OsCML3m was found in the nucleus. Previously, the rice phosphatidylethanolamine (OsPEBP) and high mobility group B1 (OsHMGB1) protein were identified as two of the putative OsCML3m target proteins. By yeast two-hybrid analysis, no interaction between OsPEBP or OsHMGB1with either OsCML3 or OsCMLs (cysteine to serine mutation at prenylation site), and strong self-activation of the OsCML3m fused with GAL4 DNA-binding domain were detected. By Bimolecular Fluorescence Complementation (BiFC) analysis, the interaction of OsPEBP with OsCML3, OsCML3m or OsCML3s was not found whereas the interaction of OsHMGB1 with OsCML3, OsCML3m or OsCML3s was found in the nucleus, suggesting that HMGB1 is an OsCML3 target protein *in planta*. Moreover, electrophoretic mobility shift assay (EMSA) showed that, in the presence of Ca^{2+}, OsCML3m decreased HMGB1 binding to pUC19 double stranded DNA whereas OsCML3 did not. These results indicate that the OsCML3 CTE interfere the target binding ability of OsCML3 and its interaction with OsHMGB1 inhibits the DNA-binding ability of OsHMGB1.

The transcript expression analysis of *CML3* in rice (*Oryza sativa* L.) showed that was slightly down-regulated at 1 h under salt treatment. In addition, the *OsCML3* transcript level was found up-regulated at 48 h after 6-Benzylaminopurine (BA) application while slightly down-regulated at 48 h after 3-Indoleacetic acid (IAA) application. Interestingly, the transcript level of *OsCML3* was significantly up-regulated to 2-3 folds at 3 h after cold stress suggesting that the OsCML3 may involve in the response to cold stress. In the *OsCML3* promoter, two Putative ABREs (ABA-responsive element) and one putative LTRE (low temperature responsive element) were found. Finally, the transgenic *Arabidopsis* overexpressing *OsCML3* or *OsCML3m* using *Agrobacterium*-mediated transformation was generated, resulting in four independent homozygous transgenic lines harboring *OsCML3* or *OsCML3m*. Higher germination percentages of all transgenic lines at 11 ^{o}C were observed compared with those of the wild type and the control transgenic Arabidopsis transformed with the blank vector. Fresh weight and dry weight ratios of the transgenic *Arabidopsis* overexpressing *OsCML3* or *OsCML3m* seedlings grown under cold stress to those under normal condition (22 ^{o}C) were mostly higher than those of the wt and the control transgenic plant. Taken together, OsCML3 probably provides a mechanism for manipulating the DNA-binding ability of OsHMGB1 in the nucleus and its C-terminal extension provides a regulatory switch. Moreover, the overexpression of *OsCML3* or *OsCML3m* enhances cold tolerance during germination and seedling stage of *Arabidopsis*.

Department:	Biochemistry	Student's Signature	.....
Field of Study:	Biochemistry and Molecular Biology	Advisor's Signature	.....
Academic Year:	2014	Co-Advisor's Signature	.....

ACKNOWLEDGEMENTS

I would sincerely like to acknowledge the efforts of many people who contribute to this work. This thesis could not be achieved without their following assistance, my thesis advisor Associate Professor Dr. Teerapong Buaboocha and my thesis co-advisor Professor Dr. Li-Jia Qu for their generous advice, skillful assistance, technical helps, guidance, encouragement, support, fruitful and stimulating discussion through the period of my study.

Sincere thanks and appreciation are due to Professor Dr. Anchalee Tassanakajon, Professor Dr. Aran Incharoensakdi, Assistant Professor Dr. Kuakarun Krusong, and Dr. Sittiruk Roytrakul for serving as the member of the doctoral thesis committee, for their useful comments and suggestions.

I would like to thank the Royal Golden Jubilee Ph.D. program-RGJ [grant number 4.C.CU/53.G.1/P.XX] from the Thailand Research Fund for financially supporting the research through the thesis fund.

Special thanks are also extended to Dr. Srivilai Phean-o-pas, Dr. Mayura Thongchuang and other friends of the Biochemistry and Biotechnology programs for lending a helping hand whenever needed, sharing the great time in laboratory, for their friendships.

Finally, the warmest gratitude is extended to my family for their patience, understanding, help, encouragement, constant support and warmhearted love whilst I have spent many hours with this thesis rather than with them.

CONTENTS

Page

Page

Page

Page

Page

Page

LIST OF TABLE

Table **Page**

LIST OF FIGURE

Figure **Page**

Figure **Page**

Figure **Page**

Figure **Page**

Figure **Page**

LIST OF ABBREVIATIONS

A_{260}	absorbance at 260 nm
A_{280}	absorbance at 280 nm
aa	amino acid
bp	base pairs
^{o}C	degree Celsius
Ca^{2+}	calcium ion
Cam	calmodulin gene
CaM	calmodulin protein
cDNA	complementary deoxyribonucleic acid
DNA	deoxyribonucleic acid
IAA	Indole-3-acetic acid (Auxin)
BA	Benzylaminopurine (Cytokiknin)
M	molar
g	gram
xg	times gravity
IPTG	isopropyl-ß-D-thiogalactopyranoside
Kb	kilobase
KDa	kiloDalton
LB	Luria Bertani media
µg	microgram
mg	milligram

µl	microliter
ml	milliliter
µM	micromolar
mM	millimolar
mRNA	messenger ribonucleic acid
MW	molecular weight
ng	nanogram
nm	nanometer
nM	nanomolar
nmole	nanomole
OD_{600}	optical density at 600 nm
oligo (dT)	oligodeoxythymidylic acid
ORF	open reading frame
cv.	cultivar
DEPC	diethyl pyrocarbonate
DNase	deoxyribonuclease
dNTP	deoxynucleoside triphosphate
EDTA	ethylenediaminetetraacetic acid
EGTA	ethylene glycol tetraacetic acid
PAGE	polyacrylamide gel electrophoresis
PCR	polymerase chain reaction
pH	power of hydrogen ion
pmole	picomole
RNA	ribonucleic acid

RNase	ribonuclease
RT-PCR	reverse transcription-polymerase chain reaction
SDS	sodium dodecyl sulfate
TAE	Tris/acetate/EDTA buffer
TBE	Tris/borate/EDTA buffer
TBS	Tris buffer saline
TEMED	N,N,N’,N’- tetramethylethylenediamine
UV	ultraviolet
v/v	volume by volume
w/v	weight by volume
X-gal	5-bromo-4-chloro-3-indolyl-ß-D-galactopyranoside

CHAPTER I

INTRODUCTION

Plants have specific mechanisms to adapt and survive stressful events. Exposure of plants to biotic and abiotic stress induces disruption in plant metabolism imposing physiological costs (Bolton 2009; Heil and Bostock 2002; Swarbrick et al. 2006). Abiotic stress is one of the most important features and has a huge impact on growth and, consequently, it is responsible for severe losses in the field. The resulting growth reduction can reach >50% in most plant species (Wang et al. 2003). Previously, although research has mainly concentrated on understanding plant responses to individual abiotic or biotic stress (Qin et al. 2011; Stotz et al. 2014; Thakur and Sohal 2013; Todaka et al. 2012), its mechanism in the response to stresses is still largely unknown.

One of well-known mechanisms in plant response involves Ca^{2+} signaling in which Ca^{2+} concentration is maintained at low levels in the cytosol via the activation of calcium pumps and storage in multiple intracellular compartments as well as extracellular spaces and transiently increased via the activation of calcium channels upon specific stimulation (Figure 1.1) (Sanders et al. 2002).

1.1 Calcium signaling

Calcium ions (Ca^{2+}) play a crucial role in organisms. Ca^{2+} is a key second messenger and important component of signal transduction machinery in many cellular processes. In plants, Ca^{2+} plays a vital role during various developmental

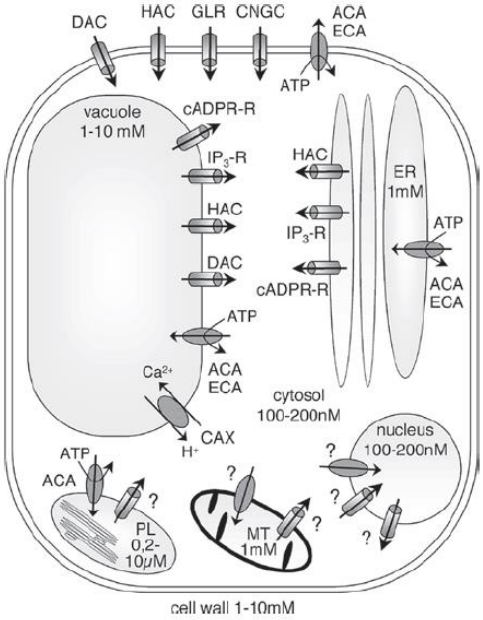

Figure 1.1 Schematic representation of Ca^{2+}-permeable channels, pumps and transporters that are proposed to be involved in calcium signaling in response to abiotic stresses. Ca^{2+}- permeable channels (cylinders) can be regulated by voltage, either hyperpolarization (HAC) or depolarization (DAC) or ligands. The ligand-gated channels include IP3 receptors (IP3-R), cADPR receptors (cADPR-R), glutamate receptors (GLR) and cyclic nucleotide-gated channels (CNGC). Genes encoding HAC, DAC, IP3-R and cADPR-R have not been identified in plants. Ca^{2+}-pumps and transporters (ovals) comprise ACA and ECA Ca^{2+}-ATPases, and the CAX Ca^{2+}/H^{+}-antiporters. Biochemical and electrophysiological evidence indicate the presence of Ca^{2+} transport systems involved in stress responses in the mitochondria (MT) and the nucleus, but their molecular identity is not clear yet. Currently, there is no evidence for the involvement of plastids (PL) in regulating abiotic stress Ca^{2+} signals. The estimated calcium concentration is indicated for each cellular compartment (Pauly et al. 2001; Reddy and Reddy 2004) (Adapted from Reddy and Reddy, 2004).This figure was taken from (Boudsocq and Sheen 2010).

processes and in response to environmental stimuli (Clapham 2007). Ca^{2+} concentration in the cytosol is very low, in the range of nM, with higher levels of Ca^{2+} (mM) in many organelles such as ER and vacuole where they are stored (Bush et al. 1989; Clarkson 1988). Upon perception of a stimulus by receptors, Ca^{2+} channels open to release Ca^{2+} from different stores into the cytosol and these elevations in cytosolic Ca^{2+} activate signaling pathways leading to specific responses. Calcium ions are involved in many kinds of abiotic and biotic stress responses in plant (Sanders et al. 1999). Examples of abiotic stress factors that change the Ca^{2+} concentration include osmotic stress, salt stress, low temperature, touch and light (Sai and Johnson 2002).

1.2 Ca^{2+}-binding proteins

The involvement of Ca^{2+} as a second messenger in a wide variety of cellular and physiological processes is well documented (Zhang et al. 2002). To respond appropriately to a specific calcium concentration in cytosol perturbation, a cell must activate a unique combination of Ca^{2+}-binding proteins. Most Ca^{2+} sensors bind Ca^{2+} using the EF-hand motif, a helix-loop-helix structure that binds one Ca^{2+} ion. EF-hands often occur in pair forming a domain with positive co-operativity, thereby minimizing the Ca^{2+} signal required to reach protein saturation (Gifford et al. 2007). Typically, Ca^{2+} binding to a Ca^{2+} sensor induces a conformational change of the protein that either promotes its interaction with downstream effectors or modulates its own catalytic activity. Plants have evolved a superfamily of EF-hand proteins represented by about 250 proteins in rice and *Arabidopsis thaliana*, a well-studied model-plant, compared to 132 and 83 EF-hand proteins in *Drosophila melanogaster*

and human, respectively (Day et al. 2002).These EF-hand proteins can be grouped into four major classes as shown in Figure 1.2. These include (A) Ca^{2+}-dependent protein kinase (CPK) that contains CaM-like Ca^{2+} binding domains and a kinase domain in a single protein. Each individual CPK protein is expected to detect changes in the Ca^{2+} parameters and translate these changes into the regulation of a protein kinase activity (Roberts and Harmon 1992), (B) Calmodulin (CaM) which contains four EF-hand domains but has no enzymatic activity themselves and functions by interacting with their target proteins (Zielinski 1998), (C) other EF-hand motif-containing Ca^{2+}- binding proteins and Calcineurin B-like (CBL) proteins that are similar to both the regulatory B subunit of calcineurin and the neuronal Ca^{2+} sensor (NCS) in animals (Klee et al. 1998) and (D) Ca^{2+}-binding proteins without EF-hand motifs.

1.3 Calmodulin and Calmodulin-like protein in plants

CaM is a small (148 residues) multifunctional protein that transduces the signal of increased Ca^{2+} concentration by binding to and altering the activities of a variety of target proteins. It contains two globular regions, each possessing a pair of Ca^{2+} binding domains (termed EF hands). CaM relays the Ca^{2+} signal by binding free Ca^{2+} ions to its C- and N terminal EF-hand pairs. Upon binding Ca^{2+}, CaM undergoes a major shift in conformation which exposes hydrophobic regions and facilitates its interaction with specific targets in a calcium dependent manner. Ca^{2+}-bound-calmodulin-mediated signal transduction in plants is shown in Figure 1.3. Structural analysis of the Ca^{2+}-free and Ca^{2+}-bound states of CaM proteins reveals the conformational changes induced by Ca^{2+} binding as shown in Figure 1.4.

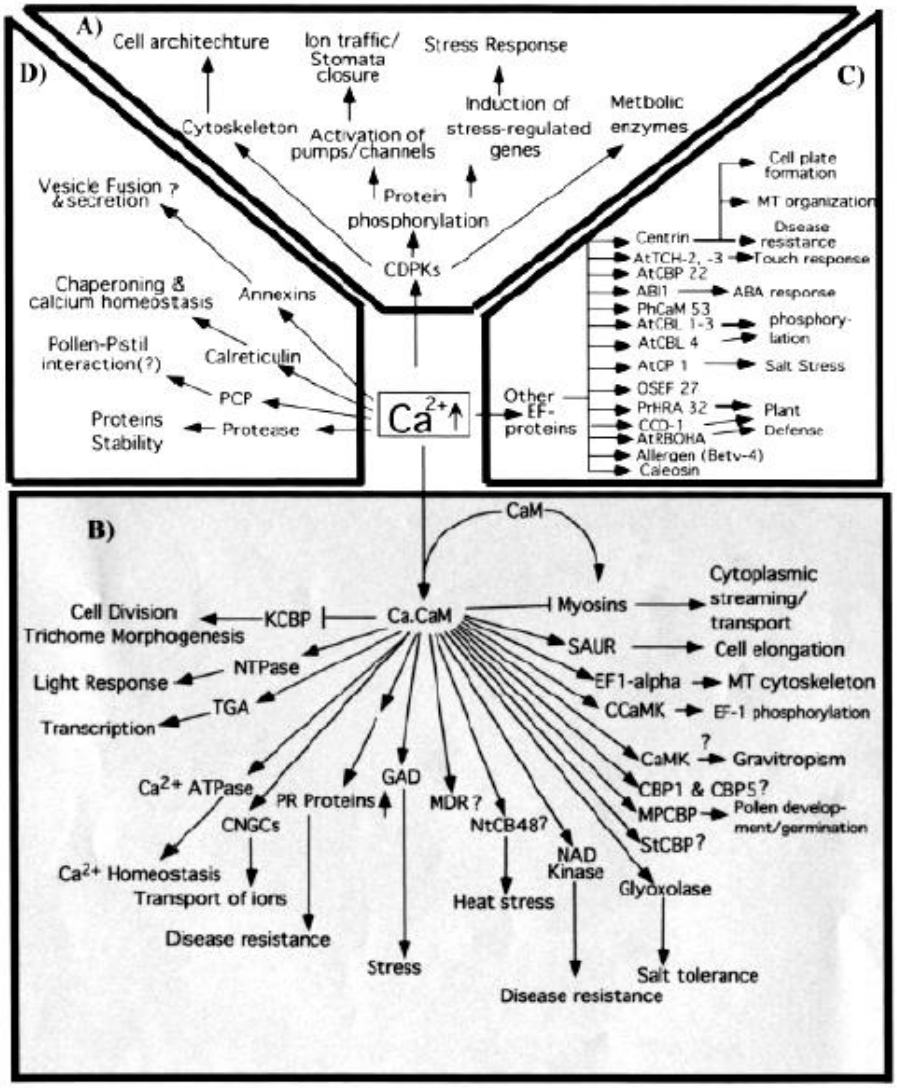

Figure 1.2 Ca^{2+} sensing proteins and their functions in plants. Four major groups of Ca^{2+} sensors (indicated in four boxes) have been described in plants: (A) Ca^{2+}-dependent protein kinase (CDPK or CPK), (B) Calmodulin (CaM), (C) other EF-hand motif containing Ca^{2+}-binding proteins and Calcineurin B-like (CBL) protein, (D) Ca^{2+}-binding proteins without EF-hand motifs (Reddy 2001).

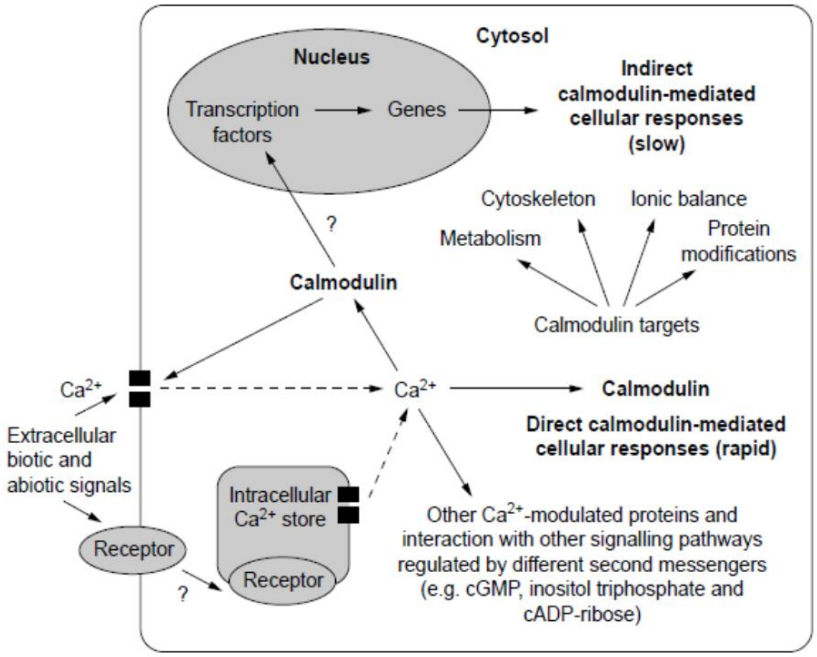

Figure 1.3 The Ca^{2+}-bound-calmodulin-mediated signal transduction in plants. Broken arrows denote Ca^{2+} fluxes from extracellular or intracellular stores, and question marks signify unknown signal transduction intermediates (Snedden and Fromm 1998).

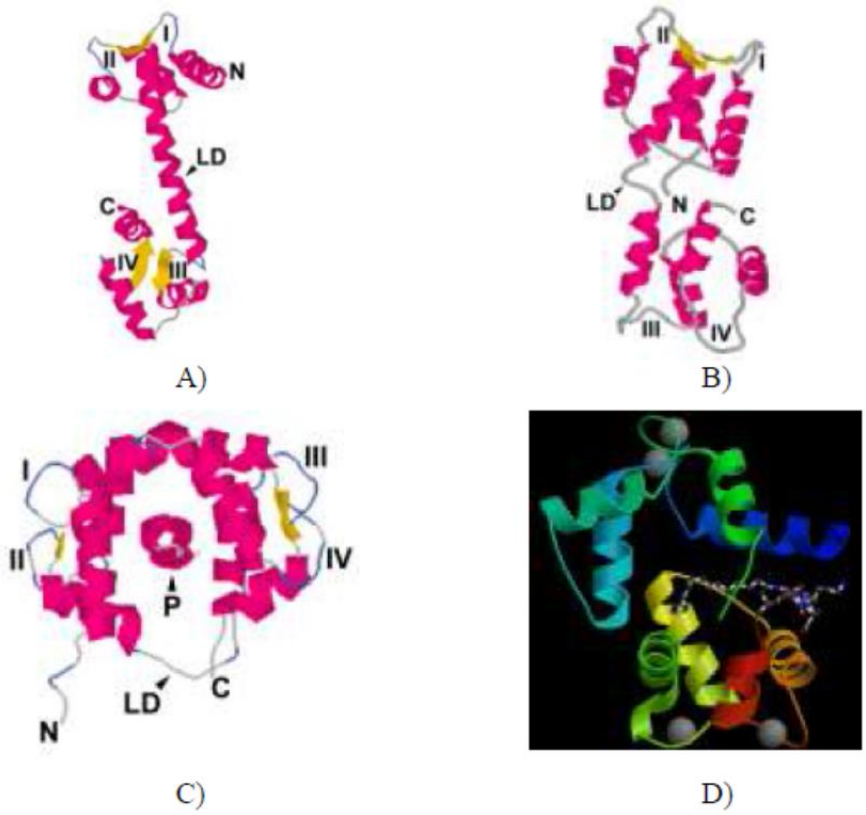

Figure 1.4 Ribbon presentations of calmodulin. (A) Ca^{2+}/CaM determined by X-ray crystallography, (B) globular domain of CaM (apo-CaM) determined by NMR spectroscopy, (C) and (D) Ca^{2+}/CaM-target peptide interaction; Peptide binding causes disruption of the flexible tether, bringing the globular domains closer to form a channel around the peptide. The majority of contacts between Ca^{2+}/CaM and target peptide are nonspecific van der Waals bonds made by residues in the hydrophobic surfaces. For (A) to (C), I-IV, Ca^{2+}-binding loops in the EF-hands; N, amino-termini of the CaM; C, carboxy-termini of the CaM; LD, central linker domain and P, target peptide. The α-helix, loop and β-sheet are colored in red, blue and yellow, respectively (Zielinski 1998).

In the Ca^{2+}-free state, CaM adopts a closed conformation. Ca^{2+} binding triggers a conformational change, and the protein adopts an open conformation with nearly perpendicular interhelical angles between the globular domains. This open conformation exposes a hydrophobic surface within each globular domain and permits the binding of protein targets (Babu et al. 1988; Kuboniwa et al. 1995; Zhang et al. 1995). In plants, CaM regulates a variety of targets including kinases, metabolic proteins, cytoskeletal proteins, ion channels and pumps, and transcription factors (Bouche et al. 2005). The Arabidopsis genome contains seven CaM genes encoding four isoforms that differ by only one to four amino acids. In addition, Arabidopsis contains 50 genes encoding CaM-like (CMLs) proteins with more divergent sequences and sometimes extra-domains that confer additional properties (McCormack and Braam 2003). Those proteins share at least 16% amino acid identity with CaM and have 2-6 identifiable EF-hand motifs. In rice, *Oryza sativa* L., five CaM and 32 CML genes have been classified (Boonburapong and Buaboocha 2007). A summary of their characteristics is shown in Table 1.1. They were named according to their percentages of amino acid identity with OsCaM1, which were calculated by dividing the number of identical residues by the total number of residues that had been aligned to emphasize the identical amino acids. These proteins are small proteins consisting of 145 to 250 amino acid residues and sharing amino acid identity between 30.2% to 84.6% with OsCaM1. When the full-length amino acid sequences of OsCaM and OsCML proteins were subjected to phylogenetic analysis using the neighbor-joining method and bootstrap analysis performed with ClustalX, a consensus tree, which is depicted in Figure 1.5, was generated. This analysis led to the separation of these proteins into six groups: 1-6. All the CML

Table 1.1 Characteristics of *OsCam* and *OsCML* genes and the encoded proteins.

(Boonburapong and Buaboocha 2007)

Name	Locus[1]	Chr[2]	cDNA length[3]	Amino Acids[4]	EF hands[5]	% of Met[6]	Identity to OsCaM1(%)[7]	Cys 27[8]	Lys 116[9]	Prenylation[10]	Myristoylation[11]	References
OsCam1-1	LOC_Os03g20370	3	450	149	4	6.0	100.0	+	+			[10]
OsCam1-2	LOC_Os07g48780	7	450	149	4	6.0	100.0	+	+			
OsCam1-3	LOC_Os01g16240	1	450	149	4	6.0	100.0	+	+			
OsCam2	LOC_Os05g41210	5	450	149	4	6.0	98.7	+	+			[10]
OsCam3	LOC_Os01g17190	1	450	149	4	6.0	98.7	+	+			
OsCML1	LOC_Os01g59530	1	564	187	4	4.3	84.6			+		[8, 9, 10]
OsCML2	LOC_Os11g03980	11	552	183	4	4.9	70.3			+		
OsCML3	LOC_Os12g03816	12	552	183	4	4.9	68.9			+		
OsCML4	LOC_Os03g53200	3	465	154	4	6.5	68.9	+	+			
OsCML5	LOC_Os12g41110	12	501	166	4	4.8	62.2	+	+			
OsCML6	LOC_Os11g37550	11	513	170	4	6.5	53.9	+				
OsCML7	LOC_Os08g02420	8	447	148	2	2.8	47.7		+			
OsCML8	LOC_Os10g25010	10	576	191	4	5.2	47.0					
OsCML9	LOC_Os05g41200	5	468	155	1	3.2	46.1					
OsCML10	LOC_Os01g72100	1	558	185	4	4.3	45.6		+			
OsCML11	LOC_Os01g32120	1	636	211	4	1.4	44.1					
OsCML12	LOC_Os01g41990	1	750	249	4	2.8	43.9					
OsCML13	LOC_Os07g42660	7	510	169	4	5.3	43.6					
OsCML14	LOC_Os05g50180	5	522	173	4	4.6	43.3					
OsCML15	LOC_Os05g31620	5	606	201	4	4.0	40.7					
OsCML16	LOC_Os01g04330	1	546	181	4	3.9	40.5					
OsCML17	LOC_Os02g39380	2	495	164	4	4.9	37.7		+			
OsCML18	LOC_Os05g13580	5	477	158	4	5.7	37.7		+			
OsCML19	LOC_Os01g72550	1	441	146	3	7.5	37.2					
OsCML20	LOC_Os02g50060	2	525	174	4	4.0	35.3				+	
OsCML21	LOC_Os05g24780	5	594	197	3	4.6	35.3					
OsCML22	LOC_Os04g41540	4	753	250	4	3.6	35.2					
OsCML23	LOC_Os01g72540	1	456	151	3	7.9	35.1					
OsCML24	LOC_Os07g48340	7	594	197	3	3.0	33.9					
OsCML25	LOC_Os11g01390	11	450	149	3	6.7	33.6					
OsCML26	LOC_Os12g01400	12	450	149	3	6.7	33.6					
OsCML27	LOC_Os03g21380	3	573	190	3	3.2	33.3					
OsCML28	LOC_Os12g12730	12	519	172	4	4.8	33.1		+			
OsCML29	LOC_Os06g47640	6	513	170	3	4.1	33.1					
OsCML30	LOC_Os06g07560	6	711	236	4	2.1	32.8					
OsCML31	LOC_Os01g72530	1	456	151	3	5.3	31.6					
OsCML32	LOC_Os08g04890	8	591	196	3	2.6	30.2					

[1] The Institute of Genomics Research (TIGR) gene identifier number.
[2] Chromosome number in which the gene resides.
[3] Length of the coding region in base pairs.
[4] Number of amino acids of the deduced amino acid sequence.
[5] Number of EF hands based on the prediction by InterPro Scan.
[6] Percentage of methionine (M) residues in the deduced amino acid sequence.
[7] Number of identical residues divided by the total number of amino acids that have been aligned expressed in percentage.
[8] Presence of a cysteine equivalent to Cys26 of typical plant CaMs at residue 7(-Y) of the first EF-hand.
[9] Presence of a lysine equivalent to Lys115 of typical plant CaMs.
[10] Presence of a putative prenylation site.
[11] Presence of a putative myristoylation site.

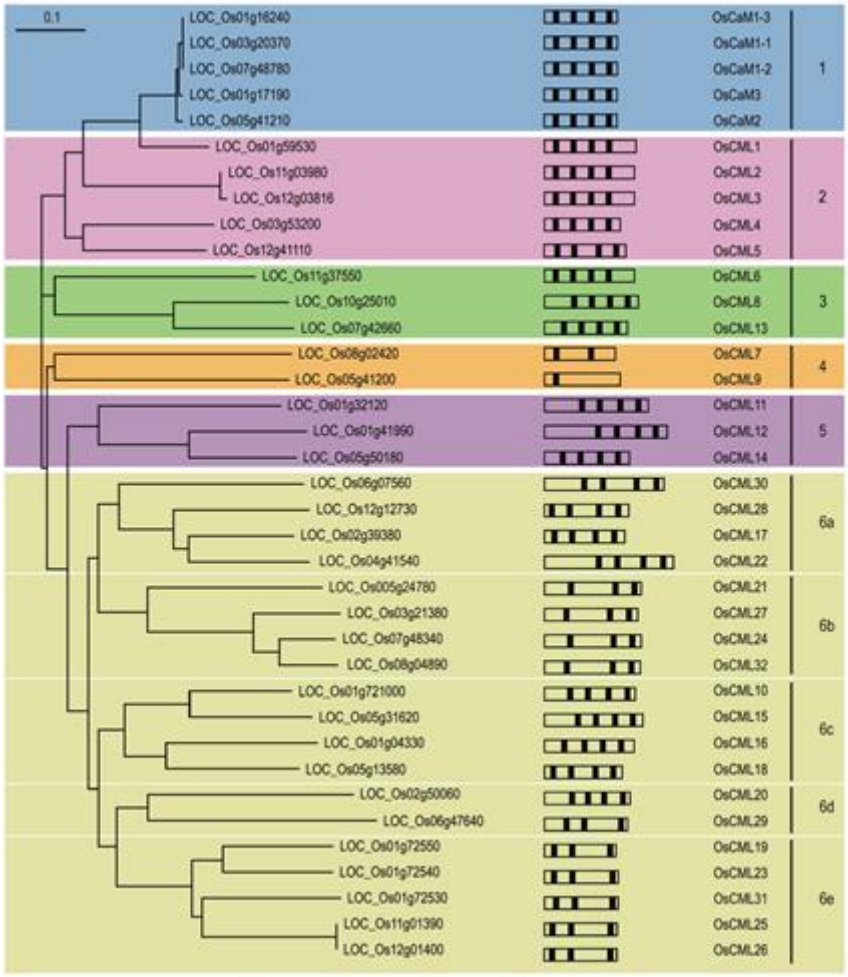

Figure 1.5 Neighbor-joining tree based on amino acid similarities among OsCaM and OsCML proteins. Tree construction using the neighbor-joining method and bootstrap analysis was performed with ClustalX. The TIGR gene identifier numbers are shown and the resulting groupings of CaM and CaM-like proteins designated as 1-6 are indicated on the right. Schematic diagrams of the OsCaM and OsCML open reading frames show their EF hand motif distribution (Boonburapong and Buaboocha 2007).

proteins in group 2 share more than 60% of amino acid sequence identity with OsCaM1. The CML proteins in groups 3, 4, and 5 have identities with OsCaM1 that average 48.2%, 46.9%, and 43.8%, respectively. By the bootstrapped phylogenetic tree based on amino acid sequence similarity of these proteins, group 6 CML proteins were separated into five subgroups: 6a-6e. These proteins share identities no more than 40.7% with OsCaM1 that average at 35.6% with the exception of OsCML10 (45.6%). All members of groups 6b and 6e contain three EF-hand motifs though with different configurations (Boonburapong and Buaboocha 2007).

Of these proteins, three OsCMLs contain an extended C-terminal basic domain and a CAAX (C is cysteine, A is aliphatic, and X is a variety of amino acids) motif, a putative prenylation site (CVIL in OsCML1 and CTIL in OsCML2 and 3). OsCML1, also known as OsCaM61 was identified as a novel CaM-like protein (Xiao et al. 1999). The CML protein was reported to be membrane-associated when it is prenylated and localized in the nucleus when it is unprenylated (Dong et al. 2002). A similar protein called CaM53 previously found in the petunia also contains an extended C-terminal basic domain and a CAAX motif, which are required for efficient prenylation in response to specific changes in carbon metabolism (Rodríguez-Concepción et al. 1999). Similar subcellular localization of CaM53 depending on its prenylation state was reported. To locate another possible modification, all proteins were analyzed by the computer program, Myristoylator (Bologna et al. 2004). As a result, OsCML20 was predicted to contain a potential myristoylation sequence. No other potential myristoylated glycines either terminal or internal were found among the rest of the OsCML proteins. In addition, to determine the possible localization of the OsCML proteins, their sequences were analyzed by

targetP (Emanuelsson et al. 2000). OsCML30 was predicted to contain an endoplasmic reticulum signal sequence, and OsCML21 was predicted to be an organellar protein. For OsCaMs and other OsCMLs, no targeting sequence was present, thus, they are probably cytosolic or nuclear proteins. The past two decades, many aspects of CaMs and CMLs in plant have been studied including biochemical function and regulation, role in plant growth and development, and in the responses to environmental stress.

1.4 Biochemical function and regulation of CaMs and CMLs

Specificity of CaM-mediated responses results from different expression patterns, specific targets, calcium affinities, sub-cellular localization and methylation (Luan et al. 2002; McCormack and Braam 2003). CaM isoforms differ in their ability to regulate target proteins (Lee et al. 2000; Yoo et al. 2005), possibly due to different structural interactions of the targets with CaM (Yamniuk and Vogel 2005). A recent protein array study has identified 173 protein targets of seven CaMs/ CMLs in Arabidopsis. Among them, about 25% interact with all CaMs/CMLs tested, 50% with at least two of them, and 25% are specific to one CaM/CML (Popescu et al. 2007). CaMs sharing the same targets can compete for binding (Lee et al. 1999), indicating that target proteins are tightly regulated depending on the amount of each CaM isoform. Interestingly, a mutation converting three amino acids of rice OsCaM1 into those of OsCaM61, confers an ability to activate OsCBK almost as efficiently as OsCaM61 (Li et al. 2006). Thus, CaMs exhibit outstanding target specificities despite high levels of sequence identity. Different Ca^{2+} sensitivities were observed depending on CaM and target proteins, adding another layer of regulation (Lee et al. 2000; Luoni

et al. 2006). Interestingly, a recent study has revealed a novel mechanism of CaM action through a direct interaction of a CaM isoform with DNA. AtCaM7, an Arabidopsis CaM isoform, was found to specifically recognize the Z-box and G- box motifs, two similar regulatory elements in light-responsive promoters, whereas AtCaM3, an isoform differing from AtCaM7 by only one amino acid, is unable to bind these promoters (Kushwaha et al. 2008). In soybean, there are five CaM isoforms (SCaM1 to -5). SCaM1, -2 and -3 that are highly conserved compared to other plant CaM isoforms including Arabidopsis CaM isoforms whereas SCaM4 and -5 are divergent and show differences in 32 amino acids with the conserved group (Lee et al. 1995). Soybean isoforms show differences in their relative abundance *in vivo*. The conserved isoforms are relatively abundant in their expression compared to the divergent forms. Surprisingly, these divergent CaM isoforms are specifically induced by fungal elicitors or pathogen (Heo *et al.*, 1999). These results provide evidence for the differential regulation of CaM isoforms in plants. Differential regulation of enzymes by soybean divergent and conserved CaM isoforms has also been reported (Lee et al. 2000). All SCaM isoforms activate phosphodiesterase (PDE) but differ in their activation of NAD kinase, calcineurin and nitricoxide synthase indicating Ca^{2+}/CaM specificity between CaM isoforms and target proteins (Lee et al. 1997). Although SCaM isoforms show similar patterns in protein blot overlay assays, they differ in their relative affinity in interacting with CaM binding proteins (Lee et al. 1999).

1.5 Roles of CaMs and CMLs in plant growth and development

The roles of CaM isoforms and CMLs in various developmental processes

including morphogenesis and reproduction have been reported. AtCaM7 is involved in light-mediated gene expression, and AtCaM7 overexpression in transgenic plants is found to promote photomorphogenic growth (Kushwaha et al. 2008). AtCaM2, another CaM isoform, appears to play a role in pollen germination. A loss-of-function mutation in the AtCaM2 gene causes a significant reduction in pollen germination (Landoni *et al*., 2010). Interestingly, several CaM-binding proteins including ACA9 (an autoinhibited Ca^{2+}-ATPase), NPG1 (No Pollen Germination) and CNGC18 (a cyclic nucleotide-gated channel) are known to play key roles in pollen germination and pollen tube growth in Arabidopsis (Frietsch et al. 2007; Golovkin and Reddy 2003; Schiott et al. 2004). Moreover, mutations in CML genes were also found to cause developmental defects. For example, a knockout mutant in the AtCML42 gene displays abnormal morphology of trichomes (Dobney et al. 2009).

1.6 CaMs and CMLs functions in the responses to environmental stress

There is considerable evidence to indicate that *Cam* genes are differentially expressed in response to different stimuli indicating that different CaM isoforms are involved in mediating a specific signal (Zielinski 1998). Three of the six Arabidopsis *Cam* genes (*Cam*1, -2 and -3) are inducible by touch stimulation (Zielinski 1998).Three CML proteins (AtCML37, AtCML38 and AtCML39) were shown to play important roles as sensors in Ca^{2+}-mediated stress response pathways (Vanderbeld and Snedden 2007). In addition, CML43 and CML18 from Arabidopsis have been implicated in pathogen response (Chiasson et al. 2005) and salinity tolerance (Yamaguchi et al. 2005), respectively. AtCML24 seems to be involved in pathogen-induced innate immune responses (Ma et al. 2008). Moreover, AtCML24

has a function in response to ABA, day length and ion stress (Delk et al. 2005). This is similar to AtCML9, which is induced by abiotic stress and ABA in young Arabidopsis seedlings; using *cml9* knock-out mutants it was demonstrated that AtCML9 has a function in modulating responses to salt stress and ABA (Magnan et al. 2008). In potato, only one of the eight CaM isoforms (PCaM1) was inducible by touch (Takezawa et al. 1995). In rice, *Oryza sativa* L., *Cam* and *CML* genes in rice exhibited differential expression patterns in tissues/organs. Under osmotic stress and salt stress, expression of *OsCam1-1*, *OsCML4*, *5*, *8*, and *11* was induced with different kinetics and magnitude. *OsCML4* and *8* mRNA levels significantly increased by 3 h after treatment and remained elevated for at least 24 h while expression of *OsCam1-1*, *OsCML5* and *11* was up-regulated as early as 1–3 h before rapidly returning to normal levels. These results indicated that *OsCam* and *OsCML* gene family members likely play differential roles as signal transducers in regulating various developmental processes and represent important nodes in the signal transduction and transcriptional regulation networks in abiotic stresss responses mediated by the complex Ca^{2+} signals in plants, which are rich in both spatial and temporal information (Chinpongpanich et al. 2012). Recently, transgenic plants over-expressing *OsCML4* showed improved growth performance and higher survival rates than the wild type (WT) under drought conditions (Yin et al. 2015).

1.7 Calmodulin-binding proteins

CaM has no catalytic activity of its own. Its regulatory activities are manifested by its ability to modulate a certain set of enzymes. Thus, it is crucial to isolate and to characterize CaM-binding proteins to understand the role of the

Ca^{2+}/CaM-mediated network. Identification of novel CaM binding proteins has also been accelerated as a result of the Arabidopsis genome project (Yang and Poovaiah 2003)). Table 1.2 shows the list of some plant CaM-binding proteins, which are involved in various functions. Interestingly, plants have a greater number and more-diversified CaM-binding proteins than animals do. Many CaM-binding proteins are plant specific, suggesting that Ca^{2+}/CaM-mediated signal networks are distinctly different in plants as compared with those in animals (Yang and Poovaiah 2003). One of the powerful molecular approaches used for screening protein–protein interaction to investigate the target of CaM in plant is cDNA expression library screening using labeled recombinant CaM as a probe. As mentioned, there have been many CaM-binding proteins identified in plants (Snedden and Fromm 1998) but still no reports of CML-binding proteins in rice. Thus, according to Phean-o-pas research (unpublished) the target proteins of OsCML3 and OsCML3m (OsCML3 lacking the C-terminal extension, CTE) were identified using cDNA expression libraries prepared from the leaf of *Oryza sativa* L. 'Khoa Dok Ma Li 105' and labeled rOsCML3 and rOsCML3m as probes. The results revealed that two of the ten putative novel OsCML3m-binding proteins were OsPEBP (Phosphatidylethanolamine-binding protein) and OsHMGB1 (High-mobility group box 1 protein). Note, however, that when the full-length rOsCML3 was used as the probe, only two target proteins were identified and these did not include OsPEBP and OsHMGB1.

1.8 Phosphatidylethanolamine-binding protein (PEBP)

The phosphatidylethanolamine-binding protein (PEBP) genes are present in all major phylogenetic divisions and have been shown to play several key roles in the

Table 1.2 CaM-binding proteins previously identified in plants (Taken from (Snedden and Fromm 1998))

Functional group	Protein	Features	References
Metabolism	Glutamate decarboxylase (GAD)	Catalyzes conversion of L-glutamate to γ-aminobutyric acid) activated by Ca^{2+}-bound calmodulin (Ca^{2+}–calmodulin) and many stresses; forms a multisubunit complex, tightly associated with calmodulin.	Baum *et al*., 1996; Snedden *et al*., 1996; Bown & Shelp, 1997
	NAD kinase	Catalyzes conversion of NAD to NADP; activated by Ca^{2+}-bound calmodulin; might be involved in oxidative burst.	Harding, Oh and Roberts, 1997
	Apyrase (Nucleoside triphosphate)	Subcellular localization is light regulated; ectopic expression affects metabolism and growth in *Arabidopsis.*	Hsieh *et al*., 1996; Roux, pers. Commun
Phosphorylation	Ca^{2+}-binding, Ca^{2+}-calmodulin-dependent kinase(CCaMK)	Has a visinin-like (three 'EF hands') and a separate Ca^{2+}–calmodulin-binding domain, which is (CCaMK) autoinhibitory.	Ramachandiran *et al*.,1997
	Kinase homologue (MCK1)	Homologous to known Ca^{2+}–calmodulin-regulated kinases 24 from other eukaryotes; isolated from maize roots; might be involved in gravitropism.	Lu, Hidaka and Feldman, 1996
Ion transport	Ca^{2+}-ATPases (BCA1 and ACA2)	Endomembrane Ca^{2+} pumps; calmodulin-binding domain autoinhibitory; localized near the N-terminus; endomembrane localization is unique to plants	Harper *et al*, 1998; Malmstrom, Askerlund and Palmgren, 1997
	Transporter-like (HvCBT1)	Probable ion transporter with putative cyclic nucleotide binding domain.	Schuurink *et al*., 1998
Cytoskeleton function	Kinesin-like (KCBP)	Motor domain protein; calmodulin modulates association with tubulin; highly expressed during mitosis; might be involved in acentriolar spindle and phragmoplast formation; involved in trichome development.	Oppenheimer *et al*., 1997; Narasimhulu, Kao and Reddy, 1997
	Elongation factor-1a (EF-1a)	Calmodulin modulates interaction of EF-1a with microtubules *in vitro*.	Durso and Cyr, 1994
	Myosin (MYA1)	Similar to class V myosins; contains IQ repeats with putative calmodulin-binding characteristics.	Kinkema and Schiefelbein, 1994
DNA binding	Basic leucine zipper protein (TGA3)	Transcription factor; interacts *in vitro* with a DNA element in the promoter of the *Cam-3 Arabidopsis* calmodulin gene.	Gawienowski *et al*., 1996

functioning of both animal and plant systems (Banfield and Brady 2000). In mammals, members of the PEBP gene family have many roles, including acting as inhibitors of the MAP kinase signalling mechanism regulating cell differentiation (Zhu et al. 2005).

In *Arabidopsis thaliana* the PEBP gene family is made up of 6 closely related genes; FT (FLOWERING LOCUS T), TFL1 (TERMINAL FLOWER1), ATC (ARABIDOPSIS CENTRORADIALIS HOMOLOGUE), TSF (TWIN SISTER OF FT), BFT (BROTHER OF FT AND TFL1), and MFT (MOTHER OF FT AND TFL1). The roles of the PEBP genes FT and TFL1 are well studied in *A. thaliana*. FT promotes flowering, acting as a signal transducer between the leaf and the shoot meristem, and TFL1 delays it by suppressing expression of FT. Functions of AtFT and AtTFL are found to be conserved in *O. sativa,* indicating conservation between monocots and dicots (Ishikawa et al. 2005; Kojima et al. 2002; Zhang et al. 2005).

In barley (*Hordeum vulgare*), five PEBP genes were analyzed to clarify their functional roles in flowering using transgenic, expression, and quantitative trait locus analyses. Overexpression of *HvFT1*, *HvFT2*, and *HvFT3* in rice resulted in early heading, indicating that these *FT*-like genes can act as promoters of the floral transition. *HvFT1* transgenic plants showed the most robust flowering initiation. In barley, *HvFT1* was expressed at the time of shoot meristem phase transition. These results suggest that *HvFT1* is the key gene responsible for flowering in the barley *FT*-like gene family (Kikuchi et al. 2009). To date the study of PEBP in rice is limited; therefore, the putative OsCML3m-binding protein, OsPEBP identified previously, may represent a novel function of OsCML3 involving in flowering.

1.9 High mobility group protein

High mobility group (HMG) proteins are among the most abundant and ubiquitous chromosomal nonhistone proteins common to eukaryotes (Wu et al. 2003). Because of their characteristic primary structures, mammalian HMG proteins have been subdivided into three distinct families (Bustin 1999; Bustin and Reeves 1996; Thomas and Travers 2001):

• HMGA proteins, containing A/T-hook DNA-binding motifs

• HMGB proteins, containing HMG-box domain(s)

• HMGN proteins, containing a nucleosome binding domain

Overall structure of the three HMG protein families is shown in figure 1.6. In plants, proteins belonging to the HMGA and HMGB families have been identified and biochemically characterized over the past years (Pedersen and Grasser 2010), but there is no evidence for the existence of HMGN proteins, which so far have been found exclusively in vertebrates. Plant proteins belonging to the HMGA family are characterized by the presence of four AT hook DNA-binding motifs (Figure 1.6), which mediate the interaction with A/T-rich DNA stretches. In contrast to HMGA proteins of other sources, the plant proteins have an N-terminal domain with sequence similarity to the globular domain of linker histone H1. In collaboration with transcription factors, the HMGA proteins contribute to the proper regulation of target genes (Grasser 2003; Klosterman and Hadwiger 2002).

HMGB proteins have been identified from various higher plants and they have in common an overall structure that is distinct from that of HMGB proteins of other organisms. Thus, in plant HMGB proteins (~13–27 kDa) the central HMG-box DNA binding domain is flanked by a basic N terminal domain and a highly acidic C-

terminal domain (Figure 1.6). The HMG-box domain of ~75 amino acid residues has a conserved L-shaped fold with an angle of ~80° between the arms, mainly consisting of three α-helices (Figure 1.7). α-helix 1 and 2 form the short arm of the L-shape, while helix 3 and the N terminal extended strand form the long arm of the L-shaped structure (Thomas and Travers 2001; Travers 2000). The basic N-terminal and the acidic C-terminal domains are variable in size and amino acid sequence, accounting for the differences in molecular mass of the members of the plant HMGB protein family (Grasser 2003).

The HMG-box domain mediates the non-sequence-specific interaction of HMGB proteins with linear double-stranded DNA. Amino acid residues of the concave face of the L shaped HMG-box domain primarily contact the minor groove of the DNA. A hydrophobic wedge is inserted deep into the minor groove, and two strategically positioned residues partially intercalate between base pairs introducing a kink, which significantly contributes to the overall bend that HMGB proteins induce upon binding to linear DNA (Thomas and Travers 2001; Travers 2000). The potential primary intercalating residue of the plant HMGB proteins is a well-conserved phenylalanine residue, while the secondary intercalating residue is less well conserved, but in many cases a valine residue is found at this position (Grasser 2003). The intercalating residues of HMG-box domains play a critical role in DNA binding and modulating DNA structure by bending and supercoiling (He et al. 2000; Klass et al. 2003; Stros and Muselikova 2000). A distinguishing feature of HMGB proteins is the specific recognition of various DNA structures including four-way junctions,

DNA minicircles and cis-platinated DNA. Another important property of the HMGB proteins in their function as architectural factors is their ability upon DNA binding

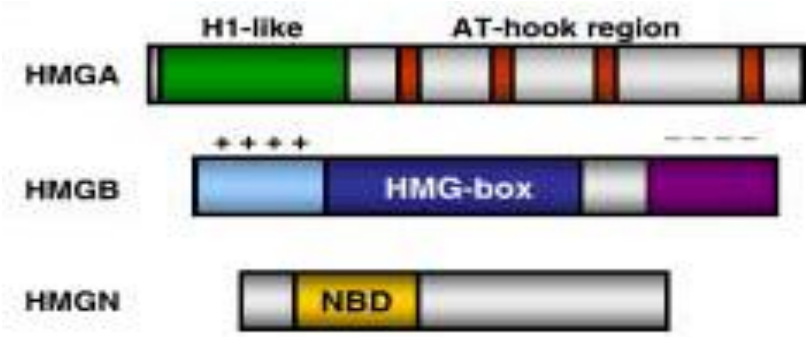

Figure 1.6 Overall structure of the three HMG protein families and structure of the HMG-box DNA-binding domain. The three HMG protein families are structurally unrelated. The plant HMGA proteins (~22 kDa) consist of a C terminal domain containing four AT-hook DNA-binding motifs (indicated by red bars) and an N-terminal domain with sequence similarity to the globular domain of linker histones (indicated by a green box). This H1-like domain is a feature specific for plant HMGA proteins (Grasser, 2003; Klosterman and Hadwiger, 2002). In plant HMGB proteins (13–27 kDa), the central HMG-box DNA-binding domain of ~75 amino acid residues is flanked by basic N-terminal and acidic C-terminal domains that are flexible in length and sequence. The acidic tail is linked to the HMG-box domain by a short linker region that is also rather variable in sequence. The HMG-box domain is indicated by a dark blue box and the basic N-terminal domain by a light blue box, while the C-terminal acidic domain is indicated by a violet box. All the HMGB proteins that have been identified from plants contain a single HMG-box domain, while HMGB proteins of other sources contain one or two HMG-box domains. For comparison, the overall structure of vertebrate HMGN proteins (~10 kDa) is shown, although this class of HMG protein apparently does not exist in plants (and insects, yeast etc.). The nucleosome binding domain (NBD) characteristic for HMGN proteins is indicated by a yellow box. Some HMGN proteins contain an acidic C-terminal region (Taken from (Grasser et al. 2007)).

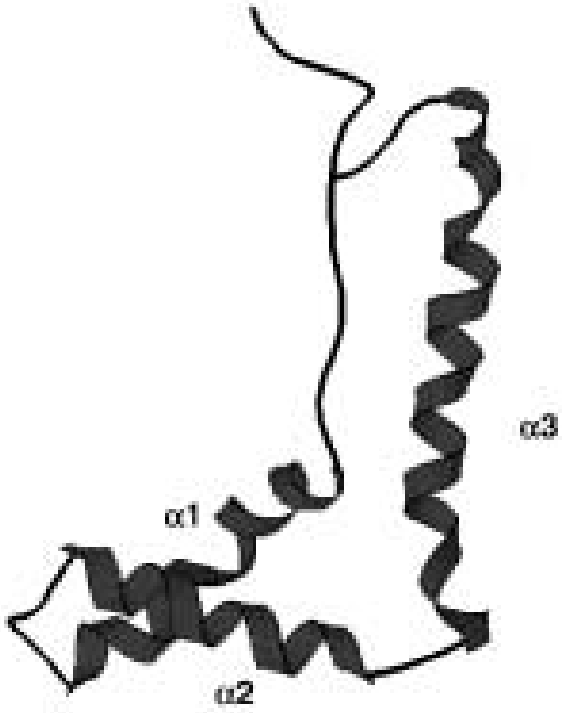

Figure 1.7 Structure of the second HMG-box (B domain) of rat HMGB1. The structure (Protein Data Bank, PDB: 1HME) has been solved by NMR (Weir et al. 1993) and is displayed using KiNG Viewer 1.39 (http://www.rcsb.org/pdb/home/home.do). Comparison of the structures of various HMG-box domains has revealed that the L-shaped fold of the HMG-box domain is well conserved (Thomas and Travers 2001; Travers 2000). The three α- helices mainly comprising the domain are indicated (α1–α3) (Taken from (Grasser et al. 2007)).

to bend linear DNA by over 90° (Agresti and Bianchi 2003; Grasser 2003; Thomas and Travers 2001; Travers 2000). Structural studies of protein/DNA-complexes have revealed a number of details regarding the DNA-interaction of non-sequence-specific HMG-box domains (Masse et al. 2002; Murphy et al. 1999; Ohndorf et al. 1999). In various studies it has been demonstrated that plant HMGB proteins bind certain DNA structures such as DNA-minicircles, four-way junctions, and supercoiled DNA with higher affinity than the corresponding linear DNA (Grasser et al. 2004; Grasser et al. 1994; Ritt et al. 1998; Webster et al. 2001; Wu et al. 2003; Zhang et al. 2003).. Previous report showed that rice HMGB1 could bind synthetic four-way junction (4H) DNA and DNA minicircles efficiently. Conformational changes were detected by circular dichroism analysis with 4H DNA bound to various concentrations of HMGB1 (Wu et al. 2003). From our previous findings, OsHMGB1 was identified as a target protein of OsCML3m. It is interesting that why OsHMGB1 was not identified using OsCML3 as a probe; therefore, the protein interaction of OsHMGB1 with OsCML3 or OsCML3m should be confirmed by other methods.

Although the studies of OsCaMs and OsCMLs in Arabidopsis functions including their target proteins have been widely performed (Snedden and Fromm 1998), there is no report of OsCML-binding proteins in rice. Recently, our research group focuses on OsCaM and OsCML biophysical properties; however, there is no detailed information on OsCML functions. Here, we examined the difference in biophysical characteristics by assessing Ca^{2+} and target peptide binding ability of the truncated version of OsCML3 lacking the CTE (OsCML3m) and its conformational changes upon Ca^{2+}-binding through measurements by circular dichroism (CD) and fluorescence spectroscopy using 8-anilino-1-naphthalene-sulfonic acid (ANS) to

investigate the effect of C-terminal extension (CTE) on the biophysical characteristics by comparing with those of OsCML3 previously characterized. The subcellular localization of OsCML3 and OsCML3m were performed to investigate the effect of the CTE. As mentioned, OsPEBP and OsHMGB1 were the putative OsCML3m-binding proteins identified earlier; consequently, we investigated their protein interactions by yeast-two hybrid and bimolecular fluorescence complementation (BiFC) assays. Moreover, electrophoretic mobility shift assay (EMSA) was used to examine the DNA-binding ability of OsHMGB1 in the presence of OsCML3 or OsCML3m. In addition, to investigate the functions of OsCML3 in rice, the transcript expression level of *OsCML3* under various stresses such as salinity, cold, auxin and cytokinin applications was determined. Last but not least, the transgenic *Arabidopsis* lines overexpressing *OsCML3* or *OsCML3m* were constructed to examine its physiological functions under cold stress.

CHAPTER II

MATERIALS AND METHODS

2.1 Materials

2.1.1 Instruments

Autoclave: Labo Autoclave MLS-3020 (Sanyo Electric Co., Ltd., Japan)

Automatic micropipette: pipetman P2, P20, P100, P1000 (Gilson Medical Electronics S.A., France)

Balance: Sartorius CP423s (Scientific Promotion, USA)

Centrifuge 5417C (Eppendorf, Germany)

CFX96 Real-Time PCR Detection System (BIO-RAD Laboratories, USA)

Dry bath incubator (Major Science, USA)

-20 °C Freezer (Sharp, Japan)

-80 °C Freezer (Forma, USA)

Confocal Microscopy (Leica, Singapore)

Confocal Microscopy (Olympus, Thailand)

Gel Doc™ (Syngene, England)

Gel mate 2000 (Toyobo, Japan)

Growth chamber PGC-432 (Human Lab, Korea)

Incubator: BM-600 (Memmert Gambh, Germany)

Incubator shaker: Innova™ 4000 (New Brunswick Scientific, UK)

Laminar flow: HS-124 (International Scientific Supply Co., Ltd., USA)

Luminescence Spectrometer LS55 (PerkinElmer, USA)

Magnetic stirrer: Fisherbrand (Fisher Scientific, USA)

Magnetic stirrer and heater: Cerastir (Clifton, USA)

Magnetic stirrer: Fisherbrand (Fisher Scientific, USA)

Microcentrifuge: PMC-880 (Tomy Kogyo, Japan)

Microwave Oven (Panasonic, Japan)

Orbital Shaker: LD-40 (Lacinco, Taiwan)

PCR workstation Model P-036 (Scientific Co., USA)

pH meter: pH900 (Precisa, Germany)

Power supply: Power PAC 1000 (Bio-RAD Laboratories, USA)

Refrigerated centrifuge 5804R (Eppendorf, Germany)

Sonicator: Vibra cell^{Tm} (Sonic, USA)

Sorvall Legend XTR centrifuge (Thermo Scientific, Germany)

Spectrophotometer: DU$^{®}$640 (Beckman Coulter, USA)

Spectropolarimeter J-715 (Jasco, Japan)

Thermo cycler: Mastercycler gradient (Eppendorf, Germany)

UV transilluminator: 2001 Microvue (LKB Bromma, Sweden)

Vortex mixer: Model K 550-GE (Scientific Inc, USA)

Water bath: Isotemp210 (Fisher Scientific, USA)

2.1.2 Materials

0.6-ml and 1.5-ml microcentrifuge tubes (ExtraGene, USA)

0.6-ml and 1.5-ml microcentrifuge tubes (Axygen, USA)

10, 100 and 1000 µl pipette tips (Axygen Hayward, USA)

Centrifugal Filters (10,000 Daltons molecular weight cut-off) (Merck, Germany)

Filter paper: Whatman No.1 (Whatman International, UK)

Filter tips 10, 20, 100, 200, 1000 µl (Extragene, USA)

Microcentrifuge tube 0.6 and 1.5 ml (Axygen, USA)

Millipore membrane filter, size of 0.22µm (Merck, Germany)

Nipro disposable syringe (Nissho, Japan)

PCR: Mastercycler gradient (Eppendorf, Germany)

PCR Thin wall microcentrifuge tube 0.2 ml (Eppendorf, Germany)

Plastic cuvette (Eppendorf, Germany)

Quartz cuvette: Hellma 105.201-QS (Sigma-Aldrich, USA)

2.1.3 Chemicals and reagents

Absolute ethanol (Carlo Erba, Italy)

Acetic acid glacial (BDH, UAE)

Acrylamide (Merck, Germany)

Agar (Merck, Germany)

Agarose (Gene Pure, USA)

Ammoniun sulfate (Sigma, USA)

Ammonium persulfate (Sigma, USA)

8-Anilino-1-naphthalenesulfonic acid (ANS, Sigma, USA)

Bacto agar (DIFCO, USA)

Bacto tryptone (Scharlau, Spain)

Bacto yeast extract (Scharlau, Spain)

Boric acid (Merck, Germany)

Bovine serum albumin (Sigma, USA)

5-Bromo-4-chloro-3-indole-beta-D-galactopyranoside; X-gal (Sigma, USA)

Bromophenol blue (Merck, Germany)

Calcium chloride dihydrate (Carlo Erba, Italy)

Casein hydrolysate (Hi media, India)

Chloroform (Merck, Germany)

Coomassie brilliant blue R-250 (Bio Basic Inc., Canada)

100 mM dATP, dCTP, dGTP, and dTTP (NEB, USA)

Dithiothreitol (Sigma, USA)

Ethidium bromide (Sigma, USA)

Ethylene diamine tetraacetic acid (EDTA) (Carlo Erba, Italy)

Ethylene diamine tetraacetic acid (EDTA) disodium salt dehydrate (Carlo Erba, Italy)

Ethylene glycol tetraacetic acid (EGTA) (Carlo Erba, Italy)

Glacial acetic acid (Labscan, Ireland)

Glycerol (BDH, UAE)

Hydrochloric acid (Carlo Erba, Italy)

Imidazole (USB, USA)

Isoamylalcohol (Merck, Germany)

Isopropyl alcohol (Carlo Erba, Italy)

Iso-1-thio-β-D-thiogalactopyranoside: IPTG (Bio Basic Inc., Canada)

Magnesium sulfate (Sigma, USA)

Methanol (Carlo Erba, Italy)

Methylenebisacrylamide (Phamacia biotech, Sweden)

Methylene blue (Carlo Erba Reagenti, Italy)

Ni-Sepharose resins (GE Healthcare, USA)

Oligo dT (Promega, USA)

Phenol Solution (Sigma, USA)

Phenyl-Sepharose resin (GE Healthcare, USA)

Polyvinyl pyrrolidone (Sigma, USA)

Potassium acetate (Merck, Germany)

Potassium hydroxide (Scharlau, Spain)

Potassium nitrate (BDH, UAE)

Sodium acetate (Carlo Erba, Italy)

Sodium chloride (Carlo Erba, Italy)

Sodium dodecyl sulfate (Sigma, USA)

Sodium dihydrogen orthophosphate (Carlo Erba Reagenti, Italy)

di-Sodium dihydrogen orthophosphate anhydrous (Carlo Erba Reagenti, Italy)

Sodium hydroxide (BDH, UAE)

Triethanolamine (Sigma, USA)

TRI Reagent (Molecular Research Center, USA)

Tris-(hydroxylmethyl)-aminomethane or Tris base (USB, USA)

Tween 20 (BIO-RAD, USA)

Triton X-100 (Merck, Germany)

Xylene cyanol FF (Sigma, USA)

Yeast Extract Powder (Himedia, India)

2.1.4 Enzymes and Restriction enzymes

Dnase I (Fermentas, USA)

KOD-Plus-Neo DNA polymerase (TOYOBO, Japan)

Pfu DNA polymerase (Fermentas, USA)

Phusion® High-Fidelity DNA polymerase (New England Biolabs, USA)

Restriction endonucleases: *Bam*HI, *Hind* III, *Nco*I, *Nde* I, *Sal*I, *Xho* I (Biolabs, USA)

RNase inhibitor (Fermentas, USA)

T4 DNA ligase (Biolabs, USA)

Taq DNA Polymerase (Fermentus, USA)

Vent DNA Polymerase (Biolabs, USA)

2.1.5 Microorganisms

***Escherichia coli* strain XLl-Blue**

(F′:: Tn*10 proA*$^{+}$*B*$^{+}$*lacI*^{q} Δ*(lacZ)M15/recA1endA1 gyrA96 (Nal* ^{r}*) thi hsdR17 (*r_k $^{-}$ *m* $_k$ $^{+}$*) supE44 relA1 lac)*

***Escherichia coli strain* BL21 (DE3)**

F^{-} *dcm ompT hsdS*($r_B$$^{-}$ $m_B$$^{-}$) *gal* λ(DE3)

***Escherichia coli* strain Top 10**

F^{-} mcrA Δ(mrr-hsdRMS-mcrBC) φ80lacZΔM15 ΔlacX74 nupG recA1 araD139 Δ(ara-leu)7697 galE15 galK16 rpsL(StrR) endA1 λ^{-}

Yeast cells MaV203

MATα, *leu*2-3,112, *trp*1-901, *his*3Δ200, *ade*2-101, *gal*4Δ, *gal*80Δ, *SPAL*10*::URA*3, *GAL*1::*lacZ*, *HIS*3UAS GAL1*::HIS*3*@LYS*2, *can*1R, *cyh*2R

Yeast cells A109

MATa, trp1-901, leu2-3, 112, ura3-52, his3-200, gal4Δ, gal80Δ, LYS2 : : GAL1UASGAL1TATA-HIS3, GAL2UAS-GAL2TATA-ADE2, URA3 : : MEL1UAS-MEL1TATA-lacZ

2.1.6 Kits

Geneaid^{TM} Gel/PCR DNA Fragment Extraction kit (Geneaid, Taiwan)

Geneaid^{TM} Genomic DNA Mini Kit (Plant) (Geneaid, Taiwan)

Geneaid^{TM} High-Speed Plasmid Mini kit (Geneaid, Taiwan)

iScript cDNA Synthesis kit (BIO-RAD Laboratories., USA)

SsoFast EvaGreen Supermix (BIO-RAD Laboratories., USA)

Pierce BCA protein assay kit (Pierce, USA)

2.1.7 DNA and plasmids

100 bp DNA ladder (Fermentus, USA)

2-Log DNA Ladder (Biolabs, USA)

Lamda DNA (Promega, USA)

pCAMBIA1301 and pCAMBIA1302 (Cambia, Australia)

pDEST22 and pDEST32 (Invitrogen, USA)

pET-21a vector system (Promega, USA)

pET-28b vector system (Promega, USA)

pENTR-D-TOPO (Invitrogen, USA)

pTZ-57R vector system (Promega, USA)

pUC19 (Promega, USA)

T&A cloning vector (RBC Bioscience, Taiwan)

2.1.8 DNA sequencing

DNA sequencing was carried out at 1st Base (Singapore) and Sangon Biotech (China)

2.1.9 Peptides

Peptide derived from CaMKII (Sigma, USA)

2.1.10 Oligonucleotide primers

Oligonucleotide primers were synthesized by First Bases (Singapore) and Sangon Biotech (China)

2.1.11 Antibiotics

Ampicilin (Sigma Chemical Co., USA)

Gentamycin (Duchefa, Netherlands)

Hygromycin (Phytotechnology, USA)

Kanamycin (Sigma, USA)

Rifampicin (Sigma, USA)

Spectinomycin (Sigma, USA)

2.1.12 Growth medium

MS medium with vitamin (PhytoTechnology Laboratories, USA)

YPAD (Takara, Japan)

2.2 Methodology

2.2.1 Cloning and biophysical characterization of OsCML3m

2.2.1.1) Sequence retrieval and analysis

Nucleotide and amino acid sequences of calmodulin-like proteins 3 (OsCML3) was obtained from GenBank databases via the National Center for Biotechnology Information (NCBI) (http://www.ncbi.mlm.nih.gov) and the rice databases via the Rice Genome Annotation Project (http://rice.plantbiology.msu.edu/) at Michigan State University and the Rice Annotation Project Database (RAP-DB) (http://rapdb.dna.affrc.go.jp/) at the National Institute of Agrobiological Sciences (NIAS). Sequencing of cDNA clones was carried out at 1st Base, Singapore. Multiple sequence alignment was performed using ClustalW2 (http://www.ebi.ac.uk/Tools/clustalw2/) at the European Bioinformatics Institute (EBI).

2.2.1.2) Primer design

Construction of the truncated OsCML3, a C-terminally truncated OsCML3 mutant that lacked the extended amino acid residues R149-L183 (shaded with gray color), termed OsCML3m, was performed (Figure 2.1). Base on the *OsCML3* cDNA

sequence, a pair of primers for amplifying the truncated *OsCML3* gene was designed with *Nde*I and *Hin*dIII restriction sites engineered at the 5′ and 3′ ends, respectively. The sequence and the length of the all oligonucleotide primers are shown in Table 2.1.

2.2.1.3) PCR amplification

The coding region of *OsCML3m* gene was amplified from the *OsCML3* cDNA clone, which was obtained from the DNA Bank of the National Institute of Agrobiological Science (NIAS) as template using gene-specific primers as described above. The amplification reaction was performed in a 50-μl reaction containing 1X *Vent* DNA polymerase buffer, 50-100 ng of DNA template, 500 μM dNTPs, 0.2 μM of each primer and 2 units of *Vent* DNA-polymerase (BioLab, Inc., USA). PCR amplification was performed as follows: pre- denaturation at 94 ºC for 5 minutes, 30 cycles of denaturation at 94 °C for 1 minutes, annealing at 55 °C for 1 minute and extension at 72 °C for 1 minute. In the final extension step, five units of *Tag* DNA polymerase (Fermentus, Inc., USA) were added.

2.2.1.4) Agarose gel electrophoresis

Agarose gel electrophoresis was used to separate, identify, and purify DNA fragments. The concentration of agarose gel used varied with the size of the DNA fragments to be separated. Generally, 1.0-1.8% agarose gel was used and the DNA samples were run in Tris-acetate-EDTA (TAE) buffer. To prepare samples, DNA was mixed with 10% (v/v) DNA gel loading buffer (0.1 M EDTA/NaOH pH 7.5, 50% (v/v) of glycerol, 1% (w/v) of SDS, 0.5% (w/v) of xylene cyanol FF, and 0.5% (w/v) of Bromophenol blue) and loaded into agarose gel. Electrophoresis was performed at a constant voltage of 100 volts until the bromphenol blue migrated to an appropiate

distance through the gel. After electrophoresis, the gel was stained with ethidium bromide solution (5-10 μg/ml in distilled water) for 5 minutes and destained with distilled water for 10 minutes. DNA fragments on agarose gel were visualized on the gel documentation and photographed. The concentration and molecular weight of DNA sample were determined by comparison of band intensity and relative mobility with those of the standard λ/*Hin*dIII DNA markers.

Figure 2.1 Comparison of the amino acid sequences of OsCML3 and OsCML3m

```
OsCML3      MDHLTKEQIAEFREAFNLFDKDGDGTITSKELGTVMGSLGQSPTEAELKKMVEEVDADGS 60
OsCML3m     MDHLTKEQIAEFREAFNLFDKDGDGTITSKELGTVMGSLGQSPTEAELKKMVEEVDADGS 60
            ************************************************************

OsCML3      GSIEFEEFLGLLARKLRDTGAEDDIRDAFRVFDKDQNGFITPDELRHVMANLSDPLSDDE 120
OsCML3m     GSIEFEEFLGLLARKLRDTGAEDDIRDAFRVFDKDQNGFITPDELRHVMANLSDPLSDDE 120
            ************************************************************

OsCML3      LADMLHEADSDGDGQINYNEFLKVMMAKRRQNMMEGHGSGGHRSSNSHKKSGCCGPNSSC 180
OsCML3m     LADMLHEADSDGDGQINYNEFLKVMMAK------------------------------ 148
            ****************************

OsCML3      TIL 183
OsCML3m     --- 
```

Table 2.1 the sequence and the length of oligonucleotide primers used for PCR amplification

Gene	Primers	Sequences 5’ to 3’	Length
OsCML3m	Forward	CATATGGACCACCTGACAAA	20
	Reverse	ATCTCGAGTCATCGCTTTGCC	21

2.2.1.5) Extraction of DNA fragment from agarose gel

The amplification products generated by PCR were purified from agarose gel using Geneaid gel extraction protocol. After electrophoresis, the desired DNA

fragment was excised as gel slice from an agarose gel using a scalpel and transferred to a microcentrifuge tube. Five hundred microliters of DF buffer were added to the gel and incubated for 10 minutes at 55-60 °C or until the gel slice was completely dissolved. During incubation, the tube was inverted every 2-3 minutes. The mixture was transferred into a DF column and centrifuged at 12,000 rpm for 1 minute. The flow through solution was discarded. Then 400 µl of W1 buffer was added, centrifuged at 12,000 rpm for 1 minute and the flow through was discarded. Six hundred µl of Wash buffer was then added to the DF column. The column was let standing for 1 minute, centrifuged at 12,000 rpm for 1 minute and the flow through was discarded. The DF column was centrifuged again for 3 minutes to remove a trace element of the Wash buffer. The DF column was then placed into a sterile 1.5 ml microcentrifuge tube. DNA was eluted by an addition of 15-50 µl of sterile water to the center of the DF column and the column was let standing for 2 minutes, and then centrifuged at 12,000 rpm for 2 minutes. DNA concentration was determined by agarose gel electrophoresis.

2.2.1.6) Ligation of CML3m gene product to T&A cloning vector

The purified PCR products were ligated to T&A cloning vector (see in Appendix A-1). A suitable molecular ratio between vector and inserted DNA in a mixture of cohesive-end ligation is usually 1:3. To calculate the appropriate amount of PCR product (insert) used in ligation reaction, the following equation was used:

$$\frac{\text{ng of vector} \times \text{kb size of insert}}{\text{kb size of vector}} \times \text{insert: vector molar ratio} = \text{ng of insert}$$

The 20 μl of ligation mixture contained appropriate amount of vector DNA and gene fragment, 1x ligation buffer and 10 U of T4 DNA ligase. The reaction was incubated overnight at 16 ^{o}C. The ligation product was then transformed into *E. coli* (Top 10).

2.2.1.7) Transformation of ligated products to E. coli host cells by $CaCl_2$ method

A) Preparation of *E. coli* competent cells

Competent *E. coli* strain Top 10 was prepared according to the method of Sambrook *et al.* (1989). A single colony of *E. coli* strain Top 10 was inoculated in 3 ml LB broth (1% (w/v) tryptone, 0.5% (w/v) yeast extract, and 1% (w/v) NaCl, pH 7.2) and incubated at 37 ºC with shaking at 250 rpm overnight. Fifty milliliters of LB medium were inoculated with two percents of the starter culture and incubated at 37 ºC with shaking at 250 rpm for 3-4 hours until the optical density at 600 nm (OD_{600}) of culture reached 0.45-0.55. The cell was chilled on ice slurry for 15-30 minutes and harvested by centrifugation at 8,000 xg, 4 ºC for 10 minutes. After the culture supernatant was decanted, the cell pellet was washed with 25 ml of fresh ice 150mM $CaCl_2$, resuspended by gently mixing and centrifuged at 8,000 xg, 4 ºC for 10 minutes. After the supernatant was discarded, the cell was resuspended with 25 ml of fresh ice 150mM $CaCl_2$ and incubated on ice for 30 minutes, then centrifuged at 8,000 xg, 4 ºC for 15 minutes. The supernatant was discarded and finally, the cells were resuspended in 1 ml of fresh ice-cold 150 mM $CaCl_2$ and incubated on ice for 1 hour. These cells were used immediately as freshly prepared competent cells (50 μL aliquot is sufficient for a transformation).

B) Transformation by $CaCl_2$ method

Sixty microliters of competent cells were mixed well with 10 µl of the ligation mixture and then placed on ice for 30 minutes. The mixture was heat-shocked for 90 minutes in a water bath set to 42 ^{o}C and the cells were quickly returned to the ice for 5 minutes. Five microliters of LB medium were then added to the cell suspension and incubated at 37 ºC with shaking at 250 rpm for 1 hour. The cells were spun down to retain 200 µl, spread onto the LB agar plates containing 100 µg/ml ampicillin, and incubated at 37 ºC overnight. The colonies which contained potential recombinant plasmids were picked and checked for the plasmid by restriction enzyme digestion.

2.2.1.8) Analysis of recombinant plasmids

A) Plasmid DNA isolation using Presto™ Mini Plasmid Kit

A single colony of recombinant cells was selected and grown in 5 ml of LB broth (1% (w/v) tryptone, 0.5% (w/v) yeast extract, and 1% (w/v) NaCl) containing 100 µg/ml of ampicillin overnight at 37 ºC with shaking at 250 rpm. The cells were spun in a microcentrifuge at 4000 rpm for 10 minutes at 4 ºC. The cells were resuspended in 200 µl of PD1 buffer containing 2 µl of TrueBlue Lysis Buffer and mixed by vortex. Then, a 200-µl of PD2 buffer was added into the sample tube, and the suspension was inverted gently several times to mix. Three hundred microliters of PD3 buffer was added to the mixture and the suspension was mixed gently. The insoluble salt-genomic DNA precipitate was then removed by centrifugation at 12,000 rpm for 15 minutes at room temperature. The supernatant was transferred to a PDH Column and then Centrifuged at 12,000 rpm for 1 minute at room temperature then the flow-through was discarded. The PDH Column was placed back in the 2-ml

Collection Tube. The PHD columns was added with 400 µl of W1 Buffer, and centrifuged at 12,000 rpm for 1 minute. The flow-through was discarded then the PDH Column was placed back in the 2-ml Collection Tube. The PHD column was added with 600 µl of Wash Buffer, and centrifuged at 12,000 rpm for 3 minutes at room temperature. The flow-through was discarded then the PDH Column was placed back in the 2-ml Collection Tube. The columns was centrifuged at 12,000 rpm for 2 minutes at room temperature to completely dry the column matrix. Finally, the dried PDH Column was transferred to a new 1.5-ml microcentrifuge tube then and the plasmid DNA was eluted with 30 µl of sterile water and stored at -20 ºC.

B) Restriction enzyme analysis

The condition of digestion was performed as recommended by the enzyme manufacturer. The recombinant plasmids isolated by Mini Plasmid kit were analyzed for the presence of the *OsCML3m* fragment by digestion with *Nde*I and *Xho*I. The reaction was carried out in 20-µl mixture at 37 ºC. The products were analyzed by 1% agarose gel electrophoresis. The size of DNA insert was compared with 100 bp standard DNA marker. .

2.2.1.9) Cloning of OsCML3m gene into expression vector (pET-21a)

A) Vector DNA preparation

The *E. coli* XL-1 Blue, which contained pET-21a plasmid was grown in 10-ml LB medium containing 100 µg/ml ampicillin at 37 ^{o}C with shaking at 250 rpm for 16 hours. The pET-21a vector (see Appendix A-2) was extracted using Alkaline lysis method as described above. The expression vector pET-21a was linearized with *Nde*I and *Xho*I digestion using the conditions recommended by the enzyme manufacturer.

The reaction was incubated at 37 ^{o}C for 3-4 hours. The linear pET-21a was harvested from agarose gel using the Geneaid gel extraction protocol as described above**.**

B) *OsCML3m* gene fragment preparation

After the *OsCML3* gene was cloned into T&A cloning vector, and the recombinant clones were checked with restriction enzyme digestion. The recombinant plasmid that contained the *OsCML3m* gene was extracted by the method as described above. The *OsCML3m* gene was digested with *Nde*I and *Xho*I using the condition of digestion recommended by the enzyme manufacturer. The reactions were incubated at 37 ^{o}C overnight. The *OsCML3m* gene fragment was harvested from agarose gel using the Geneaid gel extraction protocol and DNA size was determined by comparing with the 100 bp standard DNA marker.

C) Ligation of *OsCML3m* fragment product to pET-21a

The gene fragments were ligated to the pET-21a vector. A suitable molecular ratio of 1:5 between vector and inserted DNA in a mixture was used. The 20 µl of ligation mixture containing an appropriate amount of the vector DNA, the gene fragment, 1x ligation buffer and 10 U of T4 DNA ligase was incubated overnight at 16 ^{o}C. The mixture was then used for transformation.

D) Transformation of ligated products to *E. coli* Top 10 cell by $CaCl_2$ method

Competent cells were prepared following the protocol described above. The ligation mixtures were mixed with competent cells and then placed on ice for 30 minutes. The cells were heat-shocked for 90 minutes in a water bath set to 42 ^{o}C and quickly incubated on ice for 5 minutes. Five hundred µl of LB medium was added,

and then the cell suspension was incubated at 37 ºC with shaking at 250 rpm for 1 hour and spun down to retain 200 µl. Finally, the cell suspension was spread onto LB agar plates containing 100 µg/ml ampicillin and incubated at 37 ºC overnight. The recombinant clones that contained pET-21a vector could grow on LB agar plates containing ampicillin. A single colony was selected and checked by restriction enzyme digestion.

E) Analysis of recombinant plasmids

A single colony of recombinant cells was selected and grown in 5 ml of LB broth (1% (w/v) tryptone, 0.5% (w/v) yeast extract, and 1% (w/v) NaCl) containing 100 µg/ml of ampicillin overnight at 37 ºC with shaking at 250 rpm. The recombinant plasmids were extracted by alkaline lysis method. The recombinant plasmids were digested with *Nde*I and *Xho*I. The reaction was incubated at 37 ^{o}C overnight and the products were analyzed by 1% agarose gel electrophoresis. The size of DNA insert was compared with the 100 bp standard DNA marker.

F) Nucleotide and amino acid sequences analysis

The recombinant plasmids were extracted by Mini Plasmid Kit and nucleotide sequences of the inserts were determined. DNA sequencing was carried out at 1st Base (Singapore). The sequencing primers, T7 promoter primer and T7 terminator primer were used. The molecular weight of OsCML3m was calculated from the deduced amino acid sequence using the program Compute Mw (http://expasy.org/tools/ pi_tool.html).

2.2.1.10) Expression of the OsCML3 and OsCML3m genes

For the full-length *OsCML3*, the previously reported expression clone (Chinpongpanich et al. 2011) was used. In this study the OsCML3m gene was cloned and expressed in *E. coli* BL21 (DE3) using the protocols described below.

A) Preparation of *E. coli* BL21 (DE3) competent cell

The recombinant pET-21a plasmids containing the *OsCML3m* gene was transformed into *E. coli* strain BL21 (DE3) cell by heat shock method. Competent cells were prepared following the protocol described above. The recombinant plasmid was mixed with the competent cells and the mixture was then placed on ice for 30 minute. The cells were heat-shocked for 90 minutes in a water bath set to 42 ^{o}C and quickly incubated on ice for 5 minutes. Five hundred microliters of LB medium was then added to the cell suspension and incubated at 37 ºC with shaking at 250 rpm for 1 hour. Finally, fifty microliters of the cell suspension was spread onto the LB agar plate containing 100 μg/ml ampicillin and incubated at 37 ºC overnight.

B) Optimization for rOsCML3m production

A single colony of recombinant cells was grown overnight at 37 ^{o}C in 5 ml of LB medium, pH 7.0, containing 100 μg/ml ampicillin. Then, 2.0% of the cell culture was inoculated into 10 ml of the same medium and was incubated at 37 ^{o}C with shaking for 3-4 hours until the optical density at 600 nm (OD_{600}) of the cell culture reached 0.6. Production of recombinant proteins was induced by IPTG at a final concentration of 0, 0.2, 0.4, 0.6, 0.8 or 1.0 mM and the incubation was continued at 37 ^{o}C for 4 hours. The cells were harvested by centrifugation at 8000xg for 15 minutes, then washed twice in cold wash buffer (50 mM Tris-HCl, pH 7.5) and

collected by centrifugation. The cell pellet was stored at -80 ^{o}C. In whole cell preparation, the cell pellet was resuspended in 10 ml of cold lysis buffer (50 mM Tris-HCl, pH 7.5, 1 mM EDTA, and 1 mM DTT), and then 1 ml of cell suspenson was taken for centrifugation at 12,000 rpm for 1 minute. After that the cell pellet was resuspended with 100 μl of cold lysis buffer. Before loading into SDS-PAGE, the cell suspension was boiled at 100 ^{o}C for 10 minutes.

C) SDS-polyacrylamide gel electrophoresis

The SDS-PAGE system was performed according to the method of Bollag *et al*., 1996. The slab gel system consisted of 0.1% SDS (W/V) in 12.5% separating gel and 3.9% stacking gel. Tris-glycine (25 mM Tris, 192 mM glycine and 0.1% SDS), pH 8.3 was used as electrode buffer. The gel preparation was described in Appendix C**.** The protein samples were mixed with 5x sample buffer (60 mM Tris-HCl pH 6.9, 79% glycerol, 2% SDS, 0.1% bromophenol blue and 14.4 mM β-mercaptoethanol) by the ratio 5:1 and boiled for 10 minutes before loading to the gel. The electrophoresis was run from the cathode towards the anode at a constant current (20 mA) per gel at room temperature. The molecular weight marker proteins containing β-galactosidase (116,000 Da), bovine serum albumin (66,200 Da), ovalbumin (45,000 Da), lactate dehydrogenase (35,000 Da), restriction endonuclease Bsp98I (25,000 Da), β-lactoglobulin (18,400 Da) and lysozyme (14,400 Da) were used. After electrophoresis, the gel was stained with Coomassie blue.

D) Protein staining

The gel was transferred to a box containing Coomassie staining solution (0.25% Coomassie Blue R-250, 50% methanol, and 7% glacial acetic acid, see

Appendix C). The gel was stained for 1 hour at room temperature with gentle shaking. After staining, the stain solution was poured out, and the gel was briefly rinsed with water and incubated with Coomassie destaining solution (10% methanol and 7% glacial acetic acid, see Appendix C). The gel was gently destained several times until protein bands were readily visible.

2.2.1.11) Purification of the OsCML3 and OsCML3m proteins

A) Crude protein extracts preparation

For the large-scale protein expression, a single colony of recombinant cells was grown overnight at 37 ^{o}C for 16 hours in 25 ml of LB medium, pH 7.0, containing 100 μg/ml ampicillin. Then, 2.0% of the cell culture was inoculated into 1,000 ml of the same medium and was incubated at 37 ^{o}C with shaking for 3-4 hours until the optical density at 600 nm (OD_{600}) of the cell culture reached 0.6. Production of recombinant proteins was induced by IPTG at the final concentration of 0.4 mM and the incubation was continued at 37 ^{o}C for 4 hours. The cells were harvested by centrifugation at 8000xg for 15 minutes, and then washed twice in cold wash buffer (50 mM Tris-HCl, pH 7.5) and collected again by centrifugation. The cell pellet was stored at -80 ^{o}C until sonication. In crude extract preparation, the cell pellet was resuspended in 50 ml of cold lysis buffer (50 mM Tris-HCl, pH 7.5, 1mM EDTA, and 1mM DTT), incubated on ice for 30 minutes and then the cells were broken by sonication on ice. Unbroken cell and cell debris were removed by centrifugation at 27,000xg for 30 minutes. The supernatant was kept at 4 ^{o}C until it was used.

B) OsCML3 and OsCML3m protein purification by phenyl-Sepharose column

The phenyl-Sepharose was packed into a 4-5-ml size of resin and washed with deionized water several times. After that, the column was equilibrated with Equilibration buffer (50 mM Tris-HCl, pH 7.5, 1 mM $CaCl_2$ and 0.5 mM DTT) about 20 column volumes. Before applying the crude protein sample to the phenyl-Sepharose column, $CaCl_2$ was added to a final concentration of 5 mM to the crude protein sample and the mixture was incubated at room temperature for 10 minutes. The crude protein sample was applied to the phenyl-Sepharose column, and then the column was washed with Equilibration buffer until the absorbance at 280 nm was around 0.01. After that the column was washed with Wash buffer I (50 mM Tris-HCl, pH 7.5, 1 mM $CaCl_2$, 0.5 mM DTT and 200 mM NaCl) until the absorbance at 280 nm was near zero. Then proteins were eluted with Elution buffer I (50 mM Tris-HCl, pH 7.5, 5 mM EGTA and 0.5 mM DTT). The eluted proteins were analyzed by SDS-polyacrylamide gel electrophoresis as described above. The fractions containing OsCML3 or OsCML3m proteins were pooled and dialyzed against sufficient EGTA to remove calcium ions with 100 volumes of Dialysis buffer (1mM Tris-HCl, pH 7.5, 1mM KCl) for at least 4 hours 3 times. All proteins were concentrated using Centrifugal Filters (10000 Daltons molecular weight cut-off) (Amicon).

2.2.1.12) Determination of protein concentration by BCA protein assay

Protein concentration was determined using The Pierce BCA protein assay kit (Pierce, USA). In the first step, BCA working reagent was prepared by mixing 50 parts of reagent A with 1 part of reagent B. The second step, 25 μl of each standard

BSA or protein sample was pipetted into a microplate well, then 200 µl of working reagent was added to each well and the plate was mixed thoroughly and incubated at 37 ^{o}C for 30 minutes. After that, the plate was cooled to room temperature and the absorbance at 540 nm was measured on a microplate reader.

2.2.1.13) Characterization of OsCML3 and OsCML3m proteins

A) Ca^{2+} binding properties of OsCML3 and OsCML3m proteins

To perform the electrophoresis mobility assay of each protein, 1 mM of $CaCl_2$ or 3 mM of EGTA in the final concentration was added to each protein sample, the sample was then mixed and let stand at room temperature for 15 minutes prior to electrophoresis in a 12% (w/v) SDS-polyacrylamide gel. After electrophoresis, the gel was stained with Coomassie blue.

B) CaMKII peptide binding properties of OsCML3 and OsCML3m proteins

The ability to bind the peptide derived from CaM kinase II (CaMKII) of the OsCML3 and OsCML3m proteins was assessed by gel mobility shift assay. Two hundred picomoles of each recombinant protein in the presence of 1 mM Ca^{2+} or 3 mM EGTA were mixed with different amounts of the peptide derived from CaMKII (Sigma) and incubated for 1 hour at room temperature and then fractionated in 12.5% (w/v) polyacrylamide gel containing 4 M urea. The slab gel system consisted of 4 M urea in 12.5% seperating gel and 3.9% stacking gel. Tris-glycine (25 mM Tris, 192 mM glycine), pH 8.3 was used as electrode buffer. The preparation of gel containing 4 M urea was described in Appendix C. The protein samples were mixed with 5x sample buffer (60 mM Tris-HCl pH 6.9, 79% glycerol, 0.1% bromophenol blue) by

the ratio 5: 1. The electrophoresis was run from the cathode towards the anode at a constant current (20 mA per gel) at room temperature and the proteins were detected by Coomassie blue staining.

C) Analysis of structural changes from circular dichroism spectroscopy

Circular dichroism (CD) spectroscopy was carried out at 25 ^{o}C with constant N_2 flushing, using a CD instrument (Jasco J-715 Spectropolarimeter). The far UV CD spectra of the OsCML3 and OsCML3m proteins were measured from 190 to 250 nm in 1 mM Tris-HCl buffer, pH 7.5 and 1 mM KCl in the presence of 1 mM $CaCl_2$ or 1 mM EGTA. The final concentration of each protein used in far-UV CD analysis was 10 μM. All measurements were performed 30 min after sample preparation, using a 1-mm path length quartz cell and the parameter settings: response time 1 s; sensitivity 50 millidegrees; scan speed 50 nm/min; 2.0 nm spectral band widths, and average of three scans.

D) 8-Anilino-1-naphthalenesulphonate (ANS) fluorescence measurement

To examine Ca^{2+}-induced exposure of the hydrophobic surfaces of the recombinant OsCML3 and OsCML3m proteins, fluorescence emission spectra of 8-Anilino-1-naphthalenesulfonic acid (ANS, Sigma) in the presence of these proteins were performed on a LS55 Luminescence Spectrometer (PerkinElmer, UK) at 25 ^{o}C. Fluorescence emission spectra were monitored with excitation set at 370 nm and scan emission spectra in the range 400-650 nm. All measurements were performed using 1 μM of each protein in 1 mM Tris-HCl buffer, pH 7.5 and 1 mM KCl; and ANS at a final concentration 100 μM in the presence of 1 mM $CaCl_2$ or 3 mM EGTA.

2.2.2 Subcellular Localization

A) Construction of GFP-OsCML vectors

To construct the pCAMBIA1302 encoding either OsCML3, OsCML3m, OsCML1 or OsCML1 lacking C-terminal extension (shaded with gray color shown in Figure 2.2), termed OsCML1m, fused with GFP at the N-terminal end, the coding regions of *OsCML3* (AK111834), and *OsCML3m* were amplified from the *OsCML3* cDNA clone (J023133G18), and the coding regions of *OsCML1* (AK070889) and *OsCML1m* were PCR-amplified using the *OsCML1* cDNA clone (J023074P12). The coding region of *GFP* was also amplified from the pCAMBIA1302 as template. The PCR reactions were performed using the gene-specific primers shown in Table 2.2.

All PCR reactions contained 1X *Vent* DNA polymerase buffer, 50-100 ng of DNA template, 500 μM dNTPs, 0.2 μM of each primer and 2 units of *Vent* DNA polymerase BioLab, Inc., USA). The PCR reactions were performed with 30 cycles of 94 ^{o}C for 1 minute, annealing temperature (as shown in Table 2.2) for 1 minute and 72 ^{o}C for 1 minute and 30 seconds, and then followed by a final 72 ^{o}C for 10 minute with the addition of five units of *Tag* DNA polymerase (Fermentus, Inc., USA). The PCR products were analyzed by 1% agarose gel electrophoresis and then purified from agarose gel using Geneaid gel extraction protocol (Geneaid, USA). The ligation reaction consisted of a 1:3 molar ratio of T&A vector (RBC, Taiwan) to insert DNA, 1X T4 DNA ligase buffer, 3 units of T4 DNA ligase and Nuclease-free water added to a final volume of 20 μl. The reaction was incubated overnight at 22 ^{o}C. The ligation product was then transformed into *E. coli* (Top 10). A single colony was picked and cultured in LB medium containing 100 μg/ml ampicillin overnight. The recombinant

plasmids were extracted by Mini Plasmid kit and then digested with *Xho*I and *BstE*II with incubation at 37 ^{o}C. The products were analyzed by 1% agarose gel electrophoresis, and nucleotide sequencing was performed using M13 forward and reverse primers. The amplicons were cloned into the T&A cloning vector resulting in pTA-OsCML3, pTA-OsCML3m, pTA-OsCML1, pTAOsCML1m and pTA-GFP, respectively. After checking the sequences, all plasmids containing correct nucleotide sequence were digested with *Xho*I and *BstE*II using the conditions recommended by the enzyme manufacturer. Then, the gene fragments of *OsCML3*, *OsCML3m*,

Figure 2.2 Comparison of the amino acid sequences of OsCaM1 and OsCML1m

```
OsCML1     MADQLSEEQIGEFREAFSLFDKDGDGSITTKELGTVMRSLGQNPTEAELQDMISEVDTDS 60
OsCML1m    MADQLSEEQIGEFREAFSLFDKDGDGSITTKELGTVMRSLGQNPTEAELQDMISEVDTDS 60
           ************************************************************

OsCML1     NGNIEFKEFLGLMARKLRDKDSEEELKEAFRVFDKDQNGFISATELRHVMANIGERLTDE 120
OsCML1m    NGNIEFKEFLGLMARKLRDKDSEEELKEAFRVFDKDQNGFISATELRHVMANIGERLTDE 120
           ************************************************************

OsCML1     EVGEMISEADVDGDGQINYEEFVKCMMAKKRRKRIEEKRDHDGGSRTKSAGPSAAPASKR 180
OsCML1m    EVGEMISEADVDGDGQINYEEFVKCMMAK------------------------------ 149
           ****************************

OsCML1     GQKCVIL 187
OsCML1m    ------- 
```

Table 2.2 Gene-specific primers used for PCR amplification

Gene	Primer	Nucleotide sequence (5' to 3')	Annealing temperature (^{o}C)
OsCML3	Forward	CTCGAGGGGGGCGGAGGAATGGACC	59.3
	Reverse	GGTCACCTTTTTCAGAGGATGG	
OsCML3m	Forward	CTCGAGGGGGGCGGAGGAATGGACC	59.3
	Reverse	GGTTACCTTCACTTTGCCATCATGACC	
OsCML1	Forward	CTCGAGGGTGGTGGTGGCATGGCGG	56.8
	Reverse	GGTTACCCTACTTGGCCATCATGC	
OsCML1m	Forward	CTCGAGGGTGGTGGTGGCATGGCGG	46.9
	Reverse	GGTTACCCTACTTGGCCATCATGC	
GFP	Forward	CCATGGTAGATCTGACTAGTAAAGG	59.3
	Reverse	GGTCACCAATCTCGAGGTGGTGGTGG	
LCGFCML forward		GAGTTTGTAACAGCTGCTGG	57.0
LCNOSCML reverse		ATCGCAAGACCGGCAACAGG	

OsCML1 and *OsCML1m* were individually inserted into pTA-OsGFP via the *Xho*I and *Bst*EII sites at the 3' end of the GFP coding sequence, resulting in pTA-GFP-OsCML3 pTA-GFP-OsCML3m, pTA-GFP-OsCML1 and pTA-GFP-OsCML1m respectively. After verifying the DNA sequences by LCGFCML forward and LGNOSCML reverse primers (Table 2.2), the fragments of GFP-OsCML3, GFP-OsCML3m, GFP-OsCML1 and GFP-OsCML1m were sub-cloned into pCAMBIA1302 (see appendix A-3) using *Nco*I and *Bst*EII sites, resulting in pCAMBIA-GFP-OsCML3, pCAMBIA-GFP-OsCML3m, pCAMBIA-GFP-OsCML1 and pCAMBIA-GFP-OsCML1m, respectively, which can be expressed under the control of CaMV 35S promoter in plant. The plasmid construction diagram is shown in figure 2.3.

B) Transformation of recombinant plasmids into Agrobacterium cells

A 250 µl of *Agrobacterium* competent cells was mixed with 6-7 µl of plasmid (100 ng/µl) and then followed by the protocol as described above. After transformation, the cell suspensions were spread onto the LB agar plates containing 100 µg/ml gentamycin, 10 µg/ml rifampicin and 50 µg/ml kanamycin, and incubated at 28 ºC for 2 days. The growing colonies were picked and checked by colony PCR.

C) Colony PCR analysis

The amplification reactions were performed in a 20-µl reaction containing 1X *Taq* DNA polymerase master mix (CWBIO, China), a small amount of colony, and 0.25 µM of LCGFCML forward and LGNOSCML reverse primer. PCR amplification

Figure 2.3 A diagram of plasmid construction for subcellular localization

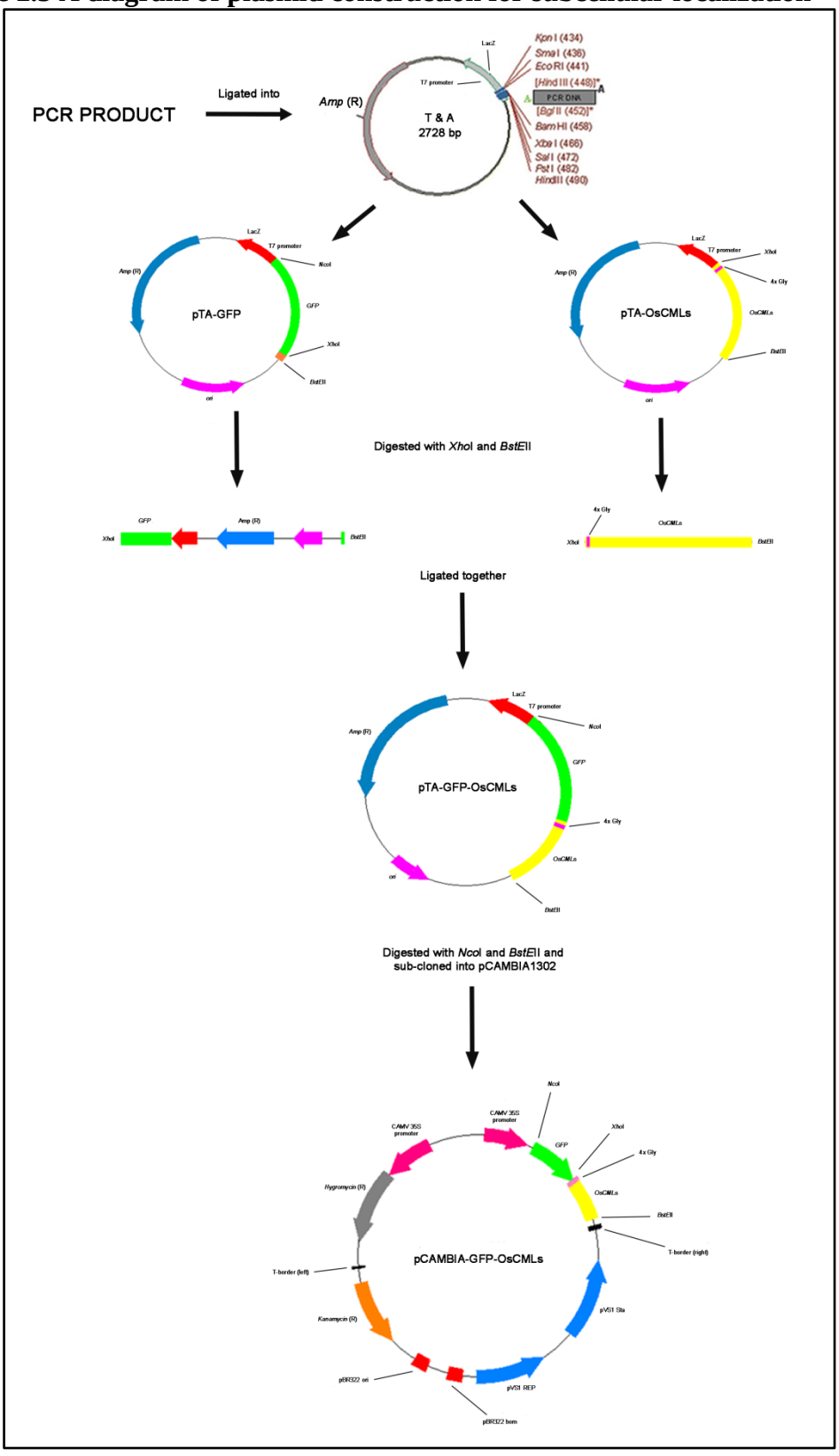

was performed as follows: pre-denaturation at 95 ºC for 5 minutes, 35 cycles of denaturation at 94 °C for 1 minutes, annealing at 57 °C for 45 second and extension at 72 °C for 1 minute and 15 seconds. In the final extension step, 72 °C for 5 minutes was set. Then, PCR products were analyzed by agarose gel electrophoresis.

D) Subcellular localization

A single colony of recombinant *Agrobacterium* was picked and cultured in 5 ml of LB broth containing 100 μg/ml gentamycin, 10 μg/ml rifampicin and 50 μg/ml kanamycin with shaking at 28 ^{o}C for 20 hours. The *Agrobacterium* cells were collected by centrifugation with velocity of 3000 rpm for 15 minutes at room temperature. The supernatant was discarded, and cell pellets were re-suspended with injection buffer (10mM MES buffer (pH 5.7), 10 mM $MgCl_2$ and 150 μM acetosyringone. Each cell suspension was diluted with injection buffer until the optical density at 600 nm (OD_{600}) reached 0.5 and then incubated in room temperature for at least 3 hours. Each *Agrobacterium* suspension was infiltrated into the leaf of 6-week-old tobacco plants at lower epidermis side. The treated plants were grown in the dark for 16 h followed by 48 h in the growth chamber (Ou et al. 2011). GFP fluorescence was examined by confocal microscopy with a Leica SPE microscope (Leica, Germany) using an excitation wavelength of 488 nm. At least 5 independent samples were examined.

2.2.3 Investigations of protein interaction of OsPEBP or OsHMGB1 with OsCML3 or OsCML3m

2.2.3.1) Sequence retrieval and analysis

Nucleotide and amino acid sequences of High mobility group B protein 1,

termed OsHMGB1 (AK062226) and phosphatidylethanolamine-binding protein, termed OsPEBP (AK241478) were obtained from databases as described above.

2.2.3.2) Confirmation of protein interactions by Yeast-two hybrid analysis

A) Primer designs

Base on the *OsCML3*, *OsCML3m*, *OsCML3s*, which had serine-to-cysteine mutation at the prenylation site, *OsHMGB1* and *OsPEBP1* cDNA sequences, a pair of primers for amplifying of each gene was designed. The forward PCR primers were designed to contain the sequence, CACC, at the 5' end of the primer to enable directional cloning into pENTR™ TOPO vector. The sequence and the length of the all five pairs of primers are shown in Table 2.3 with the CACC sequences underlined.

B) PCR amplification of *OsCML3*, *OsCML3m*, *OsCML3s*, *OsHMGB1* and *OsPEBP*

Amplification reactions were performed in a 50-μl reaction containing 1X KOD-Plus-Neo DNA polymerase buffer, 1.5 mM $MgSO_4$, 50-100 ng of DNA template, 400 μM of dNTP mixture, 0.3 μM of each pair of primer and 1 units of KOD-Plus-Neo DNA polymerase. PCR amplification was performed as follows: pre-denaturation at 94 ºC for 5 minutes, 30 cycles of denaturation at 94 °C for 1 minutes, annealing at 58.6 °C for 1 minute and extension at 68 °C for 45 seconds. In the final extension step, 68 °C for 10 minutes was set. Then, PCR products were analyzed by agarose gel electrophoresis.

C) Extraction of DNA fragment from agarose gel

The amplification products generated by PCR were purified from agarose gel using gel extraction kit (CWBIO, China). After electrophoresis, the desired DNA fragment was excised as gel slice from an agarose gel using a scalpel and transferred to a microcentrifuge tube. Three hundred microliters of PG buffer (CWBIO, China) were added to the gel and incubated for 10 minutes at 55-60 °C or until the gel slice has been completely dissolved. During incubation, the tube was inverted every 2-3 minutes. Before loading sample into column, the column was activated by addition of 200 µl of PS buffer (CWBIO, China) and then centrifuge at 12,000 to discard the supernatant. Then, the mixture was transferred into the column, the column was

Table 2.3 the sequence and the length of oligonucleotide primers used for PCR amplification in yeast-two hybrid analysis

Genes	Primers	Sequences	Length
OsCML3	Forward	5’ - CACCATGGACCACCTGACAAAGG - 3’	23
	Reverse	5’ - TCAGAGGATGGTACATGAGG - 3’	20
OsCML3m	Forward	5’ - CACCATGGACCACCTGACAAAGG - 3’	23
	Reverse	5’ - TCACTTTGCCATCATGACCTTGAG - 3’	24
OsCML3s	Forward	5’ - CACCATGGACCACCTGACAAAGG - 3’	23
	Reverse	5’ - TCAGAGGATGGTAGATGAGG - 3’	20
OsHMGB1	Forward	5’ - CACCATGAAGGGGGCCAAATCC - 3’	22
	Reverse	5’ - TCACTCGTCATCGTCTTCATCC - 3’	22
OsPEBP	Forward	5’ - CACCATGGCGCAGGAGAGCC - 3’	20
	Reverse	5’ - CTAGAAGACGGCCATGAGCTCG - 3’	22
M13	Forward	5’ - GTAAAACGACGGCCAG - 3’	16
	Reverse	5’ - CAGGAAACAGCTATGAC - 3’	17
pDEST22-GAL4-ADF		5’ - TATAACGCGTTTGGAATCACT - 3’	21
pDEST32-GAL4-BDF		5’ - AACCGAAGTGCGCCAAGTGTCTG - 3’	23

centrifuged at 12,000 rpm for 1 minute, the flow-through solution was discarded. The column was then added with 500 µl of PG buffer, centrifuged at 12,000 rpm for 1 minute and the flow through was discarded. Six hundred microliters of PW buffer (CWBIO, China) was then added to the column. The column was let standing for 1 minute, centrifuged at 12,000 rpm for 1 minute and the flow through was discarded. The column was centrifuged again for 3 minutes to remove a trace element of the PW buffer. The column was then placed into a sterile 1.5 ml microcentrifuge tube. DNA was eluted by an addition of 15-50 µl of sterile water to the center of the column. The column was let standing for 2 minutes, and then centrifuged at 12,000 rpm for 2 minutes. DNA concentration was determined by agarose gel electrophoresis.

D) Ligation of gene fragments to pENTR-D TOPO vector

In this reaction, PCR products are directionally cloned by adding four bases to the forward primer (CACC). The overhang in the cloning vector of pENTR-D TOPO (GTGG) (see appendix A-4) invades the 5' end of the PCR product, anneals to the added bases, and stabilizes the PCR product in the correct orientation by Topoisomerase I activity. To obtain the highest TOPO cloning efficiency, a 0.5:1 to 2:1 molar ratio of PCR product: TOPO vector was used (pENTR™ Directional TOPO® Cloning Kits, Invitrogen). In this study, 6-µl of ligation mixture contained appropriate amount of TOPO vector and gene fragment, 1 µl of salt solution and sterile water added to a final volume of 6 µl. The reactions were gently mixed and incubated for 5 minutes at room temperature (22-23 ^{o}C). The ligation product was used to transform *E. coli* (Top 10).

E) Transformation by $CaCl_2$ method

The ligated products were introduced into *E. coli* (Top 10) competent cells by $CaCl_2$ method. Sixty microliters of competent cells were mixed well with 2 μl of the ligation mixture and then placed on ice for 30 minutes. The mixture was heat-shocked for 90 minutes in a water bath set to 42 ^{o}C and the cells were quickly returned to the ice for 5 minutes. Five microliters of LB medium was then added to the cell suspension and incubated at 37 ºC with shaking at 250 rpm for 1 hour. The cells were spun down to retain 200 μl, spread onto the LB agar plates containing 50 μg/ml kanamycin, and incubated at 37 ºC overnight. The colonies, which contained potential recombinant plasmids were picked and checked for the plasmids by PCR.

F) Checking the gene insertions by colony PCR

The amplification reactions were performed in a 50-μl reaction containing 1X Taq DNA polymerase master mix (CWBIO, China), a small amount of colony, 400 μM of dNTP mixture, 0.3 μM of each pair of M13 Forward (-20) primer and M13 Reverse primer. PCR amplification was performed as follows: pre-denaturation at 94 ºC for 5 minutes, 35 cycles of denaturation at 94 °C for 1 minutes, annealing at 58.6 °C for 45 seconds and extension at 72 °C for 1 minute. In the final extension step, 72 °C for 10 minutes was set. Then, PCR products were analyzed by agarose gel electrophoresis.

G) Nucleotide sequences analysis

The recombinant plasmids from clones containing gene insert were extracted by Plasmid extraction kit (CWBIO, China) and nucleotide sequences of the inserts were determined using M13 Forward (-20) and M13 Reverse primers as shown in Table 2.3. DNA sequencing was carried out at Sangon Biotech, China.

H) Performing the LR Recombination Reaction to transfer the gene of interest to destination vectors (pDEST22 and pDEST32)

To individually sub-clone the gene fragment to both pDEST22 (see appendix A-5) and pDEST32 (see appendix A-6), the LR recombination reactions were performed. The reaction mixture contained 50-150 ng of purified plasmid of pENTR-D TOPO containing individual gene, 150 ng of pDEST22 or pDEST32, 2 μl of LR Clonase™ II enzyme mix, and TE buffer added to a final volume of 8 μl. The LR reactions were incubated at 25 ^{o}C for 1 hour, and then 1 μl of Proteinase K solution was added to each reaction before incubating at 37 ^{o}C for 10 minutes. The LR reactions were used to transform *E. coli* (Top 10) or could be kept at 20 ^{o}C for up to 1 week before transformation.

I) Transformation by $CaCl_2$ method

The LR reactions were introduced into *E. coli* (Top 10) competent cells by $CaCl_2$ method. Sixty microliters of competent cells were mixed well with 8 μl of each LR reaction and then placed on ice for 30 minutes. The mixture was heat-shocked for 90 minutes in a water bath set to 42 ^{o}C and the cells were quickly returned to the ice for 5 minutes. Five microliters of LB medium was then added to the cell suspension and incubated at 37 ^{o}C with shaking at 250 rpm for 1 hour. The cells were spun down

to retain 200 µl, spread onto the LB agar plates containing 100 µg/ml ampicillin for pDEST22 or 100 µg/ml gentamycin for pDEST32, and incubated at 37 ºC overnight. The colonies, which contained potential recombinant plasmids, were picked and checked for the plasmids by colony PCR.

J) Verification of gene insertion in destination vectors by colony PCR

The amplification reactions were performed in a 50-µl reaction containing 1X Taq DNA polymerase master mix (CWBIO, China), a small amount of colony, 400 µM of dNTP mixture, 0.3 µM of each pair of each gene. PCR amplification was performed as follows: pre-denaturation at 94 ºC for 5 minutes, 35 cycles of denaturation at 94°C for 1 minutes, annealing at 58.6 °C for 45 seconds and extension at 72 °C for 1 minute. In the final extension step, 72 °C for 10 minute was set. Then, PCR products were analyzed by agarose gel electrophoresis.

K) Nucleotide sequences analysis

The recombinant plasmids pDEST22 and pDEST32 containing individual gene from selected clones were extracted by Plasmid extraction kit (CWBIO, China) and nucleotide sequences of the inserts were determined using the forward primer of pDEST22-GAL4-ADF designed from the sequence at GAL4 DNA activation domain or pDEST32-GAL4-BDF designed from the sequence at GAL4 DNA binding domain for pDEST22 or pDEST32, respectively, and the suitable reverse primer as shown in Table 2.3. DNA sequencing was carried out at Sangon Biotech, China

L) Preparation of MAV203 yeast competent cell

The MAV203 yeast cell was streaked on YPAD agar (see Appendix C) and then incubated at 30 ^{o}C for 2 days. Ten ml of YPAD medium was inoculated with an

individually picked single colony of MAV203 and then shaken overnight at 30 ^{o}C. Determination of the OD600 of the culture was performed to dilute the cell culture to an OD600 of 0.4 in 50 ml of YPAD, and then the cultures were grown with an additional 2-4 hours. Cell pellets were collected by centrifugation at 2500 rpm for 10-15 minutes and resuspended in 40 ml 1X TE (see Appendix C). The cells were harvested again by centrifugation at 2500 rpm for 10-15 minutes and resuspended in 2 ml of 1X LiAc/0.5X TE (see Appendix C). The cells were incubated at room temperature for 10 minutes and used immediately for transformation.

M) Co-Transformation of recombinant plasmids into MAV203

For co-transformation, the yeast strains MAV203 was transformed with, for example, the pDEST22 harboring *OsHMGB1* paired with the pDEST32 harboring *OsCML3* or *OsCML3m* or *OsCML3s* and the pDEST22 harboring *OsPEBP* paired with the pDEST32 harboring *OsCML3* or *OsCML3m* or *OsCML3s*. All pairs of plasmids including their reciprocal pairing between bait and prey proteins in this study were shown in Table 2.4. For each transformation, 1 μg of a pair of plasmids was mixed together with 100 μl of the yeast suspension. The mixture was added with 700 μl of 1X LiAc/40% PEG-3350/1X TE (see Appendix C), mixed well, incubated at 30 ^{o}C for 30 minutes. It was then added with 88 μl of DMSO and incubated at 42 ^{o}C for 7 minutes. Centrifugation was performed for 10 seconds to remove the supernatant. The cell pellet was resuspended in 100 μl of 1X TE, plated on a selective medium plate lacking leucine and tryptophan (SC-Leu-Trp) (see Appendix C) and then incubated at 30 ^{o}C for 2-3 days.

N) Verification of Two-hybrid interaction by culturing on selective media

To investigate the protein interaction by culturing recombinant yeasts on different media, the three control MAV203 yeast cells were (see Appendix B)

Table 2.4 The pairs of plasmids used for co-transformation

Pair of Plasmids	Descriptions
pDEST22 and pDEST32	Control
pDEST32 and pDEST22-*OsPEBP*	
pDEST32 and pDEST22-*OsHMGB1*	
pDEST32-*OsCML3* and pDEST22	
pDEST32-*OsCML3m* and pDEST22	
pDEST32-*OsCML3s* and pDEST22	
pDEST32-*OsCML3* and pDEST22-*OsPEBP*	Test for protein-protein interaction
pDEST32-*OsCML3m* and pDEST22-*OsPEBP*	
pDEST32-*OsCML3s* and pDEST22-*OsPEBP*	
pDEST32-*OsCML3* and pDEST22-*OsHMGB1*	
pDEST32-*OsCML3m* and pDEST22-*OsHMGB1*	
pDEST32-*OsCML3s* and pDEST22-*OsHMGB1*	
pDEST32-*OsPEBP* and pDEST22	Control (reciprocal pair between bait and prey proteins)
pDEST32-*OsHMGB1* and pDEST22	
pDEST32 and pDEST22-*OsCML3*	
pDEST32 and pDEST22-*OsCML3m*	
pDEST32 and pDEST22-*OsCML3s*	
pDEST32-*OsPEBP* and pDEST22-*OsCML3*	Test for protein-protein interaction (reciprocal pair between bait and prey proteins)
pDEST32-*OsPEBP* and pDEST22-*OsCML3m*	
pDEST32-*OsPEBP* and pDEST22-*OsCML3s*	
pDEST32-*OsHMGB1* and pDEST22-*OsCML3*	
pDEST32-*OsHMGB1* and pDEST22-*OsCML3m*	
pDEST32-*OsHMGB1*and pDEST22-*OsCML3s*	

representing strong, weak, non-interaction (negative) when cultured on selective media were also streaked on SC-Leu-Trp agar.

To make master plates, about five single colonies growing on SC-Leu-Trp agar of each transformant including control cells were individually picked and marked on SC-Leu-Trp agar plates and then incubated at 30 ^{o}C for 2-3 days. A small amount of cells from each patch was picked, pooled and then suspended in 1 ml of sterile water. The 1:10 serial dilution suspensions from each of these cells were spotted (4 µl) onto each of the selection plates as described below;

- Selective medium plate lacking leucine and tryptophan, supplemented with 10 mM $CaCl_2$ (SC-Leu-Trp + 10 mM $CaCl_2$)
- Selective medium plate lacking leucine, tryptophan and histidine, supplemented with 10 mM $CaCl_2$ (SC-Leu-Trp-His + 10 mM $CaCl_2$)
- Selective medium plate lacking leucine, tryptophan and histidine, supplemented with 10 mM $CaCl_2$ and 10 mM 3AT (3-Amino-1,2,4-Triazole) (SC-Leu-Trp-His + 10 mM $CaCl_2$ + 10 mM 3AT)
- Selective medium plate lacking leucine, tryptophan and histidine, supplemented with 10 mM $CaCl_2$ and 25 mM 3AT (3-Amino-1,2,4-Triazole) (SC-Leu-Trp-His + 10 mM $CaCl_2$ + 25 mM 3AT)
- Selective medium plate lacking leucine, tryptophan and histidine, supplemented with 10 mM $CaCl_2$ and 50 mM 3AT (3-Amino-1,2,4-Triazole) (SC-Leu-Trp-His + 10 mM $CaCl_2$ + 50 mM 3AT)
- Selective medium plate lacking leucine, tryptophan and histidine, supplemented with 10 mM $CaCl_2$ and 100 mM 3AT (3-Amino-1,2,4-Triazole) (SC-Leu-Trp-His + 10 mM $CaCl_2$ + 100 mM 3AT)

- Selective medium plate lacking leucine, tryptophan and uracil, supplemented with 10 mM $CaCl_2$ (SC-Leu-Trp-Ura + 10 mM $CaCl_2$)

Each plate was incubated at 30 ^oC for 3 days. Protein interaction for each dilution was examined by comparing cell growth on SC-Leu-Trp + 10 mM $CaCl_2$ to the same dilution on each selection plate.

O) X-gal assay

A small amount of cells from master plates was picked and marked on filter paper placed on SC-Leu-Trp + 10 mM $CaCl_2$ and SC- Leu-Trp + 10 mM EGTA agar, and incubated 30 ^oC for 2-3 days. X-gal solution was prepared by mixing 100 μl of X-gal in DMF (10 mg of X-gal dissolved in 100 μl of DMF), 60 μl of 2-mercaptoethanol in 10 ml of Z buffer (see Appendix C). Two round 125-mm Whatman filter papers were stacked in a 15-cm petri dish, and saturated with 8 ml of the X-gal solution. Any air bubbles were removed. The membrane was carefully removed from the surface of selective medium plate using forceps. The membrane was immersed in liquid nitrogen for 30 seconds and then incubated at room temperature for 1 minute. The immersion was repeated three more times to completely break cells. The frozen membrane was placed on top of the soaked Whatman filters with colony side up and any air bubbles and excess buffer were removed. The plate was covered and incubated at 37 ^oC for 24 hours. The blue color could appear within 24 hours.

2.2.3.3 Confirmation of protein interaction by Bimolecular Fluorescence Complementation (BiFC) Assay

A) Generation of recombinant plasmids for using in BiFC assay

The plasmid of pENTR-D TOPO containing individual gene (*OsCML3*, *OsCML3m* or *OsCML3s*) used for generating recombinant pDEST22 and pDEST32, as prepared above, was used to sub-clone *OsCML3*, *OsCML3m* or *OsCML3s* into pcCFPxGW vector by LR recombination reaction, resulting in pCFP-OsCML3, pCFP-OsCML3m or pCFP-OsCML3s, respectively. Also, the *OsPEBP* and *OsHMGB1* were individually sub-cloned into pnYFPxGW vector, resulting in pYFP-OsPEBP and pYFP-OsHMGB1, respectively. The reaction mixture consisted of equal molar ratio of the recombinant pENTR-D TOPO and pcCFPxGW or pnYFPxGW , 0.7 μl of LR Clonase™ II enzyme mix and TE buffer added to a final volume of 5 μl. The LR reactions were incubated at 25 ^{o}C for 1 hour, and then followed by the same method as previously described. The LR reactions were introduced into *E. coli* (Top 10) competent cells by $CaCl_2$ method. The cell suspension was spread onto the LB agar plates containing 50 μg/ml spectinomycin and incubated at 37 ºC overnight. The colonies, which contained potential recombinant plasmids were picked and checked for the plasmids by colony PCR. The amplification reactions were performed in a 20-μl reaction containing 1X Taq DNA polymerase master mix (CWBIO, China), a small amount of colony, and 0.25 μM each primer. PCR amplification was performed as follows: pre-denaturation at 94 ºC for 5 minutes, 35 cycles of denaturation at 94°C for 1 minutes, annealing at 58.6 °C for 1 minute and extension at 72 °C for 1 minute and

15 seconds. In the final extension step, 72 °C for 10 minutes was set. Then, PCR products were analyzed by agarose gel electrophoresis.

B) Nucleotide sequences analysis

The gene-containing recombinant plasmids pcCFPxGW and pnYFPxGW from selected clones were extracted by Plasmid extraction kit (CWBIO, China) (see Appendix) and nucleotide sequences of the inserts were determined by a suitable pair of primers used for PCR amplification, shown in Table 2.3, corresponding to each gene insert. DNA sequencing was carried out at Sangon Biotech, China.

C) Preparation of *Agrobacterium tumefaciens* GV3101 competent cells

A single colony of *Agrobacterium tumefaciens* GV3101 was inoculated in 10 ml of LB broth containing 100 μg/ml gentamycin and 10 μg/ml rifampicin and then incubated at 28 ºC with shaking at 200 rpm overnight. One milliliter of cell culture was transferred into 200 ml of LB medium containing 100 μg/ml gentamycin and 10 μg/ml rifampicin and then incubated at 28 ºC with shaking at 250 rpm for 10 hours. The cells were harvested by centrifugation at 5,000 rpm at room temperature for 10 minutes. After the supernatant was discarded, the cell was re-suspended with 20 ml of TE buffer (pH 8.0), and then incubated on ice for 10 minutes. Centrifugation was performed again to harvest the cells at 5,000 rpm at room temperature for 10 minutes and then the supernatant was discarded. The cell pellet was re-suspended with 20 ml of LB broth containing 10% glycerol, and divided into 250-microliter aliquots in 1.5-ml microcentrifuge tubes. This competent cell was used immediately or stored at -70 ^{o}C.

D) Transformation of *Agrobacterium* competent cells with recombinant plasmids pcCFPxGW and pnYFPxGW

A 250 µl of *Agrobacterium* competent cells was mixed with 6-7 µl of plasmid (100 ng/µl) and then incubated on ice for 5 minutes. After that the tube was transferred into liquid nitrogen for 5 minutes and then to water bath set at 37 ^{o}C for 5 minutes. One milliliter of LB medium was then added to the cell suspension and incubated at 28 ºC with shaking at 200 rpm for 4 hours. The cells were spun down to retain 200 µl, spread onto the LB agar plates containing 100 µg/ml gentamycin, 10 µg/ml rifampicin and 50 µg/ml spectinomycin, and incubated at 28 ºC for 2 days. The growing colonies were picked and checked by colony PCR.

E) Colony PCR analysis

The amplification reactions were performed in a 20-µl reaction containing 1X *Taq* DNA polymerase master mix (CWBIO), a small amount of colony, and 0.25 µM of each primer. PCR amplification was performed as follows: pre-denaturation at 95 ºC for 5 minutes, 35 cycles of denaturation at 94 °C for 1 minutes, annealing at 58.6 °C for 1 minute and extension at 72 °C for 75 seconds. In the final extension step, 72 °C for 5 minutes was set. Then, PCR products were analyzed by agarose gel electrophoresis.

F) BiFC assay in Tobacco leaf

A single colony of *Agrobacterium* was picked and cultured in 5 ml of LB broth with shaking at 28 ^{o}C for 20 hours. The *Agrobacterium* cells were collected by centrifugation with velocity of 3000 rpm for 15 minutes at room temperature. The supernatant was discarded, and cell pellets were re-suspended with injection buffer

(10mM MES buffer (pH 5.7), 10 mM $MgCl_2$ and 150 μM acetosyringone). Each cell suspension was diluted with injection buffer until the optical density at 600 nm (OD_{600}) reached 0.5. Note that, in this study, we also used p19 to prevent co-suppression in plant cell. Thus, the p19 was also prepared with similar methods except growing on LB medium containing 100 μg/ml gentamycin, 10 μg/ml rifampicin and 50 μg/ml kanamycin, and preparing the diluted cell with its optical density of 0.3. Each pair of recombinant *Agrobacterium* (Table 2.5) was mixed with p19 and then co-infiltrated into the leaf of 6-week-old tobacco plants. The treated plants were grown in the dark for 16 h followed by 48 h in the growth chamber (Ou et al. 2011). GFP fluorescence was examined by confocal microscopy using an excitation wavelength of 488 nm. At least 5 independent samples of each pair of recombinant plasmids were examined.

Table 2.5 A pair of recombinant plasmids individually introduced into *Agrobacterium*

Pair of recombinant plasmids	Description
pcCFPxGW and pnYFPxGW	Control
pCFP-OsCML3 and pnYFPxGW	
pCFP-OsCML3m and pnYFPxGW	
pCFP-OsCML3s and pnYFPxGW	
pcCFPxGW and pYFP-OsPEBP	
pcCFPxGW and pYFP-OsHMGB1	
pCFP-OsCML3 and pYFP-OsPEBP	Verifying protein-protein interaction
pCFP-OsCML3m and pYFP-OsPEBP	
pCFP-OsCML3s and pYFP-OsPEBP	
pCFP-OsCML3 and pYFP-OsHMGB1	
pCFP-OsCML3m and pYFP-OsHMGB1	
pCFP-OsCML3s and pYFP-OsHMGB1	

2.2.3.4 Determination by Electrophoretic mobility shift assay (EMSA)

A) Primer design

To generate the recombinant plasmid pET-28b encoding HMGB1 fused with 6 x His-Tag at the N-terminal end, forward and reverse primers containing *Nde*I and *Xho*I restriction site, respectively were designed. The sequences and the length of the primers are shown in Table 2.6.

Table 2.6 the sequences and the length of oligonucleotide primers used for PCR amplification in pull-down assay

Gene	Primers	Sequences	Length
OsHMGB1	Forward	5’ - GGAATTCCATATGAAGGGGGCCAAATCC - 3’	28
	Reverse	5’ - CCGCTCGAGTCACTCGTCATCGTCTTC - 3’	27

B) PCR amplification

The coding region of *OsHMGB1* gene was amplified from the *OsHMGB1* cDNA clone, which was obtained from the DNA Bank of the National Institute of Agrobiological Science (NIAS) as template using the gene-specific primers as described above. The amplification reactions were performed in a 50-µl reaction containing 1X Phusion DNA polymerase GC buffer, 50-100 ng of DNA template, 0.2 mM dNTP, 0.5 µM of each primer and 1 unit of Phusion DNA polymerase (BioLab, Inc., USA). PCR amplification was performed as follows: pre-denaturation at 98 ºC for 30 seconds, 30 cycles of denaturation at 98 °C for 7 seconds, annealing at 58 °C

for 20 seconds and extension at 72 °C for 30 seconds. The final extension was performed at 72 °C for 10 minutes.

C) Preparation of gene fragment and linearized pET-28b fragment

The amplification product generated by PCR was purified from agarose gel using Geneaid gel extraction protocol (Geneaid, USA) as described above. The *OsHMGB1* gene fragment was digested with *Nde*I and *Xho*I using the condition of digestion recommended by the enzyme manufacturer. The reaction was incubated at 37 ^{o}C overnight. The *OsHMGB1* gene fragment was harvested from agarose gel using Geneaid gel extraction protocol and DNA size was determined by comparing with the λ / *Hin*dIII marker. For pET-28b (see Appendix A-7) fragment preparation, the *E.coli* strain Top 10 containing pET-28b was grown for extraction of plasmid in LB broth containing 50 μg/ml kanamycin. The pET-28b was isolated by High-Speed plasmid mini kit as described above. The purified pET-28b was digested with *Nde*I and *Xho*I using the condition of digestion recommended by the enzyme manufacturer. The reaction was incubated at 37 ^{o}C overnight. The linearized pET-28b fragment was harvested from agarose gel using Geneaid gel extraction protocol and DNA size was determined by comparing with the λ / *Hin*dIII marker.

D) Ligation of *OsHMGB1* gene product to pET-28b

The gene fragment was ligated to the pET-28b vector. A suitable molecular ratio of 1:5 between vector and inserted DNA in a mixture was used. The 20 μl of ligation mixture containing an appropriate amount of the vector DNA, the gene fragment, 1x ligation buffer and 10 U of T4 DNA ligase was incubated overnight at 22 ^{o}C. The mixture was then used for transformation.

E) Transformation of ligated product to *E. coli* BL21 (DE3) by $CaCl_2$ method

The competent cells were transformed with the ligation mixture by $CaCl_2$ method as described above. The cell suspension was spread onto LB agar plates containing 50 μg/ml kanamycin and incubated at 37 ºC overnight. A single colony, which could grow on LB agar plates containing kanamycin was picked to check by colony PCR.

F) Colony PCR analysis

The amplification reactions were performed in a 20-μl reaction containing 1X KAPA Taq Ready Mix (KAPABIOSYSTEMS, USA), a small amount of colony, 0.4 μM each primer shown in Table 2.4. PCR amplification was performed as follows: pre-denaturation at 98 ºC for 30 seconds, 30 cycles of denaturation at 98 °C for 10 seconds, annealing at 58.0 °C for 30 seconds and extension at 72 °C for 30 seconds. In the final extension step, 72 °C for 10 minute was set. Then, PCR productwas analyzed by agarose gel electrophoresis.

G) Analysis of recombinant plasmids

Single colonies of positive clones were selected and grown in 5 ml of LB broth (1% (w/v) tryptone, 0.5% (w/v) yeast extract, and 1% (w/v) NaCl) containing 100 μg/ml of ampicillin overnight at 37 ºC with shaking at 250 rpm. The recombinant plasmids were extracted by Mini Plasmid Kit as described above. The recombinant plasmids were digested with *Nde*I and *Xho*I at 37 ^{o}C overnight and the products were analyzed by 1% agarose gel electrophoresis. The size of DNA insert was determined by comparing with the 100 bp DNA ladder.

H) Nucleotide and amino acid sequences analysis

DNA sequencing of the purified recombinant plasmid was carried out at 1st Base, Singapore. The sequencing primers, T7 promoter primer and T7 terminator primer were used. The molecular weight of OsHMGB1 was calculated from the deduced amino acid sequence using the program Compute Mw (http://expasy.org/tools/ pi_tool.html).

I) Preparation of purified recombinant OsHMGB1 protein

A single colony of recombinant cells was grown overnight at 37 ^{o}C in 20 ml of LB medium, pH 7.0, containing 50 μg/ml kanamycin. Then, 2.0% of the cell culture was inoculated into 800 ml of the same medium and was incubated at 37 ^{o}C with shaking until the optical density at 600 nm (OD_{600}) of the cell culture reached 0.6. Production of recombinant protein was induced by IPTG at a final concentration of 0.4 mM and the incubation was continued at 37 ^{o}C for 4 hours. The cells were harvested by centrifugation at 8000xg for 15 minutes, then washed twice in cold wash buffer (50 mM Tris-HCl, pH 7.5) and collected by centrifugation. The cell pellet was stored at -80^{o}C until it was sonicated. In crude extract preparation, the cell pellet was resuspended in 40 ml of cold lysis buffer (20 mM Sodium phosphate buffer pH 7.4, 30 mM imidazole, 0.5 M NaCl, 0.5 mM dithiothreitol, 1 mM EDTA and 1X protease inhibitor mix (GE Healthcare, USA)), incubated on ice for 30 minutes and then the cells were broken by sonication on ice. Unbroken cells and cell debris were removed by centrifugation at 20000xg for 30 minutes. The supernatant was kept at 4 ^{o}C until it was used.

For OsHMGB1 purification, the Ni-Sepharose was packed into a small column and washed with deionized water several times. The column was equilibrated with Equilibration buffer (20 mM Sodium phosphate buffer pH 7.4, 30 mM imidazole, 0.5 M NaCl, 0.5 mM dithiothreitol, 1 mM EDTA) about 20 column volumes. The crude protein sample was applied to the Ni-Sepharose column, and then the column was washed with Equilibration buffer about 50 column volumes. After that the column was washed with Wash buffer I about 40 column volumes (20 mM Sodium phosphate buffer pH 7.4, 100 mM imidazole, 0.5 M NaCl, 0.5 mM dithiothreitol, 1 mM EDTA). The column was then washed with Wash buffer II (20 mM Sodium phosphate buffer pH 7.4, 200 mM imidazole, 0.5 M NaCl, 0.5 mM dithiothreitol, 1 mM EDTA). Finally, all remaining proteins in column were eluted with Wash buffer III (20 mM Sodium phosphate buffer pH 7.4, 500 mM imidazole, 0.5 M NaCl, 0.5 mM dithiothreitol, 1 mM EDTA). Five-ml per fractions were collected from washing and eluting steps. The eluted proteins were analyzed by SDS-polyacrylamide gel electrophoresis as described above. The fractions containing OsHMGB1 protein were pooled and dialyzed to reduce imidazole concentration with 100 volumes of Dialysis buffer (10 mM Tris-HCl buffer pH 7.5 for at least 4 hours 3 times. To perform the western blot analysis, after electrophoresis, the stacking gel was removed and soaked in 1X transfer buffer (25 mM Tris, 192 mM glycine, pH 8.3) for 30 minutes, twice. A piece of nitrocellulose membrane (Bio-RAD Laboratories, USA) and two sheets of filter paper was cut to the dimensions of the gel and pre-wetted with transfer buffer. The blotted sandwich was assembled in a large tray containing 1X transfer buffer in the following order: two pieces of fiber pad saturated with 1X transfer buffer, electrophoretic gel, nitrocellulose membrane and covered with two

layers of saturated filter papers. Air bubbles between layers of component were removed by rolling a clean glass rod across the surface of each component. Finally, the electroblotting of proteins on the gel to nitrocellulose membrane was carried out at 200 mA, room temperature for 5 hours. When the transfer was completed, the membrane was incubated in blocking buffer (5% milk powder in TBS buffer (20 mM Tris-HCl, pH 7.5, 0.5 M NaCl), 0.1% (v/v) Tween 20) for two and a half hours at room temperature. After blocking, the diluted Anti-His-Antibody (1:3,000) (Amersham Biosciences Inc., USA) was added in the blocking buffer and the membrane was incubated for 1 hour by shaking. Then, the membrane was washed twice in TBS-Tween buffer (TBS buffer, 0.05% (v/v) Tween 20) for 10 minutes each time at room temperature. After that, the membrane was incubated in a new blocking solution containing diluted Alkaline Phosphatase-conjugated AffiniPure Rabbit Anti-Mouse lgG (1:5,000) (Jackson ImmunoResearch Laboratories Inc. USA) for 1 hour and was washed twice in TBS-Tween buffer for 10 minutes each time. In the detection step, the membrane was incubated in 10 ml of alkaline phosphatase (100 mM Tris-HCl, pH 9.5, 100 mM NaCl and 10 mM $MgCl_2$) containing 33 µl of BCIP-T (50 mg/ml in dimethylformamide) and 44 µl of NBT (75 mg/ml in 70% (v/v) dimethylformamide) with gentle shaking. The reaction was terminated by washing the membrane several times in distilled water.

J.) Preparation of pUC19 plasmid

A single clone of *E.coli* harboring pUC19 was cultured in LB broth containing 100 µg/ml ampicillin overnight. The pUC19 plasmid was purified by Mini Plasmid Kit and then analyzed by 1% agarose gel electrophoresis as described above. The

concentration of purified pUC19 was determined using spectrophotometric analysis and then diluted to be concentration of 50 ng/ul.

K.) Preparation of recombinant OsHMGB1, OsCML3, OsCML3m and OsCaM1

Concentration of the purified rOsHMGB1, rOsCML3, rOsCML3m used in the sections above and rOsCaM1, prepared previously as described (Phean-o-pas et al. 2008) was determined by Bradford method as described above.

L.) EMSA

The purified rOsHMGB1 (1.0 uM) was mixed with 100 ng pUC19 supercoiled DNA and various amounts (0–2.0 uM) of purified rOsCML3 or rOsCML3m (0–2.0 uM) in the presence of either 5 mM $CaCl_2$ or 2 mM EGTA in binding buffer (10 mM Tris-HCl pH 7.5, 50 mM NaCl, 1 mM DTT, 5% (v/v) glycerol, 0.05% (w/v) bromophenol blue, 0.05% (w/v) xylene cyanol) and then incubated at room temperature for 10 min. In addition, purified rOsCaM1 was incubated with rOsHMGB1 as described above for direct comparison. For controls, the purified rOsCML3, rOsCML3 or rOsCaM1 was mixed with the binding buffer with the addition of either 5 mM $CaCl_2$ or 2 mM EGTA. The samples were analyzed by electrophoretic resolution in 1% (w/v) agarose-0.5x TBE, and visualized under UV-light after ethidium bromide staining, as previously described (Grasser et al. 2004).

2.2.4) Expression analysis of *OsCML3* gene in rice (*Oryza sativa* L.) under various conditions

A) Primer design

Based on the *OsCML3* (AK111834) and *OsEF1α* (AK105030) nucleotide sequences retrieved from the Rice Genome Annotation Project database (Ouyang et al. 2007) and GenBank at the National Center for Biotechnology Information (Benson et al. 2013), a pair of primers for amplifying of each gene was designed. The sequence and the length of primers are shown in Table 2.7.

B) Preparation of rice seedlings and stress treatments

Rice seedlings (Oryza sativa 'KDML105') were grown in Limpinuntana's nutrient solution (see Appendix C) under a 12 hr light/12 hr dark photoperiod. All stresses were initiated 3 hours after the start of the light period by transferring 3 week-old seedlings to various conditions as described below. Rice seedlings were grown with a completely randomized design (CRD) with at least three biological replications. Ten seedlings were pooled for each replication.

Table 2.7 List of primers used for determining *OsCML3* expression patterns

Gene	Primer	Sequence 5' to 3'	Length (bp)
OsCML3	Forward	ACTACAACGAGTTCCTCAAG	20
	Reverse	CATCAGAACAGTTGCAAACC	20
OsEF1α	Forward	ATGGTTGTGGAGACCTTC	18
	Reverse	TCACCTTGGCACCGGTTG	18

B.1) Salt stress

Rice seedlings were transfer into Limpinuntana's nutrient solution containing 150 mM NaCl to induce salt stress. Control experiment was perform with the same nutrient solution except supplemented with 150 mM NaCl. At various time 0, 1, 3, 6, 12, 24, 48h intervals after treatment, the leaves were collected immediately using liquid nitrogen and then kept at -80 ^{o}C until they were used for RNA extraction.

B.2) Cold stress

Rice seedlings were transferred to cold temperature at 15 ^{o}C in the growth chamber. Control experiment was performed using the same nutrient solution except growing at normal temperature of 25 ^{o}C. At various time 0, 1, 3, 6, 12, 24, 48h intervals after treatment, the leaves were collected immediately using liquid nitrogen and then kept at -80 ^{o}C until they were used for RNA extraction.

B.3) Auxin application

Rice seedlings were transferred into Limpinuntana's nutrient solution containing 50 μM 3-Indoleacetic acid (IAA) in 250 μM KOH. Control experiment was performed using the same nutrient solution except supplemented with 250 μM KOH. At various time 0, 1, 3, 6, 12, 24, 48h intervals after treatment, the leaves were collected immediately using liquid nitrogen and then kept at -80 ^{o}C until they were used for RNA extraction.

B.4) Cytokinin application

Rice seedlings were transferred into Limpinuntana's nutrient solution containing 50 μM 6-Benzylaminopurine (BA) in 250 μM KOH. Control experiment was performed using the same nutrient solution except supplemented with 250 μM

KOH. At various time 0, 1, 3, 6, 12, 24, 48h intervals after treatment, the leaves were collected immediately using liquid nitrogen and then kept at -80 ^{o}C until they were used for RNA extraction.

C) RNA extraction

Rice samples were ground in liquid nitrogen to a fine powder using a chilled mortar and pestle. Total RNA from the frozen tissues was extracted using the TRI REAGENT (Molecular Research Center, USA) (see appendix D) with 0.2 mL chloroform and precipitated by mixing with isopropanol.

D) Qualitative and quantitative analyses of total RNA

The concentrations of total RNA samples were determined by dilution and measurement of the absorbance at 260 nm. Calculation of RNA concentration was performed by Equation 1.

Equation 1 = RNA concentration (ng/µl/OD) = A_{260} x Dilution factor x 40

The qualitative analysis to determine the purity of RNA was determined by measuring absorbance at 260 nm and 280 nm and calculating the ratio of the A_{260} and A_{280} (A_{260}/ A_{260}).

In addition, quality of the prepared RNA was determined by TBE agarose gel electrophoresis. A 1% agarose gel containing 1x TBE buffer was prepared, and 1x TBE buffer (see appendix C) was used as a running buffer. The RNA samples were mixed with RNA-loading dye for the final concentration of 1X (5 mM Tris-HCl, pH 7.5, 0.025% bromophenol blue, 6% glycerol). The mixed samples with dye were loaded into the gel, and the gel electrophoresis was run at 100 V for 50 minutes. The gel was stained by 1 mg/ml ethidium bromide solution (see Appendix C) for 5

minutes and destained in water for 5 minutes. The stained gel was viewed on the gel documentation apparatus (Gel Doc™, Syngene).

E) DNase I treatment

Treatment of total RNA with DNase I (Fermentas, USA) was performed to remove the remaining DNA. The treatment reaction was carried out in a 30-µl reaction containing 1X DNase I buffer, 10 µg of RNA sample, 20 units of RiboLock RNase Inhibitor (Fermentas), 1 unit of DNase I and DEPC-treated H_2O added up to 30 µl. The reaction was incubated at 37 ºC for 1 hour and then heat-inactivated at 65 ºC for 10 minutes and cooled to 10 ºC. The samples were then used for reverse transcription or kept at -80 ºC.

F) Reverse transcription reaction

The reverse transcription reaction was performed using iScript™ Reverse Transcription Supermix kit (BIO-RAD, USA) following the manufacturer's instruction. The reaction was carried out in a 20-µl reaction containing 1X iScript reverse transcription supermix, 1 pg to µg of DNase I-treated RNA and Nuclease-free water added up to 20 µl. The reaction mixture was incubated at 25 ºC for 5 minutes, and the temperature was increased to 42 ºC for 30 minutes. The enzyme was heat-inactivated at 85 ºC for 5 minutes and cooled to 10 ºC. The reverse transcription reaction was subsequently used for PCR amplification or stored at -20 ºC.

G) Real-time PCR amplification

Real-time PCR reactions were performed using the SsoFast™ EvaGreen® Supermix (BIO-RAD, USA) in a 10-µl reaction containing 1X SsoFast EvaGreen Supermix, 400 nM each primer and 4 µl of DNA template. The real-time PCR was

conducted using iCycler iQ real-time system (CFX96, BIO-RAD). The reaction was pre-denatured at 95 °C for 5 minutes, followed by 40 cycles of denaturing at 95 °C for 30 seconds, annealing at 57.9 ^{o}C for 30 seconds, and extension at 72 °C for 30 seconds. The signal was read after extension of each cycle. The melting curve was constructed by increasing the PCR product after amplification from 60 to 95 °C with the increment of 0.5 °C and held for 10 seconds. The melting curve results were read at every increment.

H) Amplification efficiency

In order to determine the efficiency of the real-time PCR and optimize the running condition, a serial dilution of the template was performed and the diluted template was run in a real-time PCR. The results were utilized to generate a standard curve. The amount of template (concentration or dilution factor) was plotted in log scale on the Y-axis while the C_T value, which is the cycle number that the fluorescent signal reaches the threshold level, was on the X-axis. Amplification efficiency was then calculated using the slope of the standard curve. Each dilution was assayed in triplicate. Standard curve with the C_T was plotted against the log of the starting quantity of template. Then the efficiency was calculated by Eq. 2, and converted to percent efficiency by Eq. 3.

Eq. 2 $E = 10^{-1/slope}$

Eq. 3 $\%\ Efficiency = (E-1) \times 100$

I) Relative Quantification

The gene expression was calculated by subtracting the C_T of calibrator (untreated) from the C_T of experimental samples. The fold of gene expression was calculated and

compared by relating to the expression of the reference gene - *EF1-α* (Pfaffl 2001). Fold of expression was calculated as shown in Eq. 4.

$$\text{Eq. 4} \quad \text{Ratio} = \frac{(E_{\text{target}})^{\Delta C_T, \text{target(calibrator - test)}}}{(E_{\text{ref}})^{\Delta C_T, \text{ref(calibrator - test)}}}$$

2.2.5) The *cis*-acting elements prediction

The upstream sequence of *OsCML3* (AK111834) coding region was retrieved from GenBank (Benson *et al*., 2013) and bioinformatically analyzed using the Database of Plant Cisacting Regulatory DNA Elements (PLACE) (http://www.dna.affrc.go.jp/PLACE/) (Prestridge 1991) and the Plant Promoter Analysis Navigator (PlantPAN) (http://plantpan.mbc.nctu.edu.tw/) (Chang et al. 2008) were performed. In this study, *cis*-acting elements were considered including DREs (drought- responsive elements), ABREs (ABA-responsive elements) and LTREs (low temperature responsive elements).

2.2.6) Overexpression of *OsCML3* in *Arabidopsis thaliana*

A) Construction of the recombinant plasmids

To construct the pCAMBIA1301 encoding either OsCML3, or OsCML3m, the coding region of *OsCML3* (AK111834), or *OsCML3m* were amplified from the *OsCML3* cDNA clone using OsCML3-NcoI F and OsCML3-NheI R primers for OsCML3, and OsCML3-NcoI F and OsCML3m-NheI R primers for *OsCML3*m. The list of primer sequences and their annealing temperatures is shown in Table 2.8.

Table 2.8 List of gene-specific primers involved in construction of recombinant pCAMBIA1301

Primer	Sequence 5' to 3'	Annealing temperature (^{o}C)
OsCML3-NcoI F	CCATGGACCACCTGACAAAGGAGC	60.7
OsCML3-NheI R	GCTAGCTCAGAGGATGGTACATGAGG	
OsCML3m-NheI R	GCTAGCTCACTTTGCCATCATGACC	
35SBamF1	GGATCCTCTCGAGCTGGCGTAATAGCGA	59.0
35SSalR1	CTGGTCGACTAATTCCCGATCTAGTAAC	
Up35S	GCGGATAACAATTTCACACAGG	60.0
InCML3	TTGCCATCATGACCTTGAGG	
DonosA	GCAAGGCGATTAAGTTGGGTAACG	
PcbF	AAGCTTTCTCGAGCTGGCGTAATAGCGA	60.7
PcbR	CTGATAGTTTAATTCCCGATCTAGTAAC	

The PCR reactions comprised of 0.6 mM dNTP mixture, 0.2 μM each primer, 1X *Pfu* DNA polymerase buffer, 50 ng of DNA template, and 1.25 U of *Pfu* DNA polymerase (Biolab, USA) with an initial denaturation of 94 ^{o}C for 7 min followed by 30 cycles of denaturation at 94 ^{o}C for 1 minute, annealing temperature at 60.7 ^{o}C for 1 minute and extension at 72 ^{o}C for 1 minute and 30 seconds, and a final elongation at 72 ^{o}C for 10 min by adding five units of *Tag* DNA polymerase (Fermentus, Inc., USA). The PCR products were analyzed by 1% agarose gel electrophoresis and then purified from agarose gel using Geneaid gel extraction protocol (Geneaid, USA). The

ligation reaction consisted of a 1:3 molar ratio of T&A vector (RBC, Taiwan) to insert DNA, 1X T4 DNA ligase buffer, 3 units of T4 DNA ligase and Nuclease-free water added to a final volume of 20 μl. The reaction was incubated overnight at 22 ^{o}C. The ligation product was then transformed into *E. coli* (Top 10). A single colony was picked and cultured in LB medium containing 100 μg/ml ampicillin overnight. The recombinant plasmids were extracted by Mini Plasmid Kit and then digested with *Nco*I and *Nhe*I with incubation at 37 ^{o}C. The products were analyzed by 1% agarose gel electrophoresis and nucleotide sequencing was performed using M13 forward and reverse primers. The resulting amplicons of *OsCML3* and *OsCML3m* cloned into the T&A cloning vector were pTA-OsCML3-Over, pTA-OsCML3m-Over, respectively. After checking the sequence, all plasmids containing correct nucleotide sequence were digested with *Nco*I and *Nhe*I using the conditions recommended by the enzyme manufacturer. Then, the *OsCML3* and *OsCML3m* fragments of were individually sub-cloned into pGEM-T vector containing a CaMV35S promoter fused with *Cam1-1* (Takpirom 2007) by replacing *Cam1-1* with *OsCML3* or *OsCML3m* via the *Nco*I and *Nhe*I sites, resulting in pGEM-CAMV35S-OsCML3 or pGEM-CAMV35S-OsCML3m in order to put *OsCML3* or *OsCML3m* under the control of the 35Spromoter. The pGEM-CAMV35S-OsCML3m was partially digested using *Hin*dIII (Takara, Japan) and then ligated into *Hin*dII-digested pCAMBIA1301 (see Appemdix A-8), resulting in pCAMBIA-CAMV35S-OsCML3m. To construct pCAMBIA1301 containing *OsCML3*, pGEM-CAMV35S-OsCML3 was used as template to amplify the fragment of CaMV35S fused with *CML3* gene using a pair of primers (35SBamF1 and 35SSalR1) containing *BamH*I and *Sal* I restriction sites,

respectively. The PCR reaction comprised of 0.25 mM dNTP, 0.3 μM each primer, 1X KOD DNA polymerase buffer, 50 ng of DNA template, 1.5 mM $MgSO_4$ and 1 U of KOD-Plus-Neo DNA polymerase (TOYOBO, Japan) with an initial denaturation of 95 ^{o}C for 5 minutes followed by 30 cycles of 95 ^{o}C for 1 minute, Ta 59 ^{o}C for 45 s and 68 ^{o}C for 1 minute and 15 seconds, and a final elongation at 68 ^{o}C for 10 min. To add A-tail at the 3′ end, the PCR product was separated in 1% agarose gel and purified using Gel extraction kit (CWBIO, China), and the purified gene fragment was mixed in the 50-μl reaction containing 1X Taq DNA polymerase buffer, 0.25 mM dNTPs and 5 units of Taq DNA polymerase (CWBIO, China) and incubated at 72 ^{o}C for 30 minutes. The PCR product was ligated into EZ-T vector (GenStar) (see Appendix A-9). The reaction consisted of a 1:3 molar ratio of EZ-T vector to insert DNA, 1X Ligation buffer, 1 μl of EZ-T^{TM} DNA ligase and Nuclease-free water added to a final volume of 20 μl. The reaction was incubated at 16 ^{o}C for 30 minutes. The ligation product was then transformed into *E. coli* (Top 10). A single colony was picked and cultured in LB medium containing 100 μg/ml ampicillin overnight. The EZ-CAMV35S-OsCML3 plasmid was extracted by Plasmid extraction kit (CWBIO, China) and then digested with *Bam*HI and *Sal*I (Takara, Japan) with incubation at 37 ^{o}C. The nucleotide sequence of the insertion was determined using T7 promoter primer and T3 promoter primer. After checking the DNA sequence, the EZ-CAMV35S-OsCML3 was digested using *Bam*HI and *Sal*I (Takara, Japan) and then ligated into *Bam*HI and *Sal*I - digested pCAMBIA1301, resulting in pCAMBIA-CAMV35S-OsCML3. The nucleotide sequences of pCAMBIA-CAMV35S-OsCML3m and pCAMBIA-CAMV35S-OsCML3 were determined using Up35S,

InCML3 and DonosA primers which were designed from the upstream sequence of the CaMV35S, within *OsCML3* coding sequence and downstream of *Nos* terminator, respectively.

B) Transformation of recombinant plasmids into Agrobacterium cells

A 250 µl of A*grobacterium* competent cells was mixed with 500 ng of pCAMBIA-CAMV35S-OsCML3m, pCAMBIA-CAMV35S-OsCML3 or pCAMBIA1301 and then followed the protocol described above. After transformation, the cell suspension was spread onto LB agar plates containing 100 µg/ml gentamycin, 25 µg/ml rifampicin and 50 µg/ml kanamycin, and incubated at 28 ºC for 2 days. The growing colonies were picked and checked by colony PCR amplification.

C) Colony PCR analysis

Amplification reactions were performed in a 20-µl reaction containing 1X Taq DNA polymerase master mix (GenStar, China), a small amount of colony, 0.25 µM each of OsCML3-NcoI F and OsCML3-NheI R for *OsCML3*, OsCML3-NcoI F and OsCML3m-NheI R for *OsCML3m*, PcbF and PcbR for pCAMBIA1301. PCR amplification was performed as follows: pre-denaturation at 95 ºC for 5 minutes, 35 cycles of denaturation at 94 °C for 1 minutes, annealing at 60.7 °C for 1 minute and extension at 72 °C for 1 minute and 15 seconds. In the final extension step, 72 °C for 5 minutes was set. Then, PCR products were analyzed by agarose gel electrophoresis.

D) Growing Arabidopsis plant

Seeds of *Arabidopsis thaliana* L., ecotype Columbia were sterilized with solution containing 1.2% NaClO and 0.05% Tween-20 with shaking for 10 minutes

and then washed 7 times with sterile water. Sterilized seeds were plated on Murashige & Skoog (MS) agar (1962) containing 3% sucrose (see Appendix C) and then incubated in darkness at 4 ^{o}C for 2-3 days. The plates were then moved to the growth chamber at 22 ^{o}C under a 16:8 hour light: dark photoperiod for ten days. After that, small seedlings were transferred to soil that comprised of a 3:1:1 volume ratio of Peat moss to Vermiculite to Perlite for continuous growth.

E) Arabidopsis thaliana floral dip transformation method

One day before floral dipping, the siliques and opened inflorescences were cut and removed from 4-week old plants. For preparation of the *Agrobacterium* suspension, a single colony of recombinant *Agrobacterium* was picked and cultured in 20 ml of LB broth containing 100 μg/ml gentamycin, 25 μg/ml rifampicin and 50 μg/ml kanamycin, and incubated with shaking at 28 ºC for 1 day. After that, the cell culture was transferred into 200 ml of LB broth containing the same antibiotics with shaking at 28 ºC for 1 day. Then, the cells were collected by centrifugation at 3000 rpm for 15 minutes at room temperature. The supernatant was discarded, and cell pellets were re-suspended with transformation buffer (50-70 ml of half-strength MS medium containing 3% sucrose, 0.2% silwet L-77). *Agrobacterium* suspension was poured into big Petri dish, and then flowers of the prepared *Arabidopsis* plants were dipped into the cell suspension. The plants were allowed to soak with cell suspension for 15 minutes. After dipping, plants were moved to a big box with enough water added at the bottom. The plants were covered with another big box and transferred to darkness for 24 hours. All plants were then moved back to grow at normal condition after 24 hours in dark (Clough and Bent 1998).

F) Transgenic Arabidopsis selection

T_1 seeds were plated on MS agar containing 30 μg/ml hygromycin, and hygromycin-resisting plants were transferred to soil for self-pollination and propagation. T_1 seedlings, that showed the 3:1 segregation in hygromycin resistance, were collected. The T_2 and T_3 seeds, which were homozygous transgenic lines, were used for phenotypic investigation.

G) Preparation of Arabidopsis

The homozygous lines of transgenic *Arabidopsis* and non-transgenic *Arabidopsis* (wild type, WT) were grown on soil. After three weeks, leaves were collected and immediately frozen in liquid nitrogen and stored at -80 ^{o}C. All tissues were ground in liquid nitrogen to fine powder using a chilled mortar and pestle.

H) Extraction of genomic DNA

The genomic DNA was extracted from leaves using Genomic DNA extraction kit (see Appendix E) (Geneaid). The DNA samples were used as template for PCR to confirm whether the exogenous gene sequences were integrated into the genome of the putative transgenic plants. The amplification reactions were performed in a 20-μl reaction 1X KAPA Taq Ready Mix (KAPABIOSYSTEMS, 50-200 ng of genomic DNA, 0.4 μM each of 35Scheck-F and Guscheck-R for the transgenic 1301, 35Scheck-F and CML3check-R for the transgenic OsCML3, 35Scheck-F and CML3mcheck-R for the transgenic CML3m as shown in Table 2.9. PCR amplification was performed as follows: pre-denaturation at 95 ºC for 2 minutes, 30 cycles of denaturation at 95 °C for 30 seconds, annealing at 64 °C for 30 seconds and

extension at 72 °C for 1 minute. In the final extension step, 72 °C for 5 minutes was set. Then, PCR products were analyzed by agarose gel electrophoresis.

I) Extraction of RNA

Total RNA from the frozen tissues was extracted using the TRI REAGENT (Molecular Research Center, USA) [see in appendix A-1] mixed with 0.2 mL chloroform and precipitated by mixing with isopropanol.

J) Qualitative and quantitative analyses of total RNA

The quality and quantity of total RNA samples were determined by measurement of the absorbance at 260 and 280 nm. Calculation of RNA concentration was performed as described above.

K) DNase I treatment

Treatment of total RNA with DNase I (Fermentas, USA) was performed to remove the remaining DNA as described above.

Table 2.9 List of gene-specific primers for Arabidopsis molecular analysis

Primer	Sequence 5′ to 3′	Annealing temperature (^{o}C)
35Scheck-F	TGAAGATGCCTCTGCCGACAGTGGT	64.0
Guscheck-R	CAGGTGTTCGGCGTGGTGTAGAGCA	
CML3check-R	ATGGCCTCCACTTCCATGTCC	
CML3mcheck-R	GCCATCATGACCTTGAGGAACTCG	
AtExpCML3F	CCTCATGTACCATCCTCTGAGC ATCATCGCAAGACCGGCAACAGG	60.7

AtExpCML3R		
AtExpCML3mF	GGTCATGATGGCAAAGTGAGC	
AtExpEFalF	TTCGCTGTTAGGGACATGAGGC	
AtExpEFalR	CACCCTTCTTCACTGCAGCCTT	

L) Reverse transcription reaction

The reverse transcription reaction was performed using iScript™ Reverse Transcription Supermix kit (BIO-RAD, USA) following the manufacturer's instruction as described above.

M) Real-time PCR amplification

The Real-time PCR reactions were performed using the SsoFast™ EvaGreen® Supermix (BIO-RAD, USA). The reaction was carried out in a 10-µl reaction containing 1X SsoFast EvaGreen Supermix, 400 nM each of AtExpCML3F and AtExpCML3R pair, AtExpCML3mF and AtExpCML3R pair or AtExpEFalF and AtExpEFalR pair (Table 2.9) and 4 µl of DNA template. The real-time PCR was conducted using iCycler iQ real-time system (CFX96, BIO-RAD). The reaction was pre-denatured at 95 °C for 5 minutes, followed by 40 cycles of denaturing at 95 °C for 30 seconds, annealing at 60.7 °C for 30 seconds, and extension at 72 °C for 30 seconds. The signal was read after extension of each cycle. The melting curve was constructed by increasing temperature after amplification from 60 to 95 °C with the increment of 0.5 °C and held for 10 seconds. The melting curve results were read at every increment. The amplification efficiency was calculated as described above.

N) Relative Quantification

The gene expression level was calculated by subtracting the C_T of line 13308 (calibrator) from the C_T of the other lines (test) for the transgenic OsCML3. Also, the gene expression level of the transgenic OsCML3m was calculated by subtracting the C_T of line 23208 from the C_T of the other lines. The fold expression of the gene of interest was calculated and compared by relating its level to the expression level of the reference gene - *EF1-α* (Pfaffl 2001). Fold of expression was calculated as shown in Eq. 4.

Eq. 4 $$\text{Ratio} = \frac{(E_{\text{target}})^{\Delta C_T,\ \text{target(calibrator - test)}}}{(E_{\text{ref}})^{\Delta C_T,\ \text{ref(calibrator - test)}}}$$

O) Cold stress treatment

About sixty to seventy seeds of each transgenic lines and non-transgenic Arabidopsis (wild type) were plated on MS agar. Then the number of plates was divided into two groups with a completely randomized design (CRD) with four replicates in each line. Group one was grown under a 16 hr light/18 hr dark photoperiod at normal condition of 22 ^{o}C. The other group was grown under a 16 hr light/18 hr dark photoperiod at cold condition of 11 ^{o}C. At 22 ^{o}C, the germination rate of all lines was observed at days 3 and 9. At 11 ^{o}C, the germination rate of all lines was observed at days 9 and 14 at 11 ^{o}C,

To further investigate the cold response of Arabidopsis seedlings, the 14-day seedlings grown at 22 ^{o}C were transferred to soil with 4 plants per pot. The number of pots was divided into two groups with a completely randomized design (CRD) with four pots in each line. Group one was grown under a 16 hr light/18 hr dark

photoperiod at normal condition of 22 ^{o}C. The other group was grown under a 16 hr light/18 hr dark photoperiod at cold condition of 11 ^{o}C. After one month, the plants were weighted and then dried at 60 ^{o}C for 3 days. All dried plants were kept in the desiccator for 2 days before they were weighted.

CHAPTER III

RESULTS

3.1 Cloning of OsCML3

Based on the *OsCML3* cDNA sequence obtained from the National Institute of Agrobiological Sciences, Japan, a pair of primers for amplifying the coding region of *OsCML3m* which lacked the C-terminal extension was designed with the restriction endonuclease sites for *Nde*I and *Xho*I engineered at its 5′- and 3′-ends, respectively. The amplified PCR product of approximately 0.46 kb, which was the expected size of the *OsCML3m*, was obtained. Figure 3.1 shows the separation by agarose gel electrophoresis of the *OsCML3m* product obtained from PCR amplification using various annealing temperatures. The high yields of the PCR product of *OsCML3m* amplification were similarly found in all annealing temperatures. Because no significant amount of non-specific amplified DNA was detected, the PCR products of all annealing temperatures could be used for further cloning. The amplified *OsCML3m* gene fragment was extended by adding dA at the 3′ end using *Taq* DNA polymerase. After DNA fragment was purified using the Geneaid gel extraction kit, it was ligated into pTZ57R/T by T4 DNA ligase. Competent *E. coli* XL1-Blue cell was transformed with the ligation reaction and the transformant was selected by blue/white colony screening on LB plate containing ampicillin, X-gal and IPTG. White colonies were randomly picked and cultured for plasmid extraction. To verify insertion of the PCR product into pTZ57R/T vector, the potential recombinant plasmid containing the *OsCML3m* was digested with *Nde*I and *Xho*I at 37 °C

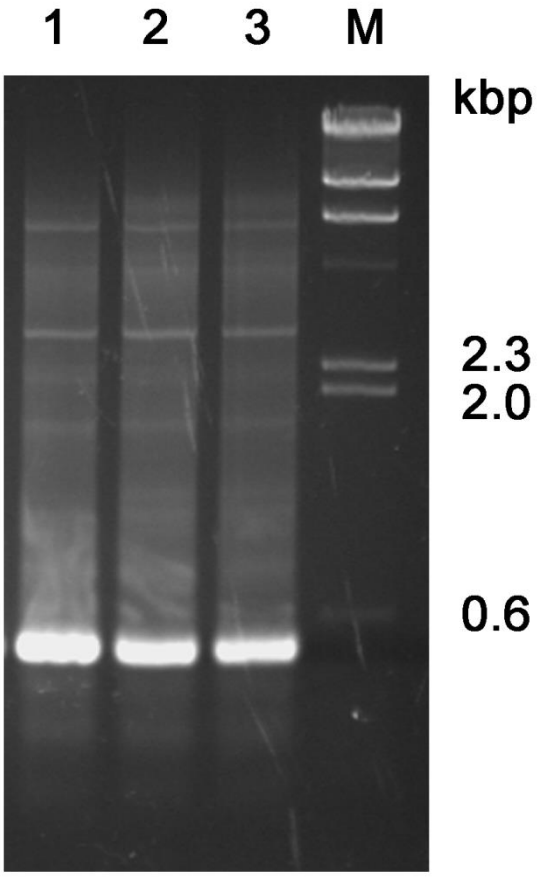

Figure 3.1 PCR products using *OsCML3* cDNA templates and varied annealing temperatures

Lane 1 = PCR product of *OsCML3m* using annealing temperature of 50 ^{o}C

Lane 2 = PCR product of *OsCML3m* using annealing temperature of 55 ^{o}C

Lane 3 = PCR product of *OsCML3m* using annealing temperature of 60 ^{o}C

Lane M = λ/*Hin*dIII standard DNA marker

overnight and analyzed by 1.0% agarose gel electrophoresis. The results show that, in addition of the 2.9-kb pTZ57R/T fragment, DNA fragment of approximately 0.46 in length was obtained as shown in Figure 3.2 (Lanes 2) as expected based on the restriction patterns of the recombinant plasmid harboring the *OsCML3m*. The resulting recombinant plasmid was called pTZ-OsCML3m. To sub-clone the *OsCML3m* into pET-21a expression vector, the pTZ-OsCML3m plasmid was extracted and digested with *Nde*I and *Xho*I. The *Nde*I and *Xho*I-digested *OsCML3m* fragment was then ligated into the same restriction sites in pET-21a vector. *E. coli* strain XL1-Blue was transformed with the ligation product and the transformant was selected by ampicillin resistance on LB agar. *E. coli* XL1-Blue single colonies were randomly picked for plasmid extraction and the purified plasmid was digested with *Nde*I and *Xho*I. After digestion, a linear pET-21a of 5.4 kb and the inserted *OsCML3m* fragment were obtained by agarose gel electrophoresis as expected based on the restriction pattern of the recombinant plasmid harboring *OsCML3m* (data not shown). The resulting recombinant plasmid was called pET21-OsCML3m. To confirm the nucleotide sequence of the *OsCML3m* inserted into pET-21a, the recombinant plasmid was subjected to DNA sequencing using T7 promoter and T7 terminator primers. The results show that the sequence of the *OsCML3m* in the recombinant plasmid shares 100 % identity with its respective cDNA sequence as shown in Figure 3.3. The coding regions of the *OsCML3m* gene was engineered to add stop codon after the last codon and did not fuse in frame with the 6x His tag coding sequence existing in pET-21a vector. Direction of the *OsCML3m* gene inserted into pET-21a is shown in Figure 3.4. The molecular weight of the recombinant

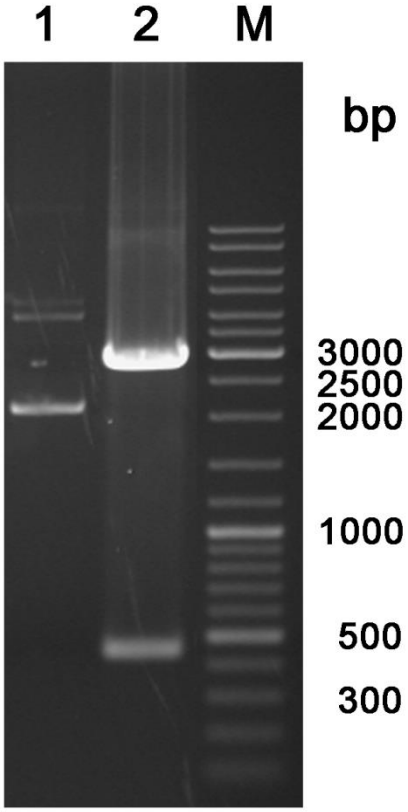

Figure 3.2 Restriction pattern of the recombinant plasmid pTZ-OsCML3m

Lane 1 = undigested pTZ-OsCML3m

Lane 2 = *Nde*I/*Hin*dIII-digested pTZ-OsCML3m

Lane M = 100 bp standard DNA marker

ATAACAATTCCCCTCTAGAAATAATTTTGTTTAACTTTAAGAAGGAGATATACAT

ATGGACCACCTGACAAAGGAGCAGATCGCCGAGTTCCGGGAGGCATTCAACCTG

M D H L T K E Q I A E F R E A F N L

TTCGACAAAGATGGAGACGGGACGATCACGAGCAAGGAGCTTGGGACGGTGAT

F D K D G D G T I T S K E L G T V M

GGGGTCGCTGGGGCAGTCGCCGACGGAGGCGGAGCTGAAGAAGATGGTGGAGG

G S L G Q S P T E A E L K K M V E

AGGTGGACGCGGACGGCAGCGGCAGCATCGAGTTCGAGGAGTTCCTGGGCCTCC

E V D A D G S G S I E F E E F L G L

TCGCCCGCAAGCTTCGCGACACCGGCGCCGAGGACGACATCCGCGACGCCTTCC

L A R K L R D T G A E D D I R D A F

GCGTCTTCGACAAGGACCAGAACGGCTTCATCACCCCCGACGAGCTCCGCCACG

R V F D K D Q N G F I T P D E L R H

TCATGGCCAACCTCAGCGACCCCCTCTCCGACGACGAGCTCGCCGACATGCTCCA

V M A N L S D P L S D D E L A D M L H

CGAGGCCGACTCCGACGGCGACGGCCAGATCAACTACAACGAGTTCCTCAAGGT

E A D S D G D G Q I N Y N E F L K V

CATGATGGCAAAGTGAAGCTCGAGA ATCTAGATGCNTNNNANNCNNNNNC

M M A K

Figure 3.3 Nucleotide and deduced amino acid sequences of the *OsCML3m* in the recombinant pET-21a. The red bold letters indicate start and stop codons. The blue letters show a partial nucleotide sequence of the T7 promoter.

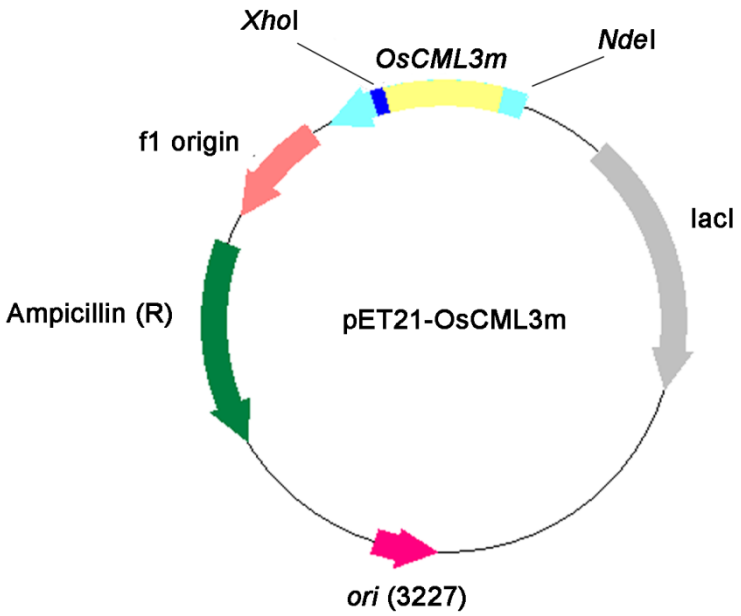

Figure 3.4 Map diagram of pET21a horboing the *OsCML3m*

OsCML3m (rOsCML3m) calculated from its deduced amino acid sequence was 16.5 kDa.

The *E. coli* BL21 (DE3) transformant containing pET21-*OsCML3m* was grown and induced by IPTG at a final concentration of 0, 0.2, 0.4, 0.6, 0.8 or 1.0 mM for 4 hours before the cells were harvested. The whole cell pellet was harvested and resuspended with 100 µl of lysis buffer containing 1 X sample buffer. Ten microliters of the mixed sample was subjected to electrophoresis on 12 % SDS-polyacrylamide gel. It was found that the expression of rOsCML3m in *E. coli* BL21 (DE3) was only detected in the presence of IPTG and its levels were similar in all concentrations of IPTG induction (Figure 3.5).

Crude protein of the recombinant OsCML3m prepared from 1 liter of LB medium was loaded into a phenyl-Sepharose column. Unbound protein was eluted from the column by Wash buffer I, and the rOsCML3m was eluted by Elution buffer I, indicating that rOsCML3m could be purified by Ca^{2+}-dependent phenyl-Sepharose hydrophobic chromatography. Figure 3.6A shows the representative protein patterns during rOsCML3m purification. The molecular weight of rOsCML3m was estimated to be approximatey 15.2 kDa by its mobility by SDS-PAGE when compared with those of standard proteins.

3.2 Biophysical characterization of OsCML3m proteins

The deduced amino acid sequences of OsCML3 and OsCML3m proteins were compared. Figure 3.7 shows the primary structures of OsCML3 and OsCML3m proteins using rOsCaM1 as a standard. Amino acids are presented in the single-letter

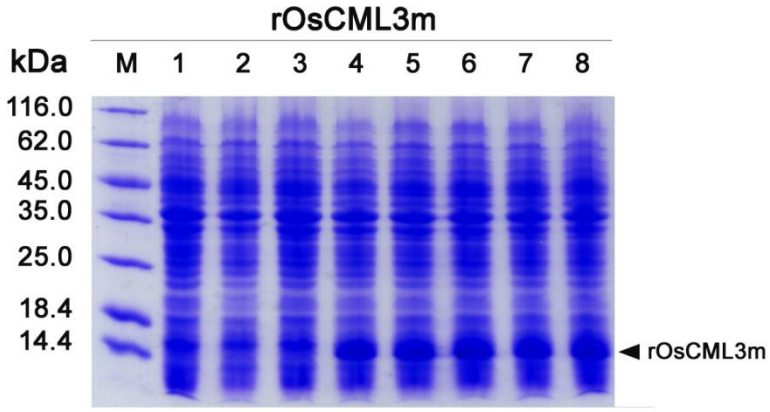

Figure 3.5 SDS-PAGE of whole cell extracts of *E. coli* BL21(DE3) harboring pET21-OsCML3m induced at various IPTG concentrations

Lane M = protein marker

Lane 1 = whole cell of *E. coli* BL21 (DE3) harboring pET-21a

Lane 2 = whole cell of *E. coli* BL21 (DE3) harboring pET-21a induced by 0.6 mM IPTG

Lane 3 = whole cell of *E. coli* BL21 (DE3) harboring pET21-OsCML3m

Lanes 4, 5, 6, 7, 8, 9 = whole cell of *E. coli* BL21(DE3) harboring pET21-OsCML3m induced by 0.2, 0.4, 0.6, 0.8 and 1.0 mM IPTG, respectively

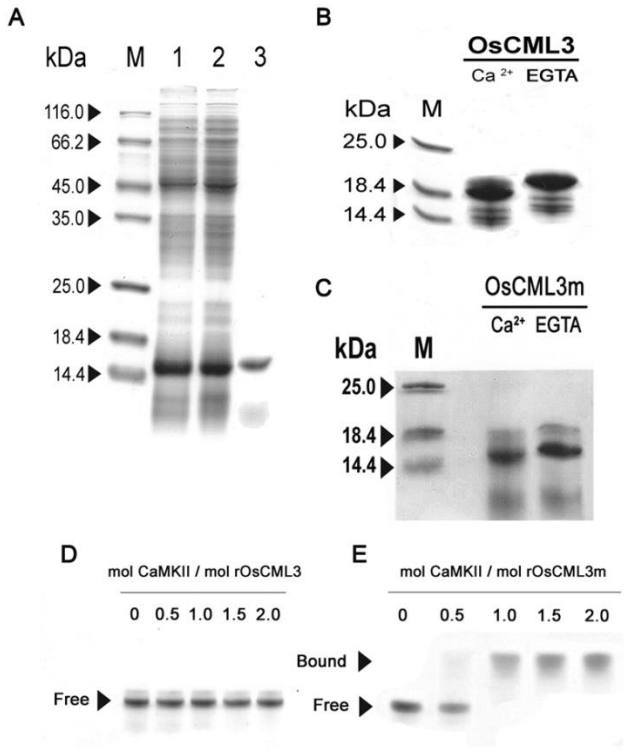

Figure 3.6 Analysis of the recombinant OsCML3m. Representative protein patterns of *E. coli* BL21 (DE3) harboring pET21-OsCML3m detected by SDS-PAGE during recombinant protein purification by a phenyl-Sepharose column (A). Lane M, molecular mass standard proteins; lane 1, crude extract; lane 2, flow-through fraction; lane 3, eluted protein. Calcium-induced electrophoretic mobility shift analysis of rOsCML3 (B, (Chinpongpanich et al. 2011)) and rOsCML3m (C). rOsCML3 and rOsCML3m proteins in the presence of 1 mM $CaCl_2$ ($+Ca^{2+}$) or 3 mM EGTA (+EGTA) was subjected to SDS-PAGE. Lane M, molecular mass standard proteins. Gel mobility shift analysis of rOsCML3 (C) and rOsCML3m (D) after incubation with increasing amounts (indicated by closed triangle) of CaMKII peptide and in the presence of Ca^{2+} and then resolved by denaturing 4 M urea/SDS-PAGE.

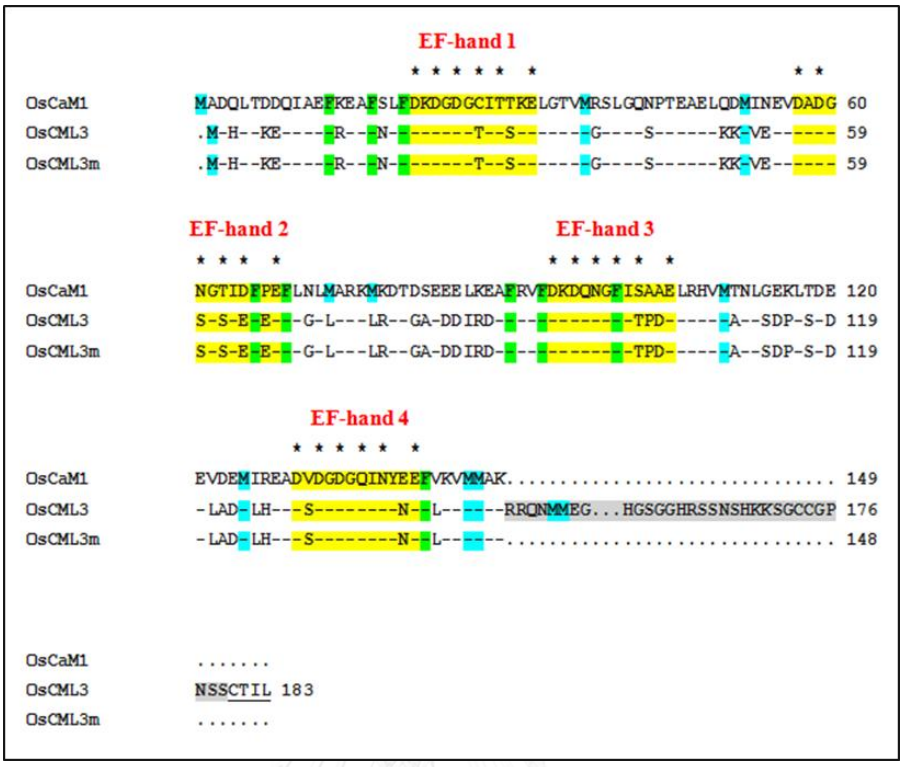

Figure 3.7 Comparison of the primary structures of OsCaM1, OsCML3 and OsCML3m proteins. The sequences are compared using OsCaM1 as a standard; identical residues in other sequences are indicated by a dash (-), and a gap introduced for alignment purposes is indicated by a dot (.). The EF-hand calcium binding motifs are marked in yellow color and residues serving as Ca^{2+}-binding ligands are marked with asterisks (*). Methionine (M) and Phenylanine (F) residues are highlighted in blue and green, respectively.

IUPAC nomenclature, and the sequences are aligned to illustrate the relationships of the four Ca^{2+}-binding loops. Table 3.1 shows characteristics of OsCML3 and OsCML3m proteins. From pairwise alignments, OsCML3 and OsCML3m share

Table 3.1 Amino acid sequence characteristics of OsCML3 and OsCML3m proteins compared with OsCaM1

Proteins	Amino acids (a)	Number of EF-hand (b)	Number of Met residues (c)	Percentage of Met residues (d)	Identity to CaM1 (%) (e)
OsCaM1	149	4	9	6.0	100
OsCML3	183	4	9	4.9	55.4
OsCML3m	148	4	7	4.7	68.5

(a) Number of amino acids of the deduced amino acid sequence. (b) Number of EF hands based on the prediction by InterProScan. (c) Number of methionine (M) residues in the deduced amino acid sequence. (d) Percentage of methionine (M) residues in the deduced amino acid sequence. (e) Number of identical residues divided by the total number of amino acids that have been aligned expressed in percentage.

55,4%, and 68.5% amino acid identities, respectively with OsCaM1. High percentage of methionine residues found in plant CaMs in general (6% in OsCaM1), is also found in OsCML3 and OsCML3m, which consist of 4.9% and 4.7% methionine residues, respectively. In addition, compared with OsCaM1, OsCML3 contains a C-terminally extended 35 amino acid tail.

One of the characteristics of CaM is its ability to bind Ca^{2+} in the presence of SDS, which increases its electrophoretic mobility relative to CaM in the absence of Ca^{2+}. Figure 3.6C shows that the degree of mobility shift of rOsCML3m appeared to be similar to that of the full-length rOsCML3 (Figure 3.6B) (Chinpongpanich et al. 2011) when incubated with 1 mM Ca^{2+} compared with 3 mM EGTA prior to electrophoresis. This result indicates that the deletion of the basic C-terminal extension (CTE) of rOsCML3 has no effect on the Ca^{2+}-binding property, which was also observed from the successful purification of rOsCML3 by Ca^{2+}-dependent hydrophobic chromatography on phenyl-Sepharose.

To further compare the properties between rOsCML3 and rOsCML3m proteins, its ability to bind the peptide derived from CaM kinase II (CaMKII) was assessed by gel mobility shift assay. Since CaM kinase II is a CaM-binding protein, examination of the ability to interact with its CaM-binding domain of particular CaM-related proteins would suggest whether they likely function similarly to and share similar sets of binding proteins with CaM. Incubation of 100 picomoles of recombinant proteins in the presence of 1 mM Ca^{2+} or 3 mM EGTA with different amounts of the peptide prior to PAGE-4 M urea resolution was performed. When incubated with the CaMKII peptide, rOsCML3m displayed a peptide-protein complex in the presence of Ca^{2+} (Figure 3.6E), whereas rOsCML3 did not (Figure 3.6D)

(Chinpongpanich et al. 2011). In the absence of Ca^{2+}, both proteins showed no binding ability to the peptide (data not shown). These results suggest that rOsCML3 has structural regions for binding the CaMKII peptide similar to those in CaM, but that the CTE domain appeared to obstruct this interaction.

Far-ultraviolet circular dichroism (far-UV CD) spectroscopy was used to determine the secondary structure of rOsCML3m protein and whether any structural changes occurred upon Ca^{2+}-binding. For CaM, major conformational changes including an increase in α-helicity upon Ca^{2+}-binding have been documented. Figure 3.8 shows that the far-UV CD spectra of rOsCML3 and rOsCML3m in the presence of 1 mM $CaCl_2$ or 1 mM EGTA have two minima near 208 and 222 nm indicating that these proteins contain substantial α-helical secondary structure. $[\theta]_n$ is molar ellipticity per residue for a residue of n amino acid residues. Table 3.2 summarizes values of $-[\theta]_n$ at 208 and 222 nm from the spectra of both proteins in the presence of 1 mM $CaCl_2$ or 1 mM EGTA and their changes upon Ca^{2+} addition, where Δ is the difference of molar ellipticity per residue between the presence and absence of $Ca^{2+}$and %Δ is the ratio of Δ and the molar ellipticity per residue in the presence of Ca^{2+} expressed in percentage form. Upon Ca^{2+} addition, an increase in molar ellipticity per residue at 208 and 222 nm was clearly observed for rOsCaM1 that displayed a large increase in $[\theta]_n$ at 222 nm with the %Δ of 23.5 when compared with the value in the absence of Ca^{2+} at 222 nm. This result indicates that the helical content was highly increased in OsCaM1 upon Ca^{2+} binding. However, rOsCML3, which shares 68.5 % identity to that of typical CaM protein, displayed a much smaller change in $[\theta]_n$ (10.6%). Surprisingly, rOsCML3m, which lacked CTE, showed higher increase in $[\theta]_n$ at 222 nm (68.7%).

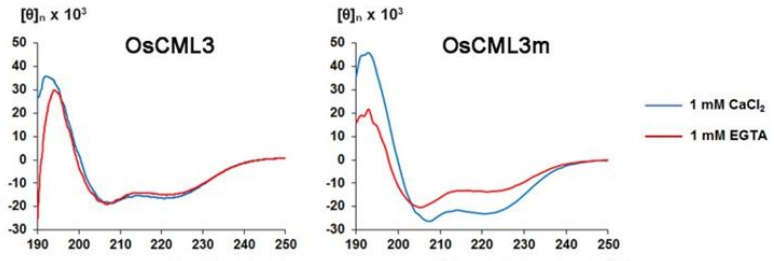

Figure 3.8 **Ca^{2+}-induced conformational changes of the rOsCML3 and rOsCML3m proteins measured by Far-UV CD spectroscopy.**

Table 3.2 Summarizes values of $-[\theta]_n$ at 208 and 222 nm from the spectra of rOsCaM1, rOsCML3 and rOsCML3m proteins in the presence of 1 mM $CaCl_2$ or 1 mM EGTA and their changes upon Ca^{2+} addition.

Recombinant protein	$-[\theta]_{n(208)}x10^{-2}$ (deg.cm^2 /dmol.residues)		Δ	%Δ	$-[\theta]_{n(222)}x10^{-2}$ (deg.cm^2 /dmol.residues)		Δ	%Δ	Reference
	$-Ca^{2+}$	+EGTA			$-Ca^{2+}$	+EGTA			
OsCaM1	14.29	15.65	1.36	9.5	11.44	14.13	2.69	23.5	(Chinpongpanich et al. 2011)
OsCML3	18.4	18.53	0.13	0.7	14.76	16.32	1.56	10.6	
OsCML3m	18.3	26.0	7.7	42.1	13.47	22.73	9.26	68.7	In this study

8-Anilino-1-naphthalenesulphonate (ANS) is a fluorescent probe that displays a blue shift when its environment is changed from an aqueous to a nonpolar medium. In addition, while its fluorescence in water is usually weak, ANS shows an enhanced fluorescence intensity in nonpolar medium. Therefore, ANS is a useful probe for Ca^{2+}-induced exposure of hydrophobic patches in the globular domains of CaMs because its fluorescence spectrum is changed and can be monitored when it binds to the accessible hydrophobic surface of the proteins. To examine Ca^{2+}-induced exposure of the hydrophobic surfaces of the rOsCML3m protein, emission spectra of 100 μM ANS in the presence of protein was monitored with the excitation wavelength set at 370 nm. Figure 3.9 shows representative emission spectra of 100 μM ANS in an aqueous buffer mixed with 1 μM of rOsCML3 (Chinpongpanich et al. 2011) and rOsCML3m in the presence of 3 mM EGTA or 1 mM Ca^{2+}. Table 3.3 summarizes the changes in ANS fluorescence in the presence of rOsCML3m upon Ca^{2+} addition in comparison with those of rOsCML3 (Chinpongpanich et al. 2011). When mixed with each protein in the presence of EGTA, ANS displayed a relatively weak fluorescence with a maximum wavelength near 520 nm, which is almost identical to that of ANS alone (data not shown). In the presence of Ca^{2+}, a significant blue shift (by 46 or 47 nm for rOsCML3 or rOsCML3m, respectively) in the maximum emission wavelength was observed. Similar large increases in the fluorescence intensity of rOsCML3 (4.75-fold) and rOsCML3m (5.31-fold) were observed, suggesting that the 35-amino-acid CTE does not impede the exposure of its hydrophobic surface upon Ca^{2+} binding.

3.3 Subcellular Localization

OsCML1 (alias OsCaM61), the CML protein most similar to OsCML3

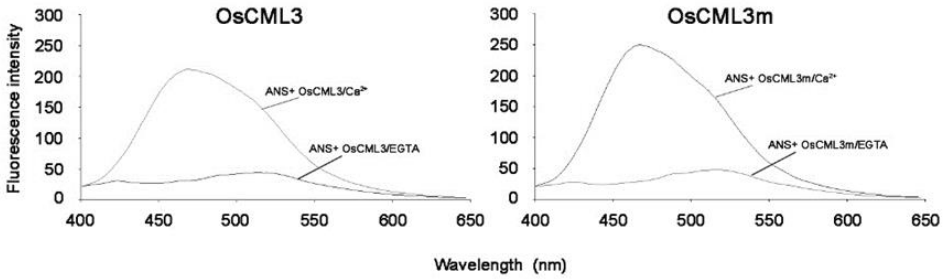

Figure 3.9 Conformational changes of the rOsCML3 and rOsCML3m proteins measured by ANS fluorescence. The fluorescence was recorded in 1 mM Tris-HCl (pH 7.5) in the presence of 1 mM $CaCl_2$ or 1 mM EGTA. Spectra shown are representatives of three independent experiments.

Table 3.3 The changes in ANS fluorescence in the presence of each of rOsCML proteins upon Ca^{2+} addition.

Recombinant Protein	Emission maximum(nm)	$\Delta\lambda_{max}$ (a)	$I_{max}(+Ca^{2+})/I_{max}(-Ca^{2+})$ (b)	Reference
rOsCML3	468	46	4.75	Chinpongpanich *et al*., 2011
rOsCML3m	467	47	5.31	In this study

(a) $\Delta\lambda_{max}$ indicates the difference of maximum fluorescence emission of ANS in the presence and in the absence of Ca^{2+}. (b) $I_{max}(+Ca^{2+})/I_{max}(-Ca^{2+})$ means the ratio of the maximum fluorescence intensity of ANS in the presence of Ca^{2+} to that in the absence of Ca^{2+}.

(Xiao et al. 1999), was reported to be membrane-associated when prenylated and localized in the nucleus when unprenylated (Dong et al. 2002). OsCML3 also contains a basic C terminal extension (CTE) and a prenylation site, called CaaX (C is cysteine, a represents an aliphatic amino acid, X is usually serine, methionine, glutamine, cysteine, alanine or leucine) motif (Rodríguez-Concepción et al. 1999). A putative prenylation site (CTIL in OsCML3) may function in membrane association similar to OsCML1 containing CVIL. To test whether the basic CTE domain containing the prenylation site imposed such a role on OsCML3, we determined the subcellular localization of the CTE-truncated OsCML3m protein compared to the full-length OsCML3. By bioinformatics analysis using PlantLoc, WoLF PSORT and Plant-mPLoc, OsCML3 and OsCML3m were predicted to localize in several compartments (Table 3.4), but the actual localization of OsCML3 and OsCML3m could not be concluded from these predictions. To clearly study the location of OsCML3 and OsCML3m in *planta*, the pCAMBIA1302 encoding either OsCML1, OsCML1m, OsCML3 or OsCML3m fused with GFP at the N-terminal end was constructed. First, the amplified PCR products of approximately 0.79, 0.59, 0.47, 0.58 and 0.47 kbp, which were the expected sizes of the *GFP*, *OsCML1*, *OsCML1m*, *OsCML3* and *OsCML3m* genes, respectively, were obtained. Figure 3.10 shows the separation by agarose gel electrophoresis of the *GFP*, *OsCML3 and OsCML3m* gene products obtained from PCR amplification using various annealing temperatures. After each DNA fragment was purified using the Geneaid gel extraction kit, it was ligated into T&A cloning vector by T4 DNA ligase. To verify insertion of the PCR product into T&A cloning vector, the potential recombinant plasmid containing each gene extracted from the transformants was digested with *Xho*I and *BstE*II at 37 °C

Table 3.4 *In silico* predicted subcellular localization of OsCML3, OsCML3m and OsHMGB1

Protein	Program for analysis		
	PlantLoc	WoLF PSORT	Plant-mPLoc
OsCML3	Chloroplast (probably in Golgi apparatus, nucleus)	Nucleus	Cell membrane, cytoplasm
OsCML3m	Nucleus, peroxisome	Cytoplasm, nucleus	Cell membrane, cytoplasm
OsHMGB1	Nucleus, cytoplasm	Nucleus	Nucleus

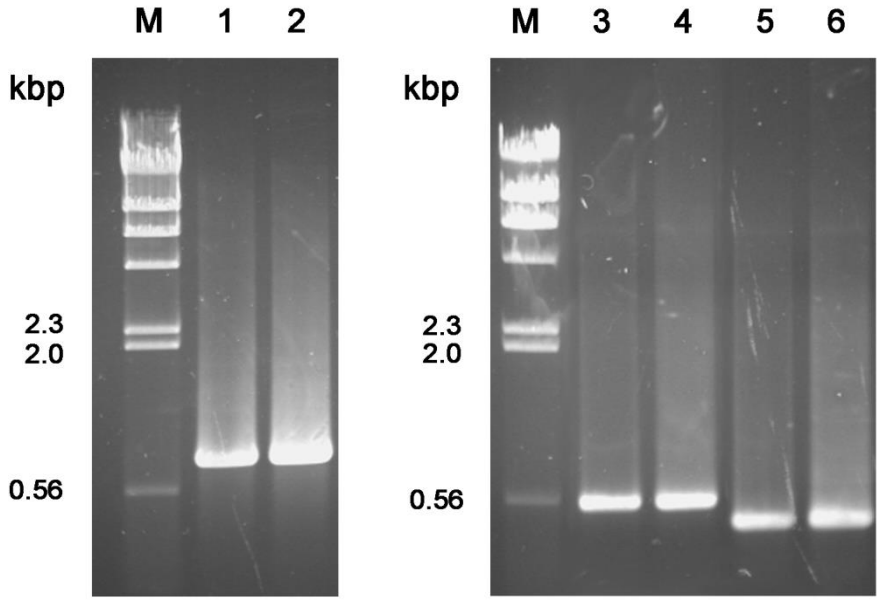

Figure 3.10 PCR products using various DNA templates and annealing temperatures

Lane M = λ/*Hin*dIII standard DNA marker

Lane 1 = PCR product of *GFP* gene using annealing temperature of 56.8 ^{o}C

Lane 2 = PCR product of *GFP* gene using annealing temperature of 59.3 ^{o}C

Lane 3 = PCR product of *OsCML3* gene using annealing temperature of 56.8 ^{o}C

Lane 4 = PCR product of *OsCML3* gene using annealing temperature of 59.3 ^{o}C

Lane 5 = PCR product of *OsCML3m* gene using annealing temperature of 56.8 ^{o}C

Lane 6 = PCR product of *OsCML3m* gene using annealing temperature of 59.3 ^{o}C

overnight and analyzed by 1.0% agarose gel electrophoresis. The results show that, in addition of the pTA fragment of 2.7 kb, DNA fragments of approximately 0.79, 0.59, 0.47, 0.58 and 0.47 kb in length were obtained as expected based on the restriction patterns of the recombinant plasmids harboring *GFP*, *OsCML1*, *OsCML1m*, *OsCML3* or *OsCML3m* as shown in Figures 3.11. After checking the sequence, all plasmids containing the correct nucleotide sequence were used to digest with *Xho*I and *BstE*II. Then, the digested fragments of *OsCML1*, *OsCML1m*, *OsCML3* and *OsCML3m* were individually inserted into pTA-GFP via the *Xho*I and *Bst*EII sites at the 3′ end of the GFP coding sequence. After transformation and digestion with *Nco*I and *Bst*EII to verify the insertion, a linear pTA vector of 2.7 kb and the inserted *OsCML* fused with *GFP* based on the restriction patterns of the recombinant plasmids harboring *OsCML1*, *OsCML1m*, *OsCML3* and *OsCML3m* were obtained as shown in Figures 3.12. The resulting plasmids were called pTA-GFP-OsCML1 pTA-GFP-OsCML1m, pTA-GFP-OsCML3 and pTA-GFP-OsCML3m respectively. After that, the fragments of GFP-OsCML1, GFP-OsCML1m, GFP-OsCML3 and GFP-OsCML3m were sub-cloned into pCAMBIA1302 using *Nco*I and *Bst*EII sites, resulting in pCAMBIA-GFP-OsCML3, pCAMBIA-GFP-OsCML3m, pCAMBIA-GFP-OsCML1 and pCAMBIA-GFP-OsCML1m, respectively, which can be expressed under the control of the CaMV 35S promoter.

To verify the gene insertion, all recombinant plasmids were digested with *Nco*I and *Xho*I. Three fragments of approximately 765, 1094, 1842 in length were obtained as expected based on the restriction pattern of all plasmids, including pCAMBIA1302. For the fourth fragment, the size of 8177, 8063, 8165 or 8060 was

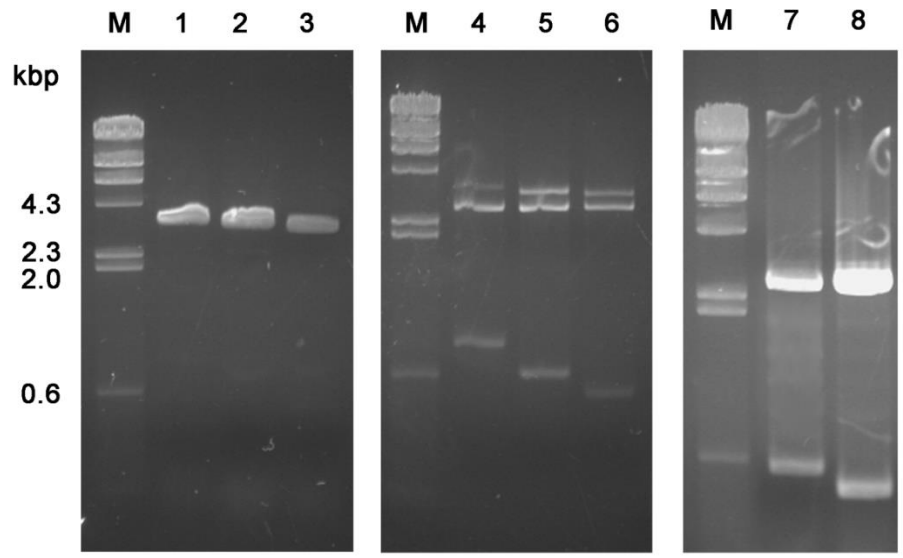

Figure 3.11 Restriction patterns of the recombinant plasmids pTA-OsCML and pTA-GFP

Lane M = λ/*Hin*dIII standard DNA marker

Lane 1 = undigested pTA-GFP

Lane 2 = undigested pTA-OsCML3

Lane 3 = undigested pTA-OsCML3m

Lane 4 = *Xho*I/*BstE*II -digested pTA-GFP

Lane 5 = *Xho*I/*BstE*II -digested pTA-OsCML3

Lane 6 = *Xho*I/*BstE*II -digested pTA-OsCML3m

Lane 7 = *Xho*I/*BstE*II -digested pTA-OsCML1

Lane 8 = *Xho*I/*BstE*II -digested pTA-OsCML1m

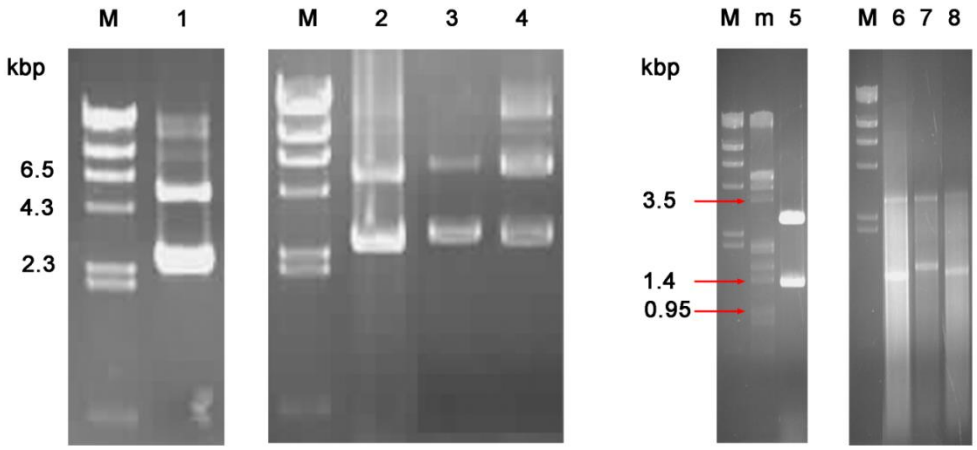

Figure 3.12 Restriction patterns of the recombinant plasmids pTA-GFP-OsCMLs

Lane M = λ/*Hin*dIII standard DNA marker

Lane 1 = undigested pTA-GFP-OsCML1

Lane 2 = undigested pTA-GFP-OsCML1m

Lane 3 = undigested pTA-GFP-OsCML3

Lane 4 = undigested pTA-GFP-OsCML3m

Lane 5 = *Nco*I/*BstE*II -digested pTA-GFP-OsCML1

Lane 6 = *Nco*I/*BstE*II -digested pTA-GFP-OsCML1m

Lane 7 = *Nco*I/*BstE*II -digested pTA-GFP-OsCML3

Lane 8 = *Nco*I/*BstE*II -digested pTA-GFP-OsCML3m

obtained from pCAMBIA-GFP-OsCML1, pCAMBIA-GFP-OsCML1m, pCAMBIA-GFP-OsCML3 or pCAMBIA-GFP-OsCML3m, respectively, whereas pCAMBIA-1302 does not show this fragment due to no additional engineered *Xho*I site as shown in Figure 3.13. After verifying the DNA sequences by LCGFCML forward and LGNOSCML reverse primers, the recombinant plasmids were individually introduced into *Agrobacterium tumefaciens* strain GV3101, and then colony PCR was performed to select the correct clones (data not shown).

The subcellular localization results revealed that the GFP signal of GFP-OsCML1 (used as positive control), which contained the prenylation site was observed mostly in the plasma membrane of the tobacco cells (Figure 3.14) while the GFP signal of GFP- OsCML1m, which lacked the predicted prenylation site was found in both cytoplasm and nucleoplasm of the tobacco cells. Similarly, the GFP signal of GFP-OsCML3 was observed in the plasma membrane of the tobacco cells while the GFP signal of GFP-OsCML3m was found in both cytoplasm and nucleoplasm of the tobacco cells. These results indicate that the OsCML3 containing the prenylation site can be located to the plasma membrane whereas OsCML3 lacking the prenylation site can enter into the nucleus.

3.4 Identification of OsCML3 and OsCML3m-binding proteins using cDNA library screening

According to Phean-o-pas (unpublished data), cDNA expression libraries were prepared from the leaf of *Oryza sativa* L. ‘Khoa Dok Ma Li 105’, and used for screening against rOsCML3 and rOsCML3m. The results revealed that two of the ten putative novel OsCML3m-binding proteins were OsPEBP and OsHMGB1. Note that,

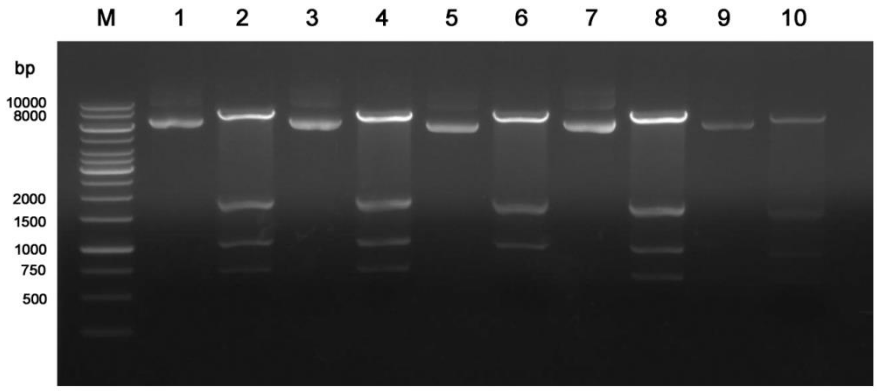

Figure 3.13 Restriction patterns of the recombinant plasmids pCAMBIA-GFP-OsCMLs

Lane M = Standard DNA marker

Lane 1 = undigested pCAMBIA-GFP-OsCML1

Lane 2 = *Nco*I/*Xho*I -digested pCAMBIA-GFP-OsCML1

Lane 3 = undigested pCAMBIA-GFP-OsCML1m

Lane 4 = *Nco*I/*Xho*I -digested pCAMBIA-GFP-OsCML1m

Lane 5 = undigested pCAMBIA1302

Lane 6 = *Nco*I/*Xho*I -digested pCAMBIA1302

Lane 7 = undigested pCAMBIA-GFP-OsCML3

Lane 8 = *Nco*I/*Xho*I -digested pCAMBIA-GFP-OsCML3

Lane 9 = undigested pCAMBIA-GFP-OsCML3m

Lane 10 = *Nco*I/*Xho*I -digested pCAMBIA-GFP-OsCML3m

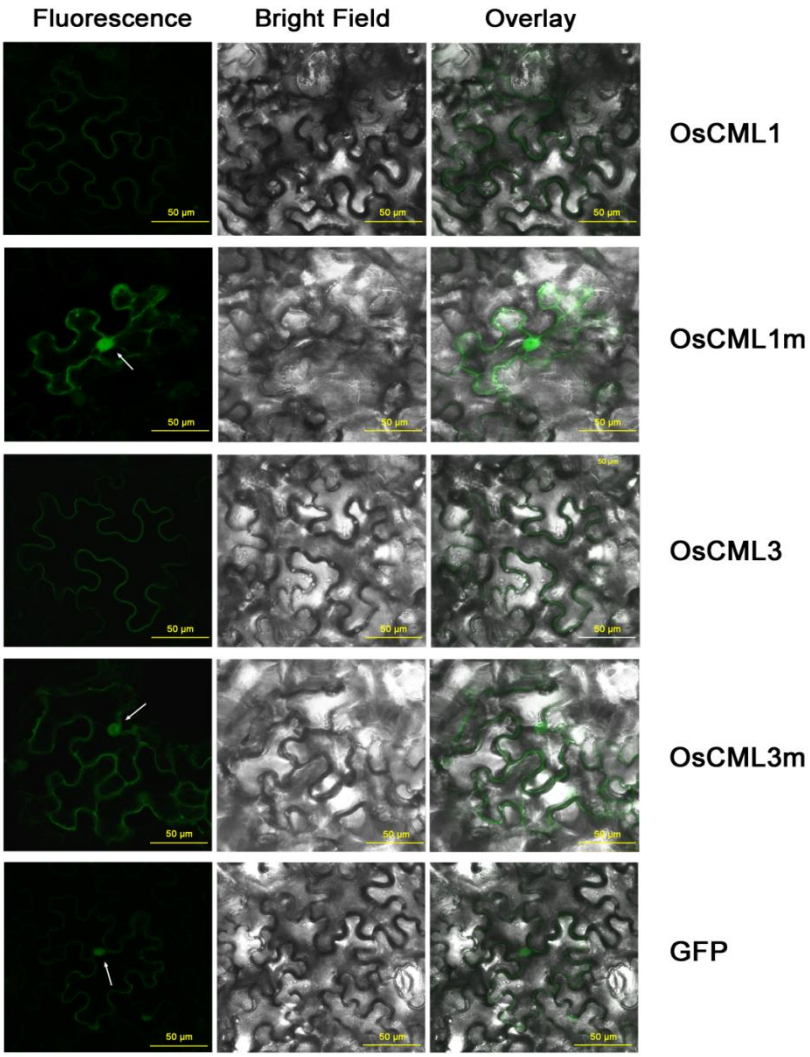

Figure 3.14 Subcellular localization of GFP and GFP-OsCMLs in tobacco leaf cells The green fluorescence, bright field and overlay images (60 x magnification) observed in tobacco leaf cells expressing the fusion proteins. Scale bar indicates 50 µm. Nucleus was indicated with white arrow.

when the full-length OsCML3 was used as the probe, only two target proteins were identified and these did not include these two proteins. Thus, the next experiments focused on confirmation of protein-protein interaction between OsCML3 or OsCML3m and these putative target proteins.

3.5 Confirmation of the protein-protein interaction using yeast-two hybrid analysis

In yeast two hybrid assay, the interested protein is fused with the DNA-binding domain (BD), which binds specifically to upstream activation sequences (UAS) of a reporter gene (Fields and Song 1989) and the activation domain (AD). When the interaction between two proteins occurs, AD and BD will reconstitute transcriptional activation together, resulting in the expression of the reporter genes such as *HIS3*, *URA3* and *LacZ*. To construct the recombinant plasmids pDEST22 and pDEST32 harboring each of *OsCML3*, *OsCML3m*, *OsCML3s*, *OsPEBP* and *OsHMGB1*, first, the PCR products obtained from PCR reactions using each corresponding cDNA template were analyzed by agarose gel electrophoresis; consequently, the *OsCML3*, *OsCML3m*, *OsCML3s*, *OsPEBP* and *OsHMGB*1 products of 556, 551, 556, 508 and 478 bp in length as expected, respectively, were obtained (Figure 3.15). After that, the purified gene fragments were individually ligated into pENTR-D TOPO vector, and then the ligation products were transformed into *E.coli* cell. Subsequently, colony PCR was performed to check gene insertion of the selected clones. The bands of expected size from each clone were obtained as shown in Figure 3.16. After verifying the DNA sequence, all plasmids containing the correct nucleotide sequence were used to individually sub-clone the gene fragment to both

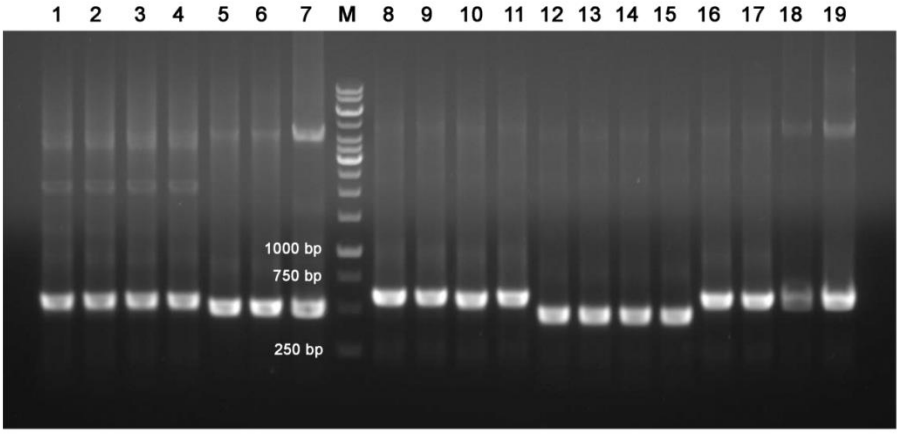

Figure 3.15 PCR products of OsPEBP, OsHMGB1, OsCML3, OsCML3m and OsCML3s gene fragments using various annealing temperatures

Lanes 1, 2, 3 and 4 are PCR product of *OsPEBP* gene using annealing temperature of 56.8, 58.6, 62.7 and 64.8 ^{o}C, respectively.

Lanes 5, 6 and 7 are PCR product of *OsHMGB1* gene using annealing temperature of 56.8, 58.6 and 62.7 ^{o}C, respectively.

Lane M = standard DNA marker

Lanes 8, 9, 10 and 11 are PCR product of *OsCML3* gene using annealing temperature of 56.8, 58.6, 62.7 and 64.8 ^{o}C, respectively.

Lanes 12, 13, 14 and 15 are PCR product of *OsCML3m* gene using annealing temperature of 56.8, 58.6, 62.7 and 64.8 ^{o}C, respectively.

Lanes 16, 17, 18 and 19 are PCR product of *OsCML3s* gene using annealing temperature of 56.8, 58.6, 62.7 and 64.8 ^{o}C, respectively.

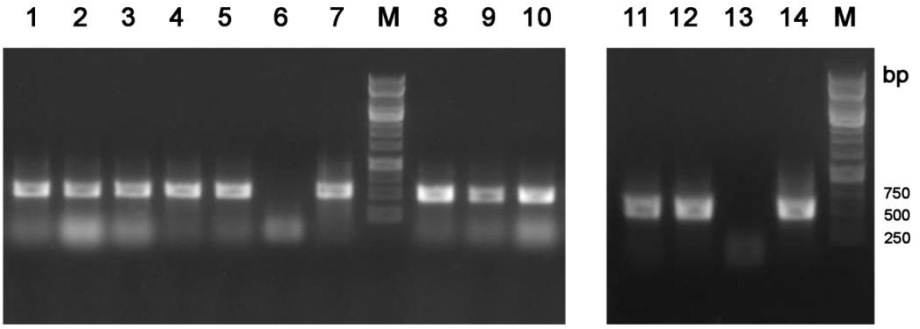

Figure 3.16 Representative colony PCR products of *OsPEBP* and *OsHMGB1* transformants

Lane 1 = Colony PCR product of transformant harboring *OsPEBP* gene clone no. 1

Lane 2 = Colony PCR product of transformant harboring *OsPEBP* gene clone no. 2

Lane 3 = Colony PCR product of transformant harboring *OsPEBP* gene clone no. 3

Lane 4 = Colony PCR product of transformant harboring *OsPEBP* gene clone no. 4

Lane 5 = Colony PCR product of transformant harboring *OsPEBP* gene clone no. 5

Lane 6 = Negative control using dH_2O instead of transformant harboring *OsPEBP* gene

Lane 7 = Positive control using *OsPEBP* PCR product as DNA template

Lane M = standard DNA marker

Lane 8 = Colony PCR product of transformant harboring *OsHMGB1* gene clone no. 1

Lane 9 = Colony PCR product of transformant harboring *OsHMGB1* gene clone no. 2

Lane 10 = Colony PCR product of transformant harboring *OsHMGB1* gene clone no. 3

Lane 11 = Colony PCR product of transformant harboring *OsHMGB1* gene clone no. 4

Lane 12 = Colony PCR product of transformant harboring *OsHMGB1* gene clone no. 5

Lane 13 = Negative control using dH_2O instead of transformant harboring *OsHMGB1* gene

Lane 14 = Positive control using *OsHMGB1* PCR product as DNA template

pDEST22 and pDEST32 by the LR recombination reactions. The LR reactions were transformed into *E. coli* (Top 10), colony PCR was then performed and analyzed by agarose gel electrophoresis. Figure 3.17 illustrates the PCR products of 556, 551, 556, 508 and 478 bp using *OsCML3*, *OsCML3m*, *OsCML3s*, *OsPEBP* and *OsHMGB1* transformed cell as template, respectively, were obtained. For co-transformation into yeast strain MAV203, for instance, the pDEST22 harboring *OsPEBP* and *OsHMGB1* were individually paired with the pDEST32 harboring *OsCML3*, *OsCML3m* or *OsCML3s*. Table 2.4 shows all plasmids paired for co-transformation. After that, the investigation of the protein interaction by culturing recombinant yeasts on different selective media as described in section 2.2.3.2.N was performed. The results revealed that when CML3m was used as the bait protein (DBD-OsCML3m), self-activation was observed as the cotransformants of DBD-CML3m and AD (pDEST22) could grow on the selective medium lacking leucine, tryptophan and histidine with the addition of high concentration of 3AT such as 25, 50 and 100 mM (Figure 3.18) for self-activation suppression at the *HIS3* gene and supplement of Ca^{2+}. Consistently, β-galactosidase activity from *Lac*Z gene was also detected in these transformants on SC-Leu-Trp supplemented with either 10 mM $CaCl_2$ (Figure 3.18) or EDTA (Figure 3.19). In contrast, no self-activation of OsCML3, OsCML3s, OsPEBP or OsHMGB1 was observed (Figure 3.18). However, no interaction of OsPEBP or OsHMGB1 with OsCML3 or with OsCML3s was observed. Note that strong positive, weak positive and negative interactions were used to compare growth on the selection plates with that of the examined transformants. The reciprocal tests between all possible combinations of bait and prey proteins were examined and they showed neither self-activation nor interaction (data not shown). These results implied that OsCML3m

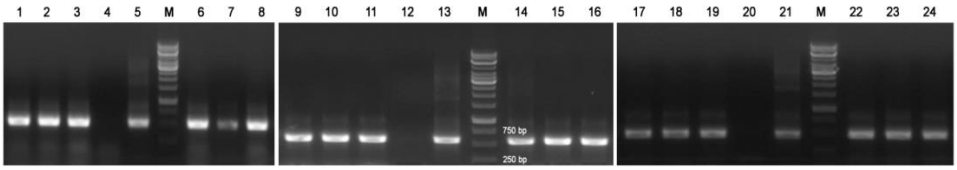

Figure 3.17 Representative colony PCR products of recombinant pDEST22 and pDEST32 transformants

Lanes 1, 2 and 3 represent colony PCR products of transformants harboring pDEST22-*OsHMGB1* clones 1, 2 and 3, respectively.

Lanes 6, 7 and 8 represent colony PCR products of transformants harboring pDEST32-*OsHMGB1* clones 1, 2 and 3, respectively.

Lanes 9, 10 and 11 represent colony PCR products of transformants harboring pDEST22-*OsCML3* of clones 1, 2 and 3, respectively.

Lanes 14, 15 and 16 represent colony PCR products of transformants harboring pDEST32-*OsCML3* of clones 1, 2 and 3, respectively.

Lanes 17, 18 and 19 represent colony PCR products of transformants harboring pDEST22-*OsCML3m* of clones 1, 2 and 3, respectively.

Lanes 22, 23 and 24 represent colony PCR products of transformants harboring pDEST32-*OsCML3m* of clones 1, 2 and 3, respectively.

Lanes 4, 12 and 20 = Negative control using dH_2O instead of transformants harboring *OsHMGB1*, *OsCML3* and *OsCML3m*, respectively

Lanes 5, 13 and 21 = Positive control using *OsHMGB1, OsCML3 and OsCML3m* PCR product, respectively, as DNA template

Lane M = standard DNA marker

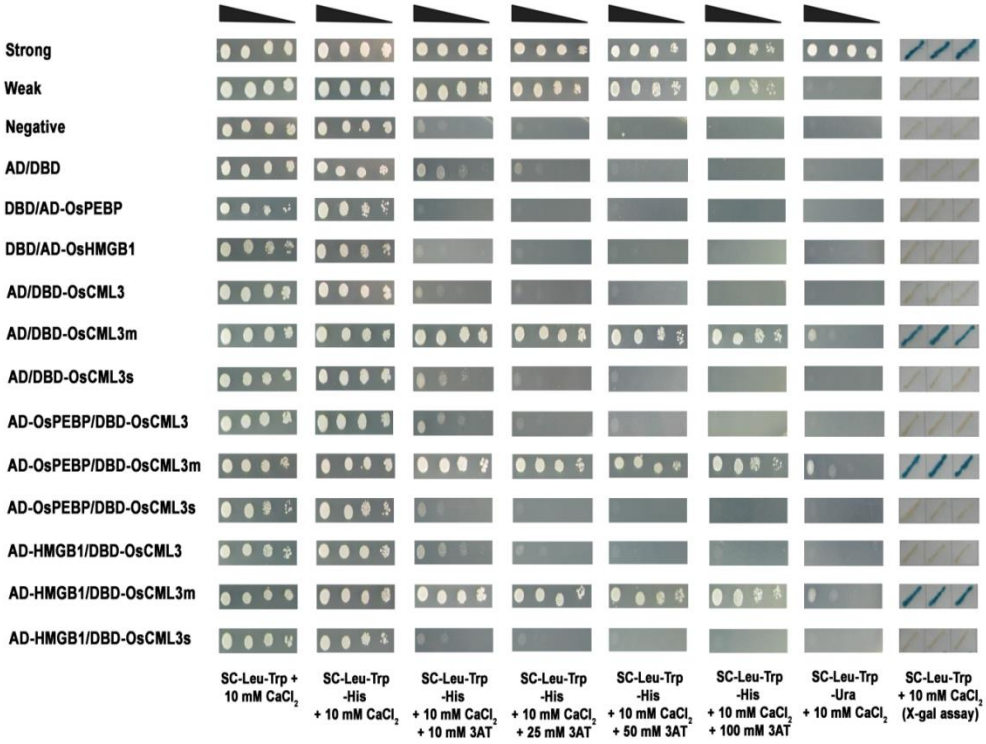

Figure 3.18 Yeast two hybrid analysis of the interaction of OsPEBP or OsHMGB1 with OsCML3, OsCML3m or OsCML3s. Each co-transformed yeast MaV203 cell was 10-fold serial diluted (10^{0}–10^{-3}, shown by closed triangle) with water and cultured on selective plates (SC-Leu-Trp, SC-Leu-Ura and SC-Leu-Trp-His supplemented with 10, 25, 50 and 100 mM 3AT). Also, X-gal assay was performed using yeast cell grown on SC-Leu-Trp. All selective plates were added with 10 mM $CaCl_2$. DBD and AD represent the GAL4 DNA binding domain and the GAL4 activation domain, respectively. Data shown are representatives of those seen from three independent repeats.

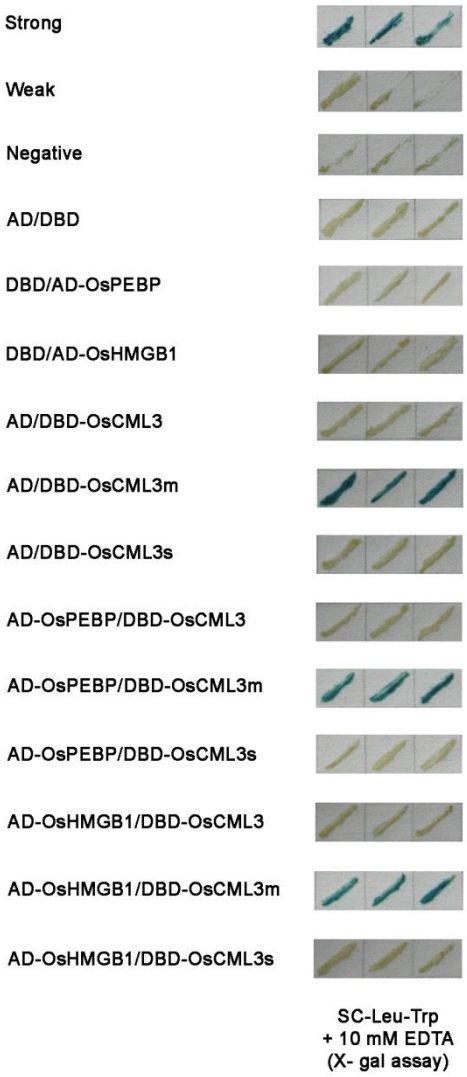

Figure 3.19 X-gal assay of each co-transformed yeast MAV203 cell grown on selective plate (SC-Leu-Trp + 10 mM EDTA). DBD and AD represent the GAL4 DNA binding domain and the GAL4 activation domain, respectively. Data shown are representatives of those seen from three independent repeats

might play function similarly to the activator (prey protein) for gene expression whereas its full-length (OsCML3) did not activate the gene expression due to the effect of the CTE, as observed in the CaM kinase II peptide-binding assay. However, the interaction of OsPEBP or OsHMGB1 with OsCML3, OsCML3m or OsCML3s could not be concluded by yeast two-hybrid assay.

3.6 Confirmation of protein interaction by BiFC assay

The *OsCML3*, *OsCML3m* or *OsCML3s* gene fragment from the recombinant pENTR-D TOPO was individually sub-cloned into pcCFPxGW vector by LR recombination reaction, resulting in pCFP-OsCML3, pCFP-OsCML3m or pCFP-OsCML3s, respectively. Similarly, the *OsPEBP* and *OsHMGB1* were individually sub-cloned into pnYFPxGW vector, resulting in pYFP-OsPEBP and pYFP-OsHMGB1, respectively. Then, the LR reactions were introduced into *E. coli* (Top 10) competent cells by $CaCl_2$ method. The cell suspension was spread onto the LB agar plates containing 50 μg/ml spectinomycin. To check the recombinant clone, resistant colonies grown on spectinomycin were picked and used as template for colony PCR using a pair of primers described in Table 2.3. Figure 3.20 shows the colony PCR product of the transformants harboring *OsPEBP*, *OsHMGB1*, *OsCML3*, *OsCML3m* and *OsCML3s*. After nucleotide sequencing, the recombinant pnYFPxGW and pcCFPxGW were individually introduced into *Agrobacterium tumefaciens* GV3101. To verify the transformant, colony PCR was performed and analyzed by agarose gel electrophoresis using *Agrobacterium* transformants harboring *OsPEBP*, *OsHMGB1*, *OsCML3*, *OsCML3m* or *OsCML3s* as template (data not shown).

To visualize protein interaction in plant cell, each pair of recombinant

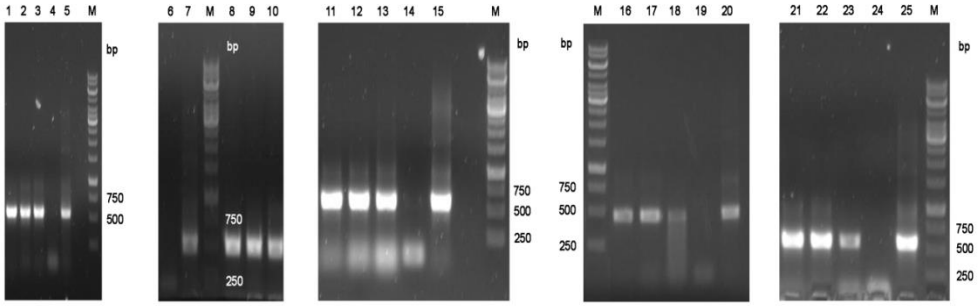

Figure 3.20 Representative colony PCR products of the recombinant pnYFPxGW and pcCFPxGW transformants

Lanes 1, 2 and 3 represent colony PCR product of transformants harboring pnYFPxGW –*OsPEBP* of clones 1, 2 and 3, respectively.

Lanes 8, 9 and 10 represent colony PCR product of transformants harboring pnYFPxGW -*OsHMGB1* of clones 1, 2 and 3, respectively.

Lanes 11, 12 and 13 represent colony PCR product of transformants harboring pcCFPxGW -*OsCML3* of clones 1, 2 and 3, respectively.

Lanes 16, 17 and 18 represent colony PCR product of transformants harboring pcCFPxGW -*OsCML3m* of clones 1, 2 and 3, respectively.

Lanes 21, 22 and 23 represent colony PCR product of transformants harboring pcCFPxGW -*OsCML3s* of clones 1, 2 and 3, respectively.

Lanes 4, 6, 14, 19 and 24 = Negative control using dH_2O instead of transformants harboring *OsPEBP*, *OsHMGB1*, *OsCML3*, *OsCML3m* and *OsCML3s*, respectively.

Lanes 5, 7, 15, 20 and 25 = Positive control using *OsPEBP*, *OsHMGB1*, *OsCML3*, *OsCML3m* and *OsCML3s* PCR product, respectively, as DNA template.

Lane M = standard DNA marker

Agrobacterium (Table 2.5) was mixed with p19 and then co-infiltrated into the leaf of 6-week-old tobacco plants. The results revealed that no green fluorescence signal was detected in leaf cells using the combination of OsPEBP with OsCML3, OsCML3m or OsCML3s (Figure 3.21). However, green fluorescence signal was clearly observed in all combination of OsHMGB1 with OsCML3, OsCML3m or OsCML3s in the nucleus (Figure 3.21 and 3.22), confirming the interaction between OsCML3 and OsHMGB1 *in planta*. The interaction in the nucleus possibly occurred through the nuclear localization signal (NLS) of OsHMGB1. The N-terminal fragment of YFP or the C-terminal fragment of CFP, used as a negative control, yielded no fluorescent signal in leaf cells co-infiltrated with the following combinations:YFP and CFP-OsCML3, YFP and CFP-OsCML3m, YFP and CFP-OsCML3s, YFP-OsPEBP and CFP, and YFP-OsHMGB1 and CFP.

3.7 Electrophoretic mobility shift assay (EMSA)

The recombinant plasmid pET28b encoding OsHMGB1fused with 6 x His-Tag at the N-terminal end was prepared. The coding region of *OsHMGB1* gene was amplified using the *OsHMGB1* cDNA clone as template. Figure 3.23 shows the band of the *OsHMGB1* PCR product at 493 bp as expected. After PCR product purification, the *OsHMGB1* fragment was cloned into pET-28b via *Nde*I and *Xho*I sites. To check the recombinant clone, the resistance colonies on kanamycin were picked and used as template for colony PCR using a pair of primers as described in Table 2.6. Figure 3.24 shows the colony PCR product obtained at 493 bp using a colony containing pET28b-*OsHMGB1* as template. In addition, the selected clone was used for plasmid extraction, and then digestion with *Nde*I and *Xho*I was performed before nucleotide

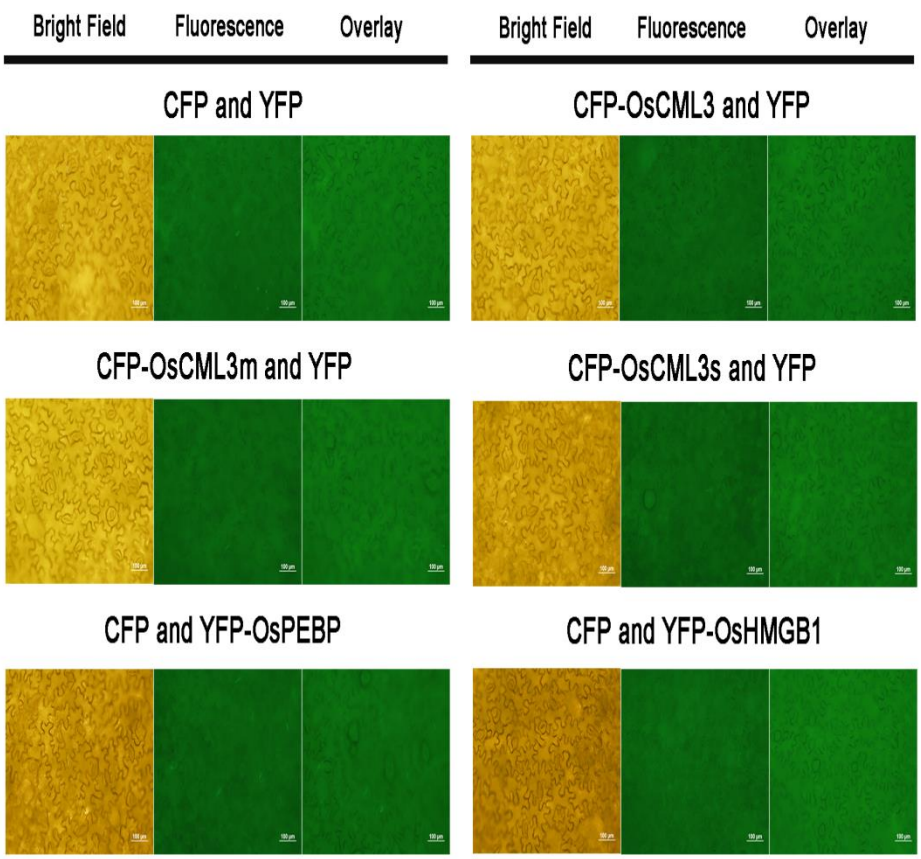

Figure 3.21 BiFC analysis of the OsPEBP and OsHMGB1 interaction with OsCML3, OsCML3m and OsCML3s. YFP represents the N-terminal fragment of yellow fluorescence protein (YFP) and CFP represents the C-terminal fragment of cyan fluorescence protein (CFP). As control, co-transformed constructs of: CFP and YFP, CFP-OsCML3 and YFP, CFP-OsCML3m and YFP, CFP-OsCML3s and YFP, CFP and YFP-OsPEBP, and CFP and YFP-OsHMGB1were analyzed. Images shown represent those seen form at least 50 such fields of view per sample and five independent samples. Scale bars represent 100 µm. Nucleus was indicated with yellow arrow. Images were taken by OLUMPUS DP Controller microscope with 20 x magnification**.**

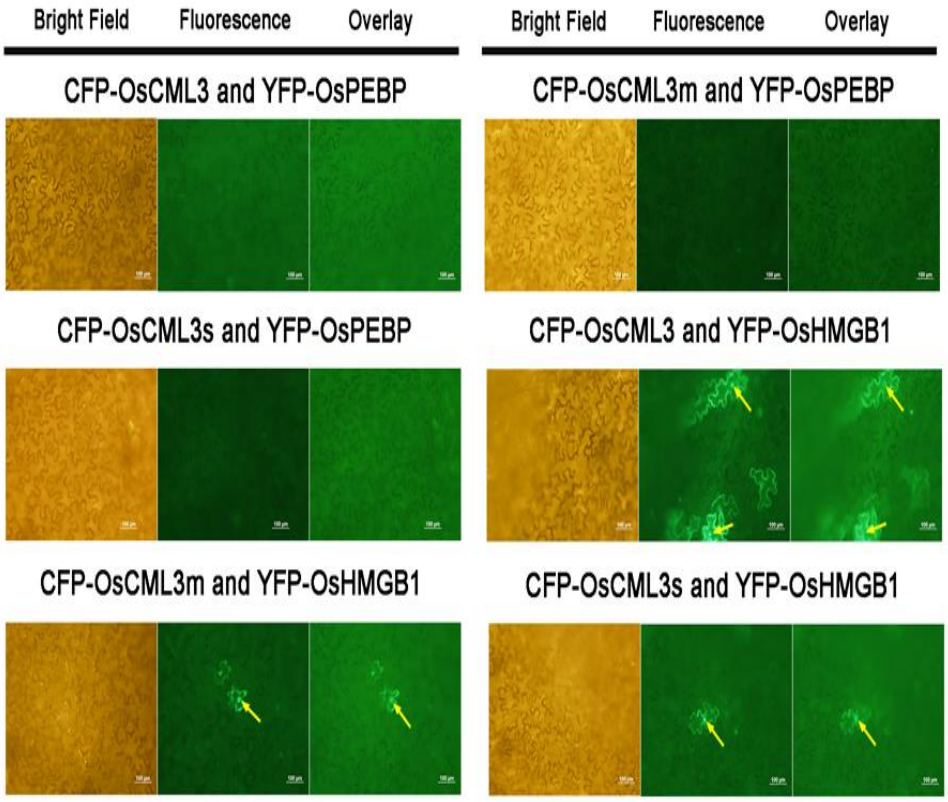

Figure 3.21 (continued) BiFC analysis of the OsPEBP and OsHMGB1 interaction with OsCML3, OsCML3m and OsCML3s. YFP represents the N-terminal fragment of yellow fluorescence protein (YFP) and CFP represents the C-terminal fragment of cyan fluorescence protein (CFP). As control, Co-transformed constructs of: CFP and YFP, CFP-OsCML3 and YFP, CFP-OsCML3m and YFP, CFP-OsCML3s and YFP, CFP and YFP-OsPEBP, and CFP and YFP-OsHMGB1were analyzed. Images shown represent those seen form at least 50 such fields of view per sample and five independent samples. Scale bars represent 100 µm. Nucleus was indicated with yellow arrow. Images were taken by OLUMPUS DP Controller microscope with 20 x magnification**.**

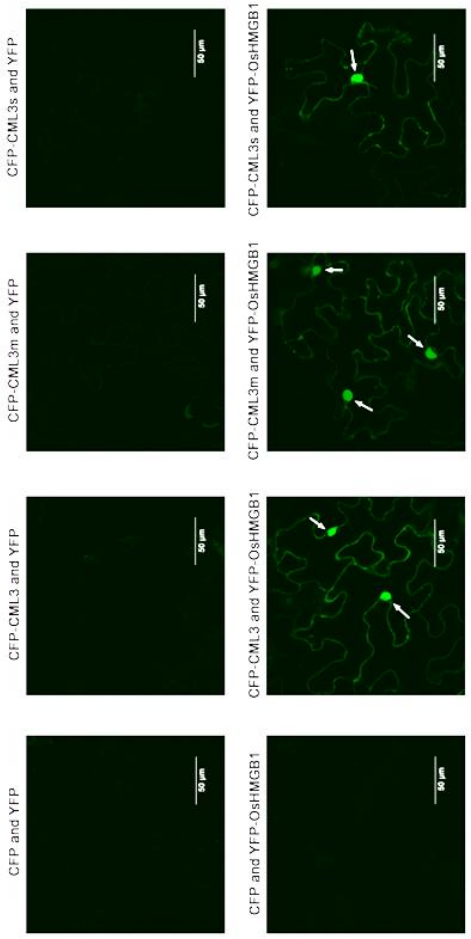

Figure 3.22 BiFC analysis of the OsHMGB1 interaction with OsCML3, OsCML3m and OsCML3s for clear visualization. Fluorescent signals were observed in the nuclei of *Nicotiana benthamiana* leaf cells co-infiltrated with a pair of *Agrobacterium* harboring YFP-HMGB1 and CFP-CML3, YFP-OsHMGB1 and CFP-CML3m, or YFP-HMGB1 and CFP-CML3s. YFP represents the N-terminal fragment of yellow fluorescence protein (YFP) and CFP represents the C-terminal fragment of cyan fluorescence protein (CFP). As control, co-transformed constructs: of CFP and YFP, CFP-CML3 and YFP, CFP-CML3m and YFP, CFP-CML3s and YFP, and CFP and YFP-HMGB1were analyzed. Images shown represent those seen form at least 100 such fields of view per sample and five independent samples. Scale bars represent 50 µm. Nucleus was indicated with white arrow. Images were taken by OLUMPUS FLUOVIEW (FV10i) microscope with 20 x magnification.

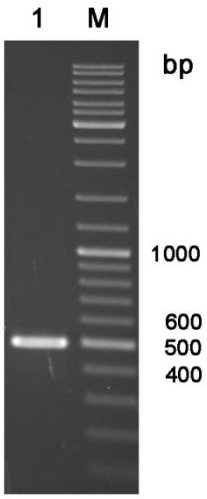

Figure 3.23 PCR product using *OsHMGB1* cDNA clone template

Lane 1 = PCR product of *OsHMGB1* gene using annealing temperature of 58 ^{o}C

Lane M = 100 bp standard DNA marker

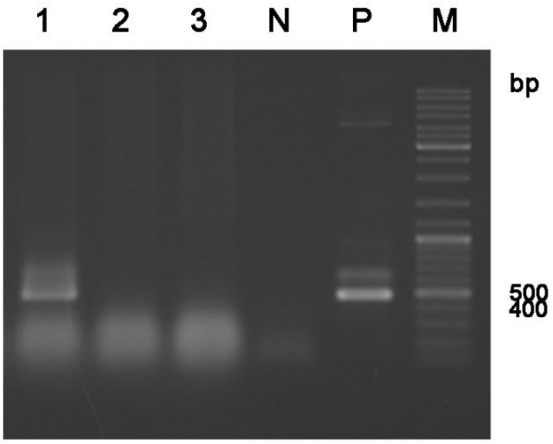

Figure 3.24 Colony PCR product of *OsHMGB1* transformant

Lane 1 = Colony PCR product using colony no.1

Lane 2 = Colony PCR product using colony no.2

Lane 3 = Colony PCR product using colony no.3

Lane N = Negative control using dH_2O instead of colony

Lane P = Positive control using *OsHMGB1* PCR product as DNA template

Lane M = 100 bp standard DNA marker

sequencing. Figure 3.25 shows the linear pET-28b and the inserted *OsHGMB1*gene fragment obtained at 5.3 kb and 0.5 kb, respectively.

A single colony of *E.coli* BL21 (DE3) containing pET-OsHMGB1 was grown in 20 ml of LB medium containing 50 μg/ml kanamycin. Two percent of the cell culture was inoculated in a large-scale LB medium and incubated at 37 ^{o}C with shaking until the optical density at 600 nm (OD_{600}) of the cell culture reached 0.6. Production of recombinant OsHMGB1 was induced by IPTG at a final concentration of 0.4 mM and the incubation was continued at 37 ^{o}C for 4 hours. The cells were harvested by centrifugation at 8000xg for 15 minutes, then washed and sonicated with buffer as described in section 2.2.3.4.I. For rOsHMGB1 purification, the crude protein was applied to the equilibrated Ni-Sepharose column, and then the column was washed with Equilibration buffer of 50 column volumes. To elute the rOsHMGB1 from column, the imidazole concentration was increased to 100, 200 and 500 mM. The eluted proteins were analyzed by SDS-polyacrylamide gel electrophoresis. Figure 3.26 shows the purified rOsHMGB1 having two major bands in the eluted fraction. The molecular weight of upper and lower bands was estimated to be 22.7 and 19.5 kDa, respectively by its mobility in SDS-PAGE when compared with those of standard proteins. Figure 3.27 shows western blot analysis with anti-His antibody confirmed the presence of rOsHMGB1, which showed the two bands corresponding to its presence in SDS-PAGE. The pUC19 plasmid was purified from *E.coli* (Top10) harboring pUC19. In addition, the recombinant rOsHMGB1, rOsCML3 (Chinpongpanich et al. 2011), rOsCML3m and rOsCaM1 (Phean-o-pas et al. 2008) prepared previously were used in this experiment. The supercoiled DNA-binding

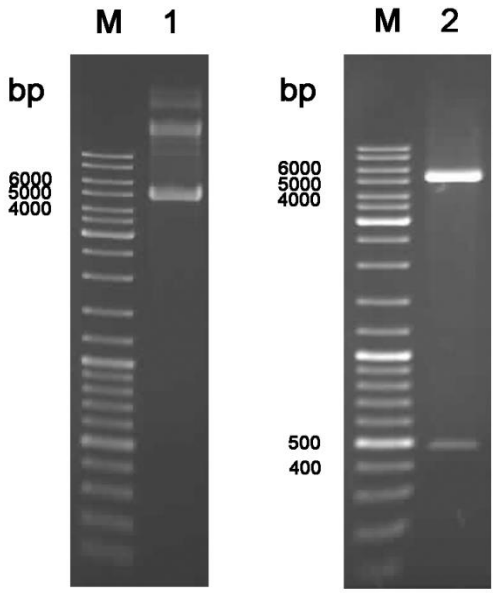

Figure 3.25 Restriction pattern of the recombinant plasmid pET-OsHMGB1

Lane 1 = undigested pET-OsHMGB1

Lane 2 = *Nde*I/*Xho*I-digested pET-OsHMGB1

Lane M = 100 bp standard DNA marker

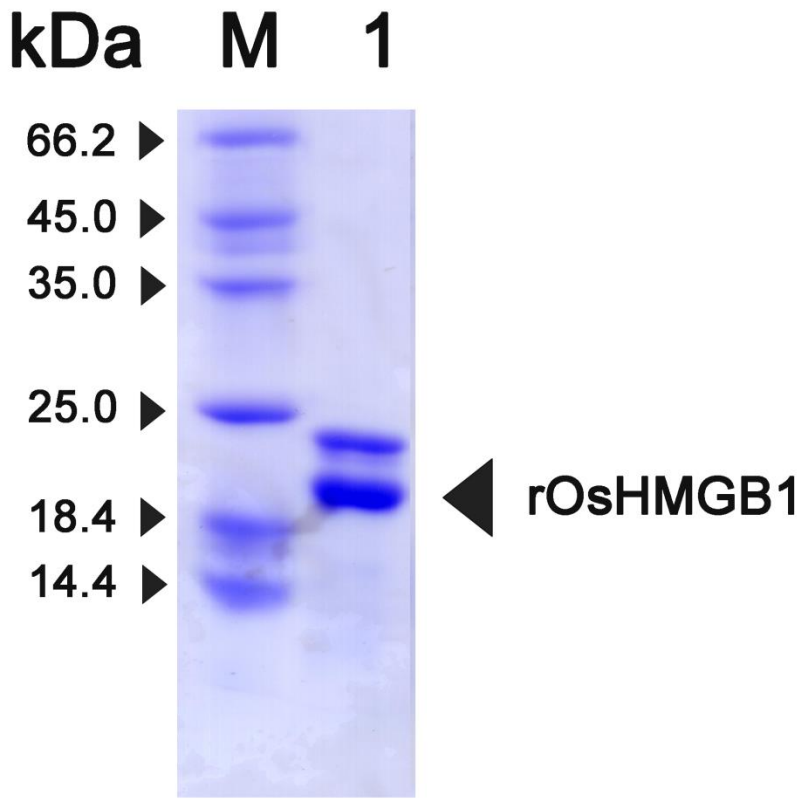

Figure 3.26 Purified rOsHMGB1. Lane M shows protein marker, Lane 1 shows purified rOsHMGB1 using Ni-Sepharose chromatography

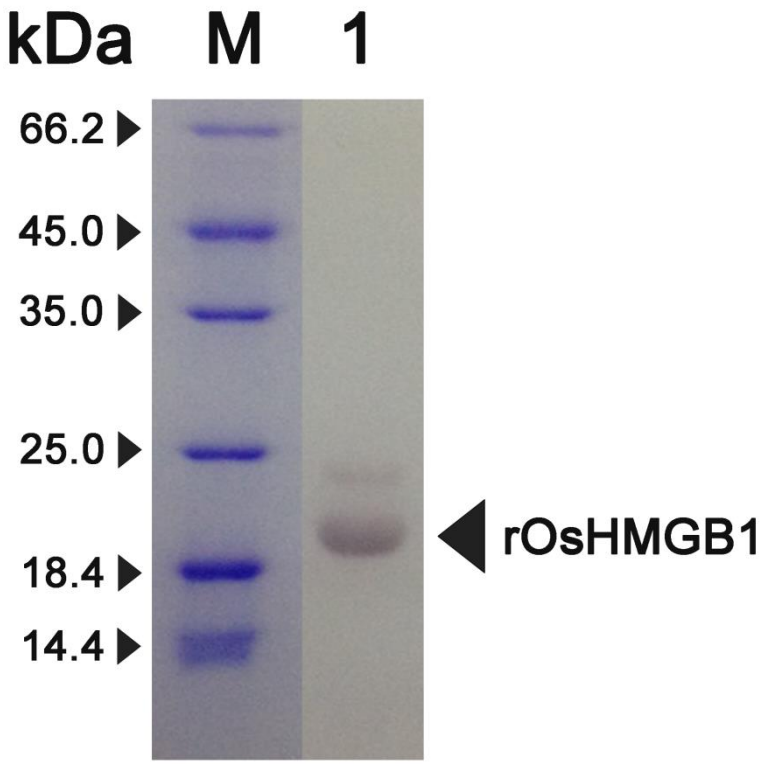

Figure 3.27 Western blot analysis of rOsHMGB1. Lane M shows molecular mass standard proteins. Lane 1 shows the Western blot analysis of the purified rOsHMGB1.

property of rOsHMGB1 was examined by incubating the supercoiled pUC19 plasmid (100 ng) with the increasing concentrations of rOsHMGB1 (0–3 μM). That the pUC19 DNA interacted with rOsHMGB1 was shown by the resolved bands of lower electrophoretic mobility of the protein-DNA complex compared to that of the free DNA. This was detected from 1.0 μM of rOsHMGB1 in the presence of Ca^{2+} (Figure 3.28A) or EGTA (data not shown). Examination of the effect of rOsCML3 or rOsCML3m upon the DNA-binding ability of rOsHMGB1 was evaluated by incubation of 1.0 μM of rOsHMGB1 and 100 ng of pUC19 at room temperature for 10 min and then adding the increasing concentrations of rOsCML3 or rOsCML3m (0–2 μM) in the presence of Ca^{2+}. With the increasing concentrations of rOsCML3, no effect on rOsHMGB1 binding to pUC19 was detected, as a similar rOsHMGB1 mobility shift as that without the addition of rOsCML3 was observed (Figure 3.28B).

In contrast, in the presence of Ca^{2+} the electrophoretic mobility of the rOsHMGB1-pUC19 complex increased in a dose-dependent manner in the presence of rOsCML3m from 0.1 μM (Figure 3.28C). Without rOsHMGB1 addition, rOsCML3, rOsCML3m and rOsCaM1 caused no mobility shift in the supercoiled pUC19 DNA (Figure 3.28E-G) Thus, only the CTE-truncated rOsCML3m in the Ca^{2+}-bound form affected the DNA-binding ability of OsHMGB1. In addition, due to the high amino acid sequence identity shared with rOsCML3m, rOsCaM1 was tested under the same conditions to examine if rOsCaM1 could also interfere with the supercoiled DNA-binding ability of rOsHMGB1. However, like rOsCML3, rOsCaM1 had no effect on the rOsHMGB1 binding to supercoiled pUC19 (Figure 3.28D), indicating that the truncated (CTE-free) rOsCML3m specifically affected the supercoiled DNA-binding ability of rOsHMGB1.In the presence of EGTA,

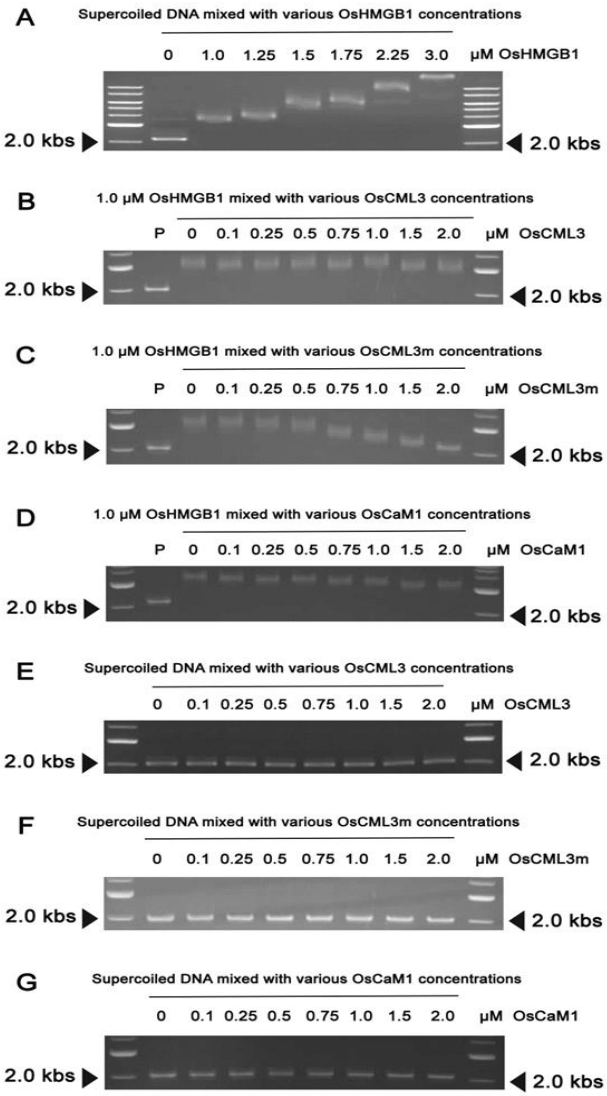

Figure 3.28. EMSA evaluation of the interaction of rOsHMGB1 with supercoiled pUC19 DNA in the presence of Ca^{2+} (A) Various rOsHMGB1 concentrations (0–3.0 μM) mixed with 100 ng supercoiled pUC19. (B–D) Mixtures of 1.0 μM rOsHMGB1, supercoiled pUC19 (100 ng) and various rOsCML3, rOsCML3m or rOsCaM1concentrations (0–2.0 μM). (E-G) Mixture of supercoiled pUC19 (100 ng) and various rOsCML3, rOsCML3m or rOsCaM1concentrations (0–2.0 μM). Gels shown are representatives of those seen from three independent repeats. Lane P represents pUC19 alone.

rOsCML3, rOsCML3m and rOsCaM1 did not affect the electrophoretic mobility of rOsHMGB1-pUC19 (data not shown).

Moreover, without rOsHMGB1 addition, rOsCML3, rOsCML3m and rOsCAM1 caused no mobility shift in the supercoiled pUC19 DNA (data not shown). These results indicated that rOsCML3m showed the inhibitory effect to binding the supercoiled DNA of rOsHMGB1 in the Ca^{2+}-dependent manner.

3.8 Expression analysis of the *OsCML3* gene in rice (*Oryza sativa* L.) under various conditions

To investigate whether *OsCML3* may possibly be involved in mediating responses to stresses, three week-old seedlings prepared in section 2.2.4.B were transferred to various conditions (salt, cold, and auxin and cytokinin application). Plants were grown with a completely randomized design (CRD) with at least three biological replicates and ten seedlings were pooled for each replication. The treated rice seedlings were collected at various time points (0, 1, 3, 6, 12, 24 and 24 h) after the beginning of treatment. Subsequently, RNA was extracted and used as template to synthesize cDNA. Then, the quantitative real-time RT-PCR using gene-specific primers of *OsCML3* and *OsEF1α*, elongation factor-1α assumed to be independent of the stresses in its expression levels (a housekeeping gene), was performed. *OsCML3* expression level was found slightly down-regulated at 1 h after the beginning of salt treatment (Figure 3.29). Interestingly, transcript expression level of *OsCML3* was significantly up-regulated 2-3-fold at 3 h after cold stress treatment compared with the control, and then declined to lower level as that of control at 6 h (Figure 3.30). This

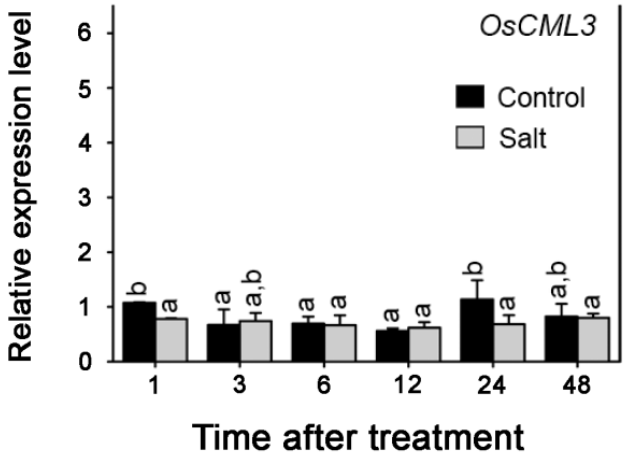

Figure 3.29 *OsCML3* transcript expression in response to salt stresses

Transcript expression levels examined in the 'KDML105' rice under salt stress showing relative transcript expression levels standardized to that of *OsEF1α* and expressed relative to the levels on day 0 of the treatment. Rice seedlings were grown in a CRD with three replicates, and for each replicate, ten seedlings were pooled for RNA extraction. The PCR reaction of the same cDNA preparation was performed in triplicate for technical replication. Data are shown as the mean ± 1 SD and means with a different lowercase letter are significantly different ($p < 0.05$) (Chinpongpanich et al. 2012).

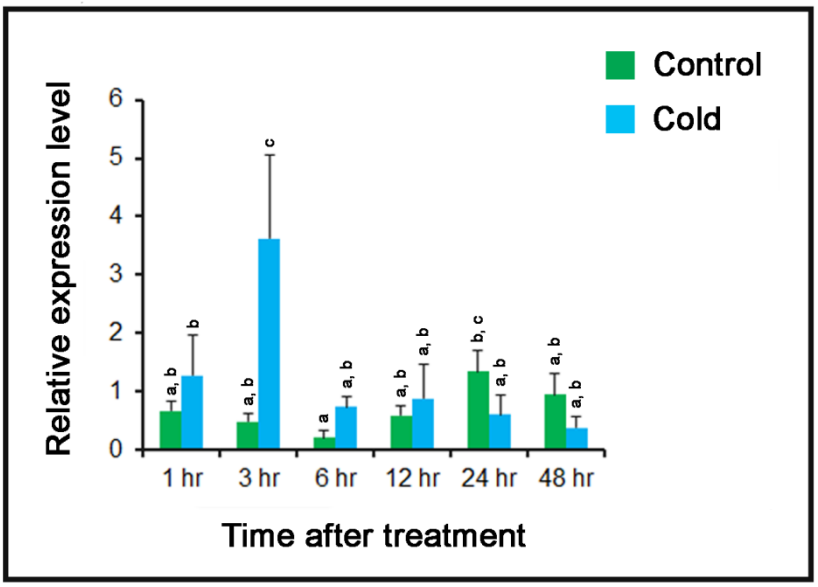

Figure 3.30 *OsCML3* transcript expression in response to cold stress

Transcript expression levels examined in the 'KDML105' rice under cold (15 ^{o}C) stress showing relative transcript expression levels standardized to that of *OsEF1α* and expressed relative to the levels on day 0 of the treatment. Rice seedlings were grown in a CRD with three replicates, and for each replicate, ten seedlings were pooled for RNA extraction. The PCR reaction of the same cDNA preparation was performed in triplicate for technical replication. Data are shown as the mean ± 1 SD and means with a different lowercase letter are significantly different ($p < 0.05$).

result suggests that OsCML3 function may involve in the response to cold stress. In addition, the *OsCML3* transcript expression level was found up-regulated at 48 h after BA application (Figure 3.31A) while slightly down-regulated at 48 h after IAA application (Figure 3.31B) when compared with their respective control.

3.9 The *cis*-acting elements prediction

To investigate the existence of *cis*-acting elements involved in stress response on the *OsCML3* promoter, the upstream sequence of its coding region was obtained from GenBank and bioinformatically analyzed using the PLACE and the PlantPAN software and databases. In this study, three *cis*-acting elements were considered including DREs (drought- responsive elements), ABREs (ABA-responsive elements) and LTREs (low temperature responsive elements). Two Putative ABREs were found in the 5′ flanking region of *OsCML3* at the -245 and -235 positions (Figure 3.32). Expectedly, one putative LTRE was observed at the– 143 position, supporting the effect of low temperature on the expression of *OsCML3* as observed earlier. In contrast, no DRE was found in the upstream region of *OsCML3*.

3.10 Overexpression of OsCML3 and OsCML3m in Arabidopsis thaliana

Construction of pCAMBIA1301containing individual *OsCML3* and *OsCML3m* were performed as follows. First of all, the coding regions of *OsCML3* and *OsCML3m* were amplified using the *OsCML3* cDNA clone used as template. Figure 3.33 shows the bands of OsCML3 and OsCML3m gene fragments at 560 and 455 bp, respectively, as expected. After PCR product purification, the *OsCML3* and

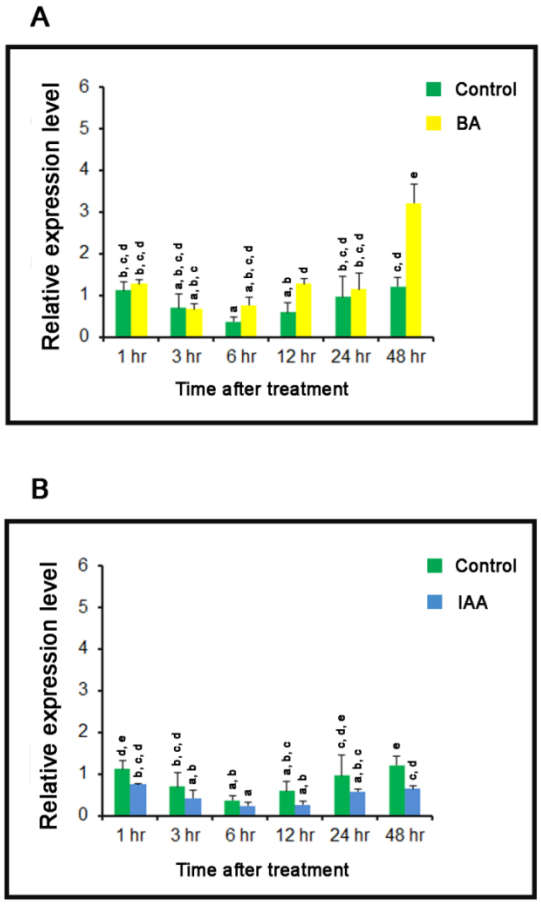

Figure 3.31 *OsCML3* transcript expression in response to cytokinin (BA) and auxin (IAA) application

Transcript expression levels examined in the 'KDML105' rice in response to cytokinin (BA) application (A) and auxin (IAA) application (B) showing relative transcript expression levels standardized to that of *OsEF1α* and expressed relative to the levels on day 0 of the treatment. Rice seedlings were grown in a CRD with three replicates, and for each replicate, ten seedlings were pooled for RNA extraction. The PCR reaction of the same cDNA preparation was performed in triplicate for technical replication. Data are shown as the mean ± 1 SD and means with a different lowercase letter are significantly different ($p < 0.05$).

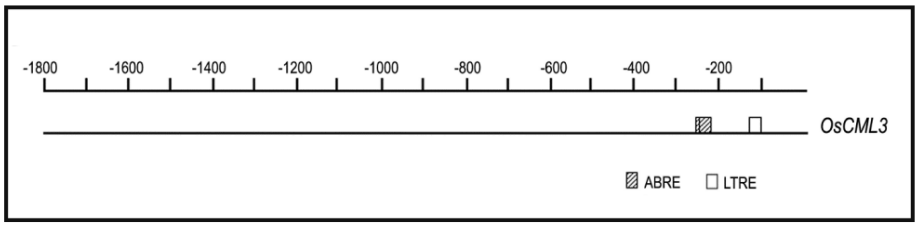

Figure 3.32 *Cis*-acting elements involved in the response to abiotic stress in the *OsCML3* promoters. The 5′ upstream regions are represented by lines and the putative ABRE (ABA-responsive elements) and LTRE (low temperature responsive elements) sequences are shown with a striped rectangle and an open rectangle, respectively.

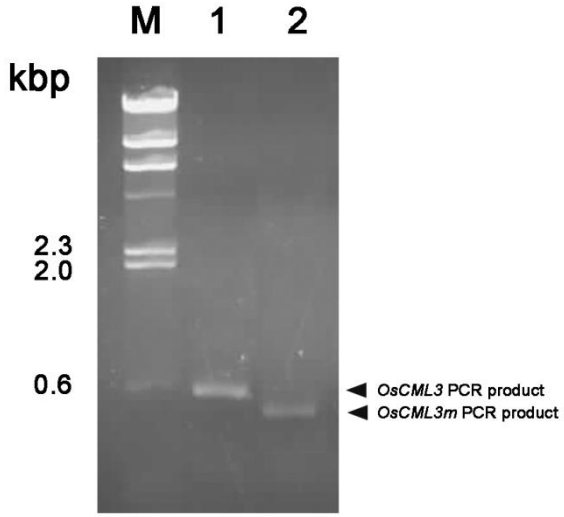

Figure 3.33 PCR products of *OsCML3* and *OsCML3m* using *OsCML3* cDNA template

Lane M = λ/*Hin*dIII standard DNA marker

Lane 1 = PCR product of *OsCML3* using annealing temperature of 60.7 ^{o}C

Lane 2 = PCR product of *OsCML3m* using annealing temperature of 60.7 ^{o}C

OsCML3m fragments were individually cloned into T&A vector, resulting in pTA-OsCML3-Over, pTA-OsCML3m-Over, respectively. Then, they were digested with *Nco*I and *Nhe*I and analyzed by agarose gel electrophoresis .resulting in the bands of linearized T&A vector, *OsCML3* and *OsCML3m* fragments of 2.7, 0.56 and 0.45 kbp, respectively, as shown in Figure 3.34. Then, the gene fragments of *OsCML3*, *OsCML3m* were individually sub-cloned into pGEM-T vector containing a CaMV35S promoter fused with *Cam1-1* by replacing *Cam1-1* with *OsCML3* or *OsCML3m* via the *Nco*I and *Nhe*I sites. After complete digestion with *Hin*dIII to verify the recombinant plasmids, three expected bands of approximately 3.0, 0.9, and 0.65 kbp for pGEM-CAMV35S-OsCML3 or 3.0, 0.9, and 0.54 kbp for pGEM-CAMV35S-OsCML3m in length were obtained as shown in Figures 3.35. Schematic diagram of the pGEM-CAMV35S-OsCML3/OsCML3m is shown in Figure 3.36. After that, the pGEM-CAMV35S-OsCML3m was partially digested using *Hin*dIII and then ligated into *Hin*dII-digested pCAMBIA1301. The recombinant plasmid was verified by complete digestion with *Hin*dIII, which showed three fragments of approximately 11.8, 0.9 and 0.54 kbp (Figure 3.37). The resulting recombinant plasmid was called pCAMBIA-CAMV35S-OsCML3m as shown with the schematic diagram in Figure 3.38. Because the partial digestion via *Hin*dIII was not successful to sub-clone the fragment of CAMV35S-OsCML3 from pGEM-CAMV35S-OsCML3 into pCAMBIA1301, the PCR reaction was performed using pGEM-CAMV35S-OsCML3 as template, and 35SBamF1 and 35SSalR1 primers to amplify the fragment of CaMV35S fused with *OsCML3* gene in order to use *BamH*I and *Sal*I sites at 5′ and 3′, respectively, instead of *Hind*III restriction site at both 5′ and 3′ end for subsequent

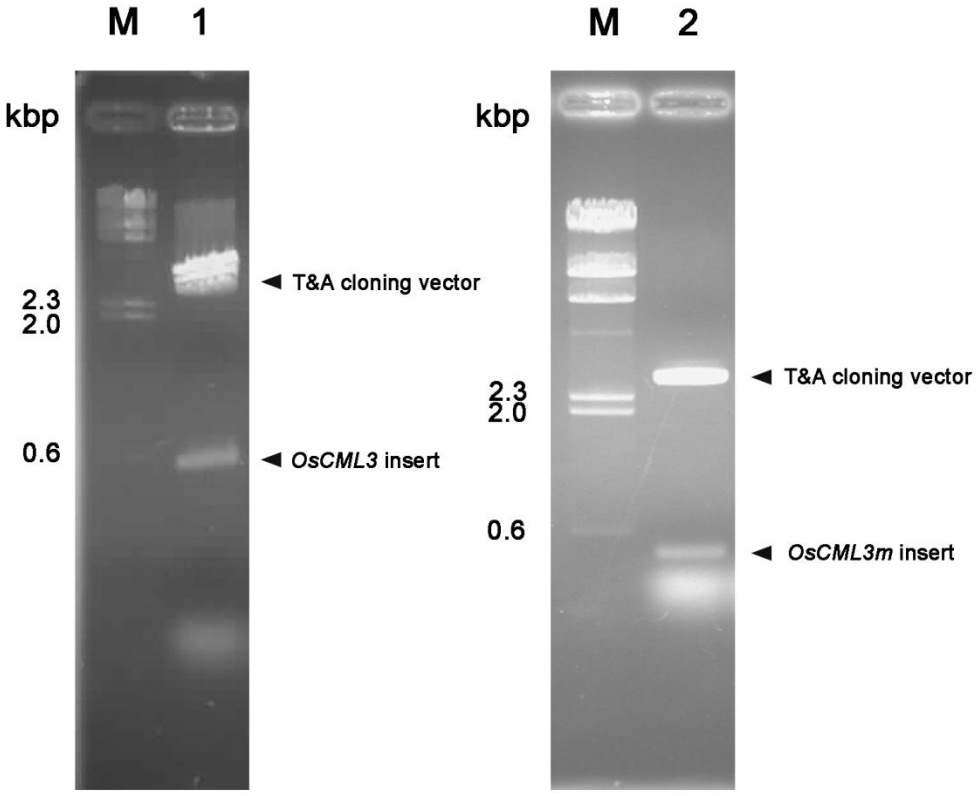

Figure 3.34 Restriction patterns of the recombinant plasmid pTA-OsCML3-Over and pTA-OsCML3m-Over

Lane M = λ/*Hin*dIII standard DNA marker

Lane 1 = *Nco*I/*Nhe*I-digested pTA-OsCML3-Over

Lane 2 = *Nco*I/*Nhe*I-digested pTA-OsCML3m-Over

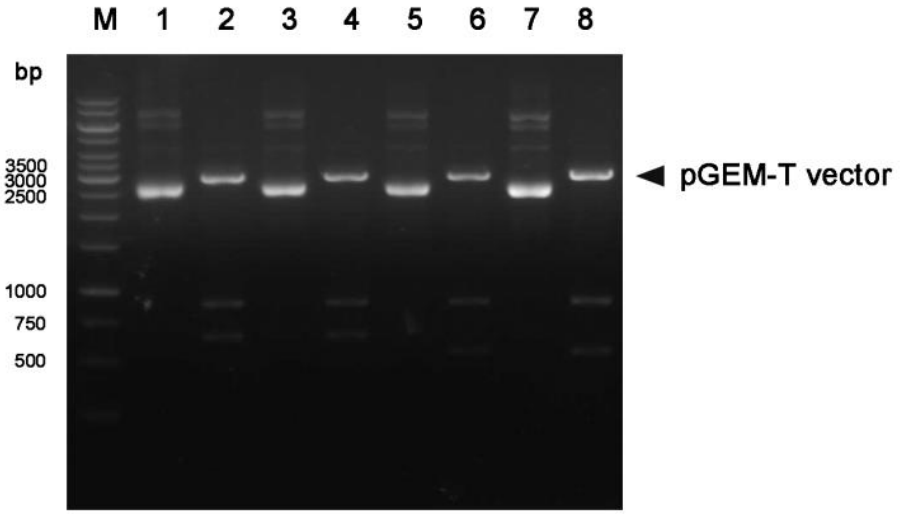

Figure 3.35 Restriction pattern of the recombinant plasmid pGEM-CAMV35S-OsCML3 and pGEM-CAMV35S-OsCML3m

Lane M = standard DNA marker

Lane 1 = undigested pGEM-CAMV35S-OsCML3 from clone no.1

Lane 2 = pGEM-CAMV35S-OsCML3 from clone no.1 digested with *Hin*dIII

Lane 3 = undigested pGEM-CAMV35S-OsCML3 from clone no.2

Lane 4 = pGEM-CAMV35S-OsCML3 from clone no.2 digested with *Hin*dIII

Lane 5 = undigested pGEM-CAMV35S-OsCML3m from clone no.1

Lane 6 = pGEM-CAMV35S-OsCML3m from clone no.1 digested with *Hin*dIII

Lane 7 = undigested pGEM-CAMV35S-OsCML3m from clone no.2

Lane 8 = pGEM-CAMV35S-OsCML3m from clone no.2 digested with *Hin*dIII

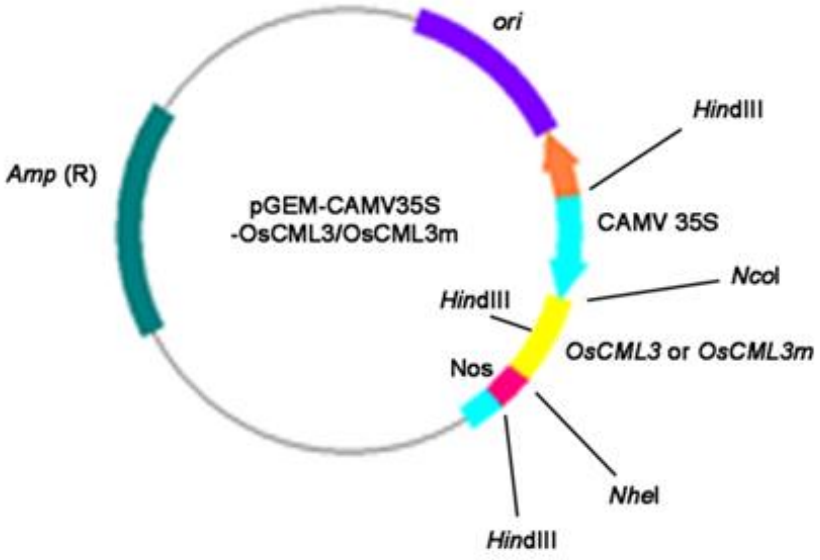

Figure 3.36 Map diagram of pGEM-CaMV35S-OsCML3 or pGEM-CaMV35S-OsCML3m

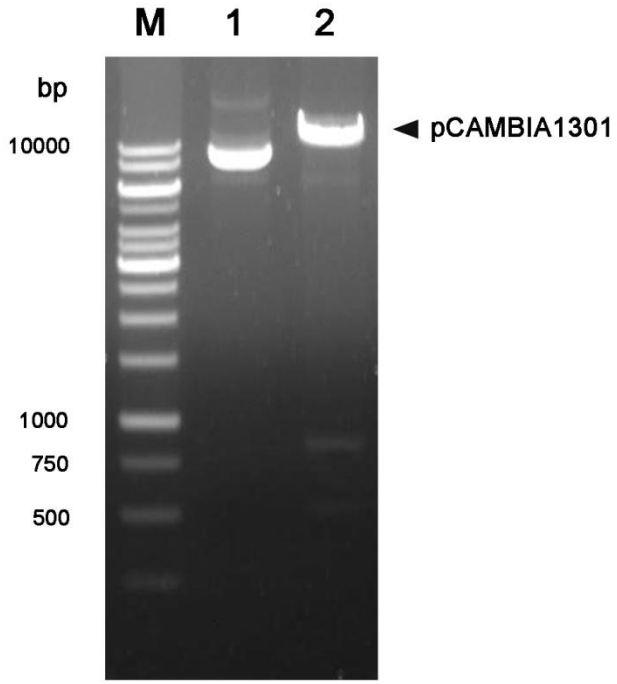

Figure 3.37 Restriction pattern of the recombinant plasmid pCAMBIA-CAMV35S-OsCML3m

Lane M = standard DNA marker

Lane 1 = undigested pCAMBIA-CAMV35S-OsCML3m

Lane 2 = *Hin*dIII -digested pCAMBIA-CAMV35S-OsCML3m

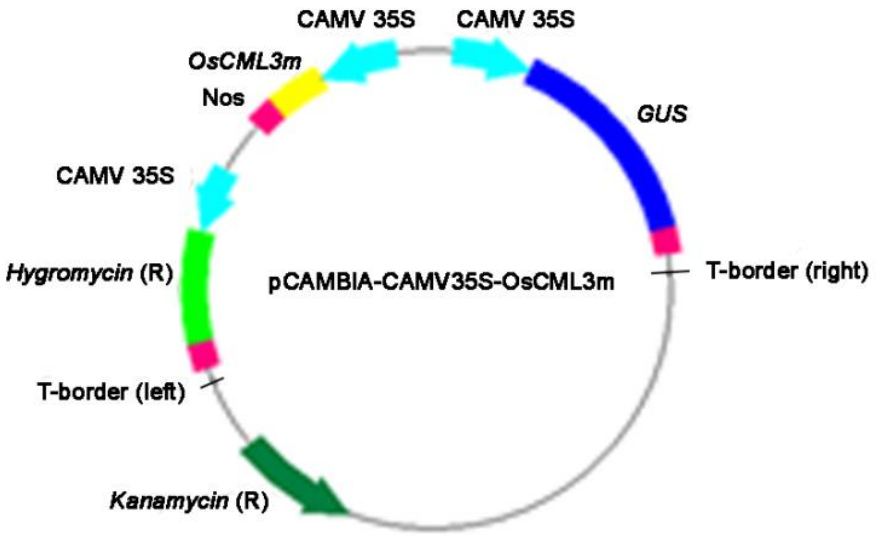

Figure 3.38 Map diagram of the pCAMBIA-CAMV35S-OsCML3m

cloning. Figure 3.39 shows the separation by agarose gel electrophoresis of the CAMV35S-OsCML3 fragment obtained from PCR amplification using various annealing temperatures, which shows the high amount of products of approximately 1.55 kbp as expected at all examined annealing temperatures. The PCR product was ligated into EZ-T vector, and the ligation product was then transformed into *E. coli* (Top 10). A single colony was picked and plasmid digestion was performed using *Bam*HI and *Sal*I. Figure 3.40 shows the two expected bands of approximately 3.0 and 1.55 kbp after digestion. The resulting plasmid was named EZ-CAMV35S-OsCML3. After determining the nucleotide sequence of the insert, the CAMV35S-OsCML3 fragment was sub-cloned into pCAMBIA1301 via *BamH*I and *Sal*I sites. Subsequently, the recombinant pCAMBIA1301 was extracted and digested with *BamH*I and *Sal*I. The separation of the DNA products by agarose gel electrophoresis resulting in two expected bands of pCAMBIA1301 and CAMV35S-OsCML3 fragments was shown in Figure 3.41. The resulting plasmid was called pCAMBIA-CAMV35S-OsCML3 as shown with the schematic diagram in Figure 3.42. After cloning, the nucleotide sequences of pCAMBIA-CAMV35S-OsCML3m and pCAMBIA-CAMV35S-OsCML3 were determined using Up35S, InCML3 and DonosA primers, which were designed from the sequences at the upstream region of the CaMV35S promoter, within the *OsCML3* coding sequence and the downstream region of of the *Nos* terminator, respectively.

The recombinant plasmids pCAMBIA-CAMV35S-OsCML3 and pCAMBIA-CAMV35S-OsCML3m were individually introduced into *Agrobacterium tumefaciens* GV3101, selected on LB agar containing 100 μg/ml gentamycin, 25 μg/ml rifampicin and 50 μg/ml kanamycin, and then the growing colonies were picked and verified by

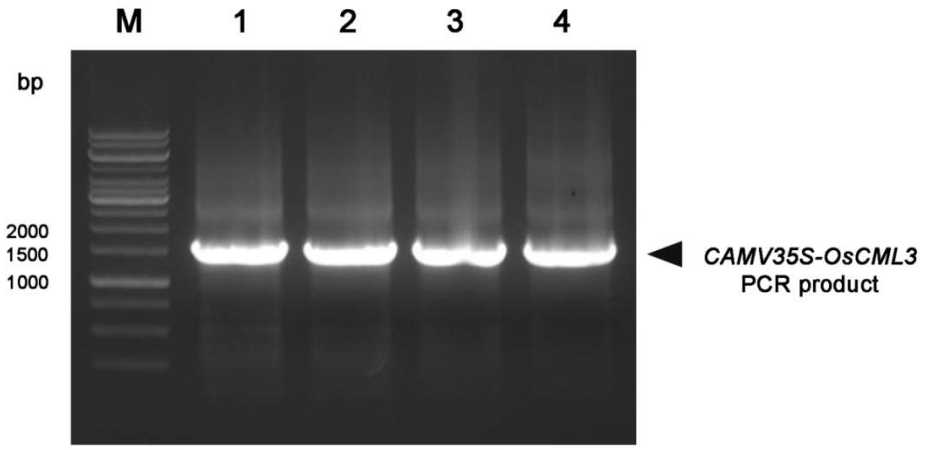

Figure 3.39 PCR products using pGEM-CAMV35S-OsCML3 as a template and varied annealing temperatures

Lane M = standard DNA marker

Lane 1 = PCR product of *CAMV35S-OsCML3* gene fragment using annealing temperature of 59 ^{o}C

Lane 2 = PCR product of *CAMV35S-OsCML3* gene fragment using annealing temperature of 61.1 ^{o}C

Lane 3 = PCR product of *CAMV35S-OsCML3* gene fragment using annealing temperature of 64.6 ^{o}C

Lane 4 = PCR product of *CAMV35S-OsCML3* gene fragment using annealing temperature of 68.2 ^{o}C

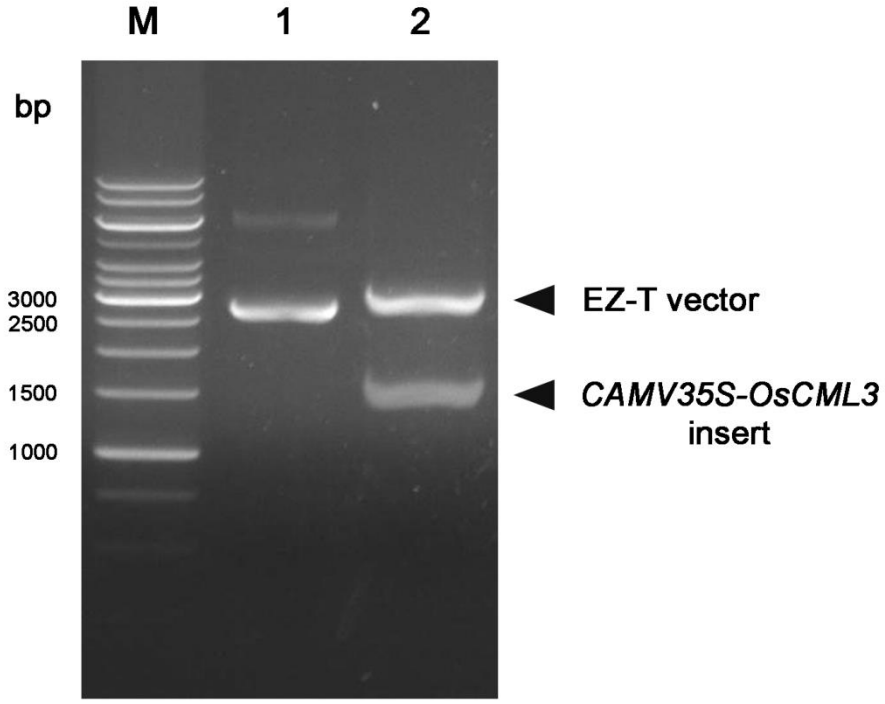

Figure 3.40 Restriction pattern of the recombinant plasmid EZ-CAMV35S-OsCML3

Lane M = standard DNA marker

Lane 1 = undigested EZ-CAMV35S-OsCML3

Lane 2 = *Bam*HI/*Sal*I-digested EZ-CAMV35S-OsCML3

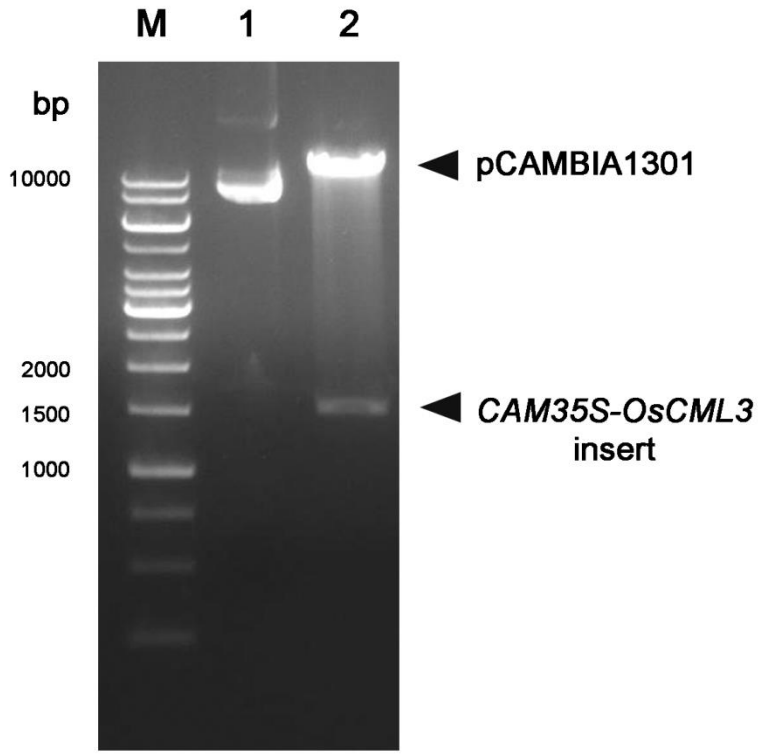

Figure 3.41 Restriction pattern of the recombinant plasmid pCAMBIA-CAMV35S-OsCML3

Lane M = standard DNA marker

Lane 1 = undigested pCAMBIA-CAMV35S-OsCML3

Lane 2 = *Bam*HI/*Sal*I-digested pCAMBIA-CAMV35S-OsCML3

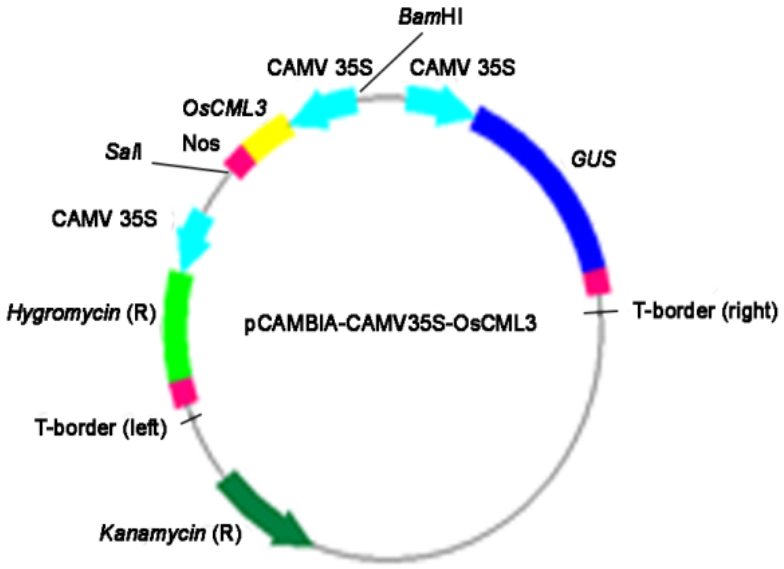

Figure 3.42 Map diagram of the pCAMBIA-CAMV35S-OsCML3

colony PCR using a pair of primers as described in section 2.2.6.C. Figure 3.43 shows the colony PCR products of approximately 3.3, 1.5 and 0.45 kbp from the transformants harboring pCAMBIA1301, pCAMBIA-CAMV35S-OsCML3 and pCAMBIA-CAMV35S-OsCML3m, respectively. Suspension culture of the recombinant *Agrobacterium* was prepared as described in section 2.2.6.E and then used to perform floral dipping with the prepared *Arabidopsis thaliana*, ecotype Columbia. The Arabidopsis transformants were grown in the green house at 22 ^{o}C under a 16:8 hour light: dark photoperiod until seeds were set and harvested. These seeds were called T1 seeds. Then, T1 seeds were plated on MS agar containing 30 μg/ml hygromycin to select resistance plant. After seeds had become seedlings, GUS activity of resistance plants were checked by cutting the leaf tissues, staining with X-Gluc solution and incubating at 37 ^{o}C overnight (see Appendix C). Figure 3.44 shows representatives of leaf tissues of OsCML3 and OsCML3m transgenic plants and the wild type stained with X-Gluc solution. From this experiment, we obtained 13, 25 and 19 lines of transgenic plants harboring OsCML3, OsCML3m and blank pCAMBIA1301 vector, called 1301 transgenic plant, respectively. After that, seeds of plants having positive GUS staining were harvested and called T2 seeds. Subsequently, T2 seeds were plated on MS agars containing 30 μg/ml hygromycin. The transgenic lines of single copy insertion with a segregation ratio of being resistant to being sensitive as 3:1 were selected under the chi-square test. We obtained 8, 8 and 6 lines of OsCML3, OsCML3m and 1301 transgenic plants, respectively, which were self-pollinated to generate T3 seeds. Next, T3 seeds were plated on MS agar containing 30 μg/ml hygromycin to select homozygous plants. The T3 transgenic plants that grew with one-hundred percent germination of plated seeds were selected

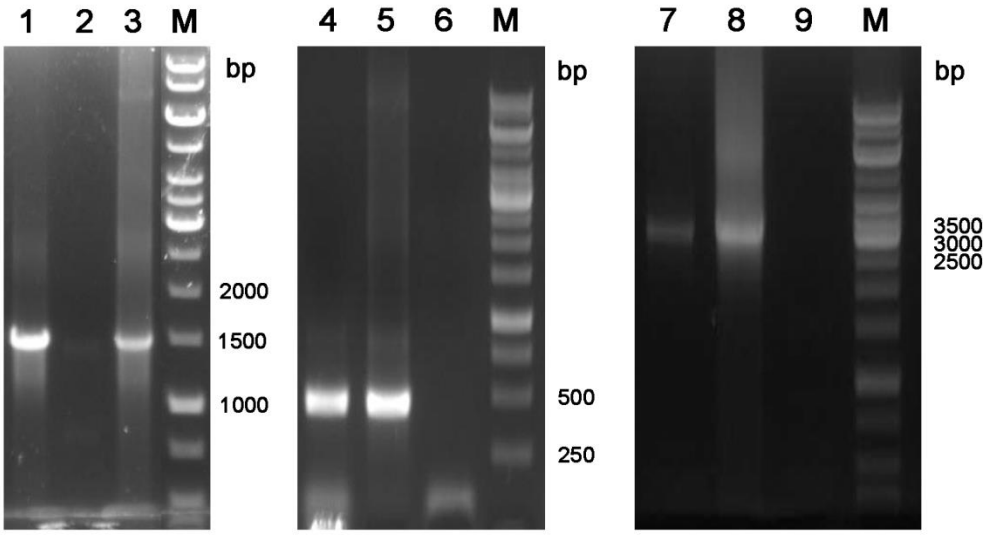

Figure 3.43 Representative colony PCR products of pCAMBIA1301, pCAMBIA-CAMV35S-OsCML3 and pCAMBIA-CAMV35S-OsCML3m transformants

Lane 1 = colony PCR product of transformant harboring pCAMBIA-CAMV35S-OsCML3

Lane 4 = colony PCR product of transformant harboring pCAMBIA-CAMV35S-OsCML3m

Lane 7 = colony PCR product of transformant harboring pCAMBIA1301

Lanes 2, 6 and 9 = Negative control using dH_2O instead of transformant harboring pCAMBIA-CAMV35S-OsCML3, pCAMBIA-CAMV35S-OsCML3m and pCAMBIA1301 respectively

Lanes 3, 5 and 8 = Positive control using pCAMBIA-CAMV35S-OsCML3, pCAMBIA-CAMV35S-OsCML3m and pCAMBIA1301 as template, respectively

Lane M = standard DNA marker

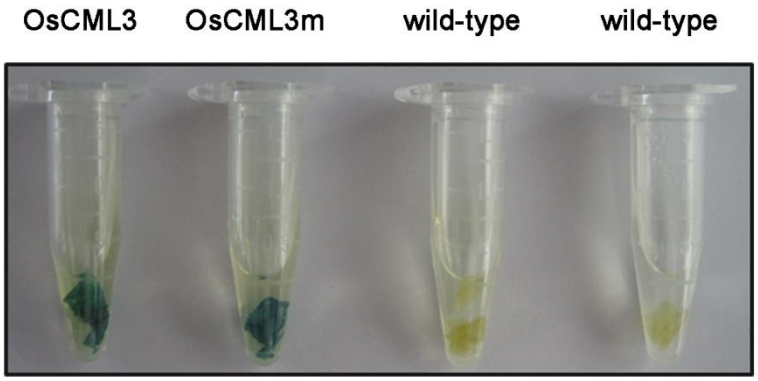

Figure 3.44 Representative histochemical analysis of GUS activity of leaf tissues stained with X-Gluc

and self-pollinated to generate T4 seeds for further studies. Finally, we obtained 4, 4 and 3 homozygous lines of OsCML3, OsCML3m and 1301 transgenic lines, respectively. Figure 3.45 shows the schematic of homozygous transgenic line selection from T1 to T4 seeds. The homozygous lines of the transgenic *Arabidopsis* and non-transgenic (wild type, WT) were grown on soil. After three weeks, the *Arabidopsis* leaves were collected and immediately frozen in liquid nitrogen and stored at -80 ^{o}C. All tissues were ground in liquid nitrogen to fine powder using a chilled mortar and pestle. To confirm whether the exogenous gene sequences were integrated into the genomic DNA of the transgenic *Arabidopsis*, the genomic DNA was extracted (see appendix E), and then the DNA samples were used as DNA template for PCR as described in section 2.2.6.H. The presence of an amplified *gus* gene fragment with the expected size of 983 bp was obtained in all transgenic lines (pCAMBIA1301 alone, pCAMBIA-CAMV35S-OsCML3 and pCAMBIA-CAMV35S-OsCML3m), except in wild-type *Arabidopsis* (Figure 3.46). The gene insert of *OsCML3* using genomic DNA of the transgenic OsCML3 *Arabidopsis* as template, and 35Scheck-F and CML3check-R primers was found with the approximate size of 707 bp (Figure 3.46). Similarly, the band of the *OsCML3m* PCR product amplified from genomic DNA of the transgenic OsCML3m *Arabidopsis* was observed at 661 bp in length. To check the contamination between the transgenic *OsCML3* Arabidopsis and the transgenic *OsCML3m* Arabidopsis, a pair of primers for amplification of the *OsCML3* gene fragment was used with genomic DNA extracted from the *OsCML3m* transgenic lines in the PCR reaction, resulting in no PCR product as shown in Figure 3.46. In contrast, the use of primers for *OsCML3m* amplification and genomic DNA of the *OsCML3* transgenic lines resulted in band product of the

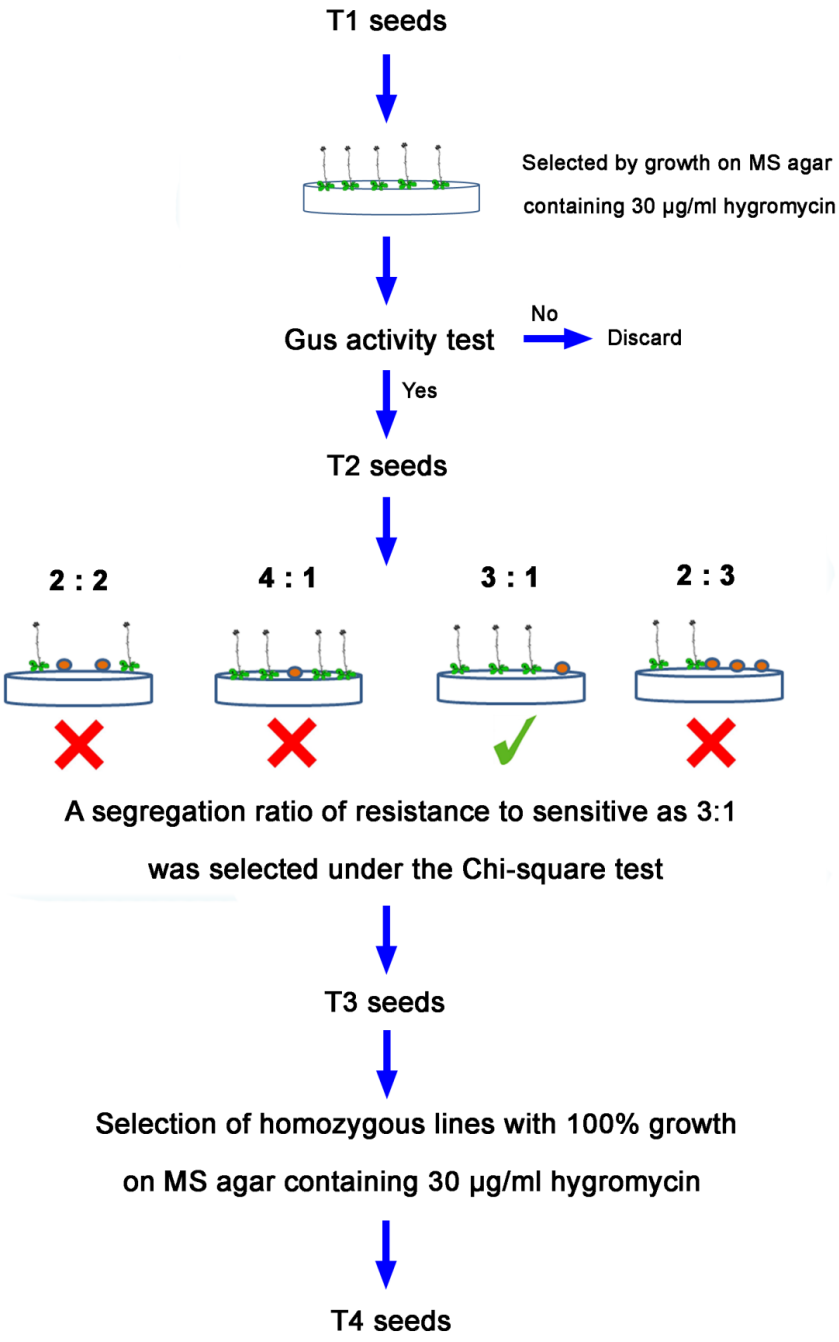

Figure 3.45 Schematic showing the selection of homozygous transgenic lines from T1 seeds to T4 seeds

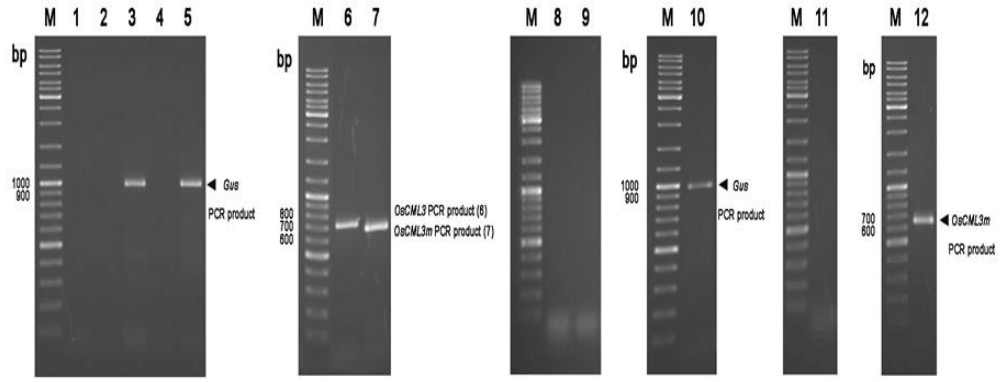

Figure 3.46 Representative PCR analyses of *gus*, *OsCML3 and OsCML3m* gene insertion in the genome of the transgenic *Arabidopsis* and the wild-type *Arabidopsis* plants. PCR products were analyzed on 1% agarose gel and visualized by ethidium bromide staining.

Lane M = 100 bp standard DNA marker

Lanes 1, 2 and 8 = PCR product using genomic DNA of the wild type *Arabidopsis* plant and a pair of primers for the amplification of *gus*, *OsCML3* and *OsCML3m* gene fragment, respectively

Lanes 3, 4 and 9 = PCR product using genomic DNA of the 1301 transgenic *Arabidopsis* and a pair of primers for the amplification of *gus*, *OsCML3* and *OsCML3m* gene fragment, respectively

Lanes 5, 6 and 7 = PCR product using genomic DNA of the *OsCML3* transgenic *Arabidopsis* and a pair of primers for amplification of *gus*, *OsCML3* and *OsCML3m* gene fragment, respectively

Lanes 10, 11 and 12 = PCR product using genomic DNA of the *OsCML3*m transgenic *Arabidopsis* and a pair of primers for amplification of *gus*, *OsCML3* and *OsCML3m* gene fragment, respectively

OsCML3m fragment. No presence of PCR product using all three pairs of primers (35Scheck-F and Guscheck-R, 35Scheck-F and CML3check-R, 35Scheck-F and CML3mcheck-R) in the wild-type Arabidopsis. These results confirm that all transgenic plants with the positive histochemical assay of the GUS reporter contained the *OsCML3 or OsCML3m* transgene in their genomes. No contamination among wild-type Arabidopsis plant and any of the transgenic lines was found.

After obtaining the homozygous transgenic plants, four independent lines of the *OsCML3* overexpressing transgenic plant, four independent lines of the *OsCML3m* overexpressing transgenic plant, one line of the pCaMBIA1301 transgenic plant and the wild-type plant were analyzed for gene expression of *OsCML3* or *OsCML3m*. Total RNA from leaves of all transgenic Arabidopsis lines and the wild-type were extracted. First-stand cDNA was synthesized and quantitative real-time PCR was performed using suitable primers as shown in Table 2.9. *EF-1* alpha was used as internal control to determine the expression level of *OsCML3* or *OsCML3m* in each independent transgenic line. Figure 3.47 shows the relative transcript expression levels of *OsCML3* and *OsCML3m* in the transgenic lines using that of line 13308 and that of line 23203 as reference, respectively. We found that the expression levels of *OsCML3* in all four lines (13308, 21014, 21411 and 23002) were numerically different, where *OsCML3* gene expression levels of lines 21014 and 21411 were statistically significantly higher than those of lines 13308 and 23002. For the expression level of *OsCML3m* in the transgenic Arabidopsis lines overexpressing *OsCML3m*, lines 9802 and 23404 showed the two highest expression levels while that of line 28307 was slightly lower and line 23208 showing the lowest expression level. There was no detection of *OsCML3* and *OsCML3m* expression in the wild-type and

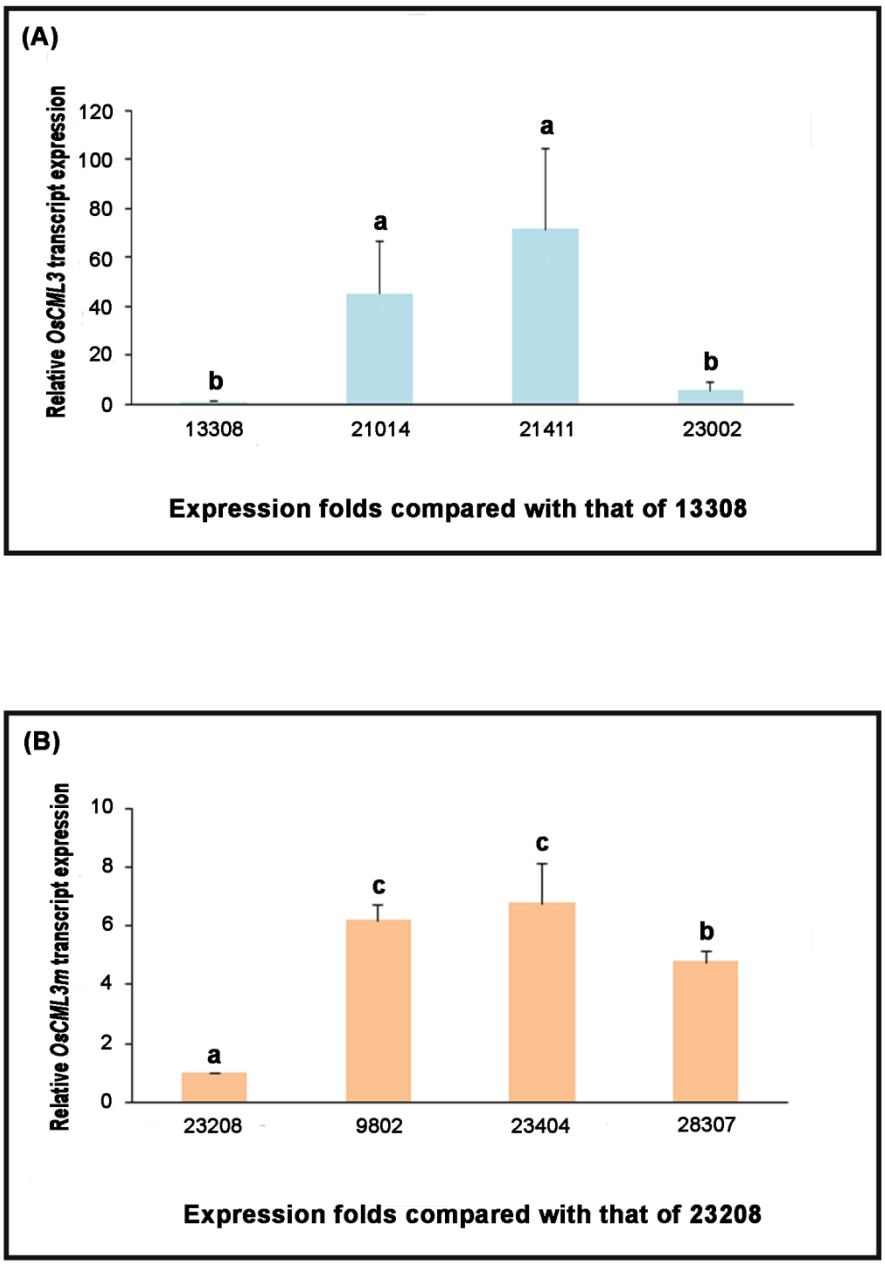

Figure 3.47 Expression levels of *OsCML3* and *OsCML3m* in the transgenic Arabidopsis lines

the pCAMBIA1301 transgenic lines (data not shown). As a result, with their high expression levels, three independent *OsCML3* transgenic lines (21014, 21411 and 23002) and all four *OsCML3m* transgenic lines were selected for phenotypic investigation.

To investigate the cold tolerance in the transgenic *Arabidopsis*, about sixty to seventy seeds of each transgenic line and non-transgenic (wild-type) *Arabidopsis* were plated on MS agar. Then, the number of plates was divided into two groups with a completely randomized design (CRD) with four replicates in each line. Group one was grown under a 16 hr light/18 hr dark photoperiod at normal condition of 22 ^{o}C. Group two was grown under a 16 hr light/18 hr dark photoperiod at cold condition of 11 ^{o}C. At 22 ^{o}C, the germination rate was observed at days 3 and 9 to check the quality of seeds. At day 3, the germination percentage of the wild type and line 21014 seeds were slightly lower than those of the other transgenic seeds (Figure 3.48A) while the germination percentage of the wild type, lines 21014 and 28307 observed at day 9 were slightly lower than the others (Figure 3.48B). Under cold stress, the germination percentages of the wild type and the 1301 transgenic *Arabidopsis* did not differ statistically. About 55% and 48% of the wild type and the 1301 transgenic seeds, respectively, could germinate at day 9 whereas more than 90% of all *OsCML3* and *OsCML3m* transgenic lines were observed except line 21014, which showed about 70% of germination (Figure 3.49A) due to the lower seed quality as observed earlier. Similarly, the higher germination percentages of all transgenic lines were observed compared with that of the wild type and the 1301 transgenic *Arabidopsis*, except line 21014 at day 14 (Figure 3.49B). Data were compared using the analysis of

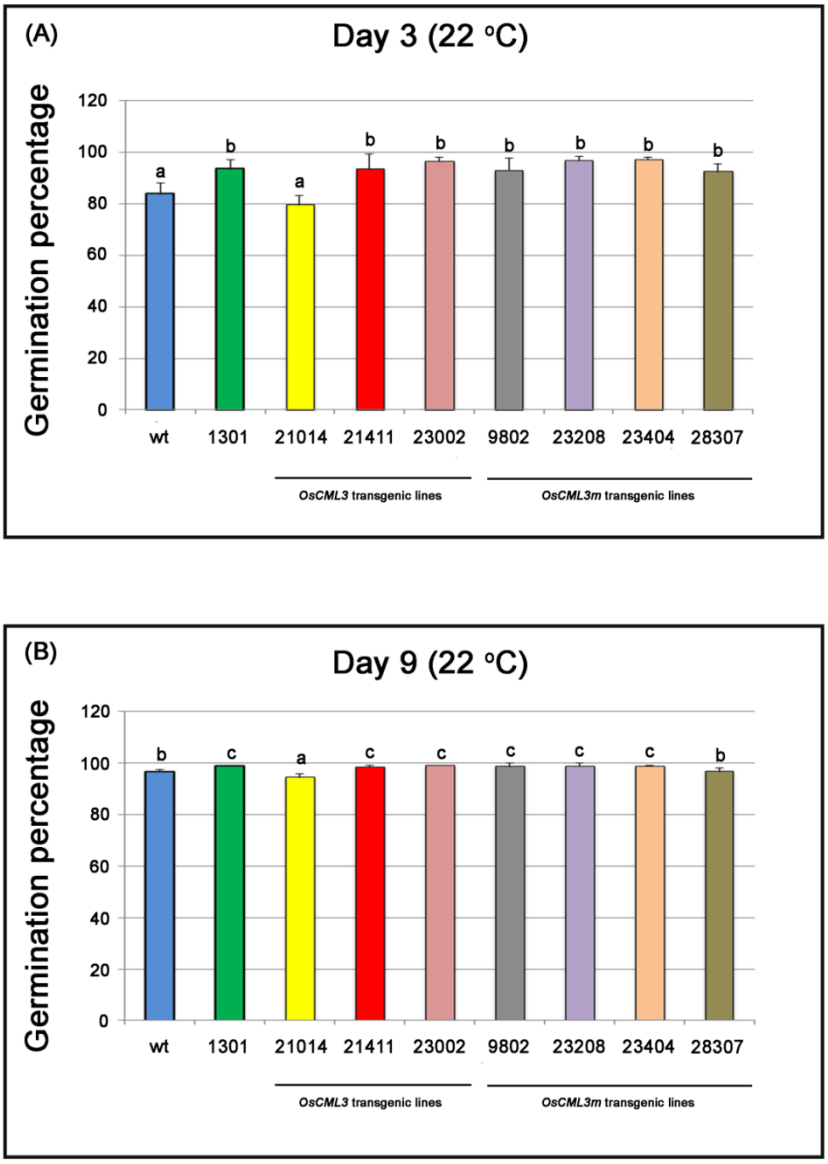

Figure 3.48 The effect of OsCML3 or OsCML3m gene overexpression in *Arabidopsis* on seed germination observed at day 3 (A), and day 9 (B) under normal condition (22 ^{o}C)

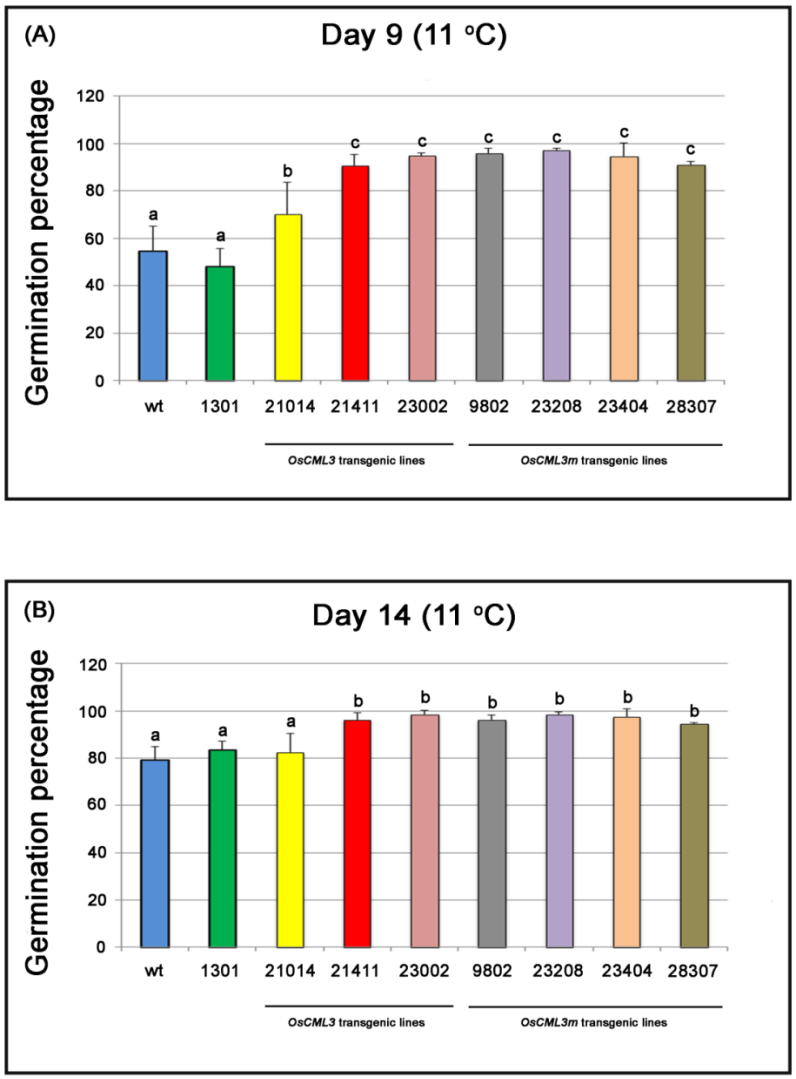

Figure 3.49 The effect of OsCML3 or OsCML3m gene overexpression in *Arabidopsis* on seed germination observed at day 9 (A), and day 14 (B) under cold stress (11 ^{o}C)

variance (ANOVA), and then the means were compared with Duncan's multiple range test (DMRT) accepting significance at the $p < 0.05$ level.

To further investigate the cold response of *Arabidopsis* seedlings, the 14-day seedlings grown at 22 ^{o}C were transferred to soil with 4 plants per pot. The number of pots was divided into two groups with a completely randomized design (CRD) with four pots for each line. Group one was grown under a 16 hr light/18 hr dark photoperiod at normal condition of 22 ^{o}C. Group two was grown under a 16 hr light/18 hr dark photoperiod at cold condition of 11 ^{o}C. After one month, the fresh weight (FW) of whole plants was measured and then plants were dried by incubation at 60 ^{o}C for 3 days. All dried plants were kept in the desiccator for 2 days before measuring dry weight (DW). Figure 3.50A presents the fresh weight of plant grown under cold stress which line 23002 and 23208 was significantly higher than that of wild type and 1301 transgenic line whereas most of *OsCML3* and *OsCML3m* transgenic lines exhibited higher fresh weight ratios of plants grown under cold stress to those under normal condition than the wild type and the 1301 transgenic line (figure 3.50B). Although most of transgenic plants exhibited lower fresh weight than the wild type and the 1301 transgenic plant grown under cold stress due to smaller size of the 14-day seedlings compared to the wild type and the 1301 transgenic plant, they exhibited higher fresh weight ratios of plants grown under cold stress to those under normal condition. Moreover, line 23404 could germinate well under cold stress as observed earlier, but its seedlings could not grow well under the same condition. This may be due to the effect of random integration of the gene insert into the genomic DNA via *Agrobacterium*-mediated transformation in different transgenic lines. Likewise, dry weight of line 23002 and 23208 was higher than control plants

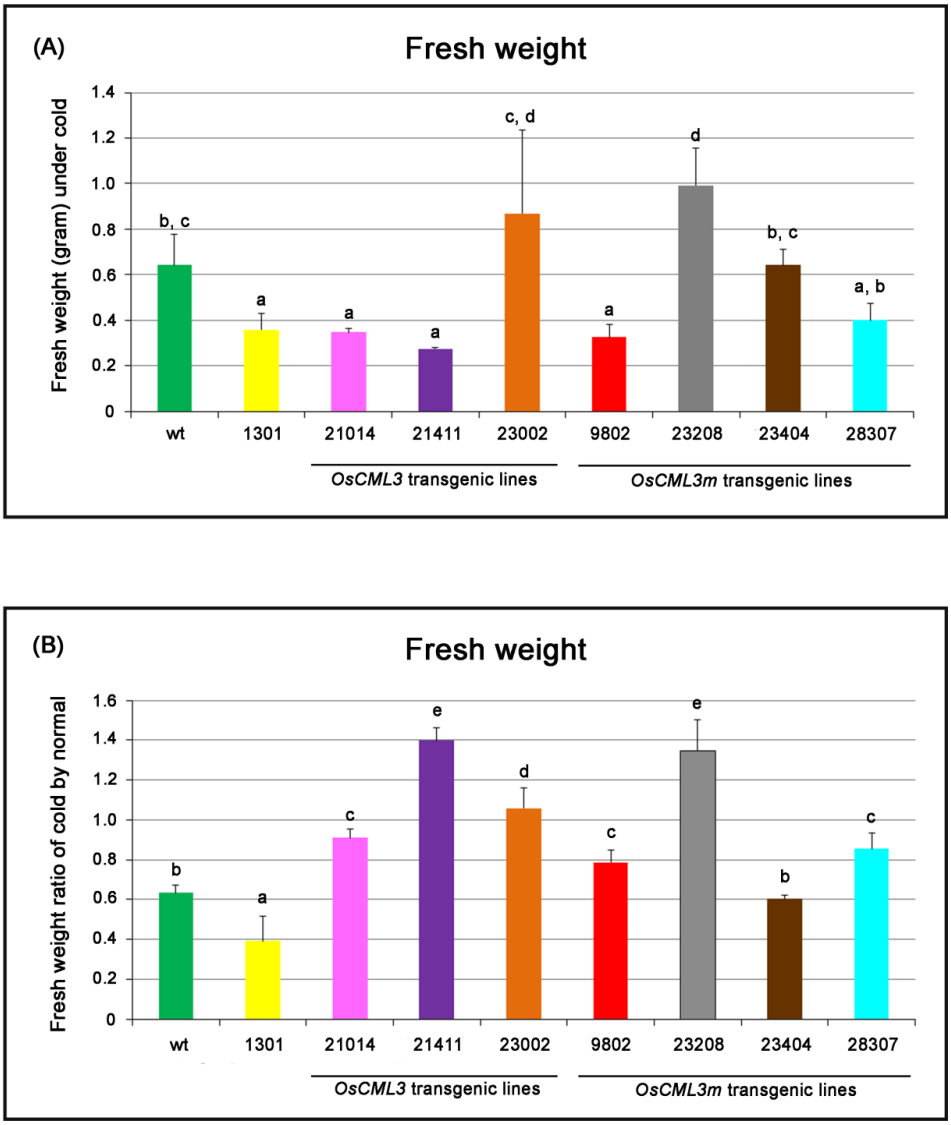

Figure 3.50 Weight of plants grown under cold (A) and weight of plants grown under cold to those grown under normal condition (B) measured in term of fresh weight

(figure 3.51A) while dry weight ratios of most of transgenic Arabidopsis overexpressing *OsCML3* or *OsCML3m* grown under cold stress to those under normal condition were higher than those of the wild type and the 1301 transgenic plant, except line 23404 (Figure 3.51B). These results suggest that the overexpression of *OsCML3* or *OsCML3m* may enhance cold tolerance during germination and seedling stage of Arabidopsis.

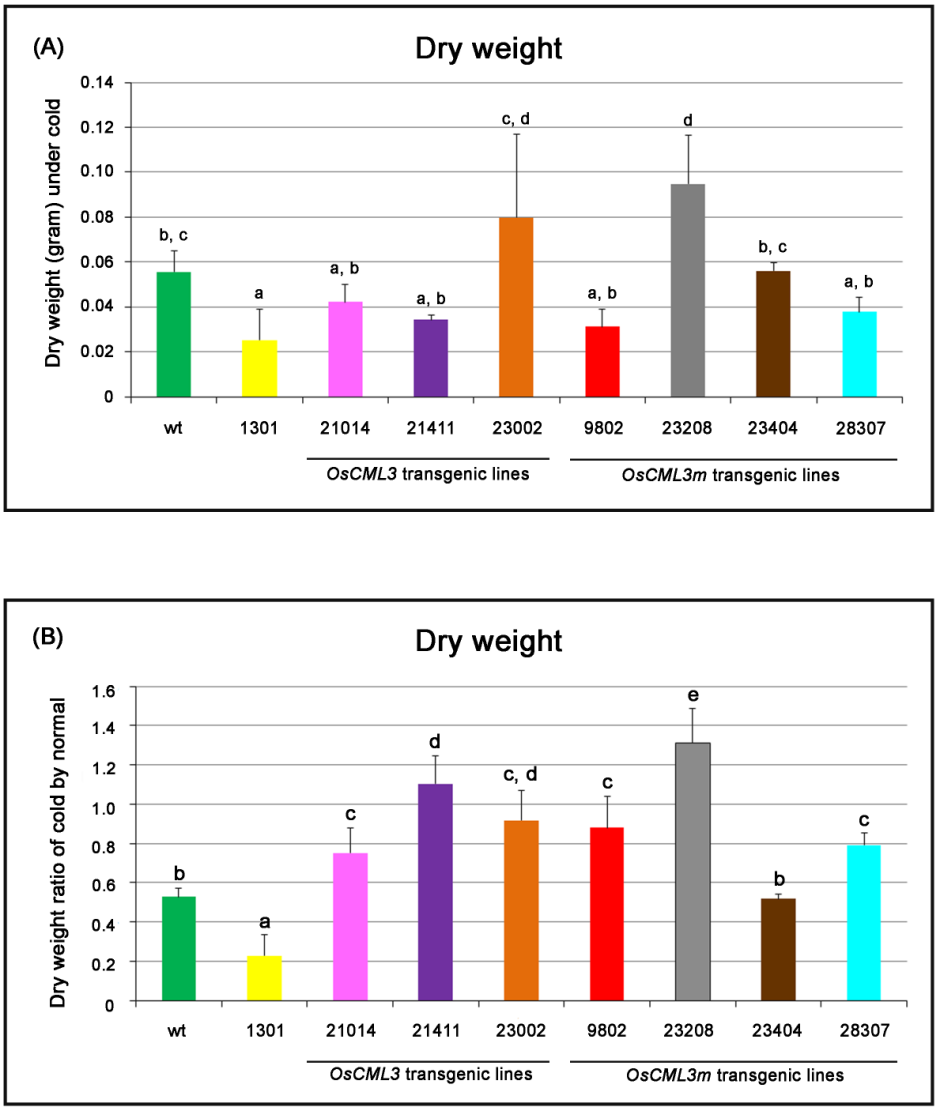

Figure 3.51 Weight of plants grown under cold (A) and weight of plants grown under cold to those grown under normal condition (B) measured in term of dry weight

CHAPTER IV

DISCUSSION

4.1 Cloning and expression of *OsCML3m* gene

In this research, *OsCML3m* gene fragment was cloned into *E. coli* BL21 (DE3) using plasmid pET-21a. For PCR amplification, the sense primer contained an *Nde*I site, while the antisense primer contained of an *Xho*I site were used. The *Nde*I site within the sense primer allowed the gene fragment to be placed at the appropriate distance behind the T7 promoter and the ribosome binding site from the phage T7 major capsid protein in pET-21a (Novagen, 2002). Therefore, this *OsCML3m* gene as well as the other previously cloned genes used in this work (*OsCam1* and *OsCML3*) (Phean-o-pas 2010) could be transcribed under the control of the T7 promoter and effectively translated within the *E. coli* BL21 (DE3) cell using the highly efficient ribosome binding site. The antisense primer, which contained an *Xho*I site and the stop codon of the gene, was designed. Thus, after translation, the resulting protein would consist of only the encoded amino acid sequence identical to the native protein. pET system has been developed for tightly-regulated expression of recombinant proteins in *E. coli* cells. The approach to control basal expression is the use of vectors that contain what is termed a T7*lac* promoter (Dubendorff and Studier 1991). These plasmids contain a *lac* operator sequence just downstream of the T7 promoter. When this type of vector is used in DE3 lysogens, the *lac* repressor acts both at the *lacUV5* promoter in the host chromosome to repress transcription of the T7 RNA polymerase gene by the host polymerase and at the T7*lac* promoter in the vector to block

transcription of the target gene by any T7 RNA polymerase that is made. For protein production under this system, addition of IPTG to a growing culture of the DE3 lysogen induces T7 RNA polymerase production , which in turn transcribes the target DNA in the plasmid. The result indicates that the *OsCML3m* gene was clearly expressed in the presence of all IPTG final concentrations.

4.2 Purification of OsCaM and OsCML proteins

In this work, OsCML3m could be expressed as an intracellular soluble protein as OsCaM1 and OsCML3 (Phean-o-pas 2010). Mechanical disruption methods are usually necessary to break down the cell wall in order to release the intracellular proteins prior to purification. The cell disintegration technique involved cell lysis by ultra-sonication or high pressure sound waves, which causes cell breakage by cavitation and shear forces, so in this work, cell wall was disrupted by ultrasonication. As a result, the control of metabolic regulation mechanism is lost when the cell is disrupted. Therefore, several potential problems may arise during disruption due to the destruction of intracellular compartmentation. In this work, addition of the reagent containing a thiol group such as dithiothreitol (DTT) in the extraction buffer would minimize the oxidation damage (Bollag 1996).

The protein purification was carried out using Ca^{2+}-dependent hydrophobic chromatography on phenyl-Sepharose, which is a medium for hydrophobic interaction chromatography (HIC). Substances are separated on the basis of the varying strength of their hydrophobic interaction with phenyl groups attached to the uncharged matrix.

It is widely used in the purification of recombinant CaM and CaM-like proteins from several sources such as CaM from *Nicotiana. tabacum* (Karita et al. 2004), CML from *Pinctada fucata* (Li et al. 2006) and CML37, CML38, CML39 from *Arabidopsis thaliana* (Vanderbeld and Snedden 2007). In the results, all proteins examined could be purified by Ca^{2+}-dependent phenyl-Sepharose hydrophobic chromatography. Although OsCML3m lacked the C-terminal extension, it still contains two globular domains, which expose their hydrophobic regions upon Ca^{2+} binding. Binding to the column was dependent on the presence of Ca^{2+}, suggesting that the proteins adopt an open conformation, which in turn exposes their hydrophobic regions in the Ca^{2+} bound state and permits the interaction with various cellular targets (Babu et al. 1988; Zhang et al. 1995). Successful purification of these proteins by the Ca^{2+}-dependent hydrophobic chromatography suggests that they are functional Ca^{2+}-binding proteins.

4.3 Characterization of OsCaM and OsCML proteins

Although the biophysical and structural properties of some CaMs and CMLs have been known in several organisms including *Oryza sativa* L. (Chinpongpanich et al. 2011), the biophysical properties and cellular functions of OsCMLs are not well-known in detail. In this study, the biophysical properties between OsCML3 and OsCML3 lacking the C-terminal extension (CTE), termed OsCML3m were compared to investigate the possible roles of the CTE in OsCML3.

The deduced amino acid sequences of OsCaM1, OsCML3 and OsCML3m proteins were compared. Due to its considerable conformational flexibility and being weakly polarized, methionine residues which are estimated to contribute nearly half of

the accessible surface area of the hydrophobic patches of CaM allow it to interact with target proteins in a sequence-independent manner (O'Neil and DeGrado 1990). All of the conserved nine methionine (M) and nine phenylalanine (F) residues among plant CaMs are present in all OsCaMs. OsCaM1, OsCML3 and OsCML3m consist of 6, 4.9 and 4.7% methionine residues, respectively. All these proteins have two pairs of EF hands with characteristic residues commonly found in plant CaMs. Moreover, the OsCML1 and OsCML3 have 38 and 35 amino acid extensions, respectively in the C-terminal extension (CTE) containing a polybasic domain in addition to the 148 amino acid sequence similar to OsCaM1. Previously, the published report shows that OsCML1 (alias OsCaM61) activated CaM-binding protein kinases (OsCBKs) in a Ca^{2+}-dependent manner, while the CTE was not required for the modulation. However, OsCaM61Δ148, OsCaM61 lacking the CTE region, was a better activator of the phosphodiesterase enzyme and showed a higher ability to activate both myosin light-chain kinase (MLCK) and Ca^{2+}/calmodulin-dependent protein kinase class II (CaMKII) compared with the full-length OsCaM61 (Dong et al. 2002).

Examination of the OsCML3 CD spectra showed a relatively small change in the $[\theta]_n$ at 208 and 222 nm upon Ca^{2+} binding, similar to that previously observed from OsCML1 (Chinpongpanich et al. 2011)). In contrast, OsCML3m displayed a significant change, indicating a large increase in the helical content of OsCML3m upon Ca^{2+} binding. However, the apo form of OsCML1 (alias OsCaM61) was previously reported to have an extended helix compared with the holo form, but the Ca^{2+}-bound form seemed to have a much shorter helix that became flexible in the Ca^{2+}-saturated protein (Jamshidiha et al. 2013). OsCML3 was predicted to have an

extended helix as well (data not shown), but it is shorter than that of OsCML1 suggesting that, if both proteins behave similarly upon Ca^{2+} binding, the increased helical content of OsCML3 likely comes from other parts of the protein. Nevertheless, these results suggest that the CTE of OsCML3 has regulatory effects on Ca^{2+} binding, and in turn upon the specific binding of OsCML3 to its targets, in which the hydrophobic patches and the helices surrounding the Ca^{2+}-binding loops are very important (Ikura et al. 1992; Kurokawa et al. 2001; O'Neil and DeGrado 1990).

Interestingly, OsCML3m interacted with the CaM-binding peptide derived from CaM kinase II (CaMKII), a target protein of typical CaMs, while the full-length OsCML3 did not. Thus, the CaM-like region of OsCML3 could interact with the CaMKII peptide upon a Ca^{2+}-induced conformational change similar to typical CaMs, but the CTE appeared to obstruct this interaction suggesting that the CTE interacts with the rest of the protein. A previous NMR study indicated that the CTE of OsCML1 indeed interacted with the rest of the protein, leading to a decreased flexibility of this region (Jamshidiha et al. 2013). The truncated OsCML1 without its CTE was shown to possess a higher ability to activate MLCK and CaMKII compared to that of the full-length OsCML1, supporting the inhibitory effect of the CTE (Dong et al. 2002).

4.4 Subcellular Localization

Subcellular localization of OsCML3 and truncated OsCML3 demonstrated that OsCML3 is localized to the plasma membrane and the truncated OsCML3 was detected in the nucleus and the cytoplasm, suggesting that the polybasic domain of the

extended C-terminus tail and the prenylation site of OsCML3 play important function in determining its cellular location. Previous report has found that PhCaM53, a similar protein from Petunia, localized at the plasma membrane whereas the non-prenylated PhCaM53 was transported to the nucleus. Also, GFP-basic domain of PhCaM53 fusion could be detected in the nucleus when the isoprenoid biosynthesis was blocked using the specific inhibitor mevinolin or by dark incubation whereas the dark exposure of the leaf explants on a medium containing 2% sucrose prevented nuclear localization, suggesting that CaM53 played a function relating to the metabolic status of the plant cells. (Rodríguez-Concepción et al. 1999). Similarly, the exposed prenylation site of OsCaM61 associated with membrane whereas the non-exposed was mainly detected in the nucleoplasm (Dong et al. 2002). These results indicated that the location of these proteins depended on the prenylation status. It was reported that the polybasic domain also involves in the prenylation status of the protein by increasing the binding affinity of GGTase-I, which is used for prenylation (James et al. 1995; Rodríguez-Concepción et al. 1999).

4.5 Identification of OsCML3 and OsCML3m-binding proteins and confirmation of the protein-protein interaction

OsPEBP and OsHMGB1 were two of the putative targets of OsCML3 identified by screening a cDNA expression library with OsCML3m as the probe. Screening with the full-length OsCML3 identified only a few targets and not these proteins, which conforms to the notion that the CTE interferes with target binding of OsCML3.

OsCML1 was reported to activate the CaM-binding protein kinases (OsCBKs) in a Ca^{2+}-dependent manner, while the CTE domain was not required for this effect (Rodríguez-Concepción et al. 1999). In contrast, the CTE of OsCML1 has been shown to decrease the activation of phosphodiesterase (Bouche et al. 2005), which is in agreement with the inhibitory effect of the CTE of OsCML3 on its interaction with targets. . These results suggest a differential activity of the CTE domain upon the binding ability of these CML proteins to different target proteins. Nonetheless, the CTE likely plays regulatory roles for the Ca^{2+}-modulated activity of these CML proteins. For OsCML3, to overcome the interfering effect of its CTE *in vivo*, we hypothesized that other proteins or mechanisms may be involved in the target binding of OsCML3, or that there are post-translation modifications of either OsCML3 or its target protein or both proteins to facilitate their interaction.

For confirmation of protein interaction of OsPEBP with OsCML3, OsCML3m or OsCML3s, the yeast two-hybrid analysis could not conclude their interaction; as no green fluorescence signal was observed from the three pairs of OsPEBP-OsCML3, OsPEBP-OsCML3m and OsPEBP-OsCML3s. These results indicate that OsPEBP, a putative OsCML3m-binding protein, may not be OsCML3 target protein. Therefore, for further investigation of protein interaction, we only focused on the interaction of OsHMGB1 with OsCML3, OsCML3m or OsCML3s.

The BiFC assay showed that OsHMGB1-OsCML3, OsHMGB1-OsCML3m and OsHMGB1-OsCML3s interaction all occurred in the nucleus. The NLS of OsHMGB1 likely facilitated the movement of these protein complexes to the nucleus. We speculate that either unknown proteins or mechanisms are involved in exposing specific regions of OsCML3 for binding to OsHMGB1, or that post-translational

modification of OsHMGB1 facilitates the interaction. The latter scenario has been observed from the phosphorylation of maize HMGB1 by protein kinase CK2 that abolishes its interaction with transcription factor Dof2 and the stimulation of Dof2 DNA binding (Krohn et al. 2002).

In general, HMGB proteins are known to play a role in the regulation of transcription and other DNA-dependent processes (Agresti and Bianchi 2003; Bustin and Reeves 1996; Reeves 2010), and OsHMGB was observed to accumulate in cold-treated rice seedlings (Cooper et al. 2003) while overexpression of AtHMGB2 reduced seed germination under dehydration conditions in Arabidopsis (Kwak et al. 2007). These indicate that HMGB proteins are likely to play a role in the responses to various stresses, possibly through DNA-binding dependent processes. Here, the examination of the effect of OsCML3 or OsCML3m on the binding of OsHMGB1 to supercoiled DNA revealed that OsCML3m decreased the binding of OsHMGB1 to the supercoiled pUC19 DNA in the presence of Ca^{2+}, while OsCML3 did not. Since the interaction between OsCML3 and OsHMGB1 was observed in the nucleus, we speculate that, probably with the help of other proteins or unknown mechanisms, the inhibitory effect of the CTE is released leading to the interaction of OsCML3 with OsHMGB1 and the transport of the complex into the nucleus (Figure 4.1), where OsCML3 might function to regulate the DNA binding of OsHMGB1 in the nucleus and subsequently affect transcription and other DNA-dependent processes (Agresti and Bianchi 2003; Bustin and Reeves 1996; Reeves 2010).

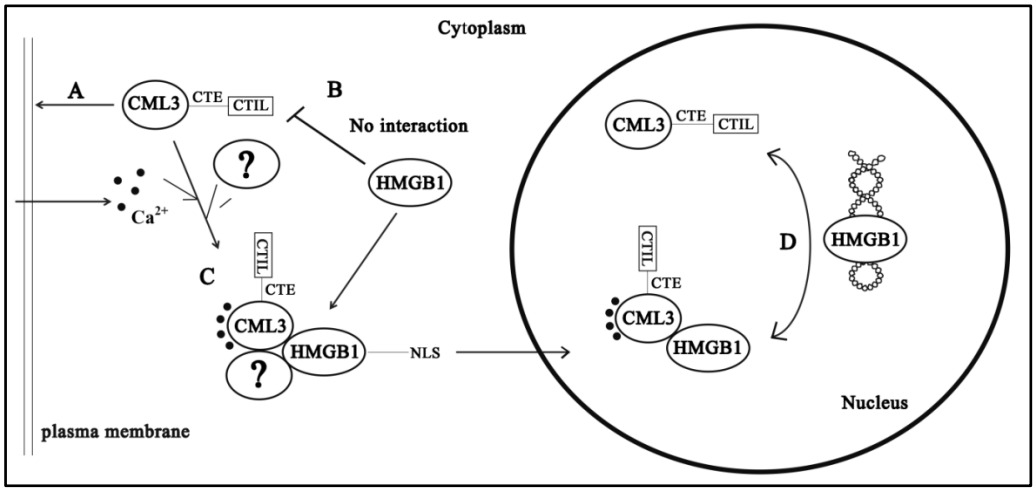

Figure 4.1 A possible model of OsCML3 functionality and interaction with HMGB1. (A) OsCML3 is localized to the plasma membrane through prenylation at the CTIL sequence in the CTE domain. (B) No interaction between OsHMGB1 and cytosolic OsCML3 occurs because of the inhibitory effect of the CTE. (C) Other proteins or an unknown mechanism (?) facilitate the interaction of OsHMGB1 with OsCML3 leading to the transportation of the HMGB1-OsCML3 complex into the nucleus through the NLS of HMGB1. (D) The supercoiled DNA-binding of OsHMGB1 is regulated by the presence of OsCML3 in the nucleus.

4.6 Transcript expression analysis of the *OsCML3* gene in rice (*Oryza sativa* L.) under various conditions

Up-regulated expression of a gene in response to a stress signal may reflect the function of the corresponding gene product, especially in signal cascades. In this study, the transcript expression analysis of *OsCML3* gene by rt-RT-PCR revealed that the expression level of *OsCML3* only exhibited a slight decrease at 1 and 24 h after

salt stress treatment, suggesting that OsCML3 may not function in the mechanism of Ca^{2+}-mediated responses to salt stress. In addition, a slight decrease of *OsCML3* transcript expression level was found at 48 h under Indole-3-acetic acid (IAA) application whereas 6-Benzylaminopurine (BA) application increased the *OsCML3* transcript expression level with a late response at 48 h.

Generally, the late response in the transcript expression levels for some of the cytokinin-responsive genes may be resulted from the multistep phosphorelay involving cytokinin receptors that relay the cytokinin signal from membrane to nucleus (Tsai et al. 2012) to regulate differential expression of target genes in response to stimuli. Although the relation between cytokinin response and Ca^{2+}/calmodulin signaling is not widely known, this finding may suggest a novel function of CMLs in rice involving with cytokinin, which plays a central role during the cell cycle and influence numerous developmental programs (Werner et al. 2001). In addition, the transcript expression level of *OsCML3* was slightly decreased under auxin treatment while its expression was increased under cytokinin application. This may be due to the control of OsCML3 function involved in auxin and cytokinin, for instance, auxin inhibits the activation of axillary buds and hence shoot branching, while cytokinin has the opposite effect (Müller and Leyser 2011).

Interestingly, the transcript expression level of *OsCML3* was early up-regulated with 2-3-folds at 3 h after cold stress treatment compared with the untreated and then declined to lower level as that of the control at 6 h. This result suggests that OsCML3 function may involve in the response to cold stress.

Previous reports have shown the functions of CaMs and CMLs involving in low temperature. For example, calmodulin was a signaling component required for

the cold induction of *COR* (cold-responsive) genes in *Arabidopsis* (Braam and Davis 1990). In *Nicotiana plumbaginifolia*, the level of *NpCAM*1 was high in response to cold and high wind, while *NpCAM*2 expression was not induced by either of the treatments (van Der Luit et al. 1999). Similarly, *AtCML9* transcript levels changed in response to NaCl, cold, and dehydration (Magnan et al. 2008). Moreover, strong induction of *OsMSR2* (a.k.a. *OsCML31*) expression by cold, drought and heat stresses was detected (Xu et al. 2011). In contrast, increased expression of *CAM*3 in *Arabidopsis* seedlings inhibited the expression of *COR* gene in response to cold (Townley and Knight 2002). This study reveals a novel function of CML3 from rice related to low temperature.

4.7 Analysis of *cis*-acting regulatory DNA elements

The *cis*-acting elements that function in stress-responsive gene expression have been analyzed to elucidate the molecular mechanisms of gene expression in response to these stresses (Maruyama et al. 2012). Three *cis*-acting elements of DREs (drought- responsive elements), ABREs (ABA-responsive elements) and LTREs (low temperature responsive elements) were considered in this study. Although the abscisic acid (ABA) -responsive element (ABRE) that regulates dehydration- and high salinity-responsive gene expression in *Arabidopsis* and *Oryza sativa* (Yamaguchi-Shinozaki and Shinozaki 1994) was found in the 5′ upstream promoter of *OsCML3* gene, its transcript expression examined by rt-RT-PCR was not clear under salt stress as well as drought stress in which no change in *OsCML3* expression level was previously found. Low temperature responsive elements (LTRE) was found in its upstream promoter corresponding to the result that its transcript expression was

increased under low temperature, confirming that OsCML3 may has function involved with cold stress. In contrast, the dehydration-responsive element (DRE) that regulates cold- and dehydration-responsive gene expression (Yamaguchi-Shinozaki and Shinozaki 1994) is not present in its upstream promoter, indicating that the regulation of *OsCML3* expression under cold stress does not involve with the DREB-CRT/DRE pathway.

4.8 Overexpression of OsCML3 and OsCML3m in Arabidopsis thaliana

Construction of pCAMBIA1301containing *OsCML3* or *OsCML3m* was successful. *OsCML3* or *OsCML3m* coding sequence was individually inserted to be over-expressed under the control of the CaMV 35S promoter. Then, the recombinant plasmids pCAMBIA-CAMV35S-OsCML3 and pCAMBIA-CAMV35S-OsCML3m were individually introduced into *Agrobacterium tumefaciens* GV3101 to prepare *Agrobacterium* cell suspension for floral dipping.

Since *Agrobacterium*-mediated genetic transformation methods such as vacuum infiltration and floral dipping methods have been developed (Clough and Bent 1998), they are currently and successfully used for the transformation of numerous plant species (Tzfira and Citovsky 2006). In this study, the floral dipping was used for transformation of Arabidopsis by integrating the gene of interest into its genome. For the floral dipping transformation, the use of sucrose and silwet L-77 mixed in *Agrobacterium suspension* is critical to success of the floral dip method (Clough and Bent 1998). After transformation, plants were grown under normal condition until T1 seeds were collected. Then, T1 seeds were plated on MS agar

containing 30 μg/ml hygromycin, subsequently, the seeds that could germinate and produced green leaves with good health were checked for Gus activity. Transgenic Arabidopsis lines exhibiting Gus activity were chosen for harvesting T2 seeds. After we checked Gus activity, the number of transgenic lines showing Gus activity was less than the number of the T1 plants that could grow on MS agar containing 30 μg/ml hygromycin, which may be because of the biological diversity in plants, as some non-transgenic Arabidopsis could show hygromycin resistance.

Then, T2 seeds were plated on MS agars containing 30 μg/ml hygromycin to select the transgenic lines that had a single copy insertion. According to Mendel's Law, the transgenic *Arabidopsis* containing a single copy of gene insertion would show a 3:1 phenotypic ratio of being resistant to being sensitive when T2 seeds were plated on MS agars containing 30 μg/ml hygromycin. The calculation was under the Chi-squared test (Pearson 1900). Then, the collected T3 seeds were checked in order to select the homozygous lines with one-hundred percent germination on MS agars containing 30 μg/ml hygromycin, and then the homozygous plants were self-pollinated to generate T4 seeds, that were used for genotypic and phenotypic investigation.

PCR reaction using suitable primers used to confirm whether the exogenous gene sequences were integrated into the genomic DNA of the transgenic *Arabidopsis*, generated correct PCR fragment size as expected of each transgenic line. These results confirmed that all homozygous transgenic plants contained the *OsCML3* or *OsCML3m* transgene in their genomes. To further determine the expression level of each independent transgenic line, q-rt-PCR was performed using the house-keeping gene *EF-1α* for internal control whose expression was stable under normal, biotic and

abiotic stresses (Nicot et al. 2005). Although the OsCML3 or OsCML3m transcript expression was similarly high under the control of the strong CaMV 35S promoter, their expression levels were numerically differentamong different independent lines. Variation of transgene expression in plants possibly comes from several factors, including the transgene insertion site and RNA silencing in the host plant (Butaye et al. 2005; Kooter et al. 1999; Matzke and Matzke 1998; Nagaya et al. 2005).

Interestingly, as mentioned earlier, the *OsCML3* transcript expression level increased under cold stress, and low-temperature responsive element (LTRE) was found in the *OsCML3* promoter. These evidences lead us to the hypothesis that the function of OsCML3 is possibly involved in the response to cold stress. Thus, this research, we aimed to investigate the effect of cold stress on the transgenic Arabidopsis overexpressing *OsCML3* or *OsCML3m* by examining germination and growth at seedling stage. From the results, overexpression of *OsCML3* and *OsCML3m* in the transgenic Arabidopsis enhanced cold tolerance both at germination and the seedling stage, indicating that OsCML3 plays a role in the response to cold stress. Although each of *OsCML3* and *OsCML3m* overexpression in the transgenic Arabidopsis exhibited similar results where their growth under low temperature was better than that of the wild type, the transcriptome profiles of cold-responsive genes induced by the overexpression *OsCML3* or *OsCML3m* may differ and should be examined, which may help us understand the molecular function of OsCML3 and the regulatory role of its CTE.

Previously, the involvement of CaM in cold induction of cold responsive (*COR*) genes and the induction of CaM by low temperature have been shown (Braam and Davis 1990). Over-expression of *CAM3* in Arabidopsis resulted in decreased

expression of cold-induced *COR* genes suggesting a negative regulatory role for CaM in the regulation of *COR* expression in plants (Townley and Knight 2002). In *Nicotiana plumbaginifolia*, the expression level of *NpCAM*1 was high in response to cold (van Der Luit et al. 1999). Moreover, AtCAMTA3, a calmodulin binding transcription activators 3 has been identified as a positive regulator of CBF2 (C-repeat binding factor 2) expression through binding to a regulatory element (CG-1 element, vCGCGb) in its promoter (Doherty et al. 2009). Overexpression of AtCBF2 showed freezing, salt and drought tolerance, which is involved with the expression of *COR* (*cold-responsive*) *gene* (Liu et al. 1998). The *camta1/camta3* double mutant exhibited decreased freezing tolerance compared with that of the wild type, suggesting that CAMTAs might be a direct link between calcium signals and cold-regulated gene expression for cold acclimation (Jeon and Kim 2013). Expression of *OsMSR2* (or *OsCML31*) was strongly up-regulated by cold, drought, and heat stresses in rice (Xu et al. 2011), and overexpression of *OsCML31* enhanced salt tolerance in Arabidopsis (Xu et al. 2011) and rice (Xu et al. 2013), but the function of OsCML31 on cold stress response was not investigated in detail.Consequently, these studies revealed a novel function of OsCML3 in the response to cold stress and it might co-function with OsHMGB1, an OsCML3 target protein, whose transcript was found accumulated in the cold-treated rice seedlings (Cooper et al. 2003) potentially regulating gene transcription and recombination processes (Bustin 1999; Thomas and Travers 2001).

Suggestions for further studies

1. From this research, OsHMGB1 was found to be a target of OsCML3 *in planta*, but their interaction is probably required unknown mechanism, other protein or post-

translational modification. It is interesting to investigate what their interaction depends on.

2. These results revealed that the CTE of OsCML3 inhibited its binding to the target protein. Thus, the protein structure of OsCML3 with its target by NMR or X-ray crystallography should be determined to explain why the CTE inhibits this interaction.

3. Overexpression of OsCML3 or OsCML3m in transgenic *Arabidopsis* enhanced cold tolerance at seed germination and seedling stage. These finding inspire us to investigate the effect of overexpressing OsCML3 or OsCML3m on the transcriptome profile in the OsCML3-overexpressing transgenic Arabidopsis by RNA-sequencing.

4. Other physiological studies such as freezing test, salt, drought and heat stresses should be investigated in the OsCML3-overexpressing transgenic Arabidopsis.

REFERENCES

Agresti A, Bianchi ME (2003) HMGB proteins and gene expression. Current Opinion in Genetics & Development 13 (2):170-178. doi:http://dx.doi.org/10.1016/S0959-437X(03)00023-6

Babu YS, Bugg CE, Cook WJ (1988) Structure of calmodulin refined at 2.2 A resolution. Journal of molecular biology 204 (1):191-204

Banfield MJ, Brady RL (2000) The structure of Antirrhinum centroradialis protein (CEN) suggests a role as a kinase regulator. Journal of molecular biology 297 (5):1159-1170. doi:10.1006/jmbi.2000.3619

Benson DA, Cavanaugh M, Clark K, Karsch-Mizrachi I, Lipman DJ, Ostell J, Sayers EW (2013) GenBank. Nucleic acids research 41 (Database issue):D36-42. doi:10.1093/nar/gks1195

Bollag DM, Rozycki, M. D., and Edelstein, S. J. (1996) Protein methods.

Bologna G, Yvon C, Duvaud S, Veuthey AL (2004) N-Terminal myristoylation predictions by ensembles of neural networks. Proteomics 4 (6):1626-1632. doi:10.1002/pmic.200300783

Bolton MD (2009) Primary metabolism and plant defense--fuel for the fire. Molecular plant-microbe interactions : MPMI 22 (5):487-497. doi:10.1094/mpmi-22-5-0487

Boonburapong B, Buaboocha T (2007) Genome-wide identification and analyses of the rice calmodulin and related potential calcium sensor proteins. BMC plant biology 7:4-4. doi:10.1186/1471-2229-7-4

Bouche N, Yellin A, Snedden WA, Fromm H (2005) Plant-specific calmodulin-binding proteins. Annual review of plant biology 56:435-466. doi:10.1146/annurev.arplant.56.032604.144224

Boudsocq M, Sheen J (2010) Calcium Sensing and Signaling. In: Abiotic Stress Adaptation in Plants. The Netherlands

Braam J, Davis RW (1990) Rain-, wind-, and touch-induced expression of calmodulin and calmodulin-related genes in Arabidopsis. Cell 60 (3):357-364

Bush D, Biswas A, Jones R (1989) Gibberellic-acid-stimulated Ca2+ accumulation in endoplasmic reticulum of barley aleurone: Ca2+ transport and steady-state levels. Planta 178 (3):411-420. doi:10.1007/BF00391870

Bustin M (1999) Regulation of DNA-dependent activities by the functional motifs of the high-mobility-group chromosomal proteins. Molecular and cellular biology 19 (8):5237-5246

Bustin M, Reeves R (1996) High-mobility-group chromosomal proteins: architectural components that facilitate chromatin function. Progress in nucleic acid research and molecular biology 54:35-100

Butaye KMJ, Cammue BPA, Delauré SL, De Bolle MFC (2005) Approaches to Minimize Variation of Transgene Expression in Plants. Mol Breeding 16 (1):79-91. doi:10.1007/s11032-005-4929-9

Chang WC, Lee TY, Huang HD, Huang HY, Pan RL (2008) PlantPAN: Plant promoter analysis navigator, for identifying combinatorial cis-regulatory elements with distance constraint in plant gene groups. BMC genomics 9:561. doi:10.1186/1471-2164-9-561

Chiasson D, Ekengren SK, Martin GB, Dobney SL, Snedden WA (2005) Calmodulin-like proteins from Arabidopsis and tomato are involved in host defense against Pseudomonas syringae pv. tomato. Plant molecular biology 58 (6):887-897. doi:10.1007/s11103-005-8395-x

Chinpongpanich A, Limruengroj K, Phean OPS, Limpaseni T, Buaboocha T (2012) Expression analysis of calmodulin and calmodulin-like genes from rice, Oryza sativa L. BMC research notes 5:625. doi:10.1186/1756-0500-5-625

Chinpongpanich A, Wutipraditkul N, Thairat S, Buaboocha T (2011) Biophysical characterization of calmodulin and calmodulin-like proteins from rice, Oryza sativa L. Acta biochimica et biophysica Sinica 43 (11):867-876. doi:10.1093/abbs/gmr081

Clapham DE (2007) Calcium Signaling. Cell 131 (6):1047-1058. doi:http://dx.doi.org/10.1016/j.cell.2007.11.028

Clarkson DT, Brownlee, C., and Ayling, S. M. (1988) Cytoplasmic calcium measurements in intact higher plant cells: Results from fluorescence ratio imaging of fura-2. J Cell Sci 91:71-80

Clough SJ, Bent AF (1998) Floral dip: a simplified method for Agrobacterium-mediated transformation of Arabidopsis thaliana. The Plant journal : for cell and molecular biology 16 (6):735-743

Cooper B, Clarke JD, Budworth P, Kreps J, Hutchison D, Park S, Guimil S, Dunn M, Luginbuhl P, Ellero C, Goff SA, Glazebrook J (2003) A network of rice genes associated with stress response and seed development. Proceedings of the National Academy of Sciences of the United States of America 100 (8):4945-4950. doi:10.1073/pnas.0737574100

Day IS, Reddy VS, Shad Ali G, Reddy AS (2002) Analysis of EF-hand-containing proteins in Arabidopsis. Genome biology 3 (10):Research0056

Delk NA, Johnson KA, Chowdhury NI, Braam J (2005) CML24, regulated in expression by diverse stimuli, encodes a potential Ca2+ sensor that functions in responses to ABA, day length and ion stress. Plant physiology 139:240-253

Dobney S, Chiasson D, Lam P, Smith SP, Snedden WA (2009) The calmodulin-related calcium sensor CML42 plays a role in trichome branching. The Journal of biological chemistry 284 (46):31647-31657. doi:10.1074/jbc.M109.056770

Doherty CJ, Van Buskirk HA, Myers SJ, Thomashow MF (2009) Roles for Arabidopsis CAMTA transcription factors in cold-regulated gene expression and freezing tolerance. The Plant cell 21 (3):972-984. doi:10.1105/tpc.108.063958

Dong A, Xin H, Yu Y, Sun C, Cao K, Shen WH (2002) The subcellular localization of an unusual rice calmodulin isoform, OsCaM61, depends on its prenylation status. Plant molecular biology 48 (3):203-210

Dubendorff JW, Studier FW (1991) Controlling basal expression in an inducible T7 expression system by blocking the target T7 promoter with lac repressor. Journal of molecular biology 219 (1):45-59

Emanuelsson O, Nielsen H, Brunak S, von Heijne G (2000) Predicting subcellular localization of proteins based on their N-terminal amino acid sequence. Journal of molecular biology 300 (4):1005-1016. doi:10.1006/jmbi.2000.3903

Fields S, Song O (1989) A novel genetic system to detect protein-protein interactions. Nature 340 (6230):245-246. doi:10.1038/340245a0

Frietsch S, Wang YF, Sladek C, Poulsen LR, Romanowsky SM, Schroeder JI, Harper JF (2007) A cyclic nucleotide-gated channel is essential for polarized tip growth of pollen. Proceedings of the National Academy of Sciences of the United States of America 104 (36):14531-14536. doi:10.1073/pnas.0701781104

Gifford JL, Walsh MP, Vogel HJ (2007) Structures and metal-ion-binding properties of the Ca2+-binding helix-loop-helix EF-hand motifs. The Biochemical journal 405 (2):199-221. doi:10.1042/bj20070255

Golovkin M, Reddy AS (2003) A calmodulin-binding protein from Arabidopsis has an essential role in pollen germination. Proceedings of the National Academy of Sciences of the United States of America 100 (18):10558-10563. doi:10.1073/pnas.1734110100

Grasser KD (2003) Chromatin-associated HMGA and HMGB proteins: versatile co-regulators of DNA-dependent processes. Plant molecular biology 53 (3):281-295

Grasser KD, Grill S, Duroux M, Launholt D, Thomsen MS, Nielsen BV, Nielsen HK, Merkle T (2004) HMGB6 from Arabidopsis thaliana specifies a novel type of plant chromosomal HMGB protein. Biochemistry 43 (5):1309-1314. doi:10.1021/bi035931c

Grasser KD, Krech AB, Feix G (1994) The maize chromosomal HMGa protein recognizes structural features of DNA and increases DNA flexibility. The Plant journal : for cell and molecular biology 6 (3):351-358

Grasser KD, Launholt D, Grasser M (2007) High mobility group proteins of the plant HMGB family: dynamic chromatin modulators. Biochimica et biophysica acta 1769 (5-6):346-357. doi:10.1016/j.bbaexp.2006.12.004

He Q, Ohndorf UM, Lippard SJ (2000) Intercalating residues determine the mode of HMG1 domains A and B binding to cisplatin-modified DNA. Biochemistry 39 (47):14426-14435

Heil M, Bostock RM (2002) Induced systemic resistance (ISR) against pathogens in the context of induced plant defences. Annals of botany 89 (5):503-512

Ikura M, Clore GM, Gronenborn AM, Zhu G, Klee CB, Bax A (1992) Solution structure of a calmodulin-target peptide complex by multidimensional NMR. Science (New York, NY) 256 (5057):632-638

Ishikawa R, Tamaki S, Yokoi S, Inagaki N, Shinomura T, Takano M, Shimamoto K (2005) Suppression of the floral activator Hd3a is the principal cause of the night break effect in rice. The Plant cell 17 (12):3326-3336. doi:10.1105/tpc.105.037028

James GL, Goldstein JL, Brown MS (1995) Polylysine and CVIM sequences of K-RasB dictate specificity of prenylation and confer resistance to benzodiazepine peptidomimetic in vitro. The Journal of biological chemistry 270 (11):6221-6226

Jamshidiha M, Ishida H, Sutherland C, Gifford JL, Walsh MP, Vogel HJ (2013) Structural analysis of a calmodulin variant from rice: the C-terminal extension of OsCaM61 regulates its calcium binding and enzyme activation properties. The Journal of biological chemistry 288 (44):32036-32049. doi:10.1074/jbc.M113.491076

Jeon J, Kim J (2013) Cold stress signaling networks in Arabidopsis. J Plant Biol 56 (2):69-76. doi:10.1007/s12374-013-0903-y

Karita E, Yamakawa H, Mitsuhara I, Kuchitsu K, Ohashi Y (2004) Three types of tobacco calmodulins characteristically activate plant NAD kinase at different Ca2+ concentrations and pHs. Plant & cell physiology 45 (10):1371-1379. doi:10.1093/pcp/pch158

Kikuchi R, Kawahigashi H, Ando T, Tonooka T, Handa H (2009) Molecular and functional characterization of PEBP genes in barley reveal the diversification of their roles in flowering. Plant physiology 149 (3):1341-1353. doi:10.1104/pp.108.132134

Klass J, Murphy FVt, Fouts S, Serenil M, Changela A, Siple J, Churchill ME (2003) The role of intercalating residues in chromosomal high-mobility-group protein DNA binding, bending and specificity. Nucleic acids research 31 (11):2852-2864

Klee CB, Ren H, Wang X (1998) Regulation of the calmodulin-stimulated protein phosphatase, calcineurin. The Journal of biological chemistry 273 (22):13367-13370

Klosterman SJ, Hadwiger LA (2002) Plant HMG proteins bearing the AT-hook motif. Plant Science 162 (6):855-866. doi:http://dx.doi.org/10.1016/S0168-9452(02)00056-0

Kojima S, Takahashi Y, Kobayashi Y, Monna L, Sasaki T, Araki T, Yano M (2002) Hd3a, a rice ortholog of the Arabidopsis FT gene, promotes transition to flowering downstream of Hd1 under short-day conditions. Plant & cell physiology 43 (10):1096-1105

Kooter JM, Matzke MA, Meyer P (1999) Listening to the silent genes: transgene silencing, gene regulation and pathogen control. Trends in plant science 4 (9):340-347

Krohn NM, Yanagisawa S, Grasser KD (2002) Specificity of the stimulatory interaction between chromosomal HMGB proteins and the transcription factor Dof2 and its negative regulation by protein kinase CK2-mediated phosphorylation. The Journal of biological chemistry 277 (36):32438-32444. doi:10.1074/jbc.M203814200

Kuboniwa H, Tjandra N, Grzesiek S, Ren H, Klee CB, Bax A (1995) Solution structure of calcium-free calmodulin. Nature structural biology 2 (9):768-776

Kurokawa H, Osawa M, Kurihara H, Katayama N, Tokumitsu H, Swindells MB, Kainosho M, Ikura M (2001) Target-induced conformational adaptation of calmodulin revealed by the crystal structure of a complex with nematode Ca(2+)/calmodulin-dependent kinase kinase peptide. Journal of molecular biology 312 (1):59-68. doi:10.1006/jmbi.2001.4822

Kushwaha R, Singh A, Chattopadhyay S (2008) Calmodulin7 plays an important role as transcriptional regulator in Arabidopsis seedling development. The Plant cell 20 (7):1747-1759. doi:10.1105/tpc.107.057612

Kwak KJ, Kim JY, Kim YO, Kang H (2007) Characterization of transgenic Arabidopsis plants overexpressing high mobility group B proteins under high salinity, drought or cold stress. Plant & cell physiology 48 (2):221-231. doi:10.1093/pcp/pcl057

Lee SH, Johnson JD, Walsh MP, Van Lierop JE, Sutherland C, Xu A, Snedden WA, Kosk-Kosicka D, Fromm H, Narayanan N, Cho MJ (2000) Differential regulation of Ca2+/calmodulin-dependent enzymes by plant calmodulin isoforms and free Ca2+ concentration. The Biochemical journal 350 Pt 1:299-306

Lee SH, Kim JC, Lee MS, Heo WD, Seo HY, Yoon HW, Hong JC, Lee SY, Bahk JD, Hwang I, et al. (1995) Identification of a novel divergent calmodulin isoform from soybean which has differential ability to activate calmodulin-dependent enzymes. The Journal of biological chemistry 270 (37):21806-21812

Lee SH, Kim MC, Heo WD, Kim JC, Chung WS, Park CY, Park HC, Cheong YH, Kim CY, Lee KJ, Bahk JD, Lee SY, Cho MJ (1999) Competitive binding of calmodulin isoforms to calmodulin-binding proteins: implication for the function of calmodulin isoforms in plants. Biochimica et biophysica acta 1433 (1-2):56-67

Lee SH, Seo HY, Kim JC, Heo WD, Chung WS, Lee KJ, Kim MC, Cheong YH, Choi JY, Lim CO, Cho MJ (1997) Differential activation of NAD kinase by plant calmodulin isoforms. The critical role of domain I. The Journal of biological chemistry 272 (14):9252-9259

Li DF, Li J, Ma L, Zhang L, Lu YT (2006) Calmodulin isoform-specific activation of a rice calmodulin-binding kinase conferred by only three amino-acids of OsCaM61. FEBS letters 580 (18):4325-4331. doi:10.1016/j.febslet.2006.06.090

Liu Q, Kasuga M, Sakuma Y, Abe H, Miura S, Yamaguchi-Shinozaki K, Shinozaki K (1998) Two transcription factors, DREB1 and DREB2, with an EREBP/AP2 DNA binding domain separate two cellular signal transduction pathways in drought- and low-temperature-responsive gene expression, respectively, in Arabidopsis. The Plant cell 10 (8):1391-1406

Luan S, Kudla J, Rodriguez-Concepcion M, Yalovsky S, Gruissem W (2002) Calmodulins and calcineurin B-like proteins: calcium sensors for specific signal response coupling in plants. The Plant cell 14 Suppl:S389-400

Luoni L, Bonza MC, De Michelis MI (2006) Calmodulin/Ca2+-ATPase interaction at the Arabidopsis thaliana plasma membrane is dependent on calmodulin isoform showing isoform-specific Ca2+ dependencies. Physiologia Plantarum 126 (2):175-186. doi:10.1111/j.1399-3054.2006.00588.x

Ma W, Smigel A, Tsai YC, Braam J, Berkowitz GA (2008) Innate immunity signaling: cytosolic Ca2+ elevation is linked to downstream nitric oxide generation through the action of calmodulin or a calmodulin-like protein. Plant physiology 148 (2):818-828. doi:10.1104/pp.108.125104

Magnan F, Ranty B, Charpenteau M, Sotta B, Galaud JP, Aldon D (2008) Mutations in AtCML9, a calmodulin-like protein from Arabidopsis thaliana, alter plant responses to abiotic stress and abscisic acid. The Plant journal : for cell and molecular biology 56 (4):575-589. doi:10.1111/j.1365-313X.2008.03622.x

Maruyama K, Todaka D, Mizoi J, Yoshida T, Kidokoro S, Matsukura S, Takasaki H, Sakurai T, Yamamoto YY, Yoshiwara K, Kojima M, Sakakibara H, Shinozaki K, Yamaguchi-Shinozaki K (2012) Identification of cis-acting promoter elements in cold- and dehydration-induced transcriptional pathways in Arabidopsis, rice, and soybean. DNA research : an international journal for

rapid publication of reports on genes and genomes 19 (1):37-49. doi:10.1093/dnares/dsr040

Masse JE, Wong B, Yen YM, Allain FH, Johnson RC, Feigon J (2002) The S. cerevisiae architectural HMGB protein NHP6A complexed with DNA: DNA and protein conformational changes upon binding. Journal of molecular biology 323 (2):263-284

Matzke AJ, Matzke MA (1998) Position effects and epigenetic silencing of plant transgenes. Current opinion in plant biology 1 (2):142-148

McCormack E, Braam J (2003) Calmodulins and related potential calcium sensors of Arabidopsis. New Phytologist 159 (3):585–598

Müller D, Leyser O (2011) Auxin, cytokinin and the control of shoot branching. Ann Bot 107 (7):1203–1212

Murphy FVt, Sweet RM, Churchill ME (1999) The structure of a chromosomal high mobility group protein-DNA complex reveals sequence-neutral mechanisms important for non-sequence-specific DNA recognition. The EMBO journal 18 (23):6610-6618. doi:10.1093/emboj/18.23.6610

Nagaya S, Kato K, Ninomiya Y, Horie R, Sekine M, Yoshida K, Shinmyo A (2005) Expression of randomly integrated single complete copy transgenes does not vary in Arabidopsis thaliana. Plant & cell physiology 46 (3):438-444. doi:10.1093/pcp/pci039

Nicot N, Hausman JF, Hoffmann L, Evers D (2005) Housekeeping gene selection for real-time RT-PCR normalization in potato during biotic and abiotic stress. Journal of experimental botany 56 (421):2907-2914. doi:10.1093/jxb/eri285

O'Neil KT, DeGrado WF (1990) How calmodulin binds its targets: sequence independent recognition of amphiphilic alpha-helices. Trends in biochemical sciences 15 (2):59-64

Ohndorf UM, Rould MA, He Q, Pabo CO, Lippard SJ (1999) Basis for recognition of cisplatin-modified DNA by high-mobility-group proteins. Nature 399 (6737):708-712. doi:10.1038/21460

Ou B, Yin KQ, Liu SN, Yang Y, Gu T, Wing Hui JM, Zhang L, Miao J, Kondou Y, Matsui M, Gu HY, Qu LJ (2011) A high-throughput screening system for Arabidopsis transcription factors and its application to Med25-dependent transcriptional regulation. Molecular plant 4 (3):546-555. doi:10.1093/mp/ssr002

Ouyang S, Zhu W, Hamilton J, Lin H, Campbell M, Childs K, Thibaud-Nissen F, Malek RL, Lee Y, Zheng L, Orvis J, Haas B, Wortman J, Buell CR (2007) The TIGR Rice Genome Annotation Resource: improvements and new features. Nucleic acids research 35 (Database issue):D883-887. doi:10.1093/nar/gkl976

Pauly N, Knight MR, Thuleau P, Graziana A, Muto S, Ranjeva R, Mazars C (2001) The nucleus together with the cytosol generates patterns of specific cellular calcium signatures in tobacco suspension culture cells. Cell calcium 30 (6):413-421. doi:10.1054/ceca.2001.0250

Pearson K (1900) On the criterion that a given system of deviations from the probable in the case of a correlated system of variables is such that it can be reasonably supposed to have arisen from random sampling. Philos Mag Series 5 50:157-175

Pedersen DS, Grasser KD (2010) The role of chromosomal HMGB proteins in plants. Biochimica et biophysica acta 1799 (1-2):171-174. doi:10.1016/j.bbagrm.2009.11.004

Pfaffl MW (2001) A new mathematical model for relative quantification in real-time RT-PCR. Nucleic acids research 29 (9):e45

Phean-o-pas S (2010) Functional characterization of OsCam1-1 from rice Oryza sativa L. in mediating salt stress response. Chulalongkorn University,

Phean-o-pas S, Limpaseni T, Buaboocha T (2008) Structure and expression analysis of the OsCam1-1 calmodulin gene from Oryza sativa L. BMB reports 41 (11):771-777

Popescu SC, Popescu GV, Bachan S, Zhang Z, Seay M, Gerstein M, Snyder M, Dinesh-Kumar SP (2007) Differential binding of calmodulin related proteins to their targets revealed using high-density Arabidopsis protein microarrays. Proc Natl Acad Sci 104:4730-4735

Prestridge DS (1991) SIGNAL SCAN: a computer program that scans DNA sequences for eukaryotic transcriptional elements. Computer applications in the biosciences : CABIOS 7 (2):203-206

Qin F, Shinozaki K, Yamaguchi-Shinozaki K (2011) Achievements and challenges in understanding plant abiotic stress responses and tolerance. Plant & cell physiology 52 (9):1569-1582. doi:10.1093/pcp/pcr106

Reddy AS (2001) Calcium: silver bullet in signaling. Plant science : an international journal of experimental plant biology 160 (3):381-404

Reddy VS, Reddy AS (2004) Proteomics of calcium-signaling components in plants. Phytochemistry 65 (12):1745-1776. doi:10.1016/j.phytochem.2004.04.033

Reeves R (2010) Nuclear functions of the HMG proteins. Biochimica et biophysica acta 1799 (1-2):3-14. doi:10.1016/j.bbagrm.2009.09.001

Ritt C, Grimm R, Fernandez S, Alonso JC, Grasser KD (1998) Four differently chromatin-associated maize HMG domain proteins modulate DNA structure and act as architectural elements in nucleoprotein complexes. The Plant journal : for cell and molecular biology 14 (5):623-631

Roberts DM, Harmon AC (1992) Calcium-Modulated Proteins: Targets of Intracellular Calcium Signals in Higher Plants. Annual Review of Plant Physiology and Plant Molecular Biology 43 (1):375-414. doi:doi:10.1146/annurev.pp.43.060192.002111

Rodríguez-Concepción M, Yalovsky S, Zik M, Fromm H, Gruissem W (1999) The prenylation status of a novel plant calmodulin directs plasma membrane or nuclear localization of the protein. The EMBO journal 18 (7):1996-2007. doi:10.1093/emboj/18.7.1996

Sai J, Johnson CH (2002) Dark-stimulated calcium ion fluxes in the chloroplast stroma and cytosol. The Plant cell 14 (6):1279-1291

Sanders D, Brownlee C, Harper JF (1999) Communicating with calcium. The Plant cell 11 (4):691-706

Sanders D, Pelloux J, Brownlee C, Harper JF (2002) Calcium at the Crossroads of Signaling. The Plant cell 14 (Suppl):s401-s417. doi:10.1105/tpc.002899

Schiott M, Romanowsky SM, Baekgaard L, Jakobsen MK, Palmgren MG, Harper JF (2004) A plant plasma membrane Ca2+ pump is required for normal pollen tube growth and fertilization. Proceedings of the National Academy of

Sciences of the United States of America 101 (25):9502-9507. doi:10.1073/pnas.0401542101

Snedden WA, Fromm H (1998) Calmodulin, calmodulin-related proteins and plant responses to the environment. Trends in plant science 3 (8):299-304. doi:http://dx.doi.org/10.1016/S1360-1385(98)01284-9

Stotz HU, Mitrousia GK, de Wit PJ, Fitt BD (2014) Effector-triggered defence against apoplastic fungal pathogens. Trends in plant science 19 (8):491-500. doi:10.1016/j.tplants.2014.04.009

Stros M, Muselikova E (2000) A role of basic residues and the putative intercalating phenylalanine of the HMG-1 box B in DNA supercoiling and binding to four-way DNA junctions. The Journal of biological chemistry 275 (46):35699-35707. doi:10.1074/jbc.M007167200

Swarbrick PJ, Schulze-Lefert P, Scholes JD (2006) Metabolic consequences of susceptibility and resistance (race-specific and broad-spectrum) in barley leaves challenged with powdery mildew. Plant, cell & environment 29 (6):1061-1076

Takezawa D, Liu ZH, An G, Poovaiah BW (1995) Calmodulin gene family in potato: developmental and touch-induced expression of the mRNA encoding a novel isoform. Plant molecular biology 27 (4):693-703

Takpirom W (2007) Overexpression of OsCam1-1 gene in transgenic rice Oryza sativa L. 'KDML105' and tobacco Nicotiana tabacum L. 'Virginia Coker'. Chulalongkorn University,

Thakur M, Sohal BS (2013) Role of Elicitors in Inducing Resistance in Plants against Pathogen Infection: A Review. ISRN biochemistry 2013:762412. doi:10.1155/2013/762412

Thomas JO, Travers AA (2001) HMG1 and 2, and related 'architectural' DNA-binding proteins. Trends in biochemical sciences 26 (3):167-174

Todaka D, Nakashima K, Shinozaki K, Yamaguchi-Shinozaki K (2012) Toward understanding transcriptional regulatory networks in abiotic stress responses and tolerance in rice. Rice (New York, NY) 5 (1):6. doi:10.1186/1939-8433-5-6

Townley HE, Knight MR (2002) Calmodulin as a potential negative regulator of Arabidopsis COR gene expression. Plant physiology 128 (4):1169-1172. doi:10.1104/pp.010814

Travers A (2000) Recognition of distorted DNA structures by HMG domains. Current opinion in structural biology 10 (1):102-109

Tsai YC, Weir NR, Hill K, Zhang W, Kim HJ, Shiu SH, Schaller GE, Kieber JJ (2012) Characterization of genes involved in cytokinin signaling and metabolism from rice. Plant physiology 158 (4):1666-1684. doi:10.1104/pp.111.192765

Tzfira T, Citovsky V (2006) Agrobacterium-mediated genetic transformation of plants: biology and biotechnology. Current opinion in biotechnology 17 (2):147-154. doi:10.1016/j.copbio.2006.01.009

van Der Luit AH, Olivari C, Haley A, Knight MR, Trewavas AJ (1999) Distinct calcium signaling pathways regulate calmodulin gene expression in tobacco. Plant physiology 121 (3):705-714

Vanderbeld B, Snedden WA (2007) Developmental and stimulus-induced expression patterns of Arabidopsis calmodulin-like genes CML37, CML38 and CML39. Plant molecular biology 64 (6):683-697. doi:10.1007/s11103-007-9189-0

Wang W, Vinocur B, Altman A (2003) Plant responses to drought, salinity and extreme temperatures: towards genetic engineering for stress tolerance. Planta 218 (1):1-14. doi:10.1007/s00425-003-1105-5

Webster CI, Packman LC, Gray JC (2001) HMG-1 enhances HMG-I/Y binding to an A/T-rich enhancer element from the pea plastocyanin gene. European journal of biochemistry / FEBS 268 (11):3154-3162

Weir HM, Kraulis PJ, Hill CS, Raine AR, Laue ED, Thomas JO (1993) Structure of the HMG box motif in the B-domain of HMG1. The EMBO journal 12 (4):1311-1319

Werner T, Motyka V, Strnad M, Schmulling T (2001) Regulation of plant growth by cytokinin. Proceedings of the National Academy of Sciences of the United States of America 98 (18):10487-10492. doi:10.1073/pnas.171304098

Wu Q, Zhang W, Pwee KH, Kumar PP (2003) Rice HMGB1 protein recognizes DNA structures and bends DNA efficiently. Archives of biochemistry and biophysics 411 (1):105-111

Xiao C, Xin H, Dong A, Sun C, Cao K (1999) A novel calmodulin-like protein gene in rice which has an unusual prolonged C-terminal sequence carrying a putative prenylation site. DNA research : an international journal for rapid publication of reports on genes and genomes 6 (3):179-181

Xu GY, Cui YC, Li MJ, Wang ML, Yu Y, Zhang B, Huang LF, Xia XJ (2013) OsMSR2, a novel rice calmodulin-like gene, confers enhanced salt tolerance in rice (Oryza sativa L.). Australian Journal of Crop Science 7 (3)

Xu GY, Rocha PS, Wang ML, Xu ML, Cui YC, Li LY, Zhu YX, Xia X (2011) A novel rice calmodulin-like gene, OsMSR2, enhances drought and salt tolerance and increases ABA sensitivity in Arabidopsis. Planta 234 (1):47-59. doi:10.1007/s00425-011-1386-z

Yamaguchi-Shinozaki K, Shinozaki K (1994) A novel cis-acting element in an Arabidopsis gene is involved in responsiveness to drought, low-temperature, or high-salt stress. The Plant cell 6 (2):251-264. doi:10.1105/tpc.6.2.251

Yamaguchi T, Aharon GS, Sottosanto JB, Blumwald E (2005) Vacuolar Na+/H+ antiporter cation selectivity is regulated by calmodulin from within the vacuole in a Ca2+- and pH-dependent manner. Proceedings of the National Academy of Sciences of the United States of America 102 (44):16107-16112. doi:10.1073/pnas.0504437102

Yamniuk AP, Vogel HJ (2005) Structural investigation into the differential target enzyme regulation displayed by plant calmodulin isoforms. Biochemistry 44 (8):3101-3111. doi:10.1021/bi047770y

Yang T, Poovaiah BW (2003) Calcium/calmodulin-mediated signal network in plants. Trends in plant science 8 (10):505-512. doi:10.1016/j.tplants.2003.09.004

Yin XM, Huang LF, Zhang X, Wang ML, Xu GY, Xia XJ (2015) OsCML4 improves drought tolerance through scavenging of reactive oxygen species in rice. J Plant Biol 58 (1):68-73

Yoo JH, Park CY, Kim JC, Heo WD, Cheong MS, Park HC, Kim MC, Moon BC, Choi MS, Kang YH, Lee JH, Kim HS, Lee SM, Yoon HW, Lim CO, Yun DJ,

Lee SY, Chung WS, Cho MJ (2005) Direct interaction of a divergent CaM isoform and the transcription factor, MYB2, enhances salt tolerance in arabidopsis. The Journal of biological chemistry 280 (5):3697-3706. doi:10.1074/jbc.M408237200

Zhang L, Liu BF, Liang S, Jones RL, Lu YT (2002) Molecular and biochemical characterization of a calcium/calmodulin-binding protein kinase from rice. The Biochemical journal 368 (Pt 1):145-157. doi:10.1042/bj20020780

Zhang M, Tanaka T, Ikura M (1995) Calcium-induced conformational transition revealed by the solution structure of apo calmodulin. Nature structural biology 2 (9):758-767

Zhang S, Hu W, Wang L, Lin C, Cong B, Sun C, Luo D (2005) TFL1/CEN-like genes control intercalary meristem activity and phase transition in rice. Plant Science 168 (6):1393-1408. doi:http://dx.doi.org/10.1016/j.plantsci.2004.10.022

Zhang W, Wu Q, Pwee KH, Manjunatha Kini R (2003) Interaction of wheat high-mobility-group proteins with four-way-junction DNA and characterization of the structure and expression of HMGA gene. Archives of biochemistry and biophysics 409 (2):357-366

Zhu S, Mc Henry KT, Lane WS, Fenteany G (2005) A chemical inhibitor reveals the role of Raf kinase inhibitor protein in cell migration. Chemistry & biology 12 (9):981-991. doi:10.1016/j.chembiol.2005.07.007

Zielinski RE (1998) Calmodulin and calmodulin-binding proteins in plants. Annu Rev Plant Physiol Plant Mol Biol 49:697-725. doi:10.1146/annurev.arplant.49.1.697

APPENDIX

Appendix A

Appendix A-1

Map of RBC T & A cloning vector

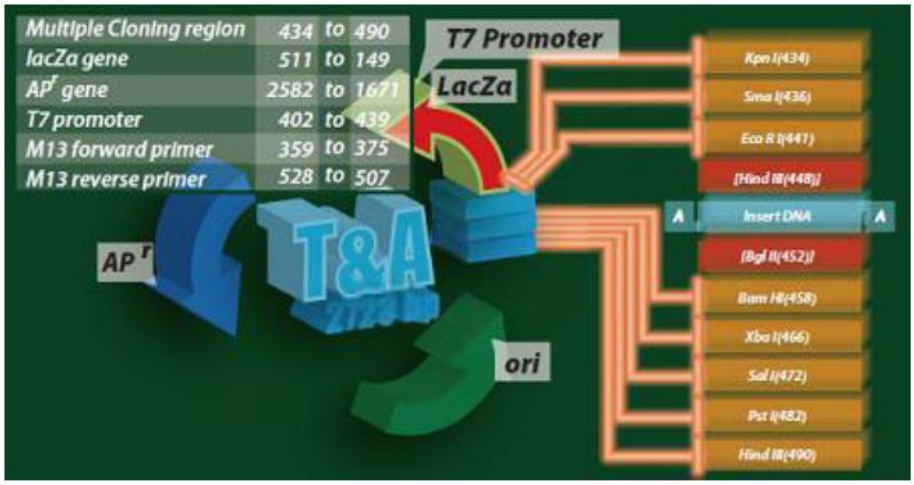

Appendix A-2

Restriction map of pET-21a(+)

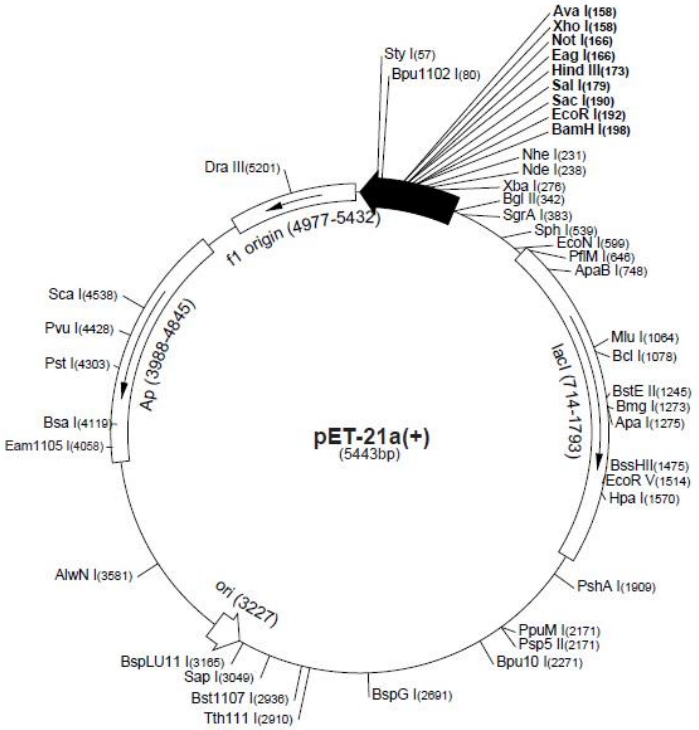

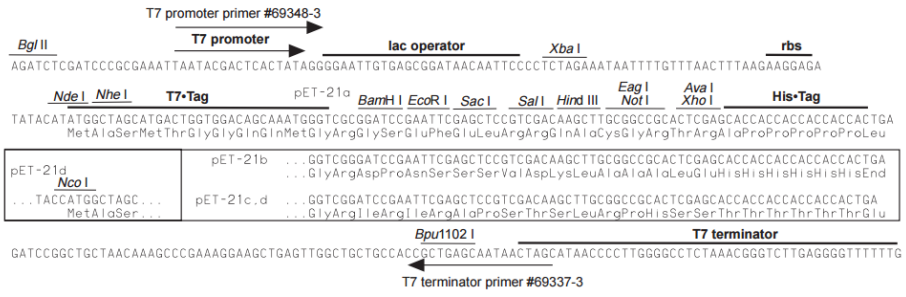

pET-21a-d(+) cloning/expression region

Appendix A-3

Restriction map of pCAMBIA 1302

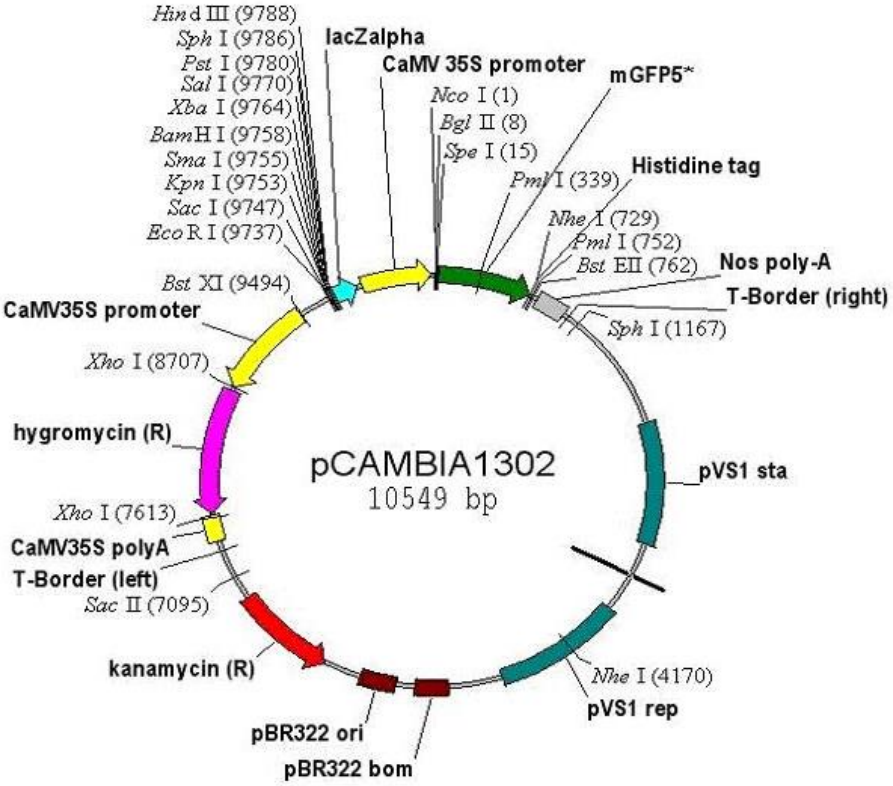

Appendix A-4

Directional TOPO® cloning

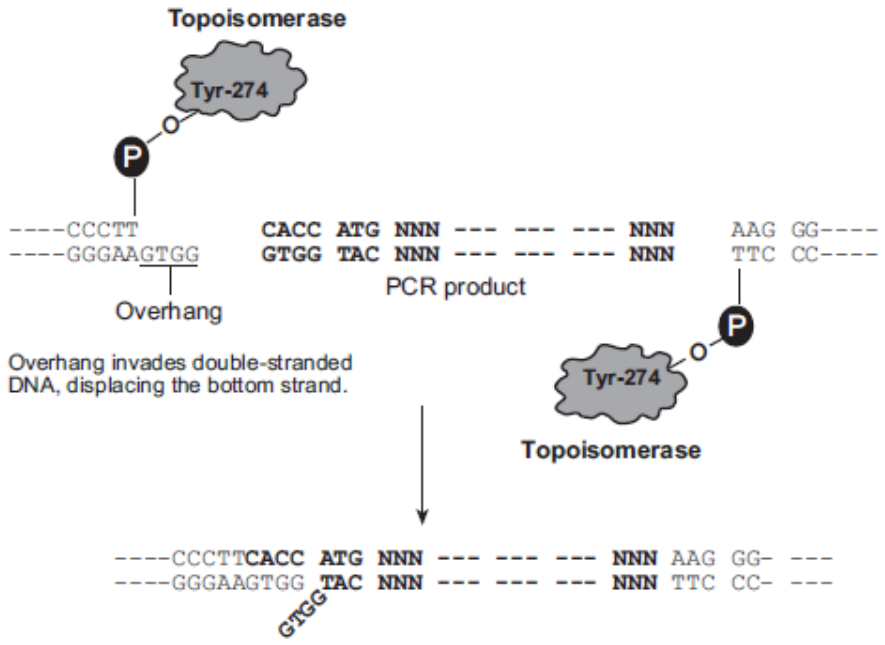

Directional joining of double-strand DNA using TOPO®-charged oligonucleotides occurs by adding a 3′ single-stranded end (overhang) to the incoming DNA (Cheng and Shuman, 2000). This single-stranded overhang is identical to the 5′ end of the TOPO®-charged DNA fragment. At Invitrogen, this idea has been modified by adding a 4 nucleotide overhang sequence to the TOPO®-charged DNA and adapting it to a 'whole vector' format. In this system, PCR products are directionally cloned by adding four bases to the forward primer (CACC). The overhang in the cloning vector (GTGG) invades the 5′ end of the PCR product, anneals to the added bases, and stabilizes the PCR product in the correct orientation. Inserts can be cloned in the correct orientation with efficiencies equal to or greater than 90%.

Appendix A-5

Map of pDEST™ 22

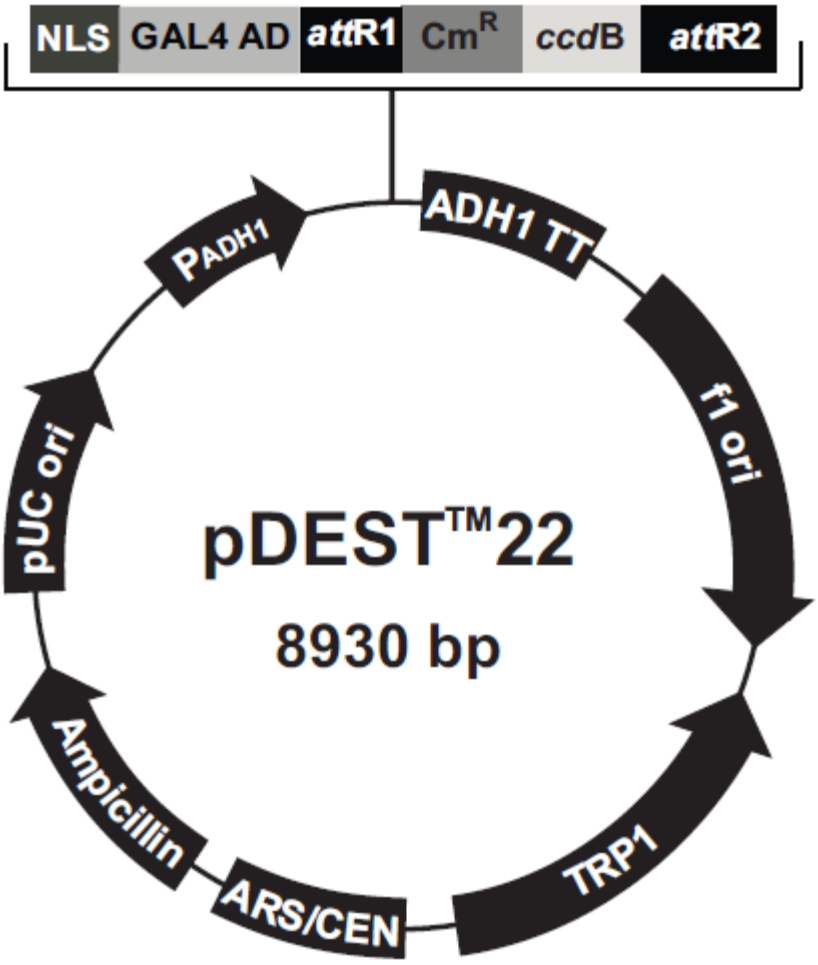

Appendix A-6

Map of pDEST™ 32

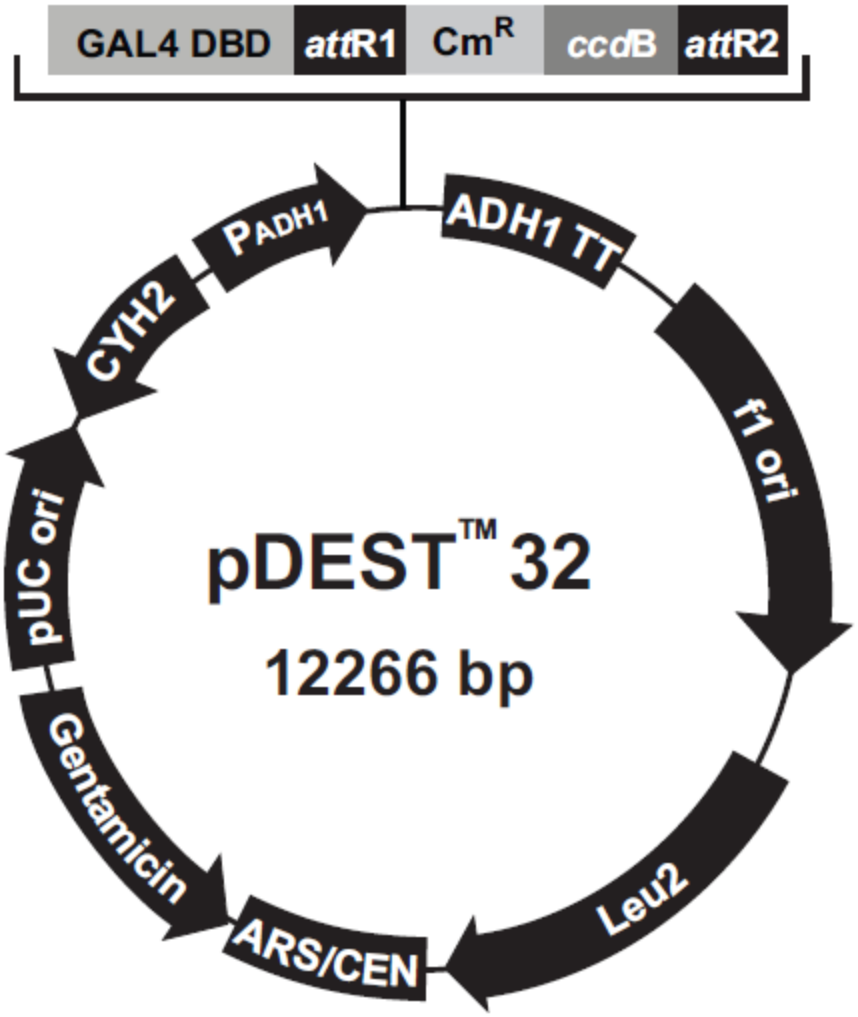

Appendix A-7

Restriction map of pET-28b(+)

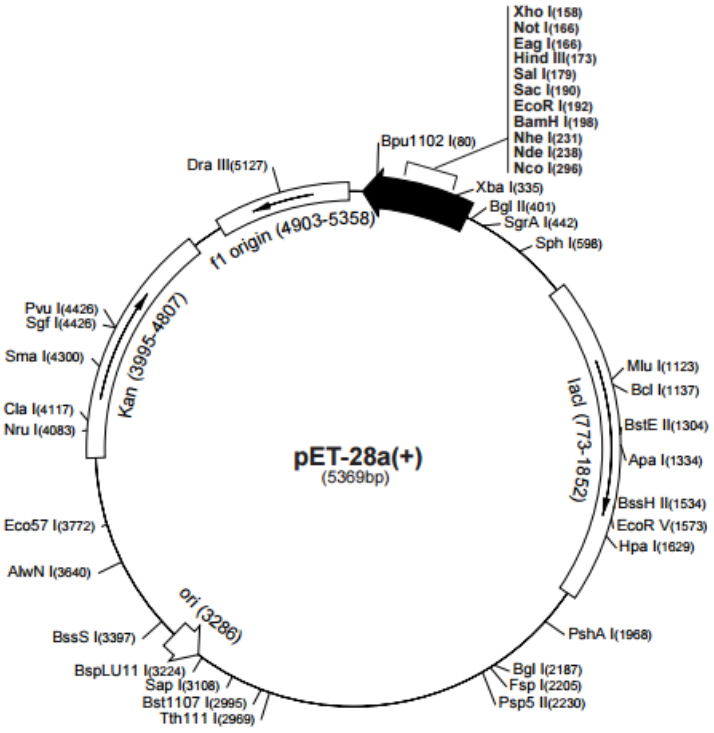

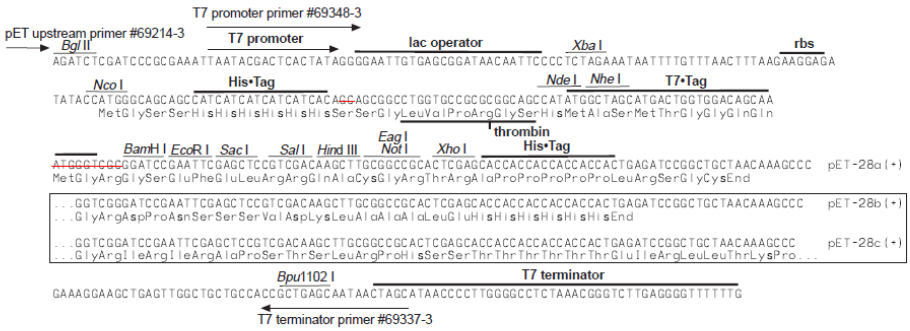

pET-28a-c(+) cloning/expression region

Appendix A-8

Restriction map of pCAMBIA 1301

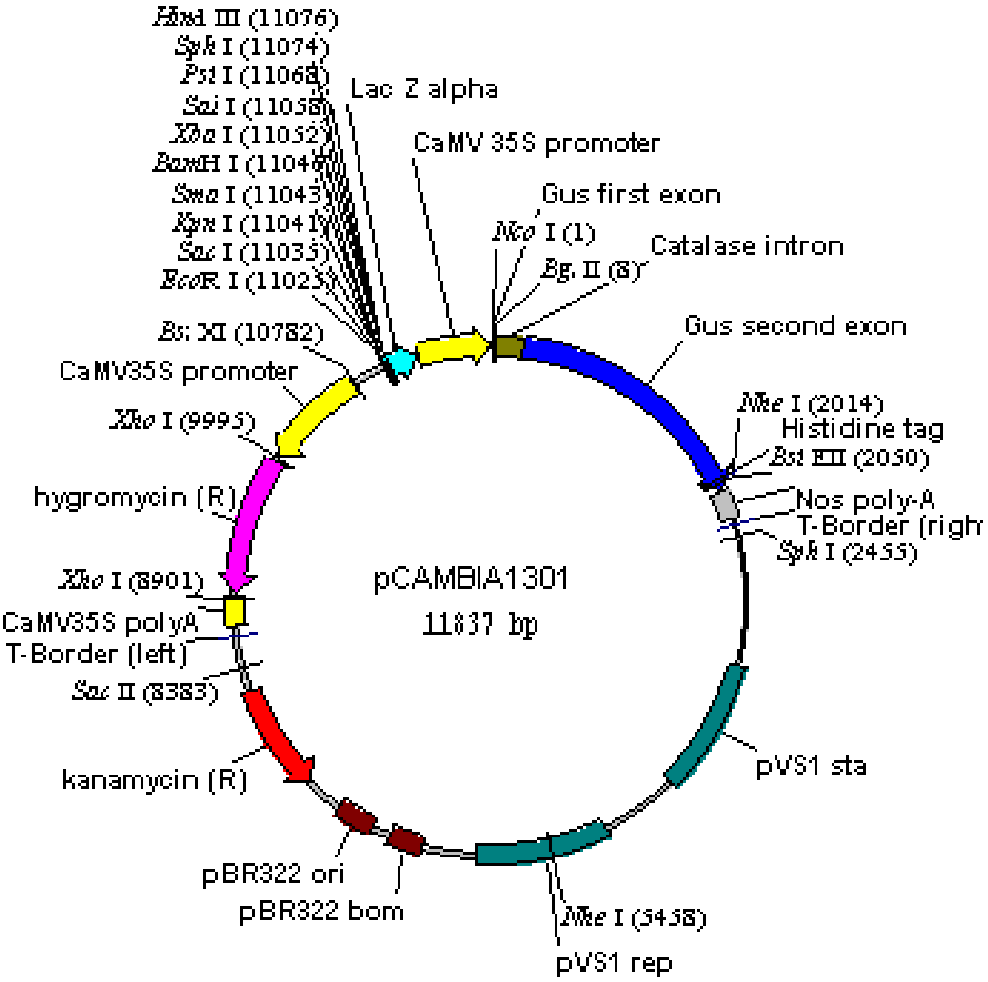

Appendix A-9

Map of EZ-T vector

图 1. EZ-T™ Simple 载体环形图谱

M13 Forward Primer (-20)
T7 Promoter

GTAAAACGACGGCCAGTGAGCGCGCGTAATACGACTCACTATAGGGCGAATTGGGCCAATACT PCR product TTCTTGGGAGTTCCTACAGCCCGGCGGATCGACAA
CATTTTGCTGCCGGTCACTCGCGCGCATTATGCTGAGTGATATCCCGCTTAACCCGGTTATG TAAGAACCCTCAAGGATGTCGGGCCGCCTAGCTGTT

GTTCTAGTGCCGCCGCCACGGCGGTCGACCAGCTTTTGTTCCCTTTAGTGAGGGTTAATTGCGCGCTTGGCGTAATCATGGTCATAGCTG
CAAGATCACGGCGGCGGTGCCGCCAGCTGGTCGAAAACAAGGGAAATCACTCCCAATTAACGCGCGAACCGCATTAGTACCAGTATCGAC

T3 Promoter
M13 Reverse Primer
β-galactosidase-α

Appendix B

Three control yeast cells

Control plasmid	Backbone	Insert	Mutant	Interaction with pEXP™ 32/Krev1
pEXP™22/ RalGDS-*wt*	pDEST™22	ras association domain of RalGDS, *wt*	wt	Strong
pEXP™22/ RalGDSm1	pDEST™22	ras association domain of RalGDS, m1	I77T	Weak
pEXP™22/ RalGDSm2	pDEST™22	ras association domain of RalGDS, m2	L65P	Not detectable

Appendix C

Chemical solution

1. Preparation for protein determination by Bradford, M. M. (1976)

Bradford solution

Coomassie Brilliant Blue (G250)	100 mg
Absolute ethanol	50 ml

Stir the solution in a container protected from light for 2 hours and adjust 100 of 85% phosphoric acid. Bring the volume to 1 L with distilled water and filter through a sterile, 0.22 μm nitrocellulose filter. Store the solution in a brown glass bottle (usable for several weeks).

2. Preparation for polyacrylamide gel electrophoresis

Separating gel buffer 8X

Tris base	181.7 g
H_2O	250 ml

Adjust pH to 8.8 with conc. HCl, bring the volume to 500 ml with distilled water. Filter through a 0.22 μm nitrocellulose and store at room temperature.

Stacking gel buffer 4X

Tris base	15.1 g
H_2O	150 ml

Adjust pH to 6.8 with conc. HCl, bring the volume to 250 ml with distilled water. Filter through a 0.22 μm nitrocellulose and store at room temperature.

Acrylamide, 30% A: 0.8% B

Acrylamide	150 g
Bisacrylamide	4 g

Dissolve in final volume of 500 ml in distilled water. Filter through a 0.22 μm nitrocellulose and store at 4 °C in a dark bottle.

Reservoir buffer 10X

Tris base	60.5 g
Glycine	288 g

Dissolve in final volume of 2 L in distilled water. Store at room temperature. Before use, add 2 g of SDS (0.1% SDS).

20% (w/v) SDS

Sodium dodecylsulfate	20 g

Adjust the volumn to 100 ml with distilled water. Stir rapidly to dissolve completely and filter through a sterile, 0.22 μm nitrocellulose filter.

Sample buffer 5X

1M Tris-HCl, pH 6.9	60 μl

20% (w/v) SDS	100 µl
Glycerol	790 µl
2-mercaptoethanol	50 µl
Bromophenol blue	1 mg

Adjust the volume to 1 ml with distilled water. Store at -20 °C in 1 ml aliquots.

Sample buffer 5X for Urea-PAGE

1M Tris-HCl, pH 6.9	60 µl
Glycerol	790 µl
Bromophenol blue	1 mg

Adjust the volume to 1 ml with distilled water. Store at -20 °C in 1 ml aliquots.

10% (w/v) Ammonium Persulfate

Ammonium persulfate	0.5 g

Dissolve in a final volume of 5 ml in H_2O. Store at 4 °C. Prepare fresh every two weeks.

SDS-PAGE

12.5% Separating gel

Acrylamide, 30% A: 0.8% B	5 ml
Separating gel buffer 8X	1.5 ml
20% (w/v) SDS	30 µl
Distilled water	5.4 ml
10% (w/v) Ammonium persulfate	60 µl
TEMED	6 µl

4% Stacking gel

Acrylamide, 30% A: 0.8% B	0.65 ml
Stacking gel buffer 4X	1.25 ml
20% (w/v) SDS	12.5 µl
Distilled water	3 ml
10% (w/v) Ammonium persulfate	37.5 µl
TEMED	2.5 µl

Polyacrylamide gel containing 4 M urea

12.5% Separating gel

Acrylamide, 30% A: 0.8% B	5 ml
Separating gel buffer 8X	1.5 ml
Urea	2.88 g
100 mM $CaCl_2$ or	120 µl (final concentration 1 mM)
150 mM EGTA	240 µl (final concentration 3 mM)

Adjust the volumn to 12 ml with distilled water

10% (w/v) Ammonium persulfate	60 µl
TEMED	6 µl

4% Stacking gel

Acrylamide, 30% A: 0.8% B	0.65 ml
Stacking gel buffer 4X	1.25 ml
Urea	1.2 g
100 mM $CaCl_2$ or	50 µl (final concentration 1 mM)
150 mM EGTA	100 µl (final concentration 3 mM)

Adjust the volumn to 5 ml with distilled water

10% (w/v) Ammonium persulfate	37.5 µl

TEMED	2.5 µl

3. Protein staining solution

Staining solution, 1 litre

Coomassie Brilliant Blue R250	2.5 g
Methanol	500 ml
Glacial acetic acid	70 ml
H_2O	430 ml

Dissolve with rapid stirring and store at room temperature.

Destaining solution

Methanol	100 ml
Glacial acetc acid	70 ml
H_2O	830 ml

Dissolve with rapid stirring and store at room temperature.

4. Media and reagents for yeast two hybrid assay

YPAD medium and plates

Component Amount

YPD 50 g

Adenine sulfate 100 mg

Distilled water to 1 liter

Autoclaved

For agar plates, add 20 g bacteriological-grade agar per liter of non-autoclaved YPAD medium. Adjust the pH to 6.0 with HCl. Autoclave at 121 ºC for 15 minutes. Cool to 55 ºC and dispense into sterile Petri dishes. Store plates when solidified upside down at 4 ºC.

Minimal Media

Minimal SD Base 26.7 g

-Leu/-Trp DO Supplement 0.64 g **or**

-His/-Leu/-Trp DO Supplement 0.62 g

Verify that the medium has a pH of 5.8; adjust if necessary.

Distilled water to 1 liter

Autoclaved

For agar plates, add 20 g bacteriological-grade agar per liter of non-autoclaved

minimal media. Adjust the pH to 5.8. Autoclave at 121 ºC for 15 minutes. Cool to 55 ºC and dispense into sterile Petri dishes. Store plates when solidified upside down at 4 ºC.

10X TE

100 mM Tris-HCl

10 mM EDTA

Adjust pH to 7.5

Autoclave

10X LiAc

1 M Lithium Acetate

Filter sterilize

1X LiAc/0.5X TE

10X LiAc 10 ml

10X TE 5 ml

Sterile water 85 ml

Filter sterilize

1X LiAc/1X TE

10X LiAc 10 ml

10X TE 10 ml

Sterile water 80 ml

Filter sterilize

1X LiAc/40% PEG-3350/1X TE

10XLiAc	10 ml
10XTE	5 ml
PEG-3350	40 g
Sterile water up to	100 ml

Filter sterilize

Z buffer

$Na_2HPO_4 . 7H_2O$	16.1 g (or 8.52 g anhydrous)
$NaH_2PO_4 . H_2O$	5.5 g (or 4.8 g anhydrous)
KCl	0.75 g
$MgSO_4 . 7H_2O$	0.246 g (or 0.12 g anhydrous)

Add sterile water up to 1000 ml

Adjust pH to 7.0

Filter sterilize

5. Reagents used for agarose gel electrophoresis

40x TAE Buffer

Tris base	193.6 g
$Na_2EDTA.2H_2O$	15.2 g

Add 700 ml deionizes water.

Adjust pH to 7.2 with glacial acetic acid.

Adjust volume to 1L with deionized water.

Autoclave and store at room temperature.

20x TBE buffer (2L)

Tris base	242.2 g
H_3BO_3	132.6 g
$Na_2EDTA.2H_2O$	29.6 g

Add 800 ml deionized water, and stir to dissolve completely.

Check pH that should be around 8.3. If not, adjust pH with solid Tris base or H_3BO_3.

Add deionized water to a final volume of 2L.

Autoclave and store at room temperature.

1% Agarose gel in TAE buffer

Agarose 1 g

1X TAE buffer 100 ml

Melt agarose in a microwave until the mixture dissolve completely.

1% Agarose gel in TBE buffer

Agarose 1 g

1X TBE buffer 100 ml

Melt agarose in a microwave until the mixture dissolve completely.

10x DNA loading buffer (10X sample buffer) (10ml)

0.5 M EDTA 2 ml (0.1M)

Glycerol 5 ml (50%)

20% (w/v) SDS 0.5 ml (1%)

Sterile deionized water 2.5 ml

Bromophenol blue 5-10 mg

Xylene cyanol FF 5-10 mg

Divide into 1-ml aliquots, Store at 4 ºC.

Warm at 65 ºC before use.

1 mg/ml Ethidium bromide

Ethidium bromide 0.1 g

H_2O to 100 ml

Store at 4 ^oC in a darkened bottle.

6. Media for plant growth

Limpinuntana's nutrient solution

300X Solution A (1 L)

KNO_3	30.333 g (0.10 g/L)
$Ca(NO_3)_2.4H_2O$	47.230 g (0.16 g/L)

300X Solution B (1 L)

$MgSO_4.7H_2O$	12.324 g (41 mg/L)
$NH_4H_2PO_4$	11.502 g (38 mg/L)
NaCl	16.577 g (55 mg/L)

300X Solution C (1 L)

$FeSO_4.7H_2O$	6 g (20 mg/Ll)
Na_2EDTA	8 g (27 mg/L)

300X Solution D (1 L)

$MnCl_2.4H_2O$	0.4323 g (1.44 mg/L)
H_3BO_3	0.342 g (1.14 mg/L)
$Na_2MoO_4.2H_2O$	0.0075 g (0.025 mg/L)
$ZnSO_4.7H_2O$	0.0264 g (0.088 mg/L)
$CuSO_4.5H_2O$	0.0117 g (0.039 mg/L)

1X Limpinuntana's solution (300 ml)

Mix solution A, B, C and D together (1 ml each).

Add deionized water to 300 ml

Autoclave for 15 minutes at 121 °C.

Murashige & Skoog (MS) agar

MURASHIGE & SKOOG BASAL Medium with Vitamin	4.43 g
Sucrose	30 g
Agar	7.5 g

Adjust pH to 5.7-5.8

Autoclave for 15 minutes at 121 °C.

Appendix D

TRI REAGENT®

Abbreviated protocol for RNA isolation

1. HOMOGENIZATION

- One ml TRI reagent per 50-100 mg tissue
- Store homogenate for 5 minutes (RT)

2. RNA EXTRACTION

- Add 0.2 ml chloroform, mix vigorously.
- Store sample for 2-15 minutes (RT)
- Centrifuge 12,000 g for 15 minutes (4 ^{o}C)

3. RNA PRECIPITATION

- Transfer aqueous phase to a clean tube
- Add 0.5 ml isopropanol and mix
- Store for 5 – 10 minutes (RT)
- Centrifuge 12,000 g for 8 minutes (4-25 ^{o}C)

4. RNA WASH

- Wash RNA pellet with 1 ml 75% ethanol
- Centrifuge 7,500 g for 5 minutes (4-25 ^{o}C)

5. SOLUBIKIZATION

- Air dry the RNA pellet for 5-10 minutes
- Dissolve by pipetting in 40-100 μl of DEPC-treated water and incubate at 55-60 ^{o}C for 10 minutes

Appendix E

Geneaid® Genomic DNA Mini Kit

Tissue Dissociation

- Cut off 50 mg (up to 100 mg) of fresh or frozen plant tissue or 10 mg (up to 25 mg) of dried sample.
- Freeze the sample with liquid nitrogen.
- Grind the sample to a fine powder then transfer it to a 1.5 ml microcentrifuge tube.

Lysis

NOTE: Mix GP1 Buffer or GPX1 Buffer and RNase A immediately prior to use.

- Add 400 µl of GP1 Buffer or GPX1 Buffer and 5 µl of RNase A into the sample tube and mix by vortex.
- Incubate at 60oC for 10 minutes. During incubation, invert the tube every 5 minutes.
- Add 100 µl of GP2 Buffer and mix by vortex then incubate on ice for 3 minutes. At this time, pre-heat the required Elution Buffer (200 µl per sample) to 60oC (for Step 4 DNA Elution).
- Place a Filter Column in a 2 ml Collection Tube then transfer the mixture to the Filter Column.
- Centrifuge for 1 minute at 1,000 x g then discard the Filter Column.
- Carefully transfer the supernatant from the 2 ml collection tube to a new 1.5 ml microcentrifuge tube

DNA Binding

- Add a 1.5 volume of GP3 Buffer (make sure isopropanol was added) then vortex immediately for 5 seconds. E.g. Add 750 µl of GP3 Buffer to 500 µl of lysate.

NOTE: If precipitate appears, break it up as much as possible with a pipette.

- Place a GD Column in a 2 ml Collection Tube.
- Transfer 700 µl of mixture (and any remaining precipitate) to the GD Column.
- Centrifuge at 14-16,000 x g for 2 minutes.
- Discard the flow-through then place the GD Column back in the 2 ml Collection Tube.
- Add the remaining mixture to the GD Column then centrifuge at 14-16,000 x g for 2 minutes.
- Discard the flow-through then place the GD Column back in the 2 ml Collection Tube.

Wash

- Add 400 µl of W1 Buffer to the GD Column then centrifuge at 14-16,000 x g for 30 seconds.
- Discard the flow-through then place the GD Column back in the 2 ml Collection Tube.
- Add 600 µl of Wash Buffer (make sure ethanol was added) to the GD Column.
- Centrifuge at 14-16,000 x g for 30 seconds.
- Discard the flow-through then place the GD Column back in the 2 ml Collection Tube.
- Centrifuge for 3 minutes at 14-16,000 x g to dry the column matrix.

Optional Step: Residue Pigment Removal (If pigments remain on the column, perform this optional step)

- Following Wash Buffer addition, add 400 µl of absolute ethanol to the GD Column.
- Centrifuge at 14-16,000 x g for 30 seconds.

- Discard the flow-through then place the GD Column back in the 2 ml Collection Tube.
- Centrifuge for 3 minutes at 14-16,000 x g to dry the column matrix.

DNA Elution

Standard elution volume is 100 µl. If less sample is to be used, reduce the elution volume (30-50 µl) to increase DNA concentration. If higher DNA yield is required, repeat the DNA Elution Step to increase DNA recovery and the total elution volume to approximately 200 µl.

- Transfer the dried GD Column to a clean 1.5 ml microcentrifuge tube.
- Add 100 µl of pre-heated Elution Buffer or TE to the center of the column matrix.
- Let stand for 3-5 minutes to ensure the Elution Buffer or TE is completely absorbed.
- Centrifuge at 14-16,000 x g for 30 seconds to elute the purified DNA

VITA

Mr. Aumnart Chinpongpanich was born on June 20, 1983 in Bangkok. After he finished high school in 1999 from Bangkok Christian College School in Bangkok, he was enrolled in the Department of Biochemistry at Kasetsart University and graduated with the degree of Bachelor of Science in 2003. He had studied for the degree of Master of Science at the Department of Biochemistry, Faculty of Science, Chulalongkorn University since 2006. Then, he keeps on studying for Doctoral degree of Science in Biochemistry and molecular biology at the Department of Biochemistry, Chulalongkorn University.